

**Paleoenvironmental and Paleoecological Changes during Deposition of  
the Late Eocene Kiliran Oil Shale, Central Sumatra Basin, Indonesia**

Dissertation  
for attaining the PhD degree  
of Natural Sciences

submitted to the Faculty of Geosciences/Geography  
of the Johann Wolfgang Goethe University  
in Frankfurt am Main

by  
Agus Haris Widayat  
from Kulonprogo (Indonesia)

Frankfurt (2011)

(D 30)

accepted by the Faculty of Geosciences/Geography of the  
Johann Wolfgang Goethe University as a dissertation.

Dean:

Prof. Dr. Robert Pütz

Expert assessors:

Prof. Dr. Wilhelm Püttmann

Prof. Dr. Wolfgang Oschmann

Prof. Dr. Jörg Pross

Apl.-Prof. Dr. Fathi Zereini

Date of the disputation: 14 April 2011

## **Acknowledgement**

The PhD study had been carried out from October 2007 to January 2011 at the Institute of Atmospheric and Environmental Sciences, Johann Wolfgang Goethe University in Frankfurt am Main, Germany. The PhD scholarship was obtained from the German Academic Exchange Service (DAAD) to which first of all my great thanks are delivered.

I express my sincere gratitude and appreciation to Prof. Dr. Wilhelm Püttmann as my supervisor for his guidance, comments and constructive discussions during the whole project. I also thank for his patience, encouragements and motivations, so that my research program can be fulfilled as scheduled. I am also very grateful to Prof. Dr. Wolfgang Oschmann (Institute of Geosciences, Section Paleontology of Johann Wolfgang Goethe University) for his willingness to be co-supervisor and his advices regarding my dissertation.

My special thanks are due to Dr. Komang Anggayana and Prof. Dr. Sudarto Notosiswoyo for their encouragement to apply for the PhD scholarship of DAAD. They are members of the Faculty of Mining and Petroleum Engineering, Institut Teknologi Bandung, Indonesia. I equally thank Dr. Hadiyanto, the Head of Indonesian Center for Geological Resources (PSDG) for providing the oil shale samples required for this project.

Many thanks are also addressed to Dr. Sri Widodo (Hasanuddin University, Indonesia) and Dr. Bas van de Schootbrugge (Institute of Geosciences, Section Paleontology of Johann Wolfgang Goethe University) for valuable comments and discussions during the interpretation of analytical data. Discussions with Dr. Achim Bechtel (Leoben University, Austria) on compound-specific carbon isotopic data are highly appreciated. I also thank all current and former members of the Department of Environmental Analytical Chemistry for their assistance, support and cooperation within the working group.

Greatest thank are due to my wife (Irayanti Widayat), my little son (Faiz Aulia Widayat) and my parents for the encouragement and understanding.

## Abstract

Forty two samples of the Late Eocene Kiliran oil shale, Central Sumatra Basin, Indonesia were collected from a 102 m long drill core. The oil shale core represents the deposition time of about 240.000 years. Palynofacies and geochemical analyses have been carried out to reconstruct the paleoenvironmental conditions and paleoecology during deposition of the oil shale. Amorphous organic matter (AOM) is very abundant (>76%). *B. braunii* palynomorphs are present (3-16%) as the only autochthonous structured organic matter and generally more abundant in the middle part of the profile. The stable carbon isotopic composition of bulk organic matter ( $\delta^{13}\text{C}$ ) varies from -27.0 to -30.5‰ and is generally more depleted in the middle part of the profile. The ratio of total organic carbon to sulfur (TOC/S), used as salinity indicator, ranges from 2.5 to 15.8 and shows variations along the profile. Slightly less saline environments are observed in the middle part of the profile. Fungal remains are generally present only in this part with a distinct peak of abundance. The presence of fungal remains is regarded as an indication for a relatively warmer climate during deposition of the middle part of the profile. The warmer climate is thought to influence the establishment of a thermocline, limiting the supply of recycled nutrients to epilimnion. Consequently, the primary productivity in the Kiliran lake decreased during deposition of the middle part of the profile as indicated by the relatively depleted  $\delta^{13}\text{C}$  values and the blooming of *B. braunii*. The chemocline was also shoaling during the deposition according to the higher abundance of total isorenieratane and its derivatives originated from green sulfur bacteria dwelling in the photic zone euxinia. The warmer climate is also thought to influence the slightly decrease of water salinity during deposition of the middle part of the profile.

The occurrence of *B. braunii* in Kiliran lake is also recognized from organic geochemical data. The distribution of *n*-alkanes is characterized by the unusual high amount of C<sub>27</sub> *n*-alkane relative to the other long-chain *n*-alkanes. The concentrations of C<sub>27</sub> *n*-alkane vary from 30.1 to 393.7 µg/g TOC and are generally in parallel with the abundances of *B. braunii* palynomorphs along the profile. The  $\delta^{13}\text{C}$  values of this compound are about -31‰ and up to 2‰ enriched relative to those of the adjacent long-chain *n*-alkanes. *B. braunii* race A can thus be regarded as the significant biological source of the C<sub>27</sub> *n*-alkane. Lower amounts of lycopane are observed in many oil shale samples (0 to 54.7 µg/g TOC). The  $\delta^{13}\text{C}$  value of this compound is

-17.2‰. This strong enrichment of  $^{13}\text{C}$  suggests that the lycopane was derived from *B. braunii* race L. The concentrations of lycopane develop generally in opposite with those of  $\text{C}_{27}$  *n*-alkane. It is likely that both *B. braunii* races bloomed in alternation in the lake, probably due to changes on specific water chemistry.

Norneohop-13(18)-ene and neohop-13(18)-ene derived from methanotrophic bacteria are the dominant hopanoid hydrocarbons. The sum of their concentrations varies from 40.6 to 360.0  $\mu\text{g/g}$  TOC. The  $\delta^{13}\text{C}$  of these compounds are extremely depleted (-45.2 to -50.2‰). The occurrence of abundant bacteria including methanotrophic bacteria was responsible for the recycling of carbon below the chemocline of the lake. The effect of the recycling of carbon is observed by the presence of a concomitant depletion (about 7-9‰) in  $^{13}\text{C}$  of some specific biomarkers derived from organisms dwelling in the whole phototrophic zone.

4-Methylsterane and 4-methyldiasterene homologues occur in the oil shale as the predominant biomarkers. The sum of the concentrations of all homologues are about 40.3-1,009.2  $\mu\text{g/g}$  TOC with generally higher values in the uppermost and lower parts of the profile. Calcium (Ca) accounts as the predominant element in the oil shale, ranging from 5.0 to 16.7%. This element shows generally parallel variation with the 4-methylsterane and 4-methyldiasterene homologues along the profile. This suggests that these compounds were derived from biological sources favoring more alkaline and more trophic environments. On the other hand, these compounds were less abundant in the middle part of the profile which is consistent with less alkaline and less trophic environments promoting *B. braunii* to bloom. Alternation between *Dinoflagellates* and *B. braunii* in ancient lacustrine environments due to water chemistry changes have been known from previous studies. In the present case, distinct alternation between *B. braunii* abundances and concentrations of 4-methylsterane and 4-methyldiasterene homologues along the studied oil shale profile suggest a hypothesis that these compounds were derived from freshwater *Dinoflagellates* although dinosterane is not present in the sediment extracts. Water alkalinity and trophic level changes were most likely responsible for the alternation of *Dinoflagellates* and *B. braunii* blooming.

## **Zusammenfassung**

Im Rahmen der vorliegenden Dissertation sind detaillierte palynologische und geochemische Untersuchungen an einem Obereozänen Ölschiefer aus dem Kiliran Sub-Becken, einem Teil des Central Sumatra Beckens (Indonesien) durchgeführt worden. Das Central Sumatra Becken gehört zu den erdölreichsten Becken in Indonesien, mit einer Gesamtmenge an Kohlenwasserstoffen von etwa 13,67 Milliarden Barrel Öl-Äquivalenten (Doust und Noble, 2008).

Die Ziele dieses Projekts bestand in:

1. Rekonstruktion der Umweltbedingungen während der Ablagerung der Sedimente im früheren Kiliran See unter Berücksichtigung der klimatischer Veränderungen und tektonischen Subsidenz.
2. Charakterisierung der organisch-geochemischen Zusammensetzung des Ölschiefers zur Bestimmung der aquatischen Bedingungen und möglicher Bioproduzenten in der Wassersäule und im Sediment.
3. Rekonstruktion der paläoökologischen Entwicklung des früheren Kiliran Sees.

Im frühen Tertiär wurde das Central Sumatra Becken durch einen Grabenbruch als Folge der Ost-West-Ausdehnung während der nordwärts gerichteten Bewegung sowohl der australischen Platte im Osten und den indischen Platte im Westen gebildet (z.B. de Coster, 1974). Anschließend Sedimentation führte während des Tertiärs zur Ablagerung der Pematang Schichten, die aus den Lower Red Bed, Brown Shale und Lake Fill Formationen besteht. Daran anschließend folgen die Sihapas Schichten (Menggala, Bangko-Bekasap, Telisa Formationen) sowie die Petani und Minas Formationen. Das Kiliran Sub-Becken befindet sich am südöstlichen Rand des Beckens. Die Brown Shale Formation (Fm) ist in diesem Teilgebiet ausgebildet und enthält Ölschiefer.

In diesem Projekt wurden zweiundvierzig Proben aus einem 102 m langen Bohrkern, der im Jahr 2006 vom Indonesian Center for Geological Resources (PSDG) im Padanglawas Graben erbohrt wurde, gesammelt. Der analysierte Abschnitt des Bohrkerns enthält Sedimente, die in einem Zeitrahmen von etwa 240.000 Jahren abgelagert wurden. Der Kern enthält feinlaminierte Ölschiefer von unterschiedlicher Zusammensetzung, wobei zunächst

Farbwechsel entlang des Profils auffallen. Der untere Teil des Profils besteht im Wesentlichen aus dunkelgrauen bis braunen Ölschiefen, während der obere Teil des Profils aus dunkelgrauen bis grauen Ölschiefen besteht.

Unter Einsatz von Durchlichtmikroskopie wurden Analysen der Palynofazies durchgeführt, um die Zusammensetzung der organischen Substanz des Kiliran Ölschiefers zu ermitteln. Durch geochemische Analysen wurden sowohl die anorganischen als auch die organischen Bestandteile des Ölschiefers untersucht. Durch Messung der Kohlenstoff-Isotop-Zusammensetzung am Bulkmaterial und an Einzelkomponenten (Biomarker) in den Extrakten der Ölschiefer konnten zusätzliche Informationen über die Herkunft und Zusammensetzung der organischen Bestandteile im Sediment gewonnen werden.

Terrigene und autochthone Einträge wurden an den Kiliran Ölschiefen durch Elementanalyse und palynologische Analysen untersucht. Aluminium (Al) und Pollen werden als terrigene Einträge angesehen, während der gesamte organische Kohlenstoff (TOC), Schwefel (S), Uran (U) und Molybdän (Mo) als autochthone Einträge angesehen werden. Die Al-Konzentrationen variieren von 3,6 bis 8,1%, wobei die Konzentrationen im Ölschiefer-Profil nach oben hin tendenziell ansteigen. Pollen haben einen Anteil von 0 bis 6% an der palynologisch identifizierten organischen Substanz und treten im allgemeinen im unteren Teil des Profils mit geringerer Häufigkeit auf als in den oberen Profilbereichen. Die Proben enthalten zwischen 1,9 und 12,5% TOC, wobei sich die TOC- und Al-Konzentrationen entlang des Profils meist gegenläufig entwickeln. S, U und Mo sind in den Ölschieferproben in Konzentrationen von 0,1 bis 2,0%, 3,2 bis 7,5 ppm bzw. 0,2 bis 6,8 ppm enthalten. Die Konzentrationen dieser Elemente korrelieren entlang des Profils in der Regel mit dem TOC, was darauf hinweist, dass diese Elemente gemeinsam mit dem organischen Material in einem reduzierenden Milieu in das Sediment eingetragen werden.

Das TOC/S-Verhältnis wurde bestimmt um Rückschlüsse auf den Bodenwassersalzgehalt des Kiliran Sees ziehen zu können. Die Verhältnisse liegen im Bereich von 2,5 bis 15,8 und deuten auf Brack- und Süßwasser hin. Generell hat der Salzgehalt im See während der Ablagerung des analysierten Sedimentabschnitts von unten nach oben abgenommen. Während der Ablagerung des obersten Teils des Profils herrschten Süßwasserbedingungen.

Die Veränderung in der Zusammensetzung der Primärproduzenten im früheren Kiliran See konnten anhand der Variation der Häufigkeit von *B. braunii* und der Änderungen in der isotopischen Zusammensetzung des Kohlenstoffs ( $\delta^{13}\text{C}$ ) der organischen Substanz nachvollzogen werden. *B. braunii* macht etwa 3 bis 16% der palynologisch identifizierten organischen Substanz in den Ölschieferproben aus. Diese Alge ist in der Regel weniger häufig im unteren Teil des Profils, und häufiger im mittleren Teil des Profils vorhanden. Im oberen Teil des Profils nimmt die Häufigkeiten der Alge wieder ab. Die  $\delta^{13}\text{C}$ -Werte variieren von -27,0 bis -30,5‰. Die Variation der  $\delta^{13}\text{C}$ -Werte entwickelt sich gegenläufig zur Häufigkeit der Alge *B. braunii*. Dies deutet auf eine erhöhte Bioproduktivität im Kiliran See während der Sedimentation des oberen und unteren Teil des Profils hin, während die Produktivität bei Ablagerung des mittleren Teils des Profils geringer war.

Zr und Rb sind terrigene Elemente. Das Verhältnis von Zr/Rb wurde ermittelt um relative Veränderungen der Korngröße des Ölschiefers zu bestimmen. Die Zr/Rb-Verhältnisse liegen im Bereich von 0,4 bis 1,3 und zeigen entlang des Profils an ansteigenden Tendenz, die durch drei abrupte Abnahmen unterbrochen wird. Die drei abrupten Abnahmen des Zr/Rb-Verhältnisses deuten auf eine rasche Vertiefung durch Absenkungen des Kiliran-Beckens hin. Tektonische Subsidenz während der Ablagerung der Sedimente war verantwortlich für die Schaffung eines größeren Sedimentationsraumes.

Überreste von Pilzen machen etwa 0 bis 3% der palynologisch identifizierten organischen Substanz. Sie fehlen fast vollständig im unteren und oberen Teil des Profils. Im mittleren Teil des Profils werden dagegen relativ häufig Reste von Pilzen gefunden, die auf ein wärmeres Klima während der Sedimentation hindeuten. In diesem Teil nimmt die Häufigkeit der Pilzrückstände deutlich zu. Die Häufigkeit der Pilzreste entlang des gesamten Profils deutet also auf eine Erwärmung gefolgt von kühleren Klimatrends während der Ablagerung des Sediments hin.

Diese Klimaveränderungen sind vermutlich ebenfalls die Ursache für die Veränderung des Salzgehalts im Wassers und der Produktivität im Kiliran See. Der Salzgehalt des Wassers nahm in den wärmeren Klimaperioden ab, da dem See mehr Frischwasser zugeführt wurde. Das wärmere Klima war für die Ausbildung einer Sprungschicht verantwortlich, die die Aufnahme von Nährstoffen aus dem Tiefenwasser ins Epilimnion verringert und somit zu einer Verringerung der primären Produktivität beitrug. Der Rückgang der Produktivität und die



Erhöhung des Sedimenteintrags infolge des wärmeren Klimas führt zu einem höheren Eintrag von terrigenem Material relativ zum autochthonen Material. Im unteren Teil des Profils, in dem fast keine Überreste von Pilzen vorhanden sind, könnte die Subsidenzrate höher gewesen sein als die Sedimentationsrate, was zu einem höheren Gehalt an autochthonem Material führt. Im oberen Teil, wo Überreste von Pilzen im Profil ebenfalls fast vollständig fehlen, könnte der See flacher sein, was den Eintrag von terrigenem Material fördert und ein Süßwassermilieu schafft.

Die Ausbildung einer Sprungschicht während der wärmeren Klimaperiode wird durch die organisch-geochemischen Daten belegt. Der Biomarker Isorenieratan und Arylisoprenoide als dessen Spaltprodukte stammen von grünen Schwefelbakterien ab. Diese Substanzen konnten in allen untersuchten Proben nachgewiesen werden und zeigen ihr Maximum ebenfalls im mittleren Teil des Profils. Grüne Schwefelbakterien leben in der photischen Zone, die aber völlig sauerstofffrei ist (photic zone euxinia). Die Konzentrationen aus der Summe von Isorenieratan und aller Isorenieratan-Derivate variieren zwischen 3,6 bis 41,5 µg/g TOC, mit einer größeren Häufigkeit im mittleren Teil des Profils. Ein Anstieg der Chemokline in der Wassersäule ist aufgrund der hohen Konzentrationen von Isorenieratan und seiner Derivate bei der Sedimentation des mittleren Teil des Profils anzunehmen, da dies zu einer Erhöhung der Biomasseproduktion von grünen Schwefelbakterien in der photischen Zone führt. Abrupte Konzentrationsverringierungen von Isorenieratan und seinen Derivaten deuten auf Absenkereignisse im See hin, was auch durch die Zr/Rb-Verhältnisse bestätigt wird. Es ist davon auszugehen, dass diese tektonischen Ereignisse sowohl für die rasche Absenkung der Chemokline als auch für die Verringerung der photic zone euxinia verantwortlich waren.

Isorenieratan und dessen Derivate können auch dazu benutzt werden, Aussagen über die Veränderung der Umweltbedingungen im früheren Kiliran See zu treffen in Bezug auf den Kohlenstoffkreislauf. Die  $\delta^{13}\text{C}$ -Werte von Isorenieratane betragen -24‰. Dieser Wert ist deutlich geringer als üblicherweise für die Biomarker der grünen Schwefelbakterien gefunden wird (etwa -15‰). Dies deutet darauf hin, dass in der H<sub>2</sub>S-haltigen photischen Zone ein mit <sup>13</sup>C-abgereicherter gelöster anorganischer Kohlenstoff (dissolved inorganic carbon, DIC) vorhanden war, der von den grünen Schwefelbakterien für die Photosynthese verwendet wurde. Die Anwesenheit von <sup>13</sup>C-abgereichertem DIC wird durch die bakterielle Aktivität unterhalb des Chemokline gefördert. Der Abbau der Biomasse von Primärproduzenten mit abgereichertem <sup>13</sup>C liefert einen DIC der ebenfalls abgereichert ist. Aufgrund von

Durchmischungseffekten zwischen den Wasserschichten wurde recycelter and somit leichter DIC dem Epilimnion wieder zugeführt.

Die Aktivität methanotropher Bakterien könnte sich ebenfalls stark auf den  $^{13}\text{C}$ -abgereicherten DIC auswirken. Die in dieser Studie identifizierten Biomarker methanotropher Bakterien sind Norneohop-13(18)-en und Neohop-13(18)-en. Die Summe ihrer Konzentrationen variieren von 40,6 bis 360,0  $\mu\text{g/g}$  TOC. Diese Verbindungen weisen sehr geringe  $\delta^{13}\text{C}$ -Werte von -45,2 bis -50,2‰ auf. Methanotrophe Bakterien siedeln sich im Bereich der Chemokline an. Die Bakterien oxidieren biogenes und an  $^{13}\text{C}$  stark verarmtes Methan, welches durch Methanogenese im Bereich des Bodenwassers und/oder im Sediment gebildet wurde, zu Kohlendioxid. Dieser Prozess erzeugt einen  $^{13}\text{C}$ -abgereicherten DIC und darüber hinaus eine an  $^{13}\text{C}$  abgereicherte bakterielle Biomasse.

Die Rückführung von  $^{13}\text{C}$ -abgereichertem DIC ins Epilimnion hat folglich auch die  $\delta^{13}\text{C}$ -Werte der phototrophen Biomasse im Kiliran See beeinflusst. Das Phytoplankton im Epilimnion nahm den an  $^{13}\text{C}$  verarmten gelösten anorganischen Kohlenstoff während der Photosynthese auf, was zu den geringen  $\delta^{13}\text{C}$ -Werten ihrer Biomasse führte. Dies ist anhand der deutlich verringerten  $\delta^{13}\text{C}$ -Werte der in dieser Studie identifizierten Biomarker nachweisbar. Biomarker aus Algen, Carotinoid-Derivate und 4-Methylsterane, haben  $\delta^{13}\text{C}$ -Werte von etwa -35‰ und -37‰. Diese Werte sind im Durchschnitt etwa 7-9‰ niedriger, als dies sonst für Biomasse der Algen üblich ist. Diese Verschiebung der  $\delta^{13}\text{C}$ -Werte für die Algenbiomasse im Epilimnion ist vergleichbar mit der Verschiebung (9‰), die auch bei den Biomarkern der grünen Schwefelbakterien aus der  $\text{H}_2\text{S}$ -haltigen photischen Zone im früheren Kiliran-See gemessen wurden.

Das Vorkommen von *B. braunii* im Kiliran See kann anhand der Biomarker-Analytik nachgewiesen werden. Die Verteilung der *n*-Alkane ist durch die ungewöhnlich hohe Menge des  $\text{C}_{27}$  *n*-Alkans relativ zu den anderen langkettigen *n*-Alkanen gekennzeichnet. Die Konzentrationen des  $\text{C}_{27}$  *n*-Alkans variieren im Bereich von 30,1 bis 393,7  $\mu\text{g/g}$  TOC, und zeigen in der Regel eine Korrelation mit der Häufigkeit von *B. braunii* Palynomorphen entlang des Profils. Die  $\delta^{13}\text{C}$ -Werte dieser Verbindung liegen bei etwa -31‰ und sind um etwa 2‰ angereichert im Vergleich zu den benachbarten langkettigen *n*-Alkanen.

Es ist bekannt, dass  $^{13}\text{C}$  in der Biomasse von *B. braunii* stark angereichert wird (z.B. Murray et al., 1994). *B. braunii* (Rasse A) kann deshalb als signifikante biologische Quelle für das  $\text{C}_{27}$  *n*-Alkan angesehen werden. Geringe Mengen von Lycopane sind in den Sedimentproben nachgewiesen worden (von 0 bis 54,7  $\mu\text{g/g}$  TOC). Der  $\delta^{13}\text{C}$ -Wert dieser Verbindung beträgt -17,2‰. Diese starke Anreicherung von  $^{13}\text{C}$  lässt vermuten, dass das Lycopan aus *B. braunii* (Rasse L) abstammt. Lycopan konnte nicht in allen Proben nachgewiesen werden und seine Verteilung entlang des Profils läßt keinen Trend erkennen. Die Daten lassen aber darauf schließen, dass Lycopan einen anderen biologischen Ursprung hat, als das  $\text{C}_{27}$  *n*-Alkan. Es ist anzunehmen, dass es für die beiden *B. braunii* Rassen zu zeitlich versetzten Blüten kam, die abhängig von Veränderungen der Wasserchemie waren.

Aufgrund des Vorhandenseins von  $^{13}\text{C}$ -abgereichertem DIC im Kiliran See, zeigen die  $\text{C}_{27}$  *n*-Alkane eine Abreicherung von 7-9‰ gegenüber den üblichen Werten für langkettige *n*-Alkane die aus *B. braunii* (Rasse A) in Torbaniten anderer paläogeographischer Gebiete extrahiert wurden. Obwohl Lycopane mit einem Wert von -17,2‰ stark an  $^{13}\text{C}$  angereichert zu sein scheint, ist dieser  $\delta^{13}\text{C}$ -Wert tatsächlich um ca. 7‰ im Vergleich zu denen der anderen spezifischen Biomarker von *B. braunii* (Botryococcane) abgereichert. Dies wurde schon vorher am Beispiel der Brown Shale Fm nachgewiesen. Die deutlichen Unterschiede der  $\delta^{13}\text{C}$ -Werte von  $\text{C}_{27}$  *n*-Alkan und Lycopan in den Kiliran-Sedimenten werden zum Teil auch darauf zurückzuführen, dass das  $\text{C}_{27}$  *n*-Alkan nicht ausschließlich von *B. braunii* (Rasse A) abstammt, sondern auch von anderen biologischen Quellen generiert wird.

4-Methylsteran-Homologe ( $\text{C}_{28}$ - $\text{C}_{30}$ ) und 4-Methyldiasteren-Homologe ( $\text{C}_{28}$ ,  $\text{C}_{30}$ ) gehören zu den dominanten Komponenten in den Extrakten der Kiliran-Sedimente. Die Konzentrationen dieser Verbindungen variieren von 40,3 bis 1.009,2  $\mu\text{g/g}$  TOC. Diese Verbindungen zeigen deutliche Konzentrationsunterschiede entlang des Ölschiefer-Profiles, mit erhöhten Konzentrationen im unteren und oberen Teile des Profils und niedrigeren Konzentrationen im mittleren Profilteil. Die Konzentrationsverteilung entlang des Profils verläuft weitgehend entgegengesetzt zu der Häufigkeitsverteilung von *B. braunii*. Anhand der palynologischen Daten konnten keine Anhaltspunkte für die biologischen Quellen der 4-Methylsterole gefunden werden. Allerdings wurden sie häufig als Biomarker von Süßwasser *dinoflagellaten* in limnischen Systemen betrachtet (z.B. Fu Jiamo et al., 1990). Die  $\delta^{13}\text{C}$ -Werte dieser Verbindungen deuten ebenfalls auf eine Herkunft aus Algen (ca. -37‰) hin. Calcium (Ca) ist das vorherrschende Element in den Ölschieferproben und sein Gehalt variiert von 5,0 bis

16,7%. Ca zeigt einen parallelen Verlauf zu den 4-Methylsteroiden entlang des Profils. Dies ist wahrscheinlich darauf zurückzuführen, dass diese Verbindungen aus biologischen Quellen stammen, die eher alkalische Umweltbedingungen bevorzugen. Im mittleren Teil des Profils, wo der Ca-Gehalt geringer ist, treten diese Verbindungen in geringeren Konzentrationen auf. Hier wurde offensichtlich die Blüte von *B. braunii* aufgrund der weniger basischen und geringer trophischen Umweltbedingungen gefördert.

Antagonistischen Beziehungen zwischen *Dinoflagellaten* und *B. braunii* sind auf der Basis der Analytik von Sedimenten aus früheren Seen berichtet worden (Lenz et al, 2007; Herrmann, 2010). Veränderungen in der Wasserchemie sind die Ursache dieser inversen Korrelation. Die ausgeprägten Wechsel zwischen der Häufigkeit von *B. braunii* und der Konzentration der 4-Methylsteroiden entlang des untersuchten Ölschieferprofils deutet darauf hin, dass die 4-Methylsteroiden auf Süßwasser *dinoflagellaten* zurückgehen. Voraussetzung für ihre Blüte war offenbar eine erhöhte Basizität des Wassers und die Verfügbarkeit von Nährstoffen.

## Contents

<b>Title page</b> .....	i
<b>Acknowledgement</b> .....	iii
<b>Abstract</b> .....	iv
<b>Zusammenfassung</b> .....	vi
<b>Contents</b> .....	xiii
<b>1. Introduction</b> .....	1
1.1. Oil production and consumption in Indonesia.....	2
1.2. General geology and resources of oil shales in Indonesia.....	4
1.3. Background and aims of the study.....	6
1.3.1. Background.....	6
1.3.2. Aims of the study.....	8
<b>2. Climatic and tectonic controls during development of the Late Eocene Kiliran lake, Central Sumatra Basin, Indonesia</b> .....	9
2.1. Abstract.....	9
2.2. Introduction.....	9
2.3. Geological setting of the study area.....	10
2.3.1. Central Sumatra Basin.....	10
2.3.2. Pematang Group development.....	11
2.3.3. Geology of the Kiliran Sub-basin.....	14
2.4. Sample material and methods.....	15
2.4.1. Sample material.....	15
2.4.2. Palynofacies analysis.....	15
2.4.3. Geochemical analysis.....	16
2.5. Results.....	16
2.5.1. Organic matter composition.....	16
2.5.1.1. Amorphous organic matter.....	16
2.5.1.2. Structured organic matter.....	17
2.5.2. Geochemical composition.....	19
2.6. Discussions.....	19
2.6.1. Variations of autochthonous and terrigenous contributions.....	19
2.6.2. Variation of salinity.....	20
2.6.3. Variation of trophic level.....	20
2.6.4. Variation of grain size.....	24
2.6.5. Redox sensitive elements.....	24
2.6.6. Development of the Kiliran lake.....	26
2.7. Conclusions.....	28
<b>3. Evidence of photic zone euxinia and chemocline dynamics during deposition of the Late Eocene Kiliran lake, Central Sumatra Basin, Indonesia</b> .....	29
3.1. Abstract.....	29
3.2. Introduction.....	30
3.3. Geological setting of the study area.....	31
3.3.1. Central Sumatra Basin.....	31
3.3.2. Geology of the Kiliran Sub-basin.....	31

3.4.	Sample material and methods.....	35
3.4.1.	Sample material.....	35
3.4.2.	Elemental analysis.....	35
3.4.3.	Biomarker analysis.....	35
3.4.4.	Compound-specific isotope analysis.....	36
3.5.	Results and discussions.....	37
3.5.1.	TOC and S.....	37
3.5.2.	Biomarkers.....	38
3.5.3.	Occurrence of isorenieratane.....	43
3.5.3.1.	Review of isorenieratane origin .....	43
3.5.3.2.	Isorenieratane in the Kiliran oil shale.....	45
3.5.3.2.1.	Green sulfur bacteria vs. terrigenous origin.....	45
3.5.3.2.2.	Factors controlling the occurrence of green sulfur bacteria.....	46
3.6.	Conclusions.....	49
<b>4.</b>	<b>Biomarker evidence for the occurrence of <i>Botryococcus braunii</i> races A and L in the Late Eocene Kiliran lake, Central Sumatra Basin, Indonesia</b>	<b>50</b>
4.1.	Abstract.....	50
4.2.	Introduction.....	50
4.3.	Geological setting of the study area.....	51
4.3.1.	Central Sumatra Basin.....	52
4.3.2.	Geology of the Kiliran Sub-basin.....	52
4.4.	Sample material and methods.....	55
4.4.1.	Sample material.....	55
4.4.2.	Palynological analysis.....	55
4.4.3.	Biomarker analysis.....	56
4.4.4.	Compound-specific isotope analysis.....	56
4.5.	Results.....	57
4.5.1.	Biomarkers.....	57
4.5.1.1.	<i>n</i> -Alkanes.....	57
4.5.1.2.	Acyclic isoprenoids.....	58
4.5.2.	Compound-specific carbon isotopic composition.....	58
4.6.	Discussions.....	62
4.6.1.	<i>n</i> -Alkanes.....	62
4.6.2.	Acyclic isoprenoids .....	64
4.6.2.1.	Pristane and phytane.....	64
4.6.2.2.	Lycopane.....	64
4.6.3.	Unusual C <sub>27</sub> <i>n</i> -alkane distribution.....	66
4.6.4.	Paleoenvironmental implications.....	66
4.6.4.1.	Lycopane distribution.....	66
4.6.4.2.	Carbon isotopic composition.....	67
4.7.	Conclusions.....	69
<b>5.</b>	<b>Paleoecological changes during deposition of the Late Eocene Kiliran oil shale, Central Sumatra Basin, Indonesia</b>	<b>71</b>
5.1.	Abstract.....	71
5.2.	Introduction.....	72
5.3.	Geological setting of the study area.....	72
5.3.1.	Central Sumatra Basin.....	73
5.3.2.	Geology of the Kiliran Sub-basin.....	73

5.4. Sample material and methods.....	76
5.4.1. Sample material.....	76
5.4.2. Elemental analysis.....	76
5.4.3. Palynological analysis.....	77
5.4.4. Biomarker analysis.....	77
5.4.5. Compound-specific isotope analysis.....	78
5.5. Results.....	78
5.5.1. Elemental and palynological data.....	78
5.5.2. Biomarkers.....	79
5.5.2.1. Hopanoids.....	82
5.5.2.2. Pristane and phytane.....	82
5.5.2.3. Steroids.....	83
5.5.2.4. Compound-specific carbon isotopic composition.....	84
5.6. Discussions.....	85
5.6.1. Hopanoids.....	85
5.6.2. Pristane and phytane.....	85
5.6.3. Steroids.....	87
5.6.4. Carbon isotopic composition in response to eutrophication of lake systems.....	88
5.6.5. Carbon isotopic composition and eutrophication in the Kiliran lake.....	89
5.6.6. Paleoecological changes.....	91
5.7. Conclusions.....	91
<b>6. Summary</b>	<b>93</b>
6.1. Paleoenvironmental changes and evolution of the former Kiliran lake.....	93
6.2. Paleoecological changes.....	94
6.3. Significance of particular biomarkers.....	96
<b>7. Suggestion for further studies</b>	<b>98</b>
7.1. Carbonate as possible indicator for paleoenvironment .....	98
7.2. Artificial maturation study.....	99
<b>References</b>	<b>100</b>
<b>Appendices</b>	<b>115</b>
<b>Curriculum Vitae</b>	<b>144</b>

## Chapter 1: Introduction

Oil shales are defined as organic-rich shales containing significant amounts of oil-prone kerogen and liberating crude oil upon heating (Peters et al., 2005a). Some authors regard oil shales not only shales but also marls and carbonates with varying proportions of clay minerals, quartz and feldspars (e.g. Tissot and Welte, 1984). Oil shales were deposited in a wide range of sedimentary environments, covering terrestrial, lacustrine and marine systems (Hutton, 1987; Cook and Sherwood, 1991) from Cambrian to Tertiary age (Dyini, 2006). Consequently, oil shales consist of a diverse composition of organic matter. With respect to the sedimentary environments, Hutton (1987) classified oil shales based on their composition of liptinite macerals. According to this classification, also cannel coals are regarded as homogeneous oil shales composed mainly of liptinite derived from terrestrial vascular plants. In lacustrine systems, torbanite and lamosite are oil shales with the maceral liptinite derived from *Botryococcus* and other lacustrine algae (e.g. *Pediastrum*), respectively. Marinite, tasmanite and kuckersite are oil shales composed of liptinite from marine algae, tasmanitids and *Gloeocapsomorpha prisca*, respectively.

Oil shales containing a sufficient amount of organic matter, typically more than 5% organic content (Tissot and Welte, 1984), can be benefited as alternative sources for fossil fuels. Unlike conventional oil, gas and coal, oil shales have to be treated first to gain the shale oil. Some methods have been developed to extract shale oil by retorting, either from conventionally blasted and excavated oil shales or from in situ oil shales (Brendow, 2003; Burnham and McConaghy, 2006). The beneficiation of oil shales was initiated in 1637 by the roasting of the Swedish Cambrian and Ordovician Alum Shale to get potassium aluminum sulphate used for fixing colours in textiles. In late 1800s, the Alum Shale was retorted for production of hydrocarbons (Dyini, 2006). Since then, oil shales have been exploited in many countries majorly in Scotland, Estonia, China, Russia, Germany and Brazil. The peak of world production was reached in 1979-1980 when more than 46 million tonnes of oil shale per year were mined. Two-third of the production was in Estonia. After that, the world shale oil production has been significantly declining due to the cheaper conventional oil production. In 2008, the world oil shale exploitation was about 930.000 tonnes (WEC, 2010).



Although, the shale oil production is still economically outcompeted by conventional oil production, the world resources of shale oil are large and increasing from time to time by exploration activities. At the end of 2008, the world shale oil in-situ resources were estimated to be about 4,786 billion barrels. For comparison, the world crude oil and natural gas liquids proven recoverable reserves at the same time are about 1,239 billion barrels (WEC, 2010). The amount of world shale oil resources is of interest considering that oil shales might be used as alternative fossil energy resources in the future, facing the continuous decline of world oil reserves and increase of general production costs for conventional oil.

### 1.1. Oil production and consumption in Indonesia

Indonesia has been active as significant player in oil industry since the first discovery of oil in North Sumatra in 1885. Indonesia holds proven oil reserves of 3.99 billion barrels at the end of 2009 (EIA, 2010). Oil production in Indonesia, including crude oil and natural gas liquids, accounted about 1.3% of the world oil production in 2009 (BP, 2010). At least 9 major oil companies have been producing in oil fields throughout Indonesia (Figure 1.1, Petrominer, 2010). Oil production has been supporting the Indonesian economy as the largest contributor to state revenue. However, the oil production has been declining in recent decades (Figure 1.2), which also significantly decreases the government revenue in the oil and gas sector from 40% in 1990 to 15% in 2009 (EIA, 2010; PWC, 2010).

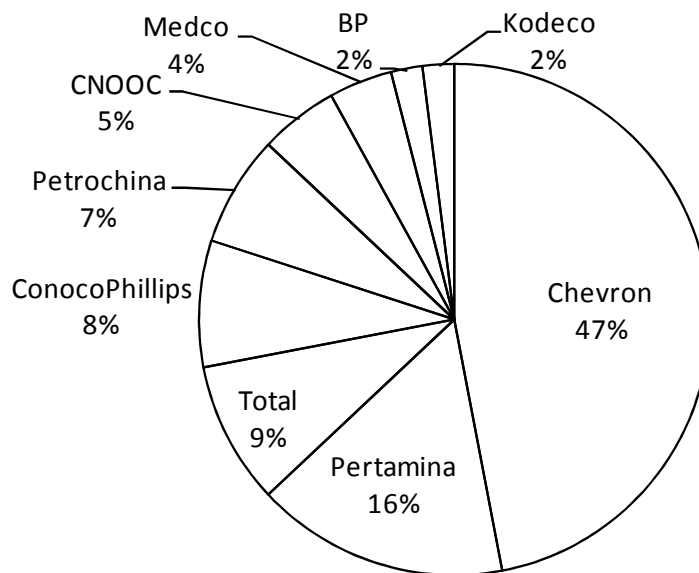


Figure 1.1. Indonesian major oil producers in 2009 (Petrominer, 2010).

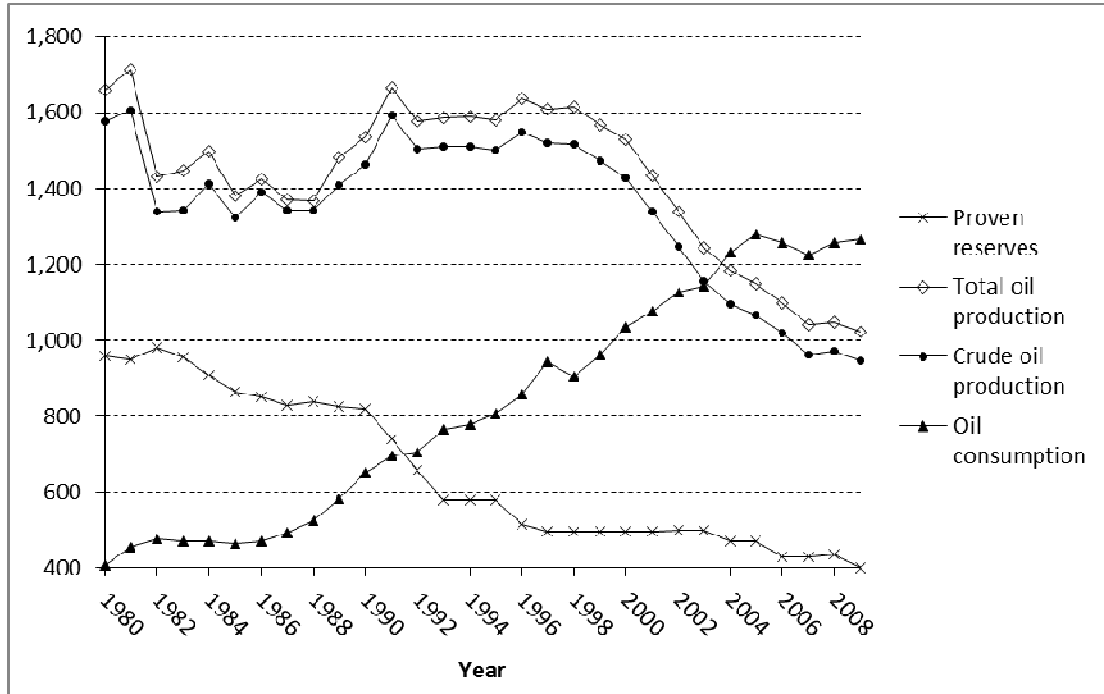


Figure 1.2. Indonesian oil statistics since the past 30 years (1980-2009) including proven reserves ( $\times 10^7$  barrels), total oil production ( $\times 10^3$  barrels/day), crude oil production ( $\times 10^3$  barrels/day) and oil consumption ( $\times 10^3$  barrels/day) (data source: EIA, 2010).

The oil production decrease is related to the production decline in giant and matured Minas and Duri oil fields, Central Sumatra Basin, operated by Chevron (EIA, 2010). On the other hand, oil consumption has been successively increasing since the past 30 years and surpassed the oil production in the end of 2004. Since then, Indonesia has been a net-oil importer country and withdrawn from the Organization of Petroleum Exporter Countries (OPEC) since 2008.

Policy has been made by the government to secure the domestic energy supply in the future. Energy diversification programs have been targeted, including the discovery of both non-conventional fossil and renewable energy sources (DJMIGAS, 2010). With respect to the non-conventional fossil resources, shale oil has been greatly expected to increase the oil production in Indonesia. Some drilling programs have been performed since the last decade to map the geological features relating to the occurrence of oil shales, explore and make inventory for its resources throughout the Indonesian basins. Several studies have also been performed assessing the possibility to utilize the oil shales (e.g. PSDG, 2006).

## 1.2. General geology and resources of oil shales in Indonesia

Numerous formations containing organic-rich sediments have been reported from different basins in Indonesia. Among Pre-Tertiary sediments, the Triassic Winto Formation (Fm) containing organic-rich shales has been found in Buton, Southeast Sulawesi (Tobing, 2005). Unlike this formation, organic-rich sediments deposited during Tertiary are well documented and more significant, and occur widespread throughout the Indonesian basins. The deposition of the Tertiary organic-rich sediments was initiated by the development of rift basins in Early Tertiary. Tectonostratigraphy divides the Tertiary sedimentation into the following stages: Early Synrift Lacustrine (Eocene-Oligocene), Late Synrift Transgressive Deltaic (Late Oligocene-Early Miocene), Early Postrift Marine (Early-Middle Miocene) and Late Postrift Regressive Deltaic (Middle Miocene-Pliocene) (Doust and Noble, 2008). Organic rich sediments deposited in these stages exhibit a wide range of depositional environments as described in the following.

Lacustrine organic rich sediments were mostly deposited in the Early Synrift stage. The organic matter consist mainly of algal type I/II kerogen which accumulated in deep to shallow and fresh to brackish water lakes. These sediments are present e.g. in Central Sumatra, West Natuna and Barito Basins. Paralic or deltaic organic rich sediments were typically developed during the Late Synrift and Late Postrift stages. The organic matter is generally composed of type II/III kerogen deposited in a variety of fluvial to estuarine lower coastal plain environments. These sediments are found e.g. in South Sumatra, East Natuna and NE Java Basins. Marine organic rich sediments were typically developed during the Early Postrift stage, consisting mainly type II kerogen. North Sumatra and Salawati Basins have been reported to generate these organic rich marine sediments (Doust and Noble, 2008; and references therein).

The organic matter in these sediments is mostly mature especially those which were deposited in deep grabens and basin centers during the Early Synrift stage. They were important as source rocks of differing petroleum systems in Indonesia (Doust and Noble, 2008). The sediments containing immature organic matter (oil shales) were typically deposited in relatively shallow environments and basin boundaries. The prospecting of oil shales which has been carried out by the government is focused on the geological features corresponding to these depositional environments.

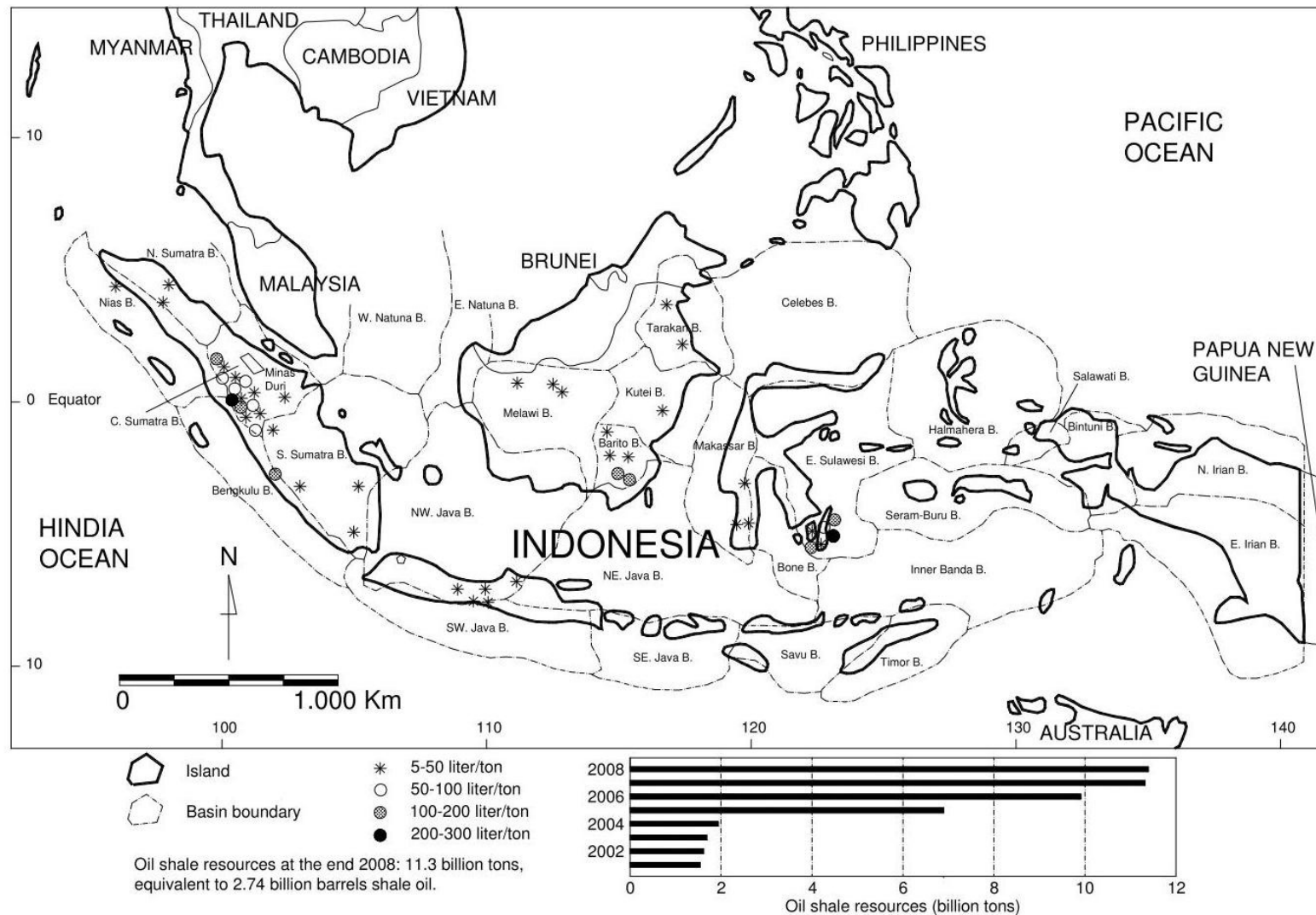


Figure 1.3. Distribution of oil shales occurrence in the Indonesian basins and the resources have been increasing since initial prospecting in 2001 (modified from DJMIGAS, 2010).

The distribution and resources of oil shales in Indonesia are summarized in Figure 1.3. Oil shales are discovered in most of the Indonesian basins, especially in the Central Sumatra Basin. The known oil shale resources were about 1,600 million tons in 2001 and successively increased in the following years until 11.3 billion tons in 2008. The oil yield varies from 5 to 300 liter oil per ton. The oil shale resources are equivalent to 2.74 billion barrels shale oil.

### 1.3. Background and aims of the study

#### 1.3.1. Background

The Central Sumatra Basin is the most prolific oil producing basin in Indonesia. Geological aspects relating to its Tertiary petroleum systems have been extensively studied (e.g. de Coster, 1974; Doust and Noble, 2008; and references therein). Brown Shale Fm has been known as the most responsible lacustrine source rocks for petroleum in the basin and has been intensively studied. The algal amorphous-rich source rocks were studied by means of palynology (Williams et al., 1985; Wain and Jackson, 1995; Carnell et al., 1998), petrography (Suwarna et al., 2001) and organic geochemistry (Williams et al., 1995; Williams and Eubank, 1995). However, the studies dealt only on spatial and spot samples throughout the Central Sumatra Basin. Comprehensive studies concerning the detailed stratigraphic succession of the Brown Shale Fm have so far never been undertaken. Additionally, most of the studies have been concentrated on the matured source rocks where petroleum systems were well developed in the basin. On the other hand, the immature source rocks or oil shales of Central Sumatra Basin have been less studied. Several authors, however, have started to pay attention to some oil shales occurrence in the basin: e.g. Williams et al., (1995), Wain and Jackson (1995) and Carnell et al. (1998).

Depositional environments of the Brown Shale Fm have previously been discussed by many authors. Both tectonic subsidence during rift development and tropical warm climates were thought to be the dominant controls of the organic matter accumulation in the formation (Williams et al., 1985; Katz, 1991; Wain and Jackson, 1995; Carnell et al., 1998). Cyclicity of the depositional environments has commonly been reported, but the reasons for the cyclicity remained unclear (Longley et al., 1990). Some authors attributed to tectonic subsidence and adjustment as the likely reasons (Wain and Jackson, 1995; Carnell et al., 1998). Williams and Eubank (1995) discussed that the occurrence of major lacustrine sequences in the Brown Shale

Fm was strongly controlled by structural evolution of the rift basin. They also suggested that climatic changes were also apparent during the sediment deposition, but their complete role was still poorly understood.

Many methods have been developed to study the depositional history of organic-rich sediments, involving both their inorganic and organic constituents. Elemental analysis has been used to reconstruct the depositional environments in many lake sediments and sedimentary rocks (e.g. Eusterhues et al., 2005). For organic matter composition, the developed classical methods are based on light microscopic analyses such as petrography and palynology. Regarding to the latter, palynofacies can be observed from the organic matter composition under a transmitted-light microscope. Palynofacies considers the total assemblages of organic matter including palynomorph, phytoclast and amorphous groups. Principal uses of palynofacies are varied including: determining the magnitude and location of autochthonous and terrigenous input, depositional polarity (onshore-offshore axes) and identifying the relative shallowing-deepening trends in stratigraphic sequences (Tyson, 1995).

Organic geochemical analysis is a further method to identify the organic matter constituents in both recent and ancient sediments. Biomarkers are the organic compounds preserved in sediments. They can be used to recognize the specific botanical input to organic matter in sediments (e.g. Koopmans et al., 1996b; Peters et al., 2005b). They have also been applied to reconstruct depositional environments of organic-rich sediments (Didyk et al., 1978; Huang and Meinschein, 1979; Moldowan et al., 1985; Peters et al., 2005b). Compound-specific isotope analysis of carbon (CSIA) has often been applied to assist the identification of source-specific biomarkers (Boreham et al., 1994; Dowling et al., 1995; Koopmans et al., 1996b; Summons et al., 2002). Additionally, the carbon isotopic composition of specific biomarker has been used to reconstruct the paleoenvironment of aquatic systems (van Breugel et al., 2005). Environmental changes during deposition of organic-rich sediments have also commonly been reconstructed using the carbon isotopic composition of bulk organic matter (Meyers and Ishiwatari, 1993; Hodell and Schelske, 1998).

### 1.3.2. Aims of the study

The general aims of this study are formulated in the following.

The lacustrine Kiliran oil shale (Brown Shale Fm) was deposited in the Kiliran Sub-basin, southeastern boundary of the Central Sumatra Basin. Forty two samples taken from a 102 m long core (represents 90 m of the formation) will be analyzed by means of palynofacies and organic geochemistry. Organic matter composition of the oil shale will be investigated to reconstruct depositional environments of the Kiliran oil shale in detail.

Developments of lakes are controlled by both tectonic subsidence creating accommodation space and climatic conditions driving sediment and water supply (e.g. Bohacs et al., 2000). In the present case, the role of both tectonic subsidence and climatic conditions during development of the former Kiliran lake will be reconstructed. This study is also aimed to assess the paleoenvironmental changes including trophic level and water salinity in a detailed stratigraphic succession during deposition of the formation.

Another aspect that will be investigated in the present study is the paleoecological condition during deposition of the oil shale. Water chemistry determines the organisms dwelling in lakes. Organisms which were present in the former Kiliran lake will be discussed with respect to water chemistry changes.

Further, organic geochemical studies will be applied to unravel the biological source of certain biomarkers. As the Brown Shale Fm is dominated by algal amorphous facies, organic geochemistry is expected to identify composition of the organic matter in more detail. To assist the biological source interpretation, compound-specific isotope analysis of carbon (CSIA) will be performed.

## **Chapter 2: Climatic and tectonic controls during development of the Late Eocene Kiliran lake, Central Sumatra Basin, Indonesia**

### **2.1. Abstract**

A 102 m long core section of the Late Eocene Kiliran oil shale has been studied by means of palynofacies and geochemistry to reconstruct the development of the former Kiliran lake. Climatic changes during deposition of the studied oil shale are interpreted from the abundance variation of fungal remains (0-3% of organic matter). Higher abundance of fungal remains in the middle part of the oil shale profile likely indicates relatively warmer climate during deposition. The warmer climate is regarded to be the cause of paleoenvironmental changes with respect to lake productivity and water salinity. Carbon isotopic compositions of bulk organic matter ( $\delta^{13}\text{C}$ ) range from -27.0 to -30.5‰. They are generally more depleted in the middle part of the profile indicating lower primary productivity of the lake during the deposition. *B. braunii* varies from 3 to 16% of organic matter and is generally more abundant in the middle part of the profile. This alga is consistent with the less trophic preference of this algal blooming. Water salinity inferred from the ratio of total organic matter to sulfur contents (TOC/S) exhibit slightly less saline environments during deposition of the middle part of the profile. The warmer climate is thought to induce thermocline establishment, limiting the reintroduction of recycled nutrients to epilimnion and thus reducing the lake productivity. The warmer climate would also decrease the lake water salinity. Tectonic is also thought to have influenced the development of the Kiliran lake. Tectonic subsidence is interpreted from periodic rapid changes to finer grain size along the oil shale profile, as indicated by the Zr/Rb ratios. The succession of the lake development is also discussed with respect to the interaction of climatic changes and periodic subsidence.

### **2.2. Introduction**

The development of lakes is strongly influenced by the interplay between subsidence rates, to create accommodation space, and sediment and water supply rates (Carroll and Bohacs, 1999). This interaction determines water level fluctuation during development of lakes and thus characterizes the associated depositional environment and organic matter facies (Carroll and



Bohacs, 1999; Bohacs et al., 2000). Relatively higher subsidence rates than sediment and water supply rates would lead to a lower water level of a lake and a higher proportion of autochthonous compared to terrigenous organic matter deposited in the sediments. On the other hand, when subsidence rates are lower than sediment and water supply rates, relatively higher lake water levels and higher terrigenous organic matter input into the sediments will be promoted.

The Late Eocene Kiliran oil shale is an immature organic-rich shale which was deposited in the Central Sumatra Basin. Sedimentological investigations of the oil shale revealed an overall shallowing upwards depositional environment as the result of higher sediment and water supply rates than subsidence rates (Carnell et al., 1998). However, the development of the former Kiliran lake has so far not been studied in detail.

The depositional environment and organic matter facies of the Kiliran oil shale are investigated in the present study. Palynofacies and geochemical analyses are carried out to characterize the organic matter and geochemical composition. The interaction between climatic and tectonic controls during the Kiliran lake development will be discussed.

### **2.3. Geological Setting of the Study Area**

Three main basins developed in Sumatra during the Early Tertiary: North, Central and South Sumatra Basins (NSB, CSB and SSB respectively) (Figure 2.1a). The Central and South Sumatra Basins have also been considered as one large basin with many troughs and grabens, as they show similar and related geological histories (de Coster, 1974). The area of the present study is located in the Kiliran Sub-basin, one of the source rock depocenters in the arbitrary boundary of the basins (Figure 2.1b). The Kiliran Sub-basin is referred as part of the Central Sumatra Basin, since they show analogous sediment successions (Wain and Jackson, 1995; Carnell et al., 1998).

#### **2.3.1. Central Sumatra Basin**

The geological setting and history of the Central Sumatra Basin have been described in detail by e.g. de Coster (1974), Williams et al. (1985) and Doust and Noble (2008). This basin is

situated in a tectonically active region as a result of the Indian-Australian plate subduction beneath the Eurasian plate. The basin development can be divided into four stages of tectonostratigraphic evolution which were responsible for petroleum system formation (Figure 2.2a): Early Synrift (Late Eocene to Oligocene), Late Synrift (Late Oligocene to Early Miocene), Early Postrift (Early to Middle Miocene) and Late Postrift (Middle Miocene to Quaternary) (Doust and Noble, 2008). Tectonic events, sedimentation rates, isostatic subsidence and eustatic sea level changes have been proposed as controlling factors for Tertiary sedimentation in the basin during these stages (de Coster, 1974).

The Early Synrift phase corresponds to the period of rift graben formation and maximum of subsidence. This rifting was triggered by an East-West extension during northward movement of both the Australian plate to the East and the Indian plate to the West. During this stage, the Pematang Group was deposited above the basement. The group consists of an association of alluvial, shallow to deep lacustrine and fluvio-deltaic facies represented by laminated shales, silts, sands with coals and conglomeratic intervals. The Brown Shale Formation (Fm) belongs to the Pematang Group and represents excellent petroleum source rocks in the basin. The Late Synrift phase corresponds to the period when subsidence rates waned. In this stage, sea level was starting to rise and influenced the deposition of the Sihapas Group. The Menggala Fm is still fluvial and overlain by shallow marine sandy (Bekasap Fm) and argillaceous (Bangko Fm) facies. The Menggala and Bekasap Fm represent excellent reservoirs, whereas the Bangko Fm is a regional seal. The Early Postrift phase corresponds to a period of tectonic quiescence. In this stage, marine transgression continued and then maximized forming distal marine facies of the Duri (delta front sands and shales) and Telisa (shales and silts) Fm. The Late Postrift phase corresponds to a period of inversion and folding. In this stage, the Petani and Minas Fm which consist of regressive deltaic and alluvial sediments were deposited during a major falling of sea levels (de Coster, 1974; Doust and Noble, 2008).

### 2.3.2. Pematang Group development

The tectonostratigraphy of the Pematang Group has been discussed by Williams et al. (1985). The Lower Red Beds Fm (Figure 2.2a) was deposited during pre-graben stage, when the basin was undergoing initial rifting (Early Eocene). It consists of grey, green and red mottled mudstones, siltstones, sandstones and minor conglomerates deposited in alluvial-lacustrine settings. Shallow lacustrine or marsh/bog environments existed in the deepest basinal areas.

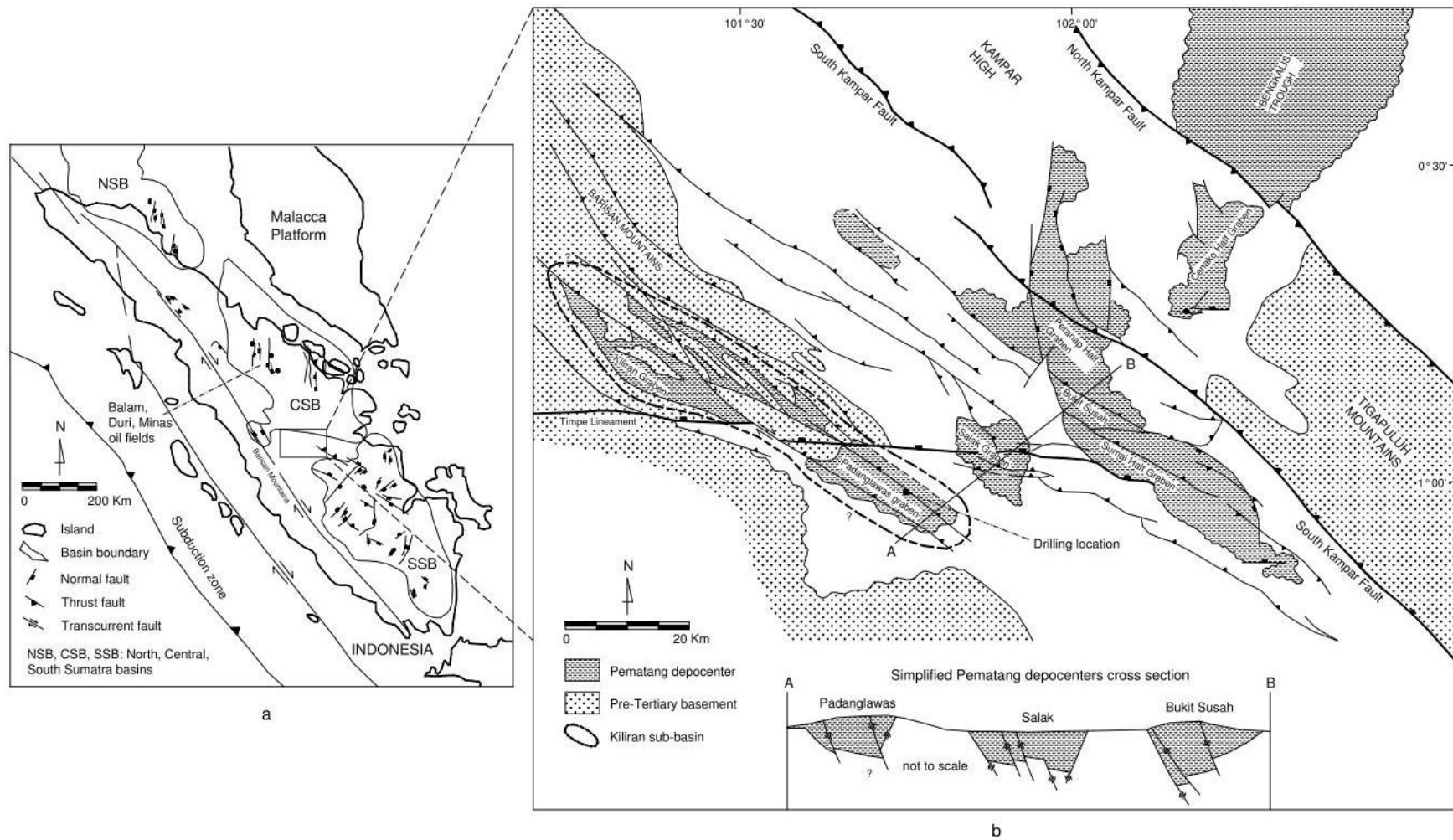


Figure 2.1. Map of Sumatra Basins with main graben structures (modified after Darman and Sidi, 2000) (a); Enlargement of the arbitrary boundary between Central and South Sumatra Basins containing Pematang depocenters, and the drilling location in Padanglawas graben (modified after Wain and Jackson, 1995 and PSDG, 2006) (b).

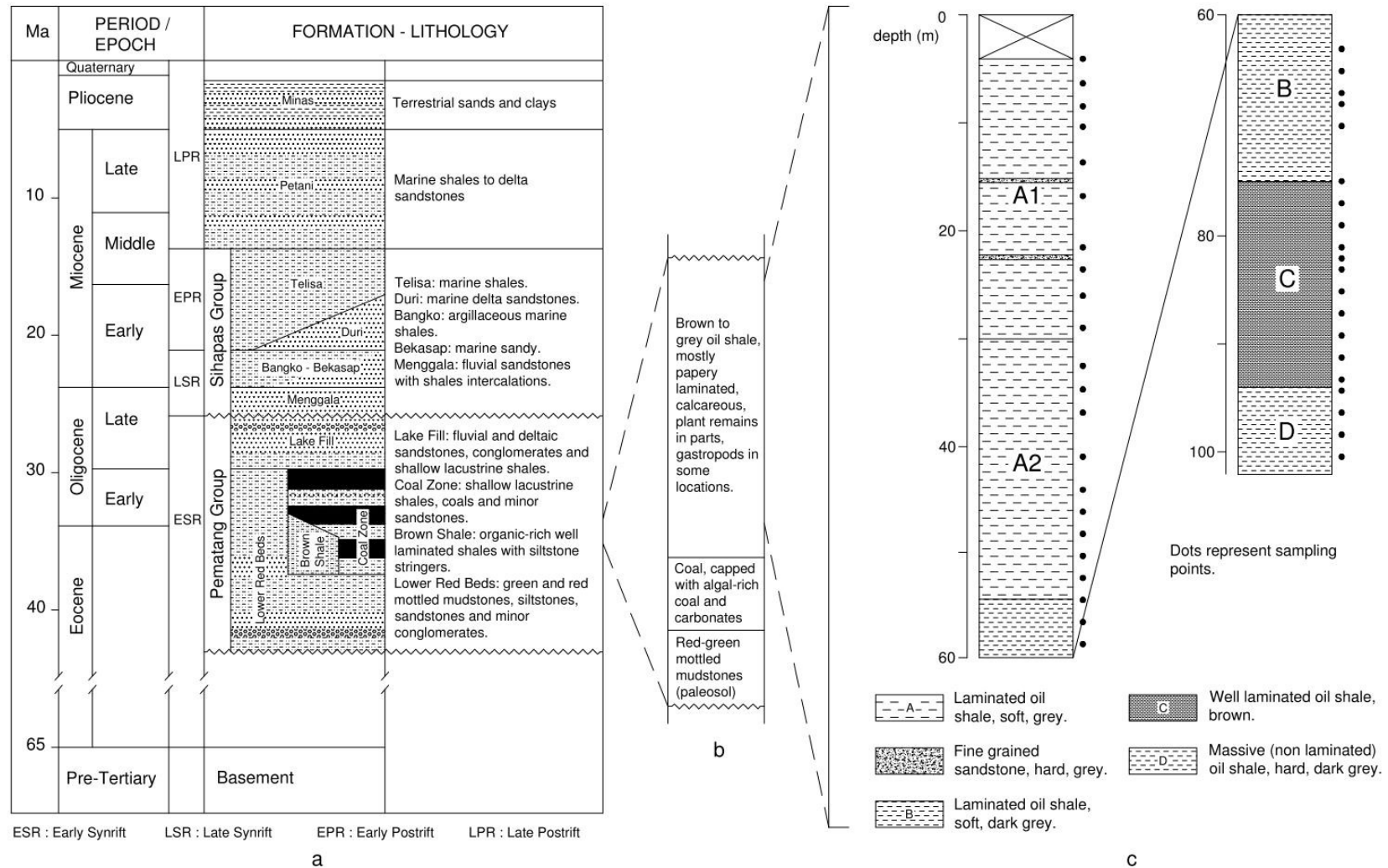


Figure 2.2. Generalized stratigraphic column of Central Sumatra Basin (adopted from Williams et al., 1985 and Doust and Noble, 2008) (a) and Kiliran Sub-basin (modified after Carnell et al., 1998 and PSDG, 2006) (b), and drill core profile of the oil shale in Padanglawas graben of Kiliran sub-basin (c).

The Brown Shale Fm either conformably overlies the Lower Red Beds Fm, or forms in some parts a lateral equivalent to the Lower Red Beds Fm. The formation is composed of organic-rich well laminated shales with siltstone stringers and deposition started during rapid rift development (Early Synrift) in deep and shallow lakes. Based on oxygen and carbon isotopic data, Williams et al. (1985) suggested that the Brown Shale Fm deposition ended with the Eocene-Oligocene global cooling. The Coal Zone Fm only occurs in a few sub-basins and consists of interbedded shallow lacustrine shales, coals and minor sandstones. This formation is laterally equivalent to the Brown Shale Fm and partly younger. In the Oligocene, a compressional phase led to uplift of the Lower Red Beds and Brown Shale Fm. During the Oligocene to Early Miocene rapid deposition of the Lake Fill Fm occurred and was characterized by uplift and rapid erosion of highland areas. It comprises fluvial and deltaic sandstones, conglomerates and shallow lacustrine shales. The deposition of this formation ended with a major unconformity.

### 2.3.3. Geology of the Kiliran Sub-basin

The Kiliran Sub-basin has been regarded as a small rift basin formed during the Early Synrift stage (Carnell et al., 1998). The morphology of the sub-basin is uncertain, since it has been integrated into the Barisan compressional belt and is now fragmented and faulted on both flanks. According to Wain and Jackson (1995), the Kiliran Sub-basin terminates abruptly against the Pre-Tertiary Timpe lineament (Figure 2.1b). Further geological mapping and drilling programs carried out by the Indonesian Center for Geological Resources (PSDG) in 2006 revealed the occurrence of a thick oil shale in Padanglawas graben, to the South of the Timpe fault. It is thought to be the extension of the Kiliran Sub-basin.

The general sediment succession of the Kiliran Sub-basin based on Carnell et al. (1998) and PSDG (2006) is presented in Figure 2.2b. The pre-graben paleosol most probably corresponds to the Lower Red Beds Fm. It is composed of carbonaceous and grey mudstones with locally red and green mottles. Above the paleosol, coal beds varying from thin to 17.5 m thick were deposited in a slowly subsiding reed swamp. A more rapid subsidence rate later resulted in the deposition of algal-rich coal interbeds which pass laterally into freshwater carbonates. A conformably lithofacies change occurred by the deposition of >90 m thick brown to grey colored calcareous shales. Assuming that the shale laminae were seasonal, Wain and Jackson

(1995) estimated a period of 240.000 years for the oil shale deposition in Kiliran graben. Sedimentological appraisal of well exposed shales in the northwestern tip of Kiliran graben suggests a shallow lake setting (10-50 m deep) which exhibit anoxic depositional environments. The presence of abundant gastropods and bioturbation in the uppermost part profile was interpreted to indicate intermittently oxic conditions of sediment deposition (Carnell et al., 1998). There is no exposure which corresponds to the Oligocene Lake Fill Fm and younger lithofacies in this area.

## **2.4. Sample Material and Methods**

### **2.4.1. Sample material**

Forty two samples were collected from a 102 m long drill core (representing about 90 m thick oil shale) available in the depository warehouse of the PSDG, Bandung, Indonesia. The sampling points are marked by dots in Figure 2.2c. The sample list is presented in Appendix 1. The core was drilled in Padanglawas graben of Kiliran sub-basin. Gastropods and bioturbation are not observed in the entire oil shale core. Plant remains are occasionally present in minor amount as woody organic detritus and leaves. The vertical section consists of fine-grained shales with the following variation of the physical characteristics:

- a. soft, grey and well-laminated shale in the upper part (section A), thin fine sandstone intervals are present in the upper part
- b. soft, dark grey and well-laminated shale (section B)
- c. soft, brown and well-laminated shale (section C)
- d. hard, dark grey and non-laminated shale in the lowermost part (section D).

Section A is further divided into A1 and A2 based on palynological and geochemical compositions (see below).

### **2.4.2. Palynofacies analysis**

Palynological processing was carried out at the Natural History Museum of London, UK. The samples were treated with HCl (37% aq.), and HF (40% aq.) in alternating steps to remove carbonates and silicates, respectively, and, after washing to neutrality, sieved with a 15

micrometer mesh sieve. Organic matter particles were counted at minimum 300 points using a transmitted-light microscope at a 400x magnification.

#### 2.4.3. Geochemical analysis

Oil shale rock samples were first crushed, pulverized and sieved to obtain particle size <63 micron. Major element (Al) and trace elements (Mo, U, Zr, Rb) were analyzed by Actlabs, Ancaster, Canada. A 0.25 g sample was totally digested at 260°C employing HF, HClO<sub>4</sub>, HNO<sub>3</sub> and HCl. The sample was then analyzed using a Perkin Elmer ELAN 9000 ICP-MS. Total organic carbon contents (TOC) and total sulfur (S) were analyzed using Euro EA (CAP 20) Elemental Analyzer. For TOC determination, pulverized samples were treated with diluted (10%) hydrochloric acid prior to the analysis to remove carbonates from the sample and then rinsed with distilled water until neutrality. The TOC values were then corrected to the original sample weight due to carbonate loss.

For analysis of carbon isotopic composition of bulk organic matter, the carbonate free samples were measured with an IsoPrime<sup>TM</sup> (GV Instruments, UK) continuous-flow isotope ratio mass spectrometer. Isotope ratios are given in  $\delta$ -notation,  $\delta = (R_s/R_{st} - 1) \times 1000$ , with  $R_s$  and  $R_{st}$  as isotope ratios of sample and the standards VPDB. Analytical precision was 0.08‰.

## 2.5. Results

### 2.5.1. Organic matter composition

#### 2.5.1.1. Amorphous organic matter

The palynofacies of the oil shale is dominated by amorphous organic matter (AOM), contributing about 76-96% of organic matter. The proportion between amorphous and structured organic matter is shown in Figure 2.3a. The detailed palynological data are presented in Appendix 2. The AOM is less abundant and decreases upwards in sections A2 and B, and is more abundant in the upper part of section A1 and section D. Higher amounts of AOM are observed in section C. Although the AOM is abundant, its structure generally can be recognized as fibrous and membraneous debris, likely supporting a lacustrine depositional environment. Batten (1983) suggested that palynofacies dominated by fibrous and/or

membranous debris commonly originate from *B. braunii*, *Pediastrum* or other non-marine algae.

### 2.5.1.2. Structured organic matter

The structured organic matter identified in the oil shale is composed of *B. braunii*, pollen, spores, phytoclasts and fungal palynomorphs. *B. braunii* accounts for the most dominant palynomorph and varies from 3 to 16% with an average value of 8% (Figure 2.3b). The proportion generally develops in opposite condition with that of AOM. The proportion of pollen ranges from ~0 to 6% averaging at 2% (Figure 2.3c) and shows moderately higher proportion in section D, lower in sections C and B, and generally increasing proportion upwards in section A. A relatively lower abundance of pollen is observed in the upper part of section A1. Bisaccate pollen are present only in a few samples with very low amount (<1%). Also, spores represent a minor component in the oil shale (<1%). Phytoclasts consist of cuticles and wood debris, varying from 0 to 3% (average 1%, not shown). Fungi are present in most samples as fruiting bodies, hyphae and spores. The proportion of fungal remains ranges from 0 to 3% with an average value of 1% (Figure 2.3d). It shows moderately higher abundances in section B and higher abundances in section A2.

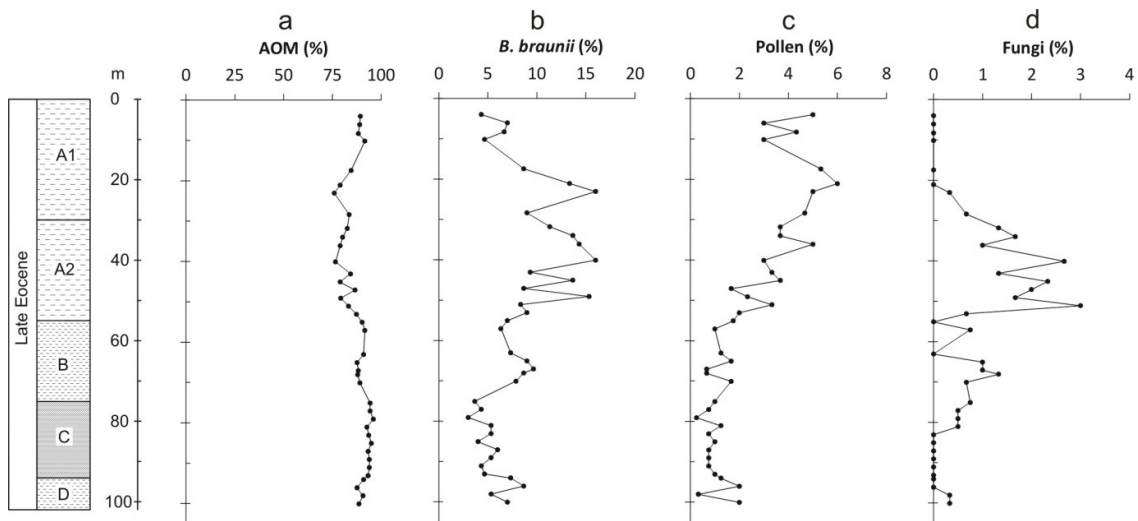


Figure 2.3. Vertical profile of the oil shale organic matter components along the profile: AOM (a), *B. braunii* (b), pollen (c) and fungal remains (d). The detailed palynological data are presented in Appendix 2.



*B. braunii* is a green colonial alga widely dispersed in temperate and tropical regions, and tolerant to seasonally cold climates. It lives in freshwater and brackish lakes, ponds and bogs (Metzger and Largeau, 2005; and references therein). *B. braunii* represents the only autochthonous organism which could be recognized as structured organic matter in the oil shale. Pollen originate mostly from angiosperm higher plants. Fungi are mostly soil organisms which degrade dead plants or fungi itself. The higher plants and fungal palynomorphs represent terrigenous organic matter input in the oil shale. The generally upwards increase of pollen along the profile especially in section A may correspond to the general shallowing upwards depositional environment of oil shale in Kiliran graben interpreted by Carnell et al. (1998).

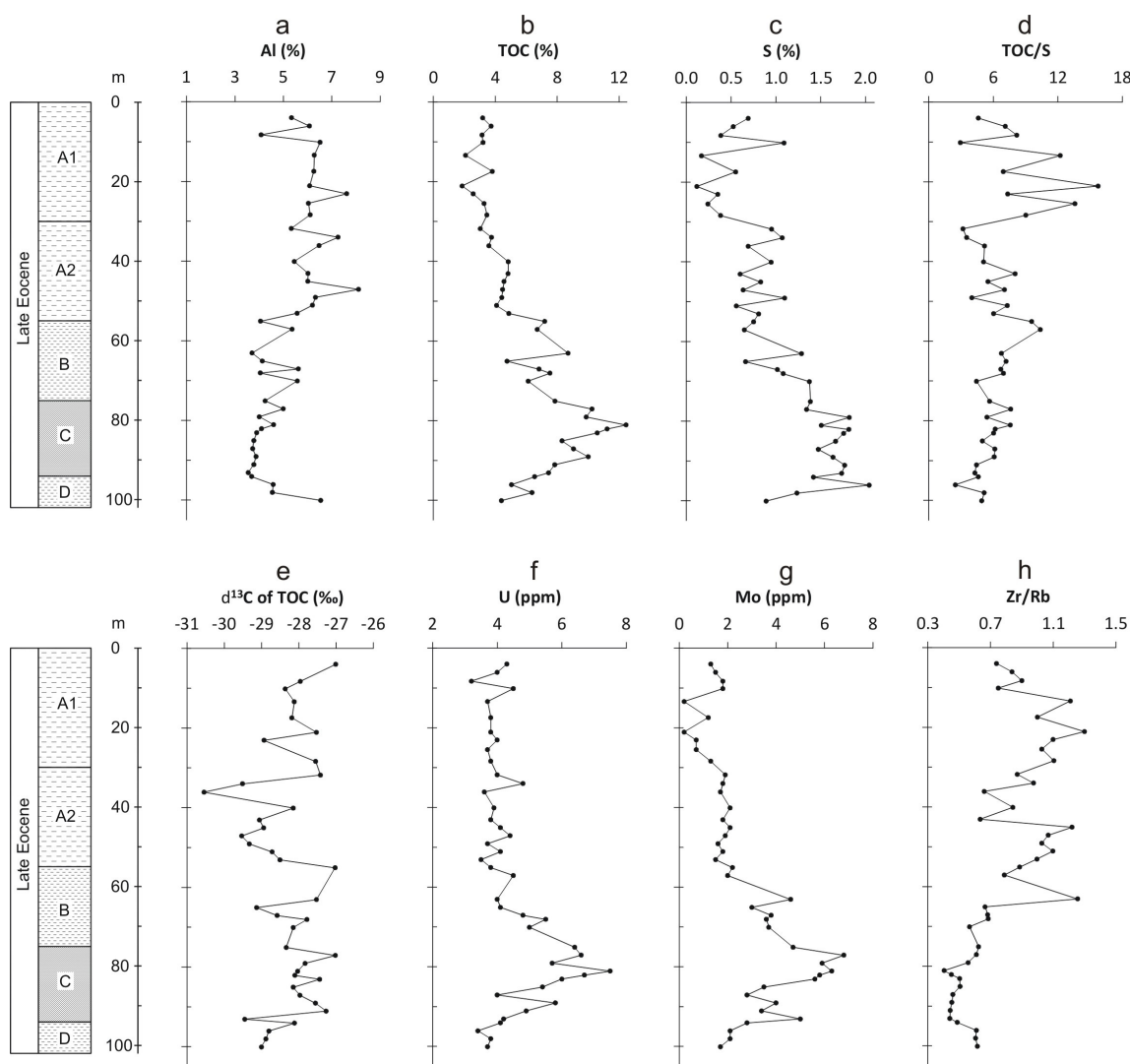


Figure 2.4. Vertical variation of geochemical parameters along the profile: Al (a), TOC (b), S (c), TOC/S (d),  $\delta^{13}\text{C}$  of bulk organic matter (e), U (f), Mo (g) and Zr/Rb (h). The detailed geochemical data are presented in Appendix 3.

### 2.5.2. Geochemical composition

Geochemical data are shown in Figure 2.4, including abundances of Al, TOC, S, U and Mo, ratios of TOC/S and Zr/Rb and carbon isotopic composition of bulk organic matter ( $\delta^{13}\text{C}$ ). The detailed geochemical data are presented in Appendix 3. Vertical variations of the major element Al and the trace elements U and Mo exhibit two distinct patterns. Concentrations of Al generally increase upwards in the profile ranging from 3.6 to 8.1% (average 5.2%). The Al concentrations are moderately higher in section D, lower in section C and increase subsequently in two steps at the beginning of deposition of sections B and A (Figure 2.4a). TOC varies from 1.9 to 12.5% (average 5.9%) and generally decrease upwards (Figure 2.4b). S percentages range from 0.1 to 2.0% averaging at 1.0% (Figure 2.4c) with a comparable variation along the profile as observed for the TOC proportion. In the lower part of section A1, S shows relatively lower concentrations. The TOC/S ratio is determined to reveal changes in the salinity condition and ranges from 2.5 to 15.8 (Figure 2.4d). The  $\delta^{13}\text{C}$  values of bulk organic matter vary along the profile, ranging from -27.0 to -30.5‰ with an average value of -28.3‰ (Figure 2.4e). The concentrations of U and Mo vary from 3.2 to 7.5 ppm (average 4.5 ppm) and from 0.2 to 6.8 ppm (average 2.7 ppm), respectively (Figure 2.4f,g). The vertical concentration variations of U and Mo are also similar with those of TOC and S percentages along the profile.

## 2.6. Discussions

### 2.6.1. Variations of autochthonous and terrigenous contributions

The higher concentrations of Al in section A indicate that in this part the terrigenous input is higher than in the other parts. Al is well known to predominate in detrital material. Their presence in sediments has been regarded as terrigenous proxy considering their immobility during diagenesis (e.g. Tribovillard et al., 2006; Dypvik and Harris, 2001). In section A pollen also show higher abundances and increase upwards successively, while in the lower sections pollen are generally less abundant, generally consistent with the Al concentration trend along the profile.

On the other hand, the higher concentrations of TOC, S, U and Mo in the lower part of the profile especially in section C suggest a higher autochthonous input compared to the upper part. The co-occurrence of these elements usually indicates sedimentation of autochthonous material due to the presence of anoxic bottom water in both marine and lacustrine environments (e.g. Tribovillard et al., 2006; Eusterhues et al., 2005). In the presence of organic matter, anoxic conditions also promote reduction of sulfate into hydrogen sulfide which can react with reduced iron to form pyrite either in the bottom water or below the sediment-water interface (e.g. Berner, 1984). U and Mo are mobile in oxygenic water and immobile or precipitated in anoxygenic water (Eusterhues et al., 2005; Tribovillard et al., 2006). In addition, the presence of organic matter also accelerates the precipitation and accumulation of these trace elements in the sediment (McManus et al., 2006; Tribovillard et al., 2006) resulting in the co-variation of them.

#### 2.6.2. Variation of salinity

Berner and Raiswell (1984) proposed the TOC/S ratio as a salinity indicator for organic-rich shales. The ratio boundaries of 2.8 ( $\pm 1.5$ ) and 10 were suggested to distinguish marine-brackish and brackish-freshwater environments of sediment deposition. They also noted that these boundaries are applicable to infer brackish depositional environments where the salinity is lower than half of normal marine salinity. The proportion of TOC relative to S in the oil shale samples confirms largely the presence of brackish (low salinity) depositional environments (Figure 2.5) except in the lower part of section A1 (Figure 2.4d) which was deposited generally under freshwater conditions.

#### 2.6.3. Variation of trophic level

The occurrence of *B. braunii* has been widely reported in less trophic environments, commonly oligotrophic-mesotrophic (e.g. Tyson, 1995) and the increase of the trophic level in aquatic environments promotes the demise of *B. braunii* (Tyson et al., 1995; Smittenberg et al., 2005; Xu et al., 2009). The disappearance of *B. braunii* in response to eutrophication has been related to the slow growth rate characteristic of this alga. With increasing availability of nutrients, *B. braunii* is outcompeted by faster-growing algae such as *Pediastrum* (Tyson, 1995), diatoms (Smittenberg et al., 2005) and freshwater *Dinoflagellates* (Herrmann, 2010). Considering its trophic level dependence, variation of the abundance of *B. braunii* might

therefore be used as a paleoenvironmental indicator for trophic level change, both anthropogenically or naturally-induced (Smittenberg et al., 2005).

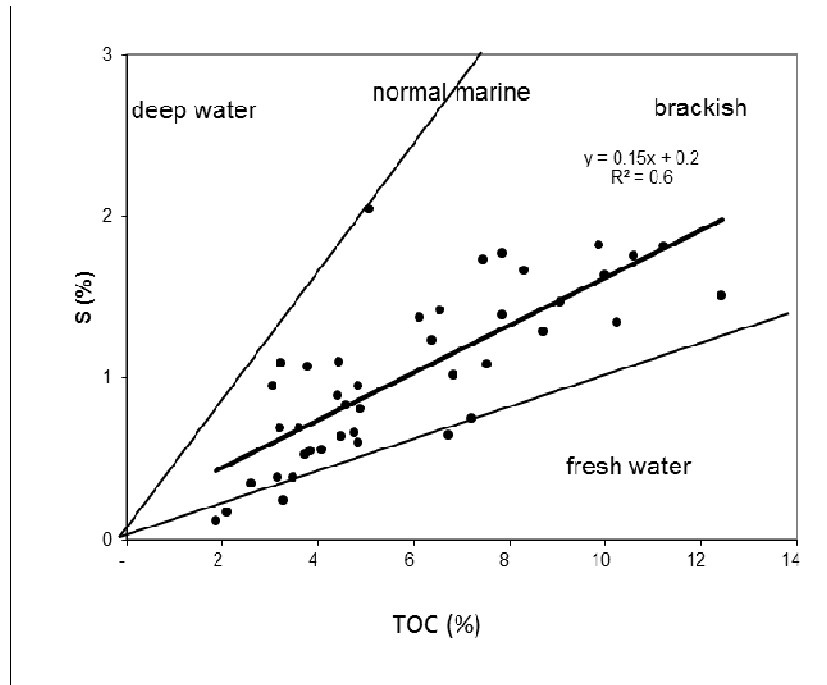


Figure 2.5. Plot of TOC vs. S indicating brackish (low salinity) to freshwater environments during deposition of the Kiliran oil shale. The salinity boundaries refer to Berner and Raiswell (1984).

*B. braunii*, together with *Pediastrum* and *Dinoflagellates*, represent the main biological source material for petroleum generation in lacustrine basins throughout Southeast Asia especially in Central Sumatra Basin (e.g. Wain and Jackson, 1995; Sladen, 1997). Additionally, Cole and Crittenden (1997) and Williams and Eubank (1995) reported that Paleogene oil source rocks of Central Sumatra depocenters are characterized either by *Pediastrum*-dominated organic matter in sediments originating from shallower lake environments or by *B. braunii*-dominated sediments originating from deeper lake environments. This particular observation was also reported from the oil shale deposited in northwestern tip of Kiliran graben (Carnell et al., 1998). During deposition of the upper part of this oil shale profile, *B. braunii* is largely replaced upwards by *Pediastrum*, which has been attributed to changes in water chemistry (Carnell et al., 1998), most likely corresponding to concentration increase of nutrients.

In the studied oil shale section deposited in Padanglawas graben, the variation of *B. braunii* abundance (Figure 2.3b) likely reflects trophic level changes during development of the former Kiliran lake. However, other algae which might take advantage from the trophic level change

based on their ecological preferences could not be observed in palynological analysis since most phytoplankton is likely incorporated into the AOM. However, the variation of  $\delta^{13}\text{C}$  along the oil shale profile is in agreement with that of the abundance variation of *B. braunii* with respect to the lake eutrophication development. Carbon isotopic composition of sedimentary organic matter have been widely regarded as indicator for lakes primary productivity (e.g. Meyers and Ishiwatari, 1993; Hodell and Schelske, 1998; O'reilly et al., 2003). In lakes where primary productivity is the main control on carbon cycling, organic matter would be progressively enriched in  $^{13}\text{C}$  with increasing productivity and inversely depleted in  $^{13}\text{C}$  with decreasing productivity. In the oil shale profile, the abundance of *B. braunii* (Figure 2.3b) tends to develop in opposite with the enrichment of  $\delta^{13}\text{C}$  values of the organic matter (Figure 2.4e). This confirms that lake trophic levels fluctuated during deposition of the oil shale and the abundances of *B. braunii* can be used to infer trophic level changes. A sudden decrease of  $\delta^{13}\text{C}$  values of bulk organic matter and a rapid increase of *B. braunii* abundance are distinctly observed at the beginning of deposition of section A2, indicating a decrease of trophic level. This sudden decrease cannot be attributed to the input of terrestrial organic matter which contributes to the oil shale in only small amounts.

Nutrients, particularly nitrates and phosphates, are the limiting factors for growing of lake aquatic plants (e.g. Seip, 1994). Nitrogen fixation occurs mainly due to soil microbes and the fixed nitrogen can be transferred into the lake by soil erosion in the surrounding land. Phosphates in the lake originate predominantly from weathering of continental rocks (e.g. Peters et al., 2005a). These external nutrients are therefore important to develop eutrophication of lakes. However, external nutrients are only relevant in the initial stage of lacustrine systems to develop the nutrient pool (Katz, 2001). In most ancient lacustrine systems responsible for organic-rich sediment deposition, long term availability of nutrients in epilimnion appears to be more maintained by remineralization (decomposition) of organic matter in anoxic hypolimnion and water overturn. Once liberated, the nutrients are reintroduced into the epilimnion through partial or complete water overturn, which can either be continuous or seasonal (see e.g. Lewis, 1987; Katz, 2001).

Bacterial processes, such as denitrification, control nutrients regeneration and mediate sulfate reduction and methanogenesis in the anoxic hypolimnion (Katz, 2001). In the former Kiliran lake, the availability of nutrients in the epilimnion was likely depending on the remineralization of organic matter rather than on the additional input of external nutrients. The

presence of anoxic bottom water during deposition of the entire oil shale section enabled regeneration of nutrients and thus methanogenesis. The latter is evident by the abundance of biomarkers from methanotrophic bacteria in all studied samples (unpublished data). The rapid decrease of the trophic level in the bottom part of section A2, therefore, should be related to a limitation of nutrient supply from the hypolimnion.

O'Reilly et al. (2003) reported the successive decreases of aquatic productivity and  $\delta^{13}\text{C}$  of sedimentary organic matter since mid of 1900s in tropical Tanganyika lake, Africa. They concluded that the productivity decrease is the effect of the present global warming. The surface temperature increase of about  $0.5^\circ\text{C}$  is decreasing aquatic productivity by about 20%. The increase of surface temperature is suggested to induce the thermal stratification establishment and oxycline shoaling of the lake, and thus limiting the nutrients supply from remineralization in the anoxic hypolimnion.

Increase of surface temperature is likely one of the possibilities controlling the marked decrease of trophic level in the former Kiliran lake especially at the beginning of deposition of section A2. Supporting data corresponding to the increase of surface temperature are provided by the variation of fungal remains along the profile (Figure 2.3d). The proportion of fungal remains develops differently from the terrigenous proxies e.g. pollen and Al abundances along the profile. The abundance of fungal remains generally changes concomitant with the abundance of *B. braunii*. Changes on diversity and relative abundance of fungal remains can reflect changes of paleoclimate during deposition of Tertiary and Quaternary sediments (Staplin et al., 1976; Elsik, 1996). The fungal remains are most diverse and abundant in sediments of the cyclic warm periods (Elsik, 1996). Additionally, the abundances of fungal remains in Neogene sediments have also been regarded to correspond with warm and humid climates during deposition (e.g. Kumar, 1990; Kalgutkar, 1997; Kar et al., 2010). The variation of fungal remains in the oil shale profile might indicate relative changes of temperature or humidity during the oil shale deposition. The increasing abundance of fungal remains in the sediments reflect more humid climate and vice versa. Additionally, under the more humid climate during deposition of sections A2 and B (Figure 2.3d), thermal stratification might have developed, limiting the remineralized nutrients input to epilimnion and thus supporting the disappearing of faster-growing algae and allowing *B. braunii* to grow.

#### 2.6.4. Variation of grain size

Zr/Rb ratios are determined to recognize relative grain size variations in the profile. In siliciclastic sediments, Zr is usually enriched in heavy minerals and associated with the relatively coarse-grained fraction, while Rb is commonly associated with the relatively fine-grained fraction and shows a positive correlation with illite and Al<sub>2</sub>O<sub>3</sub> (Dypvik and Harris, 2001). The grain size variation could not be easily recognized from the visible appearance of the studied oil shale, but the variation can be derived from the Zr/Rb ratios (Figure 2.4h). The grain sizes are relatively low in samples from the lower part and generally increase upwards with sudden decreases occurring at around 12, 45 and 96 m profile-depths.

#### 2.6.5. Redox sensitive elements

Redox sensitive elements including U and Mo have been widely used for reconstruction of bottom water redox conditions of marine systems (e.g. Tribovillard et al., 2006, and references therein). In lake system, Eusterhues et al. (2005) assessed the utility of the redox sensitive elements and found that most trace element-based redox indices failed to infer anoxicity of bottom water in Steisslingen lake (Germany). This was suggested to be due to the strong variability of the detrital input to this lake. However, they reported parallel tendency of the variation of U and Mo concentrations in sediments as a result of changes in bottom water anoxicity. These elements are relatively more abundant in sediments deposited under anoxic (sulfidic) depositional environments and are less abundant in sediments from less anoxic (non-sulfidic) environments.

In the present case, U and Mo concentrations show a remarkable variation along the profile (Figure 2.4f,g). The sharp concentration decrease of these elements from section B to A2 may lead to an interpretation of bottom water anoxicity decrease. However, the decrease of the trophic level at the beginning of deposition of section A2 requires stronger thermal stratification in the epilimnion and thus shoaling of the chemocline separating the anoxic hypolimnion from the oxic epilimnion. This implicates that U and Mo concentrations should not be used to infer anoxicity change during the deposition of these sections. It seems that the decrease of these elements concentrations rather relates to the lower primary productivity due to warmer climate. Lower amounts of organic matter sinking to hypolimnion would decrease acceleration of U and Mo precipitation. On the other hand, low productivity would also

relatively increase the fraction of detrital/terrigenous material in the sediments resulting in the dilution of organic matter especially in section A2 (Figure 2.4b). Additionally, higher precipitation during warmer climate also would increase water supply and detrital flux to the lake. But the lake might have been deep enough and thermal stratification might have been sufficiently strong to prevent water body mixing. In the present study higher concentrations of U and Mo coincide with higher concentrations of organic matter (Figure 2.4 b,f,g), and therefore reflect the input of autochthonous material into the sediment.

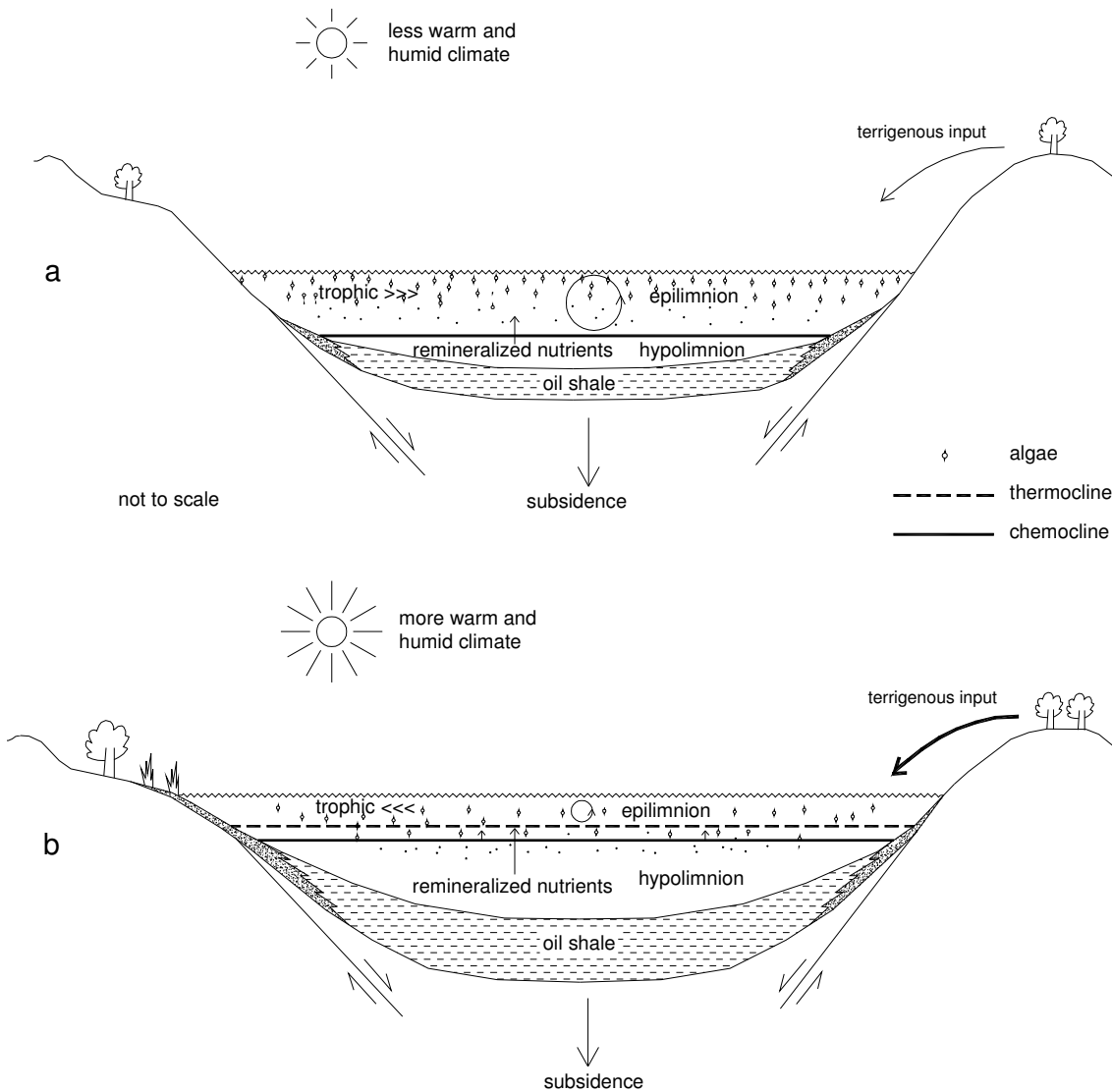


Figure 2.6. Reconstructed aquatic systems and trophic levels during deposition of section C (a) and lower part of section A2 (b). The presence of thermocline in (b) would limit the reintroduction of remineralized nutrients to epilimnion and thus decrease the primary productivity of the lake.



#### 2.6.6. Development of the Kiliran lake

Tectonic subsidence has been widely reported as the control for accommodation creation of the Paleogene lacustrine basins in Sumatra responsible for deposition of organic-rich source rocks (Williams et al., 1985; Williams and Eubank, 1995). Climatic variations have so far not been discussed as a controlling factor for changes in the composition of the sediments. In the Kiliran graben, a periodic subsidence has been thought to govern the lacustrine lithofacies sequences (Wain and Jackson, 1995). From the current study, rapid deepening due to periodic subsidence of the basin represented by the profile sections at profile-depths 96, 45 and 12 m might be interpreted from the profile of the Zr/Rb ratio (Figure 2.4h). Rapid decrease of the ratio reflects rapid change to finer grain size of the oil shale and thus also rapid change to deeper depositional environments. Although the grain size variation along the oil shale profile might also be influenced by climatic conditions, effects of climatic changes in trophic level or water salinity do not coincide with the rapid changes to the finer grain size especially at the profile-depth 45 m.

A climatic variation is also proposed to contribute to the lacustrine sequences. Remarkable climatic signals are recognized especially from the environmental change during deposition of the bottom part of section A2. Tectonic control is ruled out for this change. Periodic tectonic uplift during deposition of Kiliran oil shale is unlikely (Wain and Jackson, 1995), and can, therefore, not be used as a possible explanation for the negative excursion of  $\delta^{13}\text{C}$  values in this part. With respect to the chemical composition and palynofacies of the studied oil shale section, the interplay of subsidence and sedimentation and water supply rates during deposition of the Kiliran oil shale in Padanglawas graben can be reconstructed as follows.

The bottom part of the studied profile (section D) consists of non-laminated oil shale. A relatively low productivity in the lake is indicated by slightly higher abundances of *B. braunii* (Figure 2.3b) and lower  $\delta^{13}\text{C}$  values of the organic matter (Figure 2.4e). This section represents part of the transition facies from coal to laminated oil shale facies as a result of the increase of subsidence rates in the Padanglawas graben.

Above the transition facies, section C is composed of brown and well laminated oil shale. This section represents a lake development where subsidence rates were relatively higher than

sediment and water supply. It might have been initially deposited during relatively rapid subsidence of the basin as characterized by the sudden decrease of the grain size. The complete disappearance of fungal remains might indicate a colder period, allowing the supply of recycled nutrients to the epilimnion due to weaker or absence of thermal stratification (Figure 2.6a). Higher productivity prevailed as shown by the lower abundances of *B. braunii* (Figure 2.3b) and heavier  $\delta^{13}\text{C}$  values of organic matter (Figure 2.4e). A higher autochthonous fraction in section C is indicated by the higher concentrations of TOC, S, U and Mo (Figure 2.4) and the low abundance of pollen (Figure 2.3c). Terrigenous input was lower, due to lower sediment and water supply.

Sections B and A consist of dark grey and grey laminated oil shale, respectively. Sections B and A2 represent a lake development where sediment and water supply were relatively higher compared to section C. Two distinct increases of Al at the bottom part of the sections B and A (Figure 2.4a) coincide with the remarkable increases abundances of fungal remains (Figure 2.3d). This may indicate that warming of surface temperature was responsible for the change of the depositional environment of sections B and A2. Warmer climate would promote stronger thermocline, limiting recycled nutrients supply to epilimnion and thus decreasing productivity (Figure 2.6b). Lower proportions of the autochthonous fraction relative to the terrigenous fraction is indicated by the decreases of TOC, S, U and Mo (Figure 2.4) and the increases of Al (Figure 2.4a) and pollen (Figure 2.3c). The bottom water salinity during deposition of this part tends to be low (Figure 2.4d), most probably due to the higher water level and shoaling of the chemocline. At the profile section around 45 m, a sudden deepening of the lake apparently related to periodic subsidence is indicated by the decrease of the Zr/Rb ratio (Figure 2.4h).

Overall in section A, the fungal remains generally decrease upwards and finally disappear completely in section A1 (Figure 2.3d), indicating cooling of the climate. Salinity shows also an upwards increase in section A2 as reflected by decreasing TOC/S ratios (Figure 2.4.d). Further upwards in the sedimentary profile, in the lower part of section A1, relatively freshwater environments developed as indicated by the high TOC/S ratios. Pollen reached their maximum in abundance. This part of the oil shale (A1) most likely relates to the shallowest lake water column and intermittently oxic depositional environment, as indicated by the presence of fine sandstone intervals (Figure 2.2c). The lake might also be smaller. The shallow environments were due to both lower water level and the thick sediments previously deposited.

This lower part of section A1 most likely correlated to the presence of abundant gastropods observed in the uppermost part of oil shale in the northwestern tip of the Kiliran graben reported by Carnell et al. (1998). Subsequently, periodic subsidence probably occurred during deposition of the upper part of section A1 above depth 12 m (Figure 2.4h), resulting in increasing salinity by the less or absence of oxic intervals due to deeper environments.

## 2.7. Conclusions

Palynological and geochemical data show paleoenvironmental changes in the Late Eocene Kiliran lake as the result of the interplay between tectonic subsidence and climatic variation during the lake development. Events of lake deepening due to periodic subsidence are likely recognized from the rapid changes to finer grain size as indicated by Zr/Rb ratios. The higher abundance of fungal remains in the middle part of the profile (sections B and A2) probably indicate relatively warmer climate during deposition. The warmer climate might promote thermocline establishment of the lake and thus limiting the supply of nutrients from hypolimnion. This would decrease the lake productivity in the epilimnion. The decrease of productivity is recognized by the higher abundance of *B. braunii* and relatively lower value of  $\delta^{13}\text{C}$  especially in oil shale samples from the bottom part of section A2. The warmer climate was likely also the cause for the slight decrease of the water salinity during deposition of this part.

During deposition of the lower part of the profile (sections C and D), higher subsidence rates relative to sediment and water supply rates likely occurred, leading to the higher autochthonous input to the oil shale. During deposition of sections B and A2, the rates of sediment and water input might have been increased, promoting the higher terrigenous input to the oil shale. The shallowest depositional environments were occurred during deposition of lower part of section A1 where terrigenous input was high.

## **Chapter 3: Evidence of photic zone euxinia and chemocline dynamics during deposition of the Late Eocene Kiliran lake, Central Sumatra Basin, Indonesia**

### **3.1. Abstract**

Geochemical studies have been carried out to reconstruct the depositional environment of the former Kiliran lake with respect to chemocline dynamics. Organic geochemical analysis revealed the occurrence of isorenieratane in all 42 studied samples from a 102 m long core of the oil shale. Aryl isoprenoids (C<sub>13</sub>-C<sub>15</sub>) are also recognized in almost all samples and regarded as isorenieratane cleavage products. The carbon isotopic composition ( $\delta^{13}\text{C}$ ) of isorenieratane obtained from compound-specific isotope analysis for carbon (CSIA) is -24.0‰. Other carotenoid derivatives most likely derived from algae are also present sporadically only in a few samples. The  $\delta^{13}\text{C}$  of these compounds are about -35.0‰. The relatively stronger enrichment of isorenieratane in <sup>13</sup>C relative to the  $\delta^{13}\text{C}$  values of the algal carotenoid derivatives suggests the origin of isorenieratane and its derivatives from brown-pigmented green sulfur bacteria. Photic zone euxinia was therefore present in the Kiliran lake during the deposition of the whole oil shale profile.

The isorenieratane and its derivatives show concentration variations along the oil shale profile, probably indicating dynamics of chemocline as well as photic zone euxinia extent during the lake development. They are relatively more abundant in middle part of the profile. Palynological analysis done in earlier work revealed the occurrence of relatively abundant fungal remains in samples of this profile part, suggesting warmer climate during the deposition. The warmer climate is thought to promote establishment of the thermocline and shoaling of the chemocline in the Kiliran lake extending the photic zone euxinia and thus increasing green sulfur bacteria population.

Beside climatic variation, tectonic subsidence is also considered to induce the chemocline deepening. Periodic subsidence is recognized from the grain size variation along the oil shale profile. Rapid deepening events are interpreted from rapid decreases of the grain size indicator (Zr/Rb). Some coincident decreases between concentrations of isorenieratane and its

derivatives and Zr/Rb ratios along the oil shale profile might indicate chemocline deepening due to periodic subsidence.

### 3.2. Introduction

The studied oil shale section is an immature source rock belonging to the Late Eocene Brown Shale Formation (Fm) in Kiliran Sub-basin, the southeastern part of the Central Sumatra Basin. The oil shale was deposited in a shallowing upwards environments (Carnell et al., 1998). Based on palynological and geochemical approaches, both tectonic subsidence and climatic changes have been suggested to control the productivity of the Kiliran lake and depositional environments of the oil shale (see Chapter 2).

In the present study, additional organic geochemical data will be used to obtain further information about the influence of tectonic and climate on the dynamics of photic zone euxinia during the lake development. Analysis of the biomarker isorenieratane in sediments has been widely accepted for recognition of photic zone euxinia in former aquatic environments (Hartgers et al., 1994; Sinninghe Damsté et al., 1995, 2001; Koopmans et al., 1996a; Grice et al., 1996, 1998b, 2005; Pedentchouk et al., 2004; Brocks et al., 2005; van Breugel et al., 2005). Isorenieratane is a diagenetic product of isorenieratene and has been detected in many ancient-sediments. Isorenieratene is biosynthesized from  $\beta$ -carotene via  $\beta$ -isorenieratene by brown-pigmented strains of green sulfur bacteria (*Chlorobiaceae*) (e.g. Sinninghe Damsté et al., 2001; Maresca et al., 2008). These bacteria dwell in the oxic-anoxic interface or below it when the photic zone is reaching into the euxinic water.

Another aspect of this study is to get a better understanding of the aquatic conditions that favour green sulfur bacteria to grow in the former Kiliran Lake. The occurrence of these bacteria depends on at least three factors. Light is required to make photosynthesis possible. The presence of  $H_2S$ , which is only available in anoxic conditions, is a prerequisite because the bacteria use  $H_2S$  as electron donor instead of  $H_2O$  in the photosynthesis (e.g. Brocks et al., 2005). Another important key is the availability of nutrients which determine the productivity of aquatic plants including green sulfur bacteria (e.g. Smittenberg et al., 2004). Here, the discussion is related to the question which factors were the most important for the occurrence and abundance of green sulfur bacteria in the former Kiliran lake.

### 3.3. Geological Setting of the Study Area

The study area is located in the Kiliran Sub-basin, one of source rock depocenters in the arbitrary boundary between Central and South Sumatra Basins (Figure 3.1a). The enlarged area in Figure 3.1b shows some sub-basins in the arbitrary boundary including the Kiliran Sub-basin. The sub-basins are referred as part of Central Sumatra Basin, since they show analogous sediment succession (Wain and Jackson, 1995; Carnell et al., 1998).

#### 3.3.1. Central Sumatra Basin

The geological setting and history of Central Sumatra Basin have been described in detail by e.g. de Coster (1974), Williams et al. (1985) and Doust and Noble (2008). This rift basin is situated in a tectonically active region as a result of the Indian-Australian plate subduction beneath the Eurasian plate during Late Eocene-Oligocene. It consists of many troughs and grabens which show analogous sedimentary successions. Tectonic events, sedimentation rates, isostatic subsidence and eustatic sea level changes have been proposed as controlling factors for Tertiary sedimentation in the basin (de Coster, 1974). The generalized tectonostratigraphy of the Central Sumatra Basin is shown in Figure 3.2a. Brown Shale Fm is the most important source rocks for the occurrence of oil in the basin. It was deposited in deep and shallow anoxic lacustrine environments during rapid rift development in Late Eocene. Most of the source rocks are mature especially those that occur in the basin center and deep grabens.

#### 3.3.2. Geology of the Kiliran Sub-basin

Kiliran Sub-basin has been regarded as a small rift basin formed during Late Eocene (Carnell et al., 1998). The morphology of the sub-basin is uncertain, since it has been integrated into the Barisan compressional belt and is now fragmented and faulted on both flanks. It had also been thought to terminate abruptly against the Pre-Tertiary Timpe lineament (Wain and Jackson, 1995). Further geological mapping and drilling programs carried out by the Indonesian Center for Geological Resources (PSDG) in 2006 revealed the occurrence of thick oil shale sequences in Padanglawas graben (Figure 3.1b) in the southern part of the Timpe fault. It is thought as the extension of Kiliran Sub-basin.

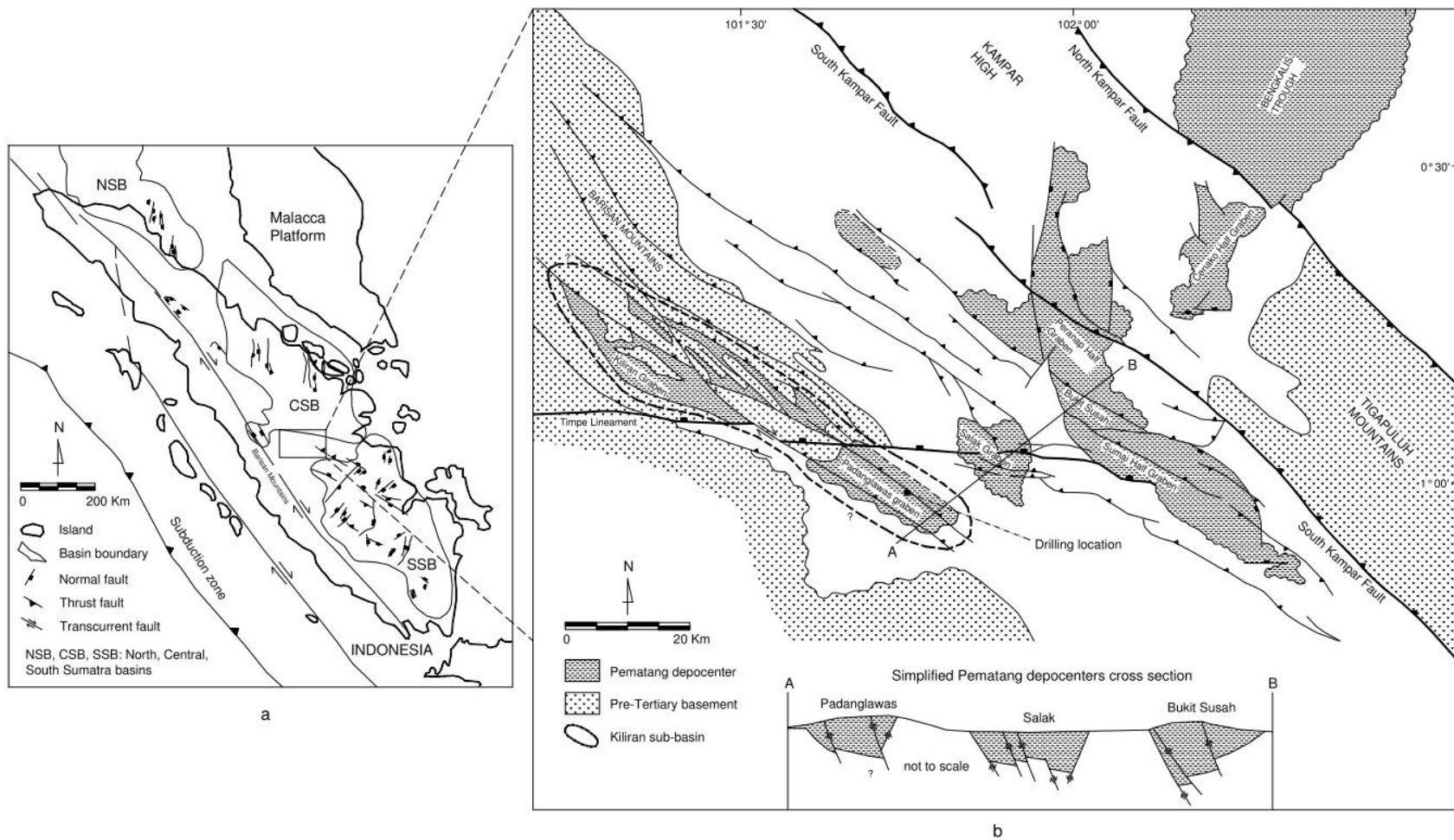


Figure 3.1. Map of Sumatra Basins with main graben structures (modified after Darman and Sidi, 2000) (a); Enlargement of the arbitrary boundary between Central and South Sumatra Basins containing Pematang depocenters, and the drilling location in Padanglawas graben (modified after Wain and Jackson, 1995 and PSDG, 2006) (b).

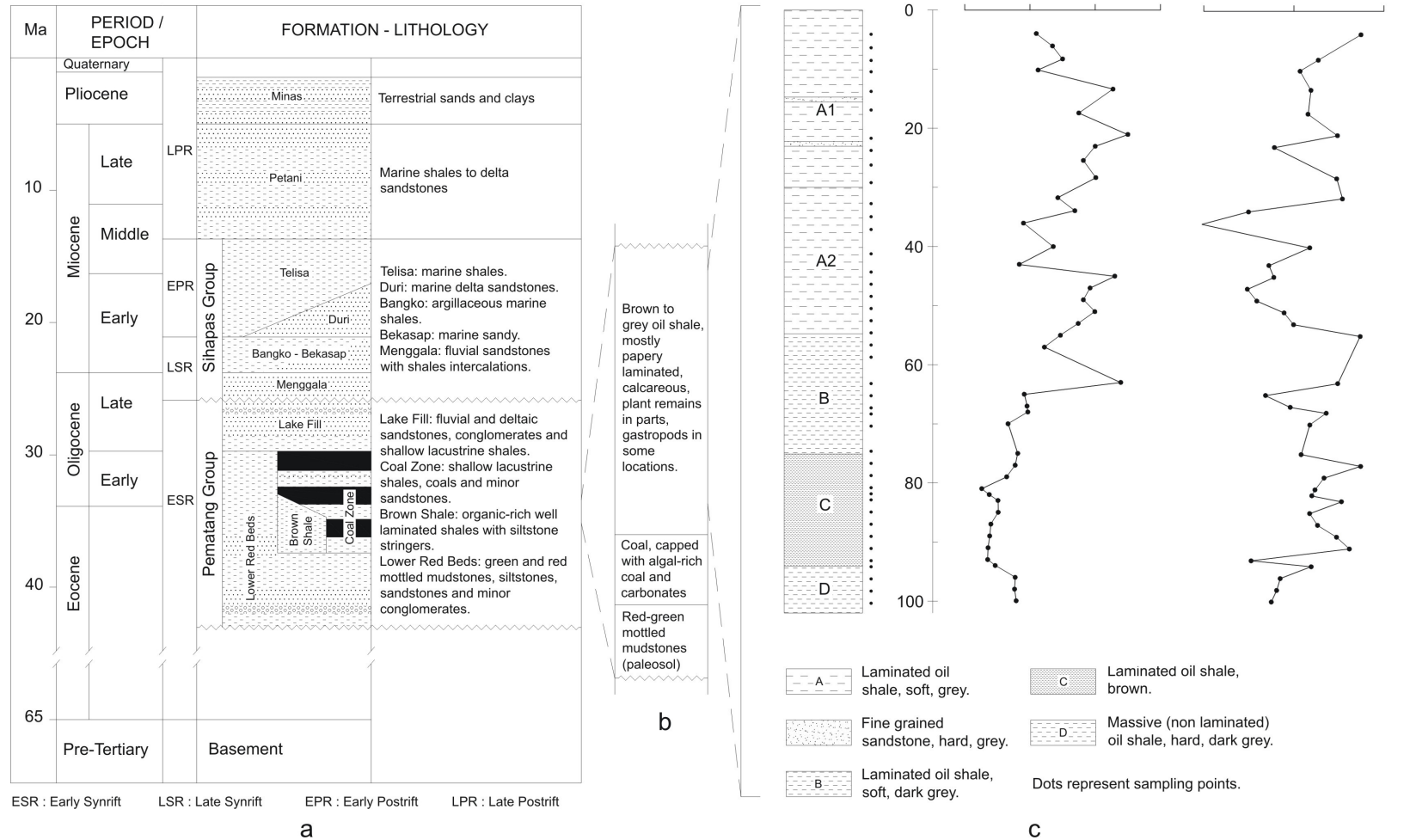


Figure 3.2. Generalized stratigraphic column of Central Sumatra Basin (adopted from Williams et al., 1985 and Doust and Noble, 2008) (a) and Kiliran Sub-basin (modified after Carnell et al., 1998 and PSDG, 2006) (b), and drill core profile of oil shale in Padanglawas graben of Kiliran Sub-basin (c).



The general sediment succession of the Kiliran Sub-basin based on Carnell et al. (1998) and PSDG (2006) is presented in Figure 3.2b. The pre-graben paleosol most probably corresponds to the Lower Red Beds Fm. It is composed of carbonaceous and grey mudstones with locally red and green mottles. Above the paleosol, coal beds varying from thin to 17.5 m thick were deposited in a slowly subsiding reed swamp. A more rapid subsidence rate later resulted in the deposition of algal-rich coal interbeds which pass laterally into freshwater carbonates. A conformably lithofacies change occurred by the deposition of >90 m thick brown to grey colored calcareous shales. Sedimentological appraisal of well exposed shale in the northwestern tip of Kiliran graben suggests a shallow lake setting (10-50 m deep) which exhibit anoxic depositional environments. The presence of abundant gastropods and bioturbation in the uppermost profile part was interpreted to indicate intermittently oxic conditions of sediment deposition (Carnell et al., 1998). There is no exposure which corresponds to the Oligocene Lake Fill Fm and younger lithofacies in this area.

The development of the Kiliran lake during deposition of the studied oil shale section has been discussed elsewhere (Chapter 2). Both, tectonic and climatic changes were thought to control the depositional environment and ecosystem of the lake. Tectonic events have been interpreted from the Zr/Rb ratio indicating variation of grain size of the oil shale (Figure 3.2c). Three subsidences observed from the sudden decreases of the grain size at profile-depths 12, 45 and 96 m suggest rapid deepening events. The climatic control has been attributed to the variation of productivity of the lake aquatic system. Productivity was interpreted from the variation of the organic matter carbon isotopic composition ( $\delta^{13}\text{C}$ , Figure 3.2c). Relatively warmer climate would lead to the establishment of a thermocline in the epilimnion of the lake. Consequently, supply of nutrients from the hypolimnion will be limited, decreasing the lake productivity and thus increasing the proportion of bacterial biomass having relatively depleted  $\delta^{13}\text{C}$ . Along the studied profile, a remarkable decrease of productivity is shown by the relatively depleted  $\delta^{13}\text{C}$  values in the bottom part of section A2.

### 3.4. Sample Material and Methods

#### 3.4.1. Sample material

Forty two samples were collected from a 102 m long drilling core available in the depository warehouse of PSDG, Bandung, Indonesia. The core was drilled in Padanglawas graben of Kiliran Sub-basin. Gastropods and bioturbation are not observed in the entire oil shale core. Plant remains are occasionally present in minor amount as woody organic detritus and leaves. The sediment profile of the core drilling and the sampling positions in the core are shown in Figure 3.2c. The vertical section consists of fine-grained shales with the following variation of the physical characteristics:

- a. soft, grey and well-laminated shale in the upper part (section A), thin fine sandstone intervals are present in the upper part
- b. soft, dark grey and well-laminated shale (section B)
- c. soft, brown and well-laminated shale (section C)
- d. hard, dark grey and non-laminated shale in the lowermost part (section D).

Section A is further divided into A1 and A2 based on geochemical composition (see below).

#### 3.4.2. Elemental analysis

Oil shale rock samples were first crushed, pulverized and sieved to obtain particle size <63 micron. Contents of total organic carbon (TOC) and total sulfur (S) were analyzed using Euro EA (CAP 20) Elemental Analyzer. For TOC determination, pulverized samples were treated with diluted (10%) hydrochloric acid prior to the analysis to remove carbonates from the samples and then rinsed with distilled water until neutrality. The TOC values are then corrected to the original sample weight due to carbonate loss.

#### 3.4.3. Biomarker analysis

Twenty five grams of pulverized oil shale sample material (<63 micron) were extracted for 24 hours in a soxhlet extraction apparatus using 200 ml dichloromethane (DCM) as solvent. The extract was then separated into four fractions using column chromatography (1.5 cm diameter) with 14 grams of activated silica gel. Sequential elution was performed to obtain fractions of saturated hydrocarbons, aromatic hydrocarbons, ketones/esters and more polar compounds

using 40 ml n-hexane, 100 ml of n-hexane/DCM (9/1 v/v), 40 ml DCM and 40 ml methanol, respectively. Gas chromatography combined with mass spectrometry (GC-MS) of the saturated and aromatic hydrocarbon fractions and total extracts was carried out on a Thermo Scientific Ultra series gas chromatograph coupled to a Thermo Scientific DSQ II mass spectrometer. GC separation of the compounds was achieved using a Thermo Scientific TR-5MS fused silica capillary column (30 m x 0.25 mm ID x 0.25  $\mu$ m film thickness). The oven temperature was programmed from 60 to 320 °C at a rate of 4 °C /min, with a 35 min isothermal period at 320 °C. The samples were injected in the splitless mode with the injector temperature at 280°C. Helium was used as carrier gas. The mass spectrometer was operated in the electron impact mode (EI) at 70 eV ionization energy. Mass spectra were obtained by scanning from 50 to 600 daltons at a cycle time of 1 second. For data processing, the Xcalibur Qual Browser software was used. 1,1'-Binaphthyl and per-deuterated tetracosane were used as internal standards for quantification of aromatic hydrocarbons and saturated hydrocarbons respectively. In this study, only certain compounds will be discussed.

#### 3.4.4. Compound-specific isotope analysis

Compound-specific isotope analysis for carbon (CSIA) was carried out in the Stable Isotope Laboratory of the Department of Applied Geosciences and Geophysics at the University of Leoben (Austria). A Thermo Fisher Delta V mass spectrometer connected to a Ultra series gas chromatograph, fitted with a similar column specification to that used in GC-MS analysis, were used for the analysis. The GC oven, injection conditions and carrier gas were also the same as those used in GC-MS analysis. Eluting compounds from the GC were converted to CO<sub>2</sub> in a combustion oven and measured relative to a reference CO<sub>2</sub>. The  $\delta^{13}\text{C}$  values were reported relative to the Pee Dee Belemnite (PDB) standard. An *n*-alkane carbon isotope external standard mixture (*n*-C<sub>15</sub>; *n*-C<sub>20</sub>; *n*-C<sub>25</sub>) was used for the control of the analytical results. Only  $\delta^{13}\text{C}$  values obtained from aromatic hydrocarbon fractions will be presented in this study.

### 3.5. Results and Discussions

#### 3.5.1. TOC and S

The TOC contents vary from 1.9 to 12.5 % (average 5.9 %) and generally decrease upwards in the profile, with lower values being observed in sections A1 and A2, moderately higher values in sections B and D, and highest values in section C (Figure 3.3a). S percentages range from 0.1 to 2.0% averaging at 1.0% (Figure 3.3b) with a variation along the profile generally similar to the one observed for the TOC values. The detailed geochemical data are presented in Appendix 3. The largely parallel variations of TOC and S may indicate relative changes of the bottom water anoxicity in the former lake. However, the lower amounts of TOC and S in sections B and A2 are rather due to lower productivity than to decreasing anoxicity of the bottom water (see Chapter 2). The warmer climate during deposition of these sections led to the establishment of a thermocline, limiting supply of nutrients from the hypolimnion of the lake. Further, the effect of the warmer climate on the chemocline dynamics of the Kiliran lake will be discussed.

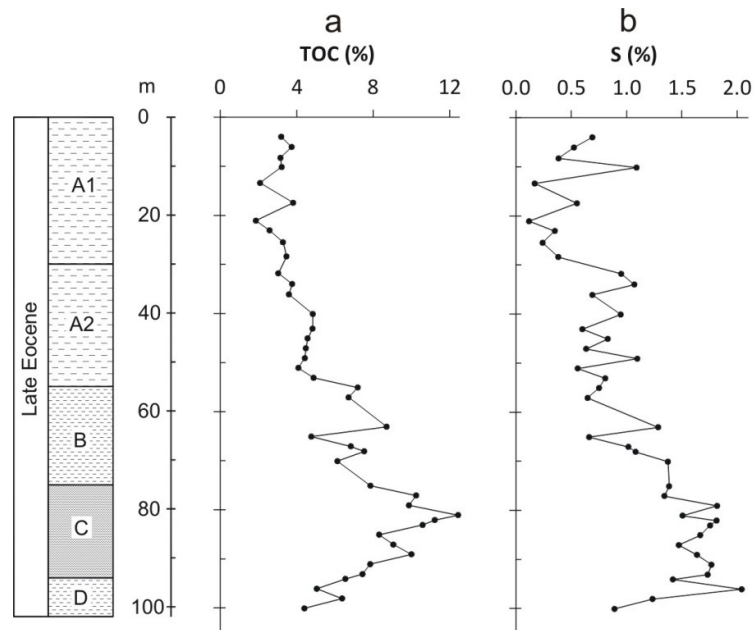


Figure 3.3. Vertical variation of TOC (a) and S (b) along the Kiliran oil shale profile. The detailed geochemical data are presented in Appendix 3.

### 3.5.2. Biomarkers

The total ion chromatograms (TIC) from GC-MS analysis of the aromatic hydrocarbon fraction (Figure 3.4a) and saturated hydrocarbon fraction (Figure 3.4b) are obtained from the solvent extract of the representative sample G-32. CSIA measurement was carried out on the aromatic hydrocarbon fraction of the same sample and the results are also shown in Figure 3.4a. The peak assignments for some selected biomarkers are listed in Table 3.1. Biomarkers in the aromatic fraction include naphthalene derivatives (C, E), alkylated benzene as cleavage products of carotenoids (A, B, D), perylene (F), methylethylcyclopentenochoyrene (G) and three carotenoids (H, I, J). Biomarkers in the saturated fraction include isoprenoids (Pr, Ph), des-A-triterpenoids (K, L, M) and regular steranes (N, O, P, Q, R, S) apart from *n*-alkanes marked with asterisks.

The detailed organic geochemical data are presented in Appendix 4. Vertical concentration variations of selected biomarkers along the profile are shown in Figure 3.5. Abundance of fungal remains from palynological analysis taken from Chapter 2 is also presented in Figure 3.5 for discussion relating to biomarker variations. The naphthalene derivatives are dominated by 1,1,5,6-tetramethyl-1,2,3,4-tetrahydronaphthalene (TMTHN, C) and cadalene (E). Cadalene concentrations generally increase upwards in the profile and vary from ~0 to 14.6 with average value of 5.4  $\mu\text{g/g}$  TOC (Figure 3.5a). In sections A and B, the concentrations show two distinct variation cycles with lower values being observed in the uppermost part of section A1. In sections C and D, the concentrations are generally lower and show a larger fluctuation. TMTHN concentrations range from ~0 to 15.2 averaging at 5.7  $\mu\text{g/g}$  TOC (Figure 3.5a) with very similar vertical variations as described for cadalene. Cadalene has been considered as biomarker for higher plants, mainly angiosperms, in the Southeast Asia region (Widodo et al., 2009; and references therein). The  $\delta^{13}\text{C}$  value of cadalene is  $-30.5\text{‰}$ , which is in the range expected for higher plants (C3 plants) as biological precursors. TMTHN has been suggested to originate from several precursors. Radke et al. (1986) reported an origin of this compound from a type III organic matter containing non specified resinous material. However, this compound was also suggested to originate probably from bacteria (Killops, 1991). The close correlation between TMTHN and cadalene concentrations suggests that both compounds are originating from higher plants in the present case.

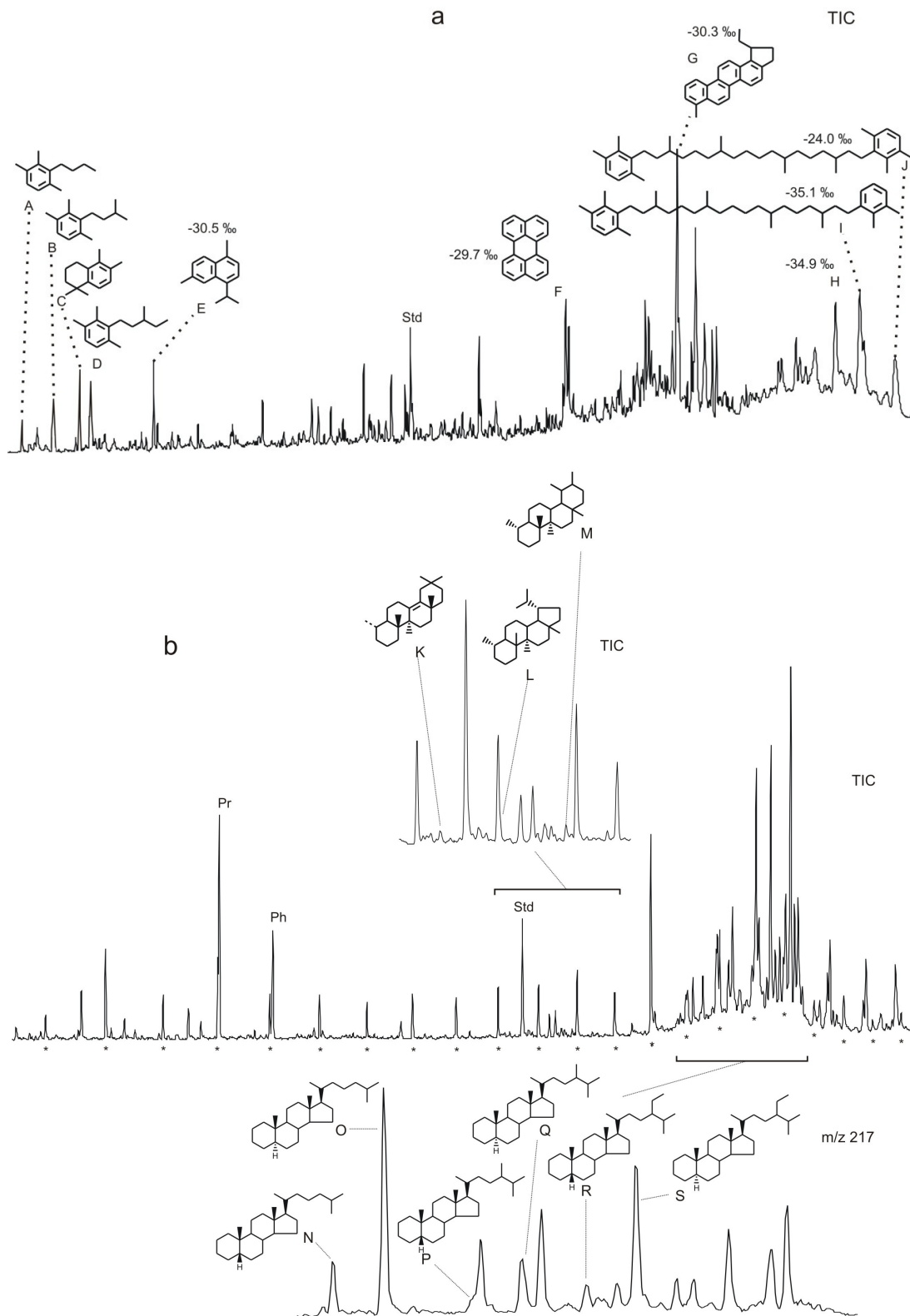


Figure 3.4. Total ion chromatograms of the aromatic hydrocarbon fraction (a) and the saturated hydrocarbon fraction (b) of the G-32 sample. The so called saturated hydrocarbon fraction also includes alkenes. Moreover the mass chromatogram of  $m/z$  217 for the recognition of steranes and an enlarged section of the total ion chromatogram with very low abundances of des-A-triterpenoids are shown. Identification of selected compounds is listed in Table 3.1.

Table 3.1. Peaks identification of biomarkers in aromatic and saturated fractions of G-32 sample.

Peak	Compound	Base peak	Mass weight	Reference
A	C <sub>13</sub> Aryl isoprenoid	133	176	1
B	C <sub>14</sub> Aryl isoprenoid	133	190	1
C	1,1,5,6-Tetramethyl-1,2,3,4-tetrahydronaphthalene	173	188	2
D	C <sub>15</sub> Aryl isoprenoid	133	204	1
E	Cadalene	183	198	9, 10
F	Perylene	252	252	9, 10
G	7-Methyl-1'-ethyl-1,2-cyclopenteno-chrysene	281	310	5, 8, 9
H	Carotenoid derivative	133	524	
I	Carotenoid derivative	133	532	6
J	Isorenieratane	133	546	7
K	des-A-olean-13(18)-ene	109	328	3
L	des-A-lupane	109	330	3, 4
M	des-A-ursane	109	330	3
N	5 $\beta$ -Sterane	217	372	4
O	5 $\alpha$ -Sterane	217	372	4
P	24-Methyl-5 $\beta$ -sterane	217	386	4
Q	24-Methyl-5 $\alpha$ -sterane	217	386	4
R	24-Ethyl-5 $\beta$ -sterane	217	400	4
S	24-Ethyl-5 $\alpha$ -sterane	217	400	4
Pr	Pristane	57	268	9
Ph	Phytane	57	282	9
Std	Internal standard			

Note: Compound identification is based on mass spectra and/or relative retention time published in the references. 1: Requejo et al. (1992), 2: Killops (1991), 3: Widodo (2008), 4: Philp (1985), 5: Dehmer (1988), 6: Pedentchouk et al. (2004), 7: Hartgers et al. (1994), 8: Stout (1992), 9: Wiley Library (2008), 10: Geopetro Library (2003).

The carotenoid cleavage products consist of C<sub>13</sub>, C<sub>14</sub> and C<sub>15</sub> aryl isoprenoids (A, B, D), and the other carotenoid derivatives are also presented by three compounds, H, I and isorenieratane (J). The isorenieratane concentrations range from 0.4 to 18.1 with an average value of 5.4  $\mu\text{g/g}$  TOC (Figure 3.5b). The concentrations generally increase upwards in several cycles along the profile with lower values being observed in section A1. The  $\delta^{13}\text{C}$  value of isorenieratane is -24.0‰, which is enriched in relation to values expected for algal and higher plant biomass. Compounds H and I occur in the samples sporadically, especially compound I is only present in two samples. Their  $\delta^{13}\text{C}$  values are -34.9 and -35.1‰ respectively, suggesting an origin from a source that differs from the biomass deriving isorenieratane. The aryl isoprenoid cleavage products (A, B, D) are most likely generated from isorenieratane, as they occur in all samples and the compounds show vertical concentration profile which vary largely parallel with isorenieratane. The sum of isorenieratane and its derivatives range from 3.6 to 41.5  $\mu\text{g/g}$  TOC averaging at 16.5  $\mu\text{g/g}$  TOC (Figure 3.5c). The  $\delta^{13}\text{C}$  values of the aryl isoprenoid cleavage products, which may be useful to confirm the relation with isorenieratane, are not available due to low concentrations or co-elution with other compounds.

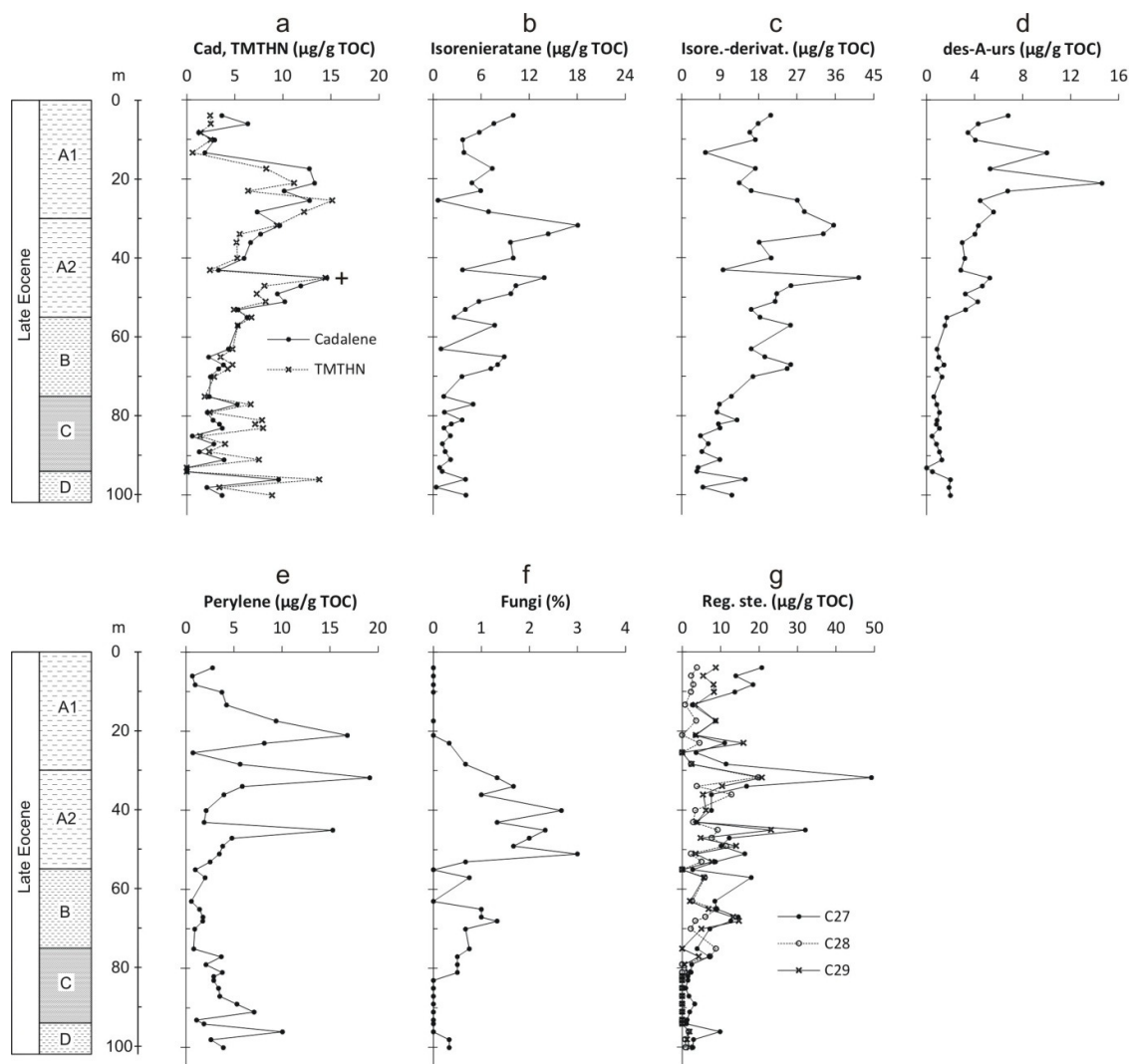


Figure 3.5. Vertical profiles of biomarkers concentrations: cadalene and TMTHN (a), isorenieratane (b), sum of isorenieratane and aryl isoprenoids (c), des-A-ursane (d), perylene (e), fungal remains (f) and sum of  $\alpha$  and  $\beta$  isomers of regular steranes (g). Sign + in (a) denotes G-32 sample. The detailed organic geochemical data are presented in Appendix 4.

Des-A-triterpenoids in the saturated hydrocarbon fraction comprise des-A-olean-13(18)-ene (K), des-A-lupane (L) and des-A-ursane (M). These biomarkers have been mentioned to originate unambiguously from higher plant (see e.g. Trendel et al., 1989; Nytoft et al., 2002; Huang et al., 2008). The concentrations of des-A-ursane vary from ~0 to 14.6 averaging at 3.0  $\mu\text{g/g TOC}$  (Figure 3.5d) and distinctly increase upwards. Both other des-A-triterpenoids have vertical variation profiles similar to des-A-ursane and are not shown here.

Perylene (F) has been reported to originate from various precursors. Aizenshtat (1973) suggested higher land plants as origin of perylene, but later Wakeham et al. (1979) questioned



this suggestion as the sediments used for the study were considered to be free of terrigenous input. Silliman et al. (2000) concluded that perylene originates from various sources including both aquatic and terrestrial organic matter and different microbial processes. Gocht et al. (2007) found perylene in a terrestrial sub-soil profile and suggested in situ biological sources. Fungi have also been reported as a major source for perylene in sediments (Jiang et al., 2000) and specifically wood-degrading fungi were hypothesized recently as a natural source of perylene by Grice et al. (2009). In the Kiliran oil shale sequence, perylene has been identified in all samples with concentrations ranging from 0.6 to 19.2 with average value of 4.3  $\mu\text{g/g}$  TOC (Figure 3.5e). The vertical variation of perylene concentrations is comparable to those of higher plant-derived des-A-triterpenoids. In the present study, perylene most likely is of terrigenous origin. Although the  $\delta^{13}\text{C}$  value of perylene (-29.7‰) is close to that of cadalene, it is difficult to distinguish whether perylene originates from higher plants or other terrigenous sources. For example Jiang et al. (2000) reported that perylene, which was suggested to originate mainly from fungi, had  $\delta^{13}\text{C}$  values (-23.6 to -24.0‰) close to those of cadalene (-24.9 to -26.6‰). In the present case, an origin of perylene from fungi is unlikely, considering the different abundance variations between perylene and fungal remains along the profile (Figure 3.5e and f).

Methylethylcyclopentenochoyrene (MECPC, L) might have a hopanoid-like structure (7-methyl-3'-ethyl-1,2-cyclopentenochoyrene) indicating a bacterial origin. However, MECPC can also be related to a 24,30-bisnorlupanoid structure (7-methyl-1'-ethyl-1,2-cyclopentenochoyrene) indicating a higher plant precursor according to Stout (1992). The  $\delta^{13}\text{C}$  value of MECPC is -30.3‰, which is very close to that of cadalene. Considering the similarity of these isotopic values, the MECPC is rather of higher plant origin which would be consistent with the presence of the latter compound, 7-methyl-1'-ethyl-1,2-cyclopentenochoyrene. This compound does not occur in all samples and shows no systematic vertical variation.

Regular steranes are present as  $\text{C}_{27}$  (N, O),  $\text{C}_{28}$  (P, Q) and  $\text{C}_{29}$  (R, S) homologues. Their concentrations ( $\alpha+\beta$  isomers) are 0.9-49.3, 0-19.8, 0-23.2 with average values of 9.3, 3.6, 5.3  $\mu\text{g/g}$  TOC respectively (Figure 3.5g). All these regular steranes reveal similar concentration variations with isorenieratane. Regular steranes are widespread in both, lacustrine and marine sediments. They originate from various eukaryotic organisms (mainly algae and higher plants) (e.g. Peters et al., 2005b). Some authors used relative contributions of the  $\text{C}_{27}$ - $\text{C}_{29}$  steranes to distinguish different ancient ecosystems and depositional environments (Huang and

Meinschein, 1979; Peters et al., 2005b). The dominance of C<sub>27</sub> steranes in the sterane composition is usually attributed to a strong algal influence, whereas the dominance of C<sub>29</sub> steranes is attributed to a strong higher plants input (e.g. Huang and Meinschein, 1979). In the present case C<sub>27</sub> steranes dominate in the sterane composition, indicating that an origin of the regular steranes from higher-plants is unlikely. Additionally, palynological data have shown the dominance of algal amorphous facies in the oil shale, whereas higher plants constitute only a minor amount (Chapter 2). Autochthonous sources, possibly certain algae, are therefore more responsible for the abundance of regular steranes in the Kiliran oil shale. Moreover, steroidal hydrocarbons were not detectable in Indonesian coals derived mostly from higher plants especially in Sumatra and Kalimantan (Anggayana, 1996; Amijaya et al., 2006; Widodo, 2008).

### 3.5.3. Occurrence of Isorenieratane

#### 3.5.3.1. Review of isorenieratane origin

The isorenieratane formation through diagenesis from various biological sources is summarized in Figure 3.6, showing pathways proposed by Koopmans et al. (1996b), Krügel et al. (1999) and Maresca et al. (2008).

Isorenieratane has been regarded as a specific biomarker of brown-pigmented green sulfur bacteria. Most green plants, including eukaryotic algae and many autotrophic bacteria, fix carbon using the C<sub>3</sub> pathway, resulting in carbon isotopic compositions ranging from about -20 to -32‰ (e.g. Peters et al., 2005a). However, brown-pigmented green sulfur bacteria do not follow this photosynthetic pathway. They fix carbon through the reverse tricarboxylic acid cycle with the key enzyme pyruvate synthase which has a low discrimination against <sup>13</sup>C. This pathway leads to an anomalous enrichment of δ<sup>13</sup>C in their biomass relative to those most of green algae using the enzyme Rubisco (van Breugel et al., 2005; and references therein). Therefore, when isorenieratane in sediments originates from brown pigmented green sulfur bacteria, δ<sup>13</sup>C enrichment of this compound by about 15‰ relative to δ<sup>13</sup>C values of algal derived compounds can be expected from CSIA measurement (Koopmans et al., 1996b). This enrichment anomaly is thus commonly used to confirm the origin of isorenieratane and its derivatives from green sulfur bacteria.

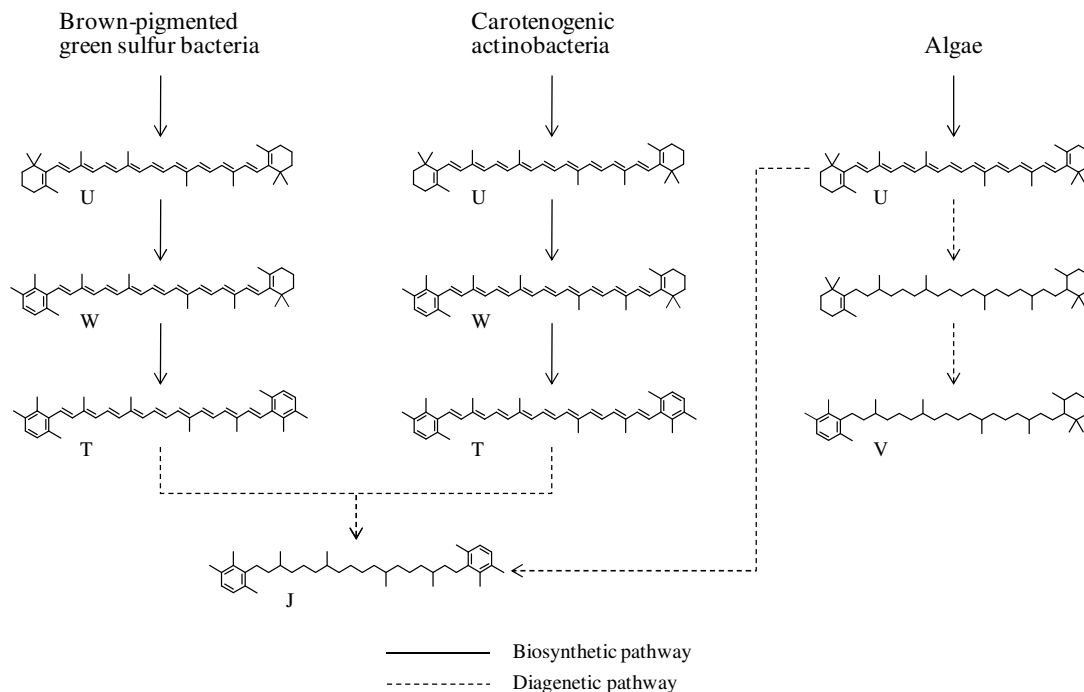


Figure 3.6. Possible sources of isorenieratane (J) in sediments including diagenetic product of: (i) isorenieratene (T) biosynthesized in brown-pigmented green sulfur bacteria and carotenogenic actinobacteria and (ii)  $\beta$ -carotene (U) from algae.  $\beta$ -Isorenieratane (V) could be derived from  $\beta$ -carotene by an abiotic process and principally isorenieratane could also originate from aromatization of both cyclohexenyl moieties. The reaction scheme has been modified after Koopmans et al. (1996b), Krügel et al. (1999) and Maresca et al. (2008).

However, the work of Koopmans et al. (1996b) revealed that  $\beta$ -isorenieratane may have  $\delta^{13}\text{C}$  values of about  $-27\text{‰}$ , which is not anomalously enriched relative to those of algal biomass.  $\beta$ -Carotene (U) was therefore considered as alternative precursor of  $\beta$ -isorenieratane as evidenced by the carbon isotopic signature similarity of the latter with  $\beta$ -carotane in North Sea oil. In a laboratory experiment Koopmans et al. (1996b) showed that a geminal methyl group of the cyclohexenyl moiety can be shifted exclusively from the 2 to the 3 position during aromatization. Moreover, they noted that in principle isorenieratane can also be formed from  $\beta$ -carotene by the abiotic aromatization of both cyclohexenyl moieties. This pathway opens the possibility of the diagenetic (abiotic) formation of isorenieratane from  $\beta$ -carotene.

Isorenieratene is also biosynthesized from a few actinobacteria (Krügel et al., 1999). Some genes in the actinobacteria are responsible to form isorenieratene from  $\beta$ -carotene via  $\beta$ -isorenieratene (W) by the desaturation/methyltransferation mechanism as shown in Figure 3.6. Actinobacteria have been considered as a less significant source of isorenieratane though they

are known from recent sediments (e.g. Bredholt et al., 2008) and sedimentary rocks (e.g. Wilkinson, 2003).

Liaaen-Jensen et al. (1982) also found isorenieratene in several species of marine sponges. However, sponges are not considered to be able to biosynthesize carotenoids *de novo*, but have the capacity to modify the chemical structure of carotenoids via the food-chain. Isorenieratene and other carotenoids were thus considered to originate either from the planktonic or bacterial diets of sponges, or their symbionts (Liaaen-Jensen et al., 1982). In addition, Chlorobiaceae (green sulfur bacteria) and actinobacteria were suggested as possible symbionts of sponges (Webster et al., 2001).

### 3.5.3.2. Isorenieratane in Kiliran oil shale

#### 3.5.3.2.1. Green sulfur bacteria vs. terrigenous origin

As shown in Figure 3.5c, the summarized concentration of isorenieratane and its derivatives generally increase upwards along the profile until section A2. On the other hand, the vertical variation of S (Figure 3.3b) disagrees with that of isorenieratane. S concentrations generally decrease from the bottom to the top of the profile. The unexpected concentration variations of isorenieratane and its derivative may lead to an alternative interpretation of its origin, because this compound could also originate from actinobacteria. These bacteria are mostly present in soil but also found in marine and freshwater environments (Ward and Bora, 2006; Allgaier and Grossart, 2006). They constitute a major component of the microbial population in most soils (e.g. Goodfellow and Williams, 1983). Moreover, fungi which may indicate soil erosion in the hinterland are present in the oil shale according to the palynological data.

However, some other parameters challenge this alternative source of isorenieratane and its derivatives. The concentration profile of isorenieratane and its derivatives and relative abundance of fungal palynomorphs do not correlate. Regular C<sub>27</sub> steranes that most likely originate mainly from algae (autochthonous) also exhibit generally an upwards increase along the profile. Concentrations of isorenieratane are positively correlated to those of the regular steranes,  $R^2 = 0.67$ , 0.56 and 0.64 for the sum of  $\alpha$  and  $\beta$  isomers of C<sub>27</sub>, C<sub>28</sub> and C<sub>29</sub> steranes respectively. Additionally, terrigenous biomarkers generally show the highest abundance in the lower part of section A1, whereas isorenieratane as well as regular steranes show low

concentrations in this part. This prefers to the common interpretation that isorenieratane in the oil shale is rather originating from green sulfur bacteria than from terrigenous organisms.

Moreover, the  $\delta^{13}\text{C}$  value of isorenieratane of  $-24\text{‰}$  argues for an origin from green sulfur bacteria. Similar  $\delta^{13}\text{C}$  values have been reported in several other studies e.g.  $-27$ ,  $-25.3$  and  $-24.2\text{‰}$  for isorenieratene or isorenieratane from Cadagno and Cisó lakes and Kyllaren fjord respectively. These intermediate values have been attributed to assimilation of  $\delta^{13}\text{C}$  depleted dissolved inorganic carbon (DIC) by the brown-pigmented green sulfur bacteria in shallow aquatic systems (Schaeffer et al., 1997; Hartgers et al., 2000; Smittenberg et al., 2004; van Breugel et al., 2005). In the Kiliran Lake, the use of  $\delta^{13}\text{C}$  depleted DIC by aquatic organisms is evident by the concomitant  $\delta^{13}\text{C}$  depletion of some phytoplankton biomarkers, including isorenieratane and the other two carotenoid derivatives (compounds H and I). The latter two compounds may originate from algae considering that the depletion of  $\delta^{13}\text{C}$  values (about  $-35\text{‰}$ ) of these compounds is also due to recycling of DIC in the water column. The significant enrichment of  $\delta^{13}\text{C}$  isorenieratane by about  $11\text{‰}$  relative to the two algal carotenoids may further confirm an origin of isorenieratane from the brown-pigmented green sulfur bacteria.

#### 3.5.3.2.2. Factors controlling the occurrence of green sulfur bacteria

Since green sulfur bacteria depend on the availability of  $\text{H}_2\text{S}$  to grow, the disagreement between concentrations of S and isorenieratane and its derivatives along the profile (Figures 3.3b and 3.5bc) may indicate that  $\text{H}_2\text{S}$  was not the limiting factor for green sulfur bacteria development. On the other hand, in marine-related environments, increase of isorenieratene abundance has previously often been related to expansions of photic zone euxinia due to an increase of the trophic level (Menzel et al., 2002; Smittenberg et al., 2004; Rohling et al., 2006). Higher productivity in the upper water column would enhance the demand of oxygen for respiration in the lower water column and thus promote to shoaling of chemocline. In shallower chemocline, the expansion of the photic zone euxinia would favour green sulfur bacteria to grow. Additionally, the increasing availability of nutrients would also increase population of the bacteria. However, the summarized concentration of isorenieratane and its derivatives in the oil shale profile develop in different variation compared to the trophic level as shown by the  $\delta^{13}\text{C}$  value as a productivity indicator (Figure 3.2c). This indicates that other factors must be responsible to control the abundances of isorenieratane and its derivatives along the profile.

O'Reilly et al. (2003) suggested that the present global warming is responsible for the decrease of aquatic productivity of Tanganyika lake, Africa. This was attributed to thermocline establishment in the Tanganyika lake. They also reported that the present global warming is also shoaling the oxycline of the lake. As mentioned above, warmer climate was present during deposition of sections B and A2 of the Kiliran oil shale profile (see Chapter 2). The fungal remains (Figure 5g) were used to indicate a relatively warmer climate. This warmer climate was related to the decrease of the Kiliran lake productivity during deposition of the sections. The climate was likely also responsible for chemocline shoaling of the Kiliran lake. The stronger thermocline during deposition of the sections might limit water mixing in the epilimnion. Below the thermocline, oxygen renewal was not possible and additionally respiration was the important biological process, decreasing the availability of oxygen. This, consequently, led to the chemocline shoaling and thus expansion of photic zone euxinia. The warmer climate is therefore a plausible explanation for the higher abundances of isorenieratane and its derivatives in sections B and A2. Additionally, the lower lake productivity during deposition of these sections probably also expanded the photic zone euxinia with respect to water transparency. Lake productivity decrease commonly corresponds to increase of water transparency, expanding the euphotic zone (see e.g. Goldman, 1988).

In the following, development of the Kiliran lake is discussed with respect to photic zone euxinia and chemocline dynamics.

A rapid subsidence occurring during deposition of the sediments of profile-depth 96 m might have instantly deepened the chemocline. Consequently, the light could not reach the chemocline effectively and the green sulfur bacteria population decreased during deposition of section C (Figure 3.7a). Additionally, higher productivity might decrease the water transparency. At the top of section C, fungal remains initially appear and subsequently increase in abundance until section A2 with only some disappearances around profile-depth 60 m. The variations of isorenieratane and its derivatives abundances generally seem to follow the variation of fungal remains except at the profile section around profile-depth 45 m. This may indicate that the stronger thermocline during warmer climate shoaled the chemocline (Figure 3.7b). Additionally, lower productivity might increase the water transparency. At profile-depth 45 m, the sudden decrease of isorenieratane and its derivatives concentrations coincide with the sudden decrease of grain size (Figure 3.2c). Subsidence is likely responsible for this rapid chemocline deepening. Afterwards, from the top of section A2 to the lower part of section A1,

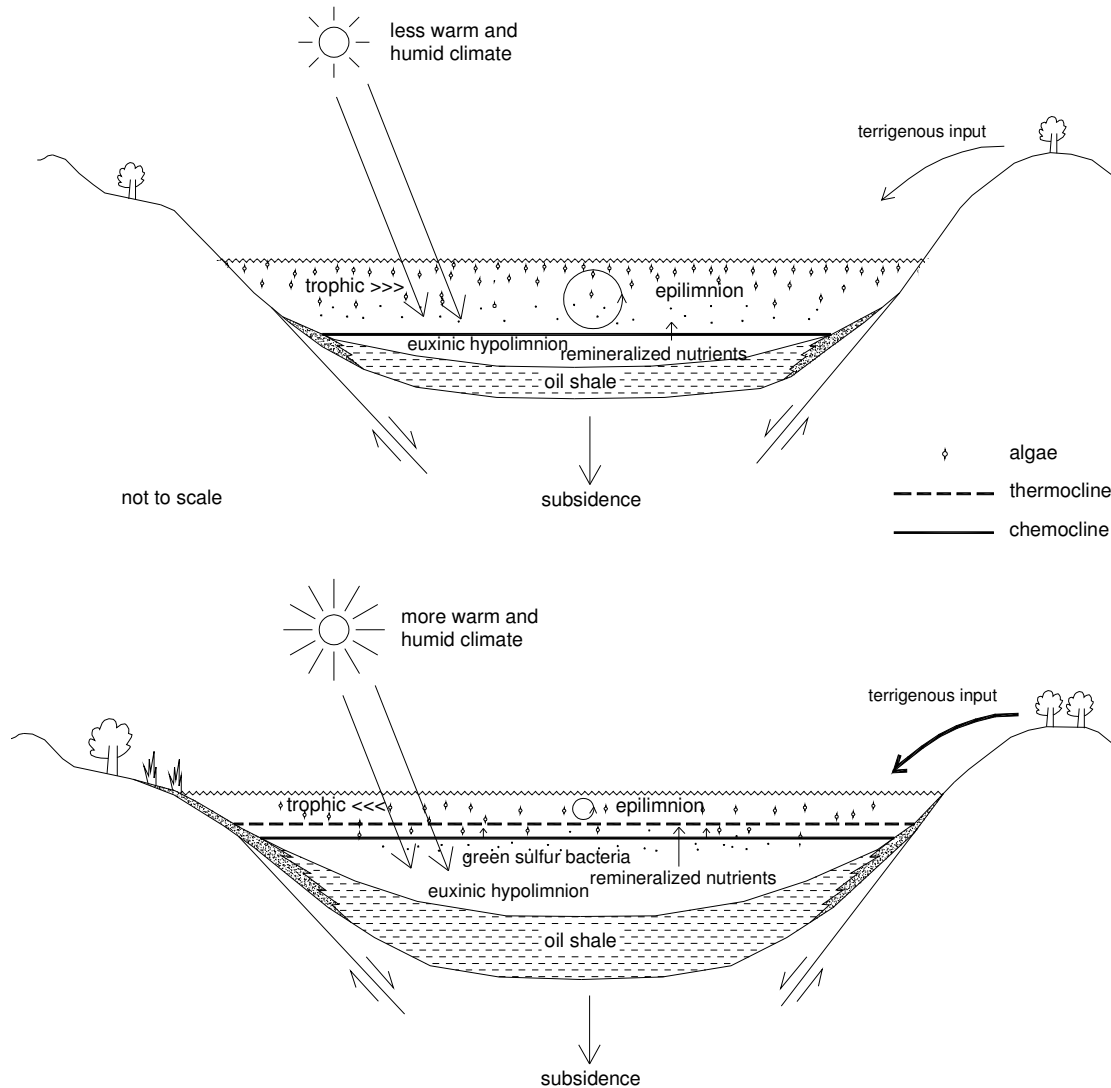


Figure 3.7. Chemocline dynamics during the deposition of section C (a) and section A2 (b) (modified from Chapter 2). Green sulfur bacteria (GSB) would bloom more effectively when the chemocline was shoaling, extending the photic zone euxinia.

the fungal remains decrease upwards and finally disappear. The sum abundance of isorenieratane and its derivatives also decreases upwards (Figure 3.5c). In the lower part of section A1, they are generally low, while terrigenous input is highest as shown by the concentrations of cadalene, TMTN and especially des-A-ursane (Figure 3.5). This indicates that during deposition of this part, the lake was shallow, as water level was decreasing and thick sediments were previously deposited. Intervals of oxic depositional environments might occur. The photic zone euxinia was consequently narrow and only temporarily present. The relatively shallow with oxic intervals environments during deposition of the lower part of section A1 are also characterized by the deposition of fine sandstone intervals (Figure 3.2c). Subsequently, subsidence occurred again at profile-depth 12 m, creating more accommodation space and thus

likely expanding the photic zone euxinia as indicated by slightly higher abundances of isorenieratane and its derivatives.

### 3.6. Conclusions

The significance of selected biomarkers from aromatic and saturated hydrocarbon fractions is discussed in this study. Biomarkers from terrigenous organic matter are cadalene, 1,1,5,6-tetramethyl-1,2,3,4-tetrahydronaphthalene (TMTHN), perylene and des-A-triterpenoids. Concentrations of these biomarkers show generally an upwards increase along the oil shale profile but decrease again at the top of the profile. Regular steranes ( $C_{27}$ - $C_{29}$ ), isorenieratane and aryl isoprenoids are also recognized in almost all samples. The aryl isoprenoids are regarded as cleavage products of isorenieratane. The concentrations of regular steranes and isorenieratane and its derivatives develop along the profile largely in parallel with the biomarkers from terrigenous organic matter except for the top of the profile where they vary differently from those of terrigenous biomarkers. It is unlikely that the regular steranes predominated by  $C_{27}$  carbon number were derived from terrigenous organic matter. Further, carbon isotopic composition ( $\delta^{13}C$ ) of isorenieratane is -24.0‰, relatively enriched from common values for lacustrine algal biomass, suggesting that the isorenieratane was derived from brown-pigmented green sulfur bacteria dwelling in the photic zone euxinia.

The upwards increases of the isorenieratane and its derivatives concentrations are more intensive in the middle part of the oil shale profile. Palynological data from earlier work revealed that fungal remains are relatively more abundant in this part, indicating warmer climate during deposition. The warmer climate likely promoted thermocline establishment in the former Kiliran lake. Consequently, the chemocline would shoal, expanding the photic zone euxinia and thus increasing the brown-pigmented green sulfur bacteria population.

Tectonic subsidence is also considered to induce the chemocline deepening. Periodic subsidence is recognized from the grain size variation along the oil shale profile. The rapid deepening events interpreted from rapid decreases of grain size indicator (Zr/Rb) coincide with the sudden decreases of isorenieratane and its derivatives concentrations suggesting deepening of chemocline. Therefore, both climatic changes and tectonic subsidence were likely the significant factors on the dynamics of chemocline as well as the extent of photic zone euxinia.



## **Chapter 4: Biomarker evidence for the occurrence of *Botryococcus braunii* races A and L in the Late Eocene Kiliran lake, Central Sumatra Basin, Indonesia**

### **4.1. Abstract**

Palynological and organic geochemical studies have been carried out to recognize the occurrence of *B. braunii* in the 102 m long core of the Late Eocene Kiliran oil shale. *B. braunii* palynomorphs are observed in varying amounts in all 42 samples (3-16% of organic matter). Heptacosane (C<sub>27</sub> *n*-alkane) is present with concentrations of up to 393.7 µg/g TOC and unusually abundant relative to the other long-chain *n*-alkane in the saturated hydrocarbon fractions. The stable carbon isotopic composition ( $\delta^{13}\text{C}$ ) of this compound shows values of about -31‰, which are up to 2‰ enriched relative to the other long-chain *n*-alkanes. The abundance of *B. braunii* and the concentration of the C<sub>27</sub> *n*-alkane develop similar along the oil shale profile. The C<sub>27</sub> *n*-alkane is regarded as biomarker for *B. braunii* race A, which is thus suggested to be dominant in the algal population. Lycopane is also observed in many samples with concentrations of up to 54.7 µg/g TOC. These values are much lower to the C<sub>27</sub> *n*-alkane. The  $\delta^{13}\text{C}$  value of lycopane is -17.2‰. This strongly enriched  $\delta^{13}\text{C}$  value is consistent with an origin from *B. braunii* race L. Both of the *B. braunii* races show generally an opposite development in abundance along the profile. This may indicate that the algal races bloomed in alternation, probably due to different specific water chemistry preferences. Although the carbon isotopic compositions of these biomarkers are quite different, they are both thought to be depleted about 7-9‰ relative to the respective expected values. Some other biomarkers are also discussed with respect to the concomitant  $\delta^{13}\text{C}$  depletion due to the presence of <sup>13</sup>C-depleted dissolved inorganic carbon (DIC) fixed by organisms dwelling in the entire phototrophic zone of the former Kiliran lake.

### **4.2. Introduction**

*B. braunii* is a worldwide dispersed green colonial alga, belonging to *Trebouxiophyceae* class (Senousy et al., 2004). It lives in lakes, ponds and bogs, and tolerates freshwater-brackish and oligotrophic-eutrophic environments (Komárek and Marvan, 1992; Metzger and Largeau,

2005; Ramírez and Corbacho, 2005). This alga is characterized by the ability to synthesis a variety of lipids with high contents of hydrocarbons. The hydrocarbons of *B. braunii* have been extensively studied. Due to the absence of obvious morphological differences, the alga strains have thus been classified based on their hydrocarbon biosynthesis. Races A, B and L were attributed to those generating odd carbon numbered *n*-alkadienes/trienes from C<sub>25</sub> to C<sub>31</sub> (Metzger et al., 1985a), triterpenoid C<sub>30</sub>-C<sub>37</sub> botryococcenes (Metzger et al., 1985a, 1985b) and tetraterpenoid lycopadiene (Metzger and Casadevall, 1987), respectively. The co-existence of the races has previously been reported, i.e. races A and B in Overjuyo lake, Bolivia (Metzger et al., 1988; Metzger et al., 1989), B and L in Khao Kho Hong lake, Thailand (Metzger and Casadevall, 1987; Metzger et al., 1988) and the three races A, B and L in El Junco lake, Galápagos (Zhang et al., 2007).

*B. braunii*, together with *Pediastrum* and other lacustrine algae, has been suggested to be the main biological source material for petroleum generation in lacustrine basins throughout Southeast Asia (e.g. Sladen, 1997). Races A and mostly B of the alga were reported to contribute significantly to crude oils and source rocks in Sumatra (Moldowan and Seifert, 1980; Sosrowidjojo et al., 1994; Dowling et al., 1995; Williams et al., 1995). The race L, however, has never been reported so far to occur in the geological record of Sumatra. The occurrence of *B. braunii* was previously also discussed as an important organic matter component of oil shale deposited in Kiliran Sub-basin (Carnell et al., 1998).

In the present study, palynological and organic geochemical approaches are carried out to obtain more understanding of the occurrence of *B. braunii* in the Kiliran oil shale. The presence of the algal races will be unraveled from the distribution of biomarkers and the application of compound specific isotope analysis (CSIA) for carbon.

### **4.3. Geological Setting of the Study Area**

The study area is located in the Kiliran Sub-basin, one of the source rock depocenters in the arbitrary boundary between Central and South Sumatra Basins (Figure 4.1a). The enlarged area in Figure 4.1b shows some sub-basins in the arbitrary boundary including the Kiliran Sub-basin. The sub-basins are referred as part of Central Sumatra Basin, since they show analogous sediment succession (Wain and Jackson, 1995; Carnel et al., 1998).

#### 4.3.1. Central Sumatra Basin

The geological setting and history of Central Sumatra Basin have been described in detail e.g. by de Coster (1974), Williams et al. (1985) and Doust and Noble (2008). This rift basin is situated in a tectonically active region as a result of the Indian-Australian plate subduction beneath the Eurasian plate during Late Eocene-Oligocene. It consists of many troughs and grabens which show analogous sedimentary successions. Tectonic events, sedimentation rates, isostatic subsidence and eustatic sea level changes have been proposed as controlling factors for Tertiary sedimentation in the basin (de Coster, 1974). The generalized tectonostratigraphy of the Central Sumatra Basin is shown in Figure 4.2a. Brown Shale Fm contains the most important source rocks for the occurrence of oil in the basin. It was deposited in deep and shallow anoxic lacustrine environments during rapid rift development in Late Eocene. Most of the source rocks are mature especially those that occur in basin centers/deep grabens.

#### 4.3.2. Geology of the Kiliran Sub-basin

Kiliran Sub-basin has been regarded as a small rift basin formed during Late Eocene (Carnell et al., 1998). The morphology of the sub-basin is uncertain, since it has been integrated into the Barisan compressional belt and is now fragmented and faulted on both flanks. It had also been thought to terminate abruptly against the Pre-Tertiary Timpe lineament (Wain and Jackson, 1995). Further geological mapping and drilling programs carried out by the Indonesian Center for Geological Resources (PSDG) in 2006 revealed the occurrence of thick oil shale sequences in Padanglawas graben (Figure 4.1b) in the southern part of the Timpe fault. It is thought as the extension of Kiliran Sub-basin.

The general sediment succession of the Kiliran Sub-basin based on Carnell et al. (1998) and PSDG (2006) is presented in Figure 4.2b. The pre-graben paleosol most probably corresponds to the Lower Red Beds Fm. It is composed of carbonaceous and grey mudstones with locally red and green mottles. Above the paleosol, coal beds varying from thin to 17.5 m thick were deposited in a slowly subsiding reed swamp. A more rapid subsidence rate later resulted in the deposition of algal-rich coal interbeds which pass laterally into freshwater carbonates. A conformably lithofacies change occurred by the deposition of >90 m thick brown to grey colored calcareous shales. Sedimentological appraisal of well exposed shales in the northwestern tip of Kiliran graben suggests a shallow lake setting (10-50 m deep) which

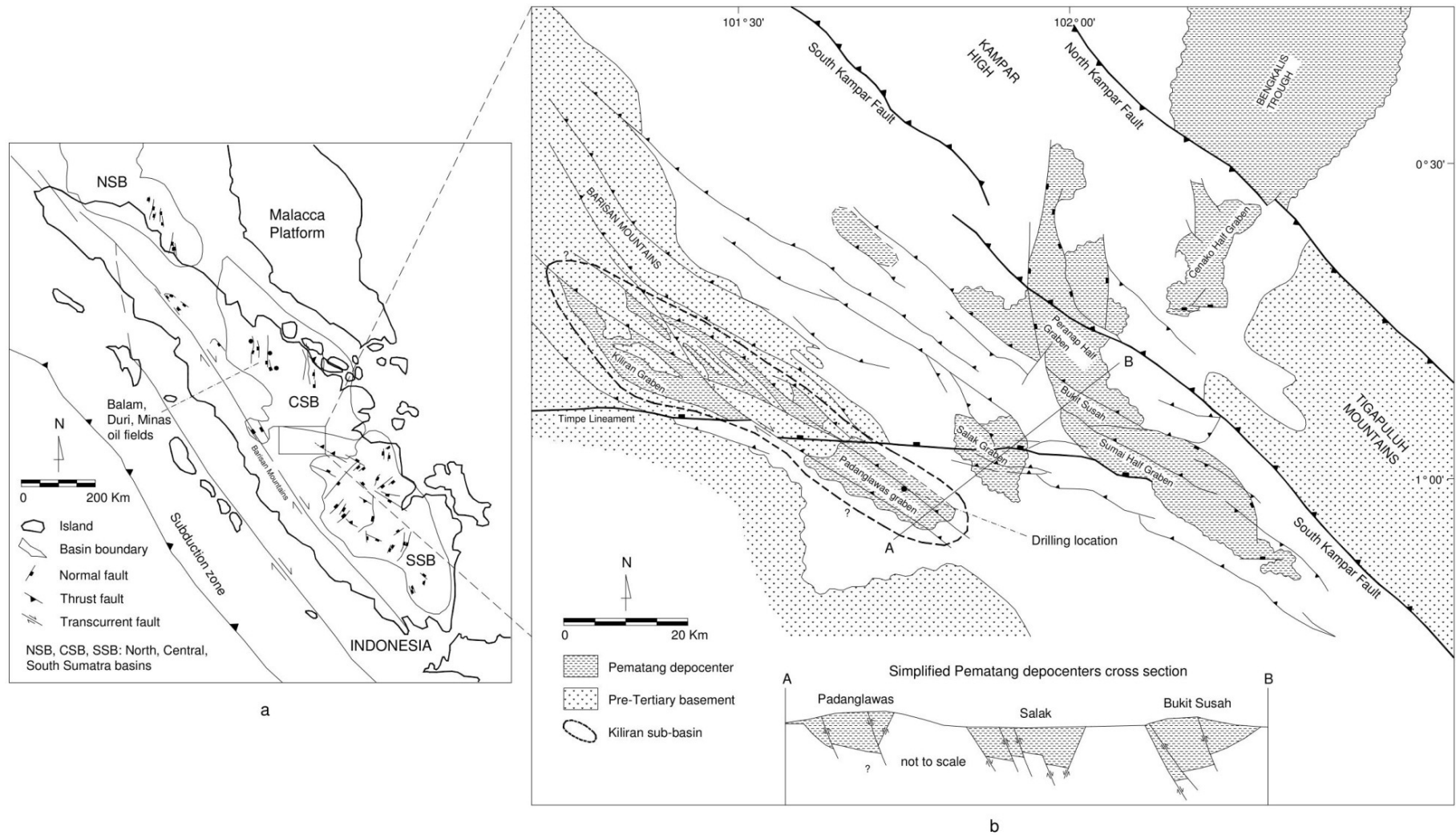


Figure 4.1. Map of Sumatra Basins with main graben structures (modified after Darman and Sidi, 2000) (a). Enlarged map of the arbitrary boundary between Central and South Sumatra Basins containing Pematang depocenters, and the drilling location in Padanglawas graben (modified after Wain and Jackson, 1995 and PSDG, 2006) (b).

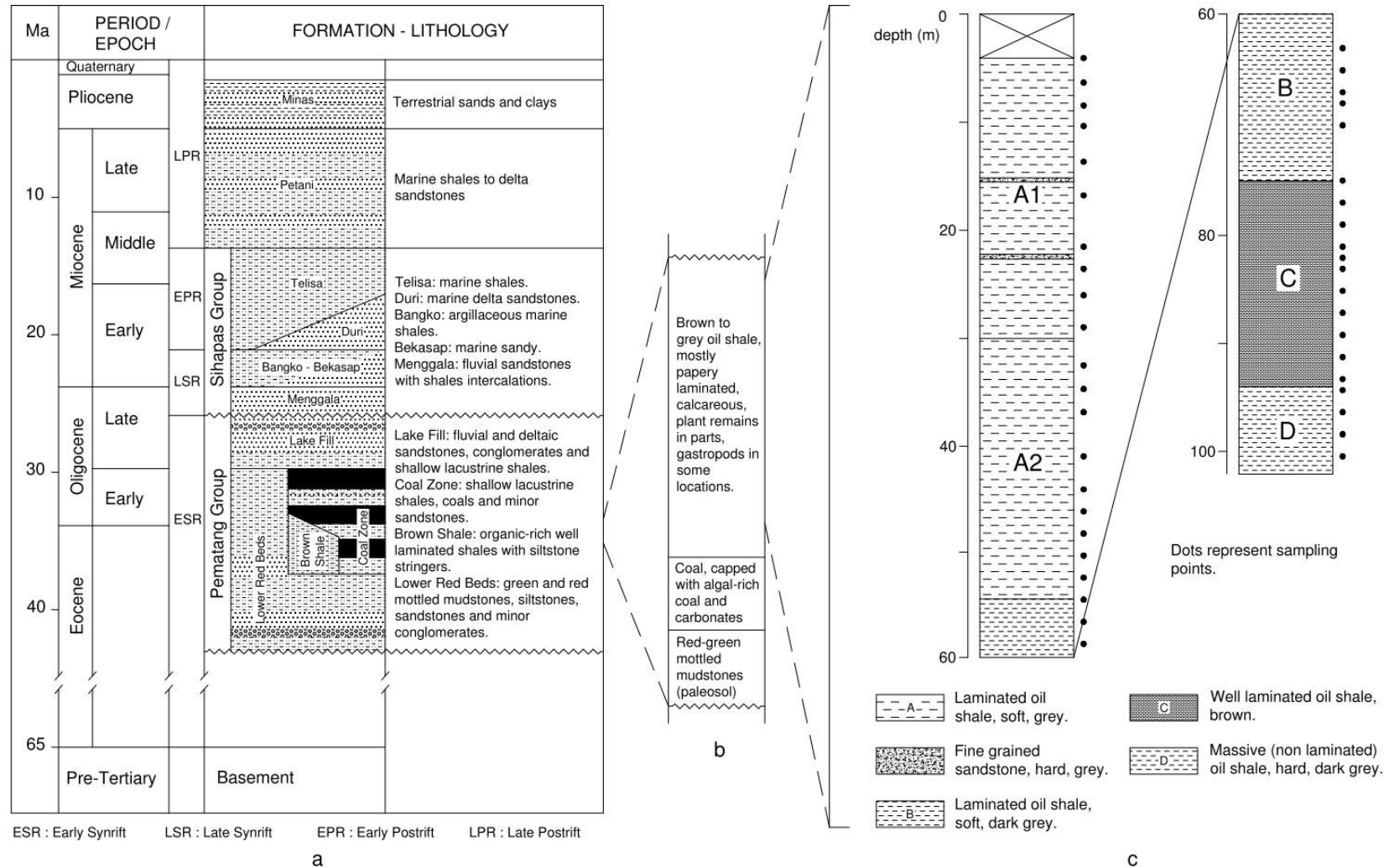


Figure 4.2. Generalized stratigraphic column of Central Sumatra Basin (adopted from Williams et al., 1985 and Doust and Noble, 2008) (a) and Kiliran Sub-basin (modified after Carnell et al., 1998 and PSDG, 2006) (b), and drill core profile of oil shale in Padanglawas graben of Kiliran sub-basin (c).

exhibit anoxic depositional environments. The presence of abundant gastropods and bioturbation in the uppermost part of the profile was interpreted to indicate intermittently oxic conditions of sediment deposition (Carnell et al., 1998). There is no exposure which corresponds to the Oligocene Lake Fill Fm and younger lithofacies in this area.

#### 4.4. Sample Material and Methods

##### 4.4.1. Sample material

Forty two samples were collected from a 102 m long drilling core available in the depository warehouse of PSDG, Bandung, Indonesia. The core was drilled in Padanglawas graben of Kiliran Sub-basin. Gastropods and bioturbation are not observed in the entire oil shale core. Plant remains are occasionally present in minor amount as woody organic detritus and leaves. The sediment profile of the core drilling and the sampling positions in the core are shown in Figure 3.2c. The vertical section consists of fine-grained shales with the following variation of the physical characteristics:

- a. soft, grey and well-laminated shale in the upper part (section A), thin fine sandstone intervals are present in the upper part
- b. soft, dark grey and well-laminated shale (section B)
- c. soft, brown and well-laminated shale (section C)
- d. hard, dark grey and non-laminated shale in the lowermost part (section D).

Section A is further divided into A1 and A2 based on geochemical composition (see below).

##### 4.4.2. Palynological analysis

Palynological processing was carried out at the Natural History Museum of London, UK. The samples were treated with HCl (37% aq.), and HF (40% aq.) in alternating steps to remove carbonates and silicates, respectively, and, after washing to neutrality, sieved with a 15 micrometer mesh sieve. Organic matter particles were counted at minimum 300 points using a transmitted-light microscope at a 400x magnification. In the present study, only the abundance of palynomorph of *B. braunii* will be presented to compare with geochemical data.

#### 4.4.3. Biomarker analysis

Twenty five grams of pulverized oil shale sample material (<63 micron) were extracted for 24 hours in a soxhlet extraction apparatus using 200 ml dichloromethane (DCM) as solvent. The extract was then separated into four fractions using column chromatography (1.5 cm diameter) over 14 grams activated silica gel. Sequential elution was performed to obtain fractions of saturated hydrocarbons, aromatic hydrocarbons, ketones/esters and more polar compounds using 40 ml n-hexane, 100 ml of n-hexane/DCM (9/1 v/v), 40 ml DCM and 40 ml methanol, respectively. In the present study, saturated and aromatic hydrocarbon fractions were analyzed by gas chromatography and mass spectrometry (GC-MS) using a Thermo Scientific Ultra series gas chromatograph coupled to a Thermo Scientific DSQ II mass spectrometer. GC separation of the compounds was achieved using a Thermo Scientific TR-5MS fused silica capillary column (30 m x 0.25 mm ID x 0.25  $\mu$ m film thickness). The oven temperature was programmed from 60 to 320 °C at a rate of 4 °C /min, with a 35 min isothermal period at 320 °C. The samples were injected in the splitless mode with the injector temperature at 280°C. Helium was used as carrier gas. The mass spectrometer was operated in the electron impact mode (EI) at 70 eV ionization energy. Mass spectra were obtained by scanning from 50 to 600 daltons at a cycle time of 1 second. For data processing, the Xcalibur Qual Browser software was used. Per-deuterated tetracosane and 1,1'-binaphthyl were used as internal standard for quantification of the saturated and aromatic hydrocarbons, respectively. In this study, only some significant compounds will be discussed.

#### 4.4.4. Compound-specific isotope analysis

Compound-specific isotope analysis (CSIA) for carbon of the saturated hydrocarbons was carried out in the Stable Isotope Laboratory of the Department of Applied Geosciences and Geophysics at the University of Leoben (Austria). A Thermo Fisher Delta V mass spectrometer connected to a Ultra series gas chromatograph, fitted with a similar column specification to that used in GC-MS analysis, were used for the analysis. The GC oven, injection conditions and carrier gas were also the same as those used in GC-MS analysis. Eluting compounds from the GC were converted to CO<sub>2</sub> in a combustion oven and measured relative to a reference CO<sub>2</sub>. The  $\delta^{13}\text{C}$  values were reported relative to the Pee Dee Belemnite (PDB) standard. An *n*-alkane carbon isotope external standard mixture (*n*-C<sub>15</sub>; *n*-C<sub>20</sub>; *n*-C<sub>25</sub>) was used for the control of the analytical results.

## 4.5. Results

### 4.5.1. Biomarkers

The total ion chromatogram (TIC) from GC-MS analysis of saturated hydrocarbon fraction obtained from the solvent extract of the representative sample G-32 is shown in Figure 4.3a. The mass chromatogram of  $m/z$  57 obtained from the saturated hydrocarbon fraction is presented in Figure 4.3b. The TIC of the aromatic hydrocarbon fraction from the same sample is shown in Figure 4.3c. Des-A-ursane (Urs) is present in low amount, ranging from ~0 to 14.6 with an average value of 3  $\mu\text{g/g}$  TOC (Figure 4.4a). The proportion of *B. braunii* varies from 3 to 16% with an average value of 8% and is presented in Figure 4.4b to compare with concentration variation of individual biomarkers. The abundances of some *n*-alkanes, pristane (Pr), phytane (Ph) and lycopane (Ly) and related parameters along the profile are shown in Figure 4.4c-i. Two compounds in the high boiling point range of the aromatic hydrocarbon fraction shown in Figure 4.3c consist of isorenieratane (Is), a specific biomarker for green sulfur bacteria (e.g. Sinninghe Damsté et al., 2001) and a carotenoid derivative (Cd). Both compounds are discussed with respect to their carbon isotopic compositions. The detailed organic geochemical data are presented in Appendix 4.

#### 4.5.1.1. *n*-Alkanes

The *n*-alkanes observed in the oil shale range from  $\text{C}_{14}$  to  $\text{C}_{35}$  showing odd over even predominance (Figure 4.3b) in almost all samples. A slightly bimodal distribution of *n*-alkanes is recognized maximizing at  $\text{C}_{17}$  and  $\text{C}_{27}$  for short and long chains *n*-alkanes respectively. Long chain *n*-alkanes in the range  $\text{C}_{25}$ - $\text{C}_{30}$  show generally higher concentrations in sections A and B and lower concentrations in sections C and D. Their concentrations decrease upwards in section A. The concentration of  $\text{C}_{27}$  *n*-alkane (heptacosane) is dominant in almost all samples and much higher compared to all other *n*-alkanes. The concentration variation of the  $\text{C}_{27}$  *n*-alkane along the profile is shown in Figure 4.4c. Its concentration ranges from 30.1 to 393.7 with an average value of 147.9  $\mu\text{g/g}$  TOC. The longer chain *n*-alkanes ( $>\text{C}_{30}$ ), especially odd-numbered, show a different distribution profile. Their concentrations are generally in parallel and increase upwards successively along the profile. The concentration profile of one of these *n*-alkanes ( $\text{C}_{33}$ ) is shown in Figure 4.4d. Its concentration varies from ~0 to 32.1 with an average value of 8.6  $\mu\text{g/g}$  TOC. The carbon preference index (CPI) based on Bray and Evans



(1961) is determined involving C<sub>24</sub>-C<sub>34</sub> *n*-alkanes. Higher CPI values (>1.0) reflect an odd over even predominance of the long chain *n*-alkanes. The CPI values range from 2.2 to 6.6 (Figure 4.4e). The short and mid chain *n*-alkanes (C<sub>14</sub>-C<sub>24</sub>) show no systematic concentration variation along the profile (not shown).

#### 4.5.1.2. Acyclic isoprenoids

Pristane and phytane are dominant compounds in the oil shale. Pristane concentrations range from 51.4 to 359.0 averaging at 142.6 µg/g TOC (Figure 4.4f). Phytane is less abundant and varies from 34.5 to 173.6 with an average value of 76.2 µg/g TOC (Figure 4.4f). Their concentration variation along the profile is parallel with no vertical variation tendency. They show consistently higher abundances in section B. The Pr/Ph ratio varies from 1.3 to 2.4 with an average value of 1.9 (Figure 4.4g). Lycopane is the only long chain acyclic isoprenoid identified in the Kiliran oil shale. The concentration varies from ~0 to 54.7 averaging at 9.2 µg/g TOC (Figure 4.4h). Lycopane is not detectable in all samples and shows generally a decreasing concentration upwards in the profile. The ratio of lycopane relative to C<sub>31</sub> *n*-alkane provides values from ~0 to 3.6 with a tendency of increasing values towards the bottom of the profile (Figure 4.4i).

#### 4.5.2. Compound-specific carbon isotopic composition

CSIA measurements were carried out on the saturated hydrocarbon fractions of samples G-30, G-32, G-50 and G-74 and the aromatic fraction of sample G-32. The results are listed in Table 2. The δ<sup>13</sup>C values of *n*-alkanes, Pr and Ph of sample G-32 are mostly higher than those of the other samples. The variation of δ<sup>13</sup>C values with chain length of *n*-alkanes is shown in Figure 4.5. The δ<sup>13</sup>C of *n*-alkanes for sample G-32 are about -29.0 to -33.9‰, whereas those for samples G-30, G-50 and G-74 are -29.3 to -35.2‰, -30.7 to -34.9‰ and -30.1 to -34.5‰ respectively. Enrichment of about 2‰ for C<sub>27</sub> *n*-alkane is observed in samples G-50 and G-74. Significant δ<sup>13</sup>C differences between odd (lighter) and even (heavier) carbon numbered mid chain *n*-alkanes are shown in case of sample G-32. δ<sup>13</sup>C Values of pristane and phytane are close to those of *n*-alkanes in all samples. The δ<sup>13</sup>C values of pristane show consistently heavier values than those of phytane. Moderate differences of δ<sup>13</sup>C values of pristane and phytane are observed, 1.8, 2.8, 1.6 and 1.1‰ for samples G-30, G-32, G-50 and G-74, respectively.

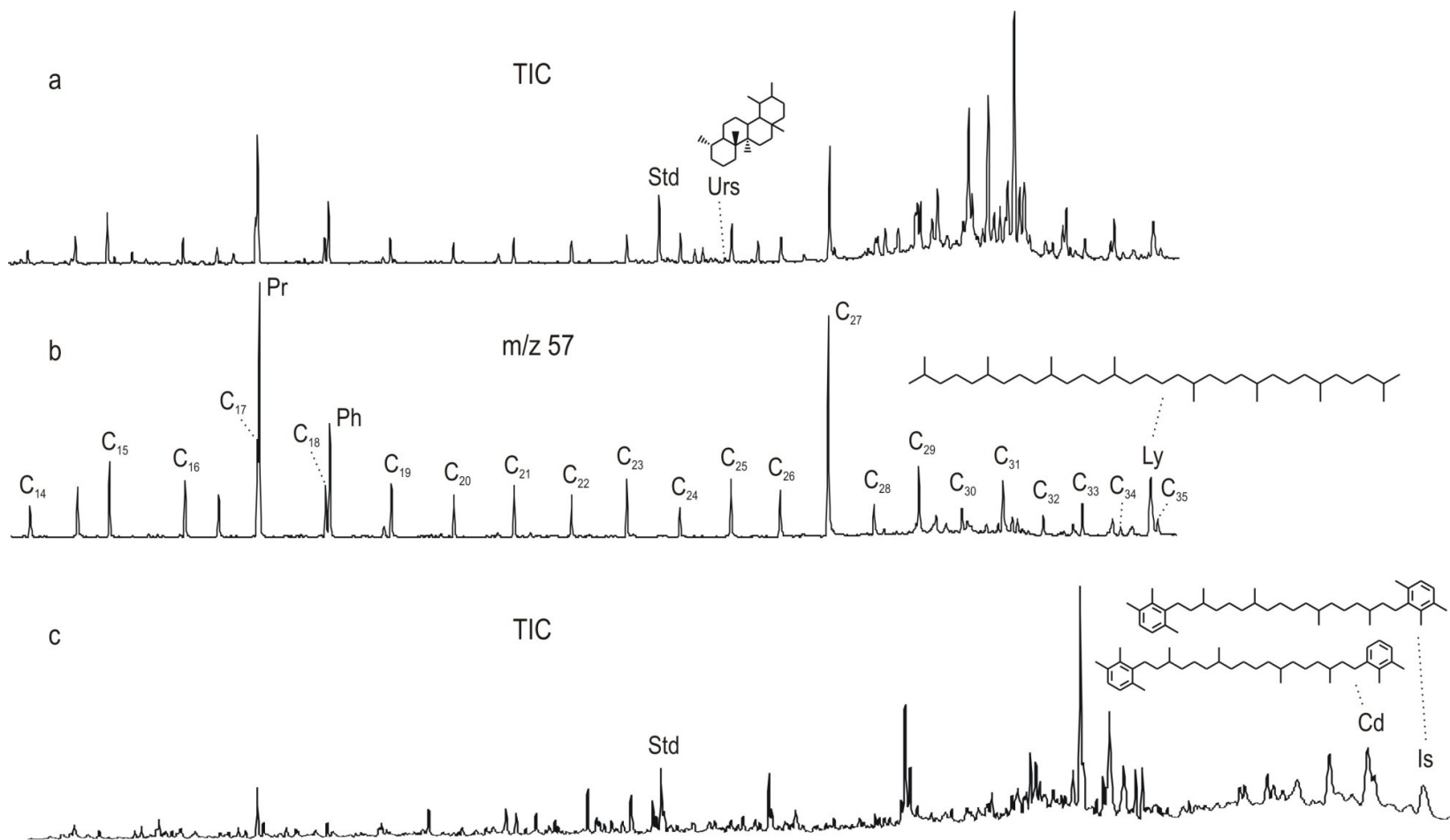


Figure 4.3. Total ion current (a) and mass chromatogram of  $m/z$  57 (b) of the saturated hydrocarbon fraction, and total ion current (c) of the aromatic hydrocarbon fraction of sample G-32. Abbreviations: Std: internal standard, Urs: des-A-ursane, carbon numbers:  $n$ -alkanes, Pr: pristane, Ph: phytane, Ly: lycopane, Cd: carotenoid derivative, Is: isorenieratane.

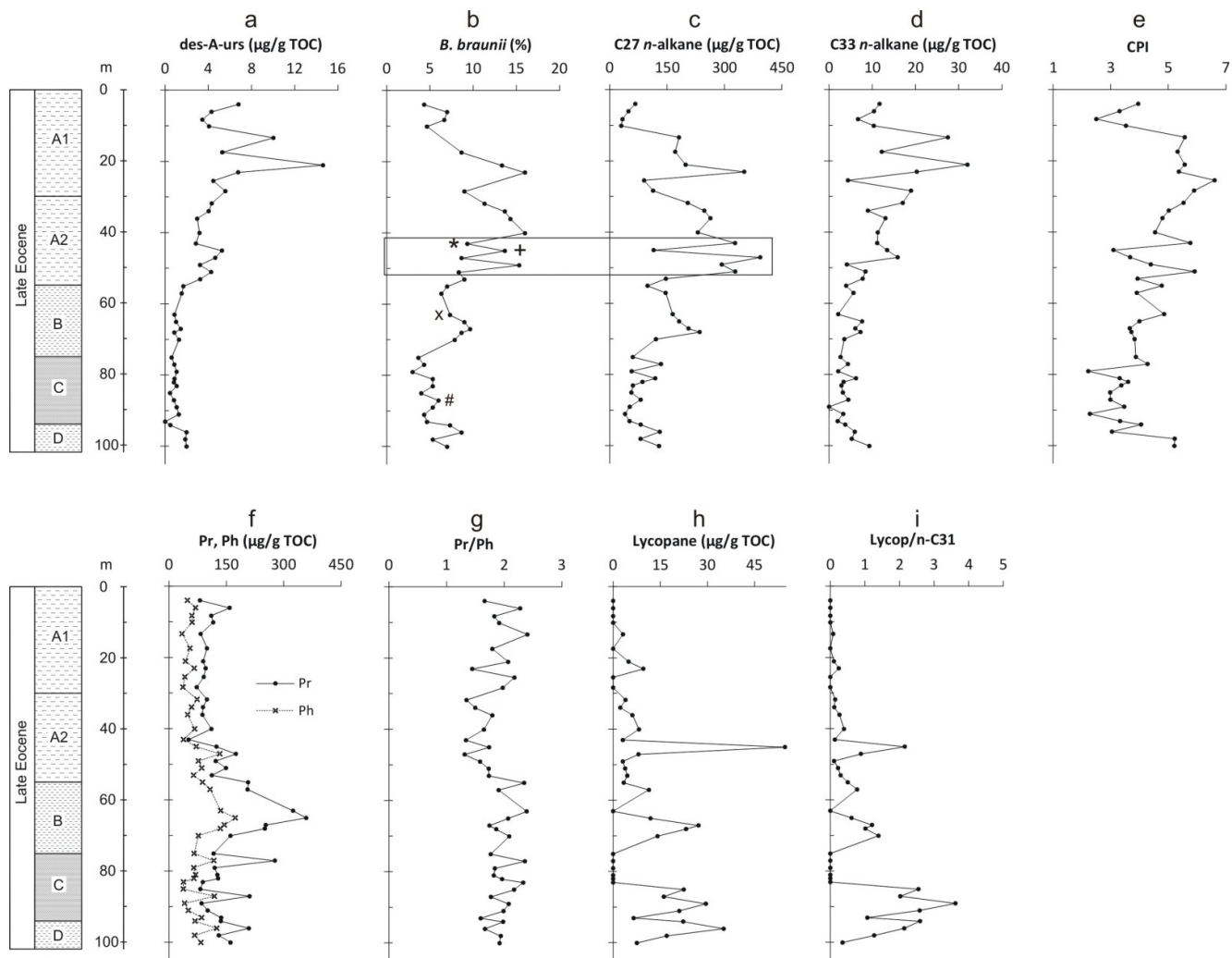


Figure 4.4. Vertical distributions of organic components in the Kiliran oil shale showing des-A-ursane (a), *B. braunii* palynomorph (b),  $\text{C}_{27,33}$  n-alkanes (c,d), CPI (e), Pr and Ph (f), Pr/Ph (g), lycopane (h) and lycopane/ $\text{C}_{31}$  n-alkane (i). Signs (a) denote samples: \* (G-30), + (G-32), x (G-50), # (G-74). The rectangular covers samples showing opposite distribution between *B. braunii* palynomorph and  $\text{C}_{27}$  n-alkane. The detailed organic geochemical data are presented in Appendix 4.

$\delta^{13}\text{C}$  Values of lycopane could only be measured from sample G-32 and show a remarkably significant enrichment in  $\delta^{13}\text{C}$  (-17.2‰). In the other three samples (G-30, G-50 and G-74) lycopane concentrations were too low. Isorenieratane and the other carotenoid derivative show  $\delta^{13}\text{C}$  values of -24 and -35.1‰, respectively.

Table 2. Carbon isotopic composition of individual compounds identified in saturated hydrocarbon fractions from 4 samples of Kiliran oil shale.

Compound	$\delta^{13}\text{C}$ (‰)			
	G-30	G-32	G-50	G-74
Pristane	-32.3	-28.5	-28.6	-29.8
Phytane	-34.1	-31.3	-30.2	-30.9
$\Delta\text{Pr-Ph}$	1.8	2.8	1.6	1.1
<i>n</i> -Alkanes:				
C <sub>15</sub>		-30.2		
C <sub>16</sub>		-29.0		
C <sub>17</sub>	-32.3	-29.5	-32.4	-31.4
C <sub>18</sub>	-30.4	-29.0	-30.9	-30.1
C <sub>19</sub>	-33.0	-30.5	-33.7	-32.9
C <sub>20</sub>	-29.3	-29.9	-31.2	-31.3
C <sub>21</sub>	-34.2	-33.5	-34.4	-34.0
C <sub>22</sub>	-33.0	-30.4	-33.1	-33.3
C <sub>23</sub>	-34.7	-33.9	-34.9	-34.0
C <sub>24</sub>	-32.3	-30.5	-33.5	-32.3
C <sub>25</sub>	-34.8	-32.2	-33.8	-34.5
C <sub>26</sub>	-34.2	-31.3	-32.9	-33.4
C <sub>27</sub>	-33.5	-31.0	-30.7	-31.4
C <sub>28</sub>	-35.2	-29.7	-32.6	-33.9
C <sub>29</sub>	-33.5	-30.8	-32.9	-33.6
Lycopane		-17.2		
Carotenoid derivative		-35.1		
Isorenieratane		-24.0		

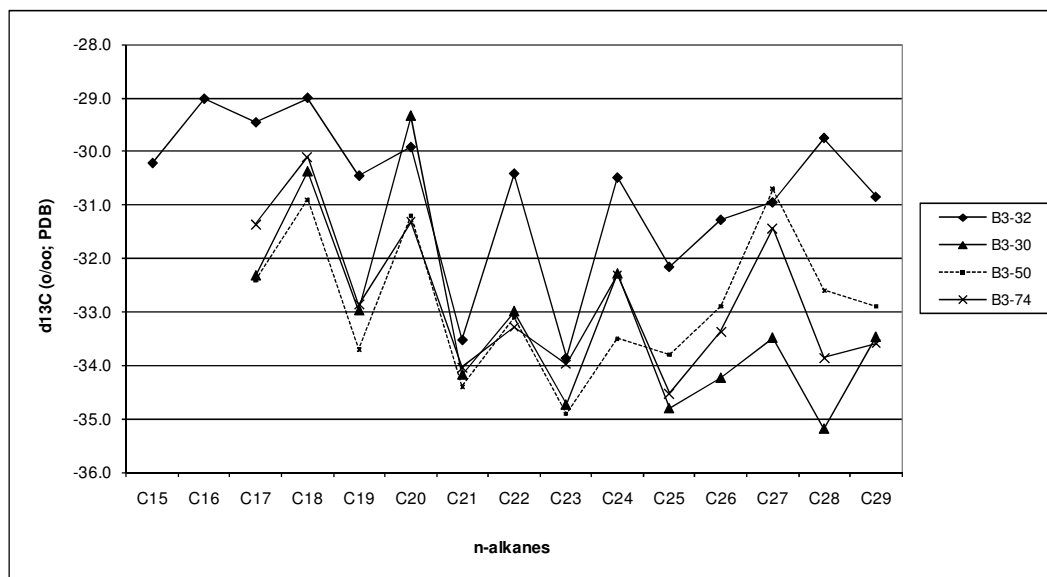


Figure 5. Carbon isotopic composition of *n*-alkanes (C<sub>15</sub>-C<sub>29</sub>) in saturated hydrocarbon fractions obtained from 4 representative oil shale samples.

## 4.6. Discussions

### 4.6.1. *n*-Alkanes

*n*-Alkanes in oil shales can originate from various biological sources. The wide range of CPI values (Figure 4.4e) confirms the presence of different sources contributing to the long chain *n*-alkanes. CPI is usually dependent on maturity, but for the studied oil shale section a wide variation of the maturity level can be excluded. Vitrinite reflectance values of about  $0.25\pm 0.03\%$  (PSDG, 2006) and  $T_{\max}$  values from Rock-Eval data around  $430\pm 4^{\circ}\text{C}$  (PSDG, 2006; Widayat et al., unpublished) with no variation trends along the oil shale profile suggest uniform immaturity. Long chain *n*-alkanes ( $>C_{25}$ ) with odd over even predominance have been reported to originate from epicuticular waxy coatings of vascular plants (e.g. Eglinton and Hamilton, 1967) and some common lacustrine green and blue-green algae including *B. braunii* (Gelpi et al., 1970; Moldowan et al., 1985; Lichtfouse et al., 1994). Algae and photosynthetic bacteria commonly also account for short chain *n*-alkanes ( $C_{15}$ - $C_{19}$ ) resulting in a bimodal distribution of *n*-alkanes (Gelpi et al., 1970; Moldowan et al., 1985; Cranwell et al., 1987). Leaves of some C3 trees, leaves and roots of some C4 grasses, certain bacteria and fungi have also been reported as the source of short chain *n*-alkanes, usually characterized by even over odd predominance (Tu et al., 2000; Kuhn et al., 2010). Mid-chain *n*-alkanes with an odd over even predominance are commonly derived from submerged and floating macrophytes (Ficken et al., 2000; Aichner et al., 2010), some lacustrine algae and photosynthetic bacteria (Gelpi et al., 1970; Peters et al., 2005b).

The presence of zigzag pattern of  $\delta^{13}\text{C}$  values comparing *n*-alkanes with odd and even carbon numbers has sometimes been related to the contribution of *n*-alkanes from higher plants.  $\delta^{13}\text{C}$  enrichment of odd-numbered relative to even-numbered *n*-alkanes beyond  $C_{21}$  or  $C_{23}$  chain length was reported to occur in some higher plants (e.g. Collister et al., 1994; Chikaraishi and Naraoka, 2003, 2007; Aichner et al., 2010). On the other hand, the relative depletion of  $\delta^{13}\text{C}$  values of odd-numbered *n*-alkanes compared to even-numbered *n*-alkanes was also attributed to a contribution of terrestrial biomass (Murray et al., 1994; Schouten et al., 2001). The occurrence of such patterns was suggested to be due to different fractionation processes in the respective biosynthetic pathways of higher plants (see Chikaraishi and Naraoka, 2007). However, the zigzag pattern may also reflect multiple sources contributing to *n*-alkanes (Ishiwatari et al., 1994b).

In the present case, major origin of long chain *n*-alkanes (C<sub>25</sub>-C<sub>30</sub>) showing odd over even predominance with the exceptional high proportion of C<sub>27</sub> *n*-alkane from higher plants is unlikely. Terrigenous organic matter contributing to Kiliran oil shale has been considered to be less significant (Carnell et al., 1998; Widayat et al., unpublished), although the C<sub>27</sub> *n*-alkane is a dominant compound in most samples. Carbon isotopic compositions of the long chain *n*-alkanes (C<sub>25</sub>-C<sub>30</sub>) do not show zigzag pattern and exhibit two distinct patterns among the samples (Figure 4.5). *n*-Alkanes (C<sub>25</sub>-C<sub>29</sub>) in sample G-32 show their heaviest  $\delta^{13}\text{C}$  value at C<sub>28</sub>, whereas those from the other three samples each show the heaviest values at C<sub>27</sub> and lighter values for the two shorter and longer even-numbered homologues. The latter pattern is similar to that reported from Central Sumatra Basin (Balam and Duri) crude oils derived most probably also from Brown Shale Fm which have not been regarded to originate mainly from higher plants (Dowling et al., 1995). Carbon isotope data therefore confirm that the long chain *n*-alkanes were not derived mainly from higher plants. Moreover, C<sub>27</sub> *n*-alkane concentrations variation along the profile is mostly similar to *B. braunii* palynomorph abundance except for the part covered with rectangle in Figure 4.4b and 4.4c. This suggests that the long chain *n*-alkanes were derived mostly from *B. braunii*. The inconsistency of C<sub>27</sub> *n*-alkane and *B. braunii* distributions of samples in the part of the profile marked by the rectangle area and the presence of two distinct  $\delta^{13}\text{C}$  patterns of long chain *n*-alkanes may indicate different organisms contributing to this compound.

The *n*-alkanes with longer carbon chain length (>C<sub>30</sub>) likely originate mostly from higher plants considering the successive upwards increase of the abundances i.e. of C<sub>33</sub> *n*-alkane in the profile (Figure 4.4d). This is evident from the close similarity of the distribution profile of C<sub>33</sub> *n*-alkane and the des-A-triterpenoids (including des-A-ursane shown in Figure 4.4a) which are commonly attributed to an origin from higher plants (e.g. Huang et al., 2008). Additionally, the  $\delta^{13}\text{C}$  values of long chain *n*-alkanes (>C<sub>30</sub>) of the Balam and Duri oils reported by Murray et al. (1994) and Dowling et al. (1995) exhibit zigzag patterns between *n*-alkanes of odd and even carbon-numbers which have also been attributed to the contribution of higher plants.

The short and mid-chain *n*-alkanes (C<sub>14</sub>-C<sub>24</sub>) might be derived from various biological sources. Although the short-chain *n*-alkanes show zigzag  $\delta^{13}\text{C}$  pattern, higher plants as main sources of odd over even predominance of the short chain *n*-alkanes are uncommon. Biological sources, most likely algae and/or photosynthetic bacteria, which have relatively heavier and lighter  $\delta^{13}\text{C}$  proportions contributing to even and odd carbon numbered *n*-alkanes, respectively, might

consequently exist in the lacustrine system. Stronger zigzag patterns of  $\delta^{13}\text{C}$  values of odd and even-numbered mid chain *n*-alkanes of sample G-32 (about 4‰) indicate an origin from multiple sources including probably a minor contribution of higher plants (macrophytes).

#### 4.6.2. Acyclic isoprenoids

##### 4.6.2.1. Pristane and phytane

Pristane and phytane are ubiquitous in sediments and usually the most dominant compounds among the acyclic isoprenoids. The common origin of them is the phytyl side chain of chlorophyll a in phototrophic organisms and bacteriochlorophyll a and b in purple sulfur bacteria (e.g. Powell and McKirdy, 1973; Peters et al., 2005b). Didyk et al. (1978) proposed the relative proportion of pristane to phytane (Pr/Ph) to indicate redox conditions of depositional environments. However, additional sources, e.g. archaeobacterial membrane lipids (Chappe et al., 1982), tocopherols (Goossens et al., 1984) and methyltrimethyltridecylchromans (Li et al., 1995), also contribute to the presence of these isoprenoids, limiting the utility of Pr/Ph ratio as redox indicator (e.g. Rontani et al., 2010). In the present case, isorenieratane has been identified in all samples (not shown) suggesting the presence of euxinic condition during deposition of the oil shale. Therefore, the Pr/Ph variation along the profile might rather be related to the variation of biological sources than to changes of the bottom water redox conditions. Moreover, Peters et al. (2005b) suggested that differences of  $\delta^{13}\text{C}$  values of pristane and phytane from common source are usually not exceeding 0.3‰. In the Kiliran oil shale, the differences take up to 2.8‰, confirming multiple sources of the isoprenoids.

##### 4.6.2.2. Lycopane

Lycopane has commonly been found in recent lacustrine sediments and some Tertiary source rocks deposited under anoxic or euxinic, freshwater to brackish lacustrine environments (Freeman et al., 1990; Grice et al., 1998a; Peters et al., 2005b). This compound has also been reported to occur in recent marine sediments and source rocks deposited in anoxic marine environments (Brassell, 1990; Wakeham et al., 1993; Sinninghe-Damsté et al., 2003). The most common lycopane source is the  $\text{C}_{40}$  carotenoid lycopene that occurs ubiquitous in phytoplankton such as purple sulfur bacteria and certain marine algae and higher plants

(Schmidt, 1978; Freeman et al., 1990; Sinninghe-Damsté et al., 2003). Lycopane can also originate from the tetraterpenoid lycopadiene biosynthesized in *B. braunii* race L (e.g. Metzger and Largeau, 2005).

Lycopane cannot be considered as specific proxy for a certain biological source considering its widespread occurrence in various organisms and depositional environments. However the use of CSIA can help to unravel its origin. Significant  $\delta^{13}\text{C}$  enrichments of lycopane and other related compounds found in lacustrine systems have commonly been attributed to the contribution of *B. braunii* race L. Lycopane identified in Sdom Formation, Dead Sea having  $\delta^{13}\text{C}$  values of  $-21\text{‰}$  was suggested to originate from *B. braunii* (Grice et al., 1998a). Also from Messel oil shale the presence of carbon isotopically enriched lycopane ( $-20.9\text{‰}$ ) has been reported (Hayes et al., 1990) and was suggested to be caused either by the occurrence of substantially  $^{13}\text{C}$ -enriched DIC or by the presence of *B. braunii* (Sinninghe-Damsté et al., 2003).

The relative  $\delta^{13}\text{C}$  enrichment of *B. braunii*-derived compounds has previously been reported by some authors (e.g. Boreham et al., 1994, Dowling et al., 1995; Summons et al., 2002). The enrichment has been suggested to be due to the thick outer walls of the alga limiting the diffusion rates for  $\text{CO}_2$ . Under such conditions, the isotopic fractionation during photosynthesis may not be fully expressed, resulting in a  $^{13}\text{C}$ -enriched biomass (Boreham et al., 1994). Alternatively, carbon fixation from bicarbonate, which has relatively more enriched  $\delta^{13}\text{C}$  than aqueous  $\text{CO}_2$ , may also increase the  $\delta^{13}\text{C}$  value of *B. braunii* biomass (Huang et al., 1999).

In the extracts from the Kiliran oil shale, the  $\delta^{13}\text{C}$  value of lycopane ( $-17.2\text{‰}$ ) is strongly enriched relative to all other compounds (Table 2). An even stronger enrichment was previously observed for botryococcanes, specific biomarkers for *B. braunii* race B, in Balam, Duri and Minas oils ( $-10$  to  $-11\text{‰}$ ) reported by Dowling et al. (1995). However, these biomarkers and other related isoprenoids could not be detected in the studied samples. To our knowledge, the  $\delta^{13}\text{C}$  value of  $-17.2\text{‰}$  is the heaviest value for lycopane reported in geological record so far. This suggests that the lycopane was derived mostly from *B. braunii* race L.



#### 4.6.3. Unusual C<sub>27</sub> *n*-alkane distribution

Specific biomarkers for *B. braunii* such as botryococcanes for the race B (Moldowan and Seifert, 1980), polymethylsqualanes (Summons et al., 2002) and their related compounds are not recognized in the studied samples. Since lycopane is not present in all samples, the presence of *B. braunii* race L throughout the whole oil shale sequence is unlikely. Apart from *B. braunii* race L additionally *B. braunii* race A is present in the oil shale as indicated by the general parallel distribution between *Botryococcus* palynomorphs and C<sub>27</sub> *n*-alkane. This compound is present in unusual high concentrations relative to the other *n*-alkanes. Metzger et al. (1997) reported the predominance of C<sub>27</sub>, C<sub>29</sub> or C<sub>31</sub> *n*-alkanes from different strains of *B. braunii* race A.

The high input of the C<sub>27</sub> *n*-alkane from *B. braunii* race A is also supported by its enrichment in  $\delta^{13}\text{C}$  (up to 2‰) relative to the other adjacent even and odd carbon numbered *n*-alkanes shown in samples G-74, G-50 and G-30 (Figure 4.5). Such enrichment is not observed in sample G-32 despite of the abundance of the algal palynomorph. Race L might be the dominant *B. braunii* in this sample as supported by the high concentration of lycopane (Figure 4.4h).

#### 4.6.4. Paleoenvironmental implications

##### 4.6.4.1. Lycopane distribution

The occurrence of lycopane in sediments may be controlled by the productivity of photoautotrophic organisms and by the presence of an anoxic depositional environment. Corresponding to the latter, Sinninghe-Damsté et al. (2002) discussed that lycopane has been considered as a relatively labile biomarker in an oxic environment and would be degraded in a greater extent than *n*-alkanes. This is because the *n*-alkanes are preferentially adsorbed to larger particles preventing effective degradation. The proportion of lycopane relative to C<sub>31</sub> *n*-alkane derived from higher plants has therefore been applied as a proxy for oxicity of the depositional environment in the Arabian sea.

The lycopane concentration in the oil shale profile shows generally an upwards decrease (Figure 4.4h) and the lycopane/C<sub>31</sub> *n*-alkane ratio generally decreases upwards (Figure 4.4i).

The variation of the lycopane abundance in the oil shale profile can be interpreted to be a result of changes of the bottom water anoxicity. However, as mentioned above, the presence of euxinic environments during the deposition of the entire oil shale profile challenges this interpretation. Additionally, the lycopane concentration is highest in sample G-32, whereas those in the adjacent samples both below and above are very low (Figure 4.4h). In these samples, drastic changes of the depositional environment and rapid variation of the bottom water anoxicity are not supported by geochemical data. On the other hand, the decrease of the C<sub>27</sub> *n*-alkane concentration in sample G-32 indicates a substitution between *B. braunii* races A and L. Therefore, the variation of lycopane concentrations along the profile would rather reflect changes in the productivity of *B. braunii* race L.

Although many authors reported co-occurrence between species of *Botryococcus*, ecological preferences of each species including the *B. braunii* chemotaxonomic races remain unclear even in living population (e.g. Zhang et al., 2007). Ramírez and Corbacho (2005) reported a substitution between different *Botryococcus* species in response to water chemistry change (NH<sub>3</sub><sup>-</sup>, free CO<sub>2</sub>, alkalinity). In the present case, the generally different developments of *B. braunii* races A and L during the oil shale deposition might also indicate an alternation between them on the algal population, probably due to their specific water chemistry preferences.

#### 4.6.4.2. Carbon isotopic composition

The occurrence of isorenieratane in the Kiliran oil shale is important regarding its carbon isotopic composition. Isorenieratane has been used to reconstruct the  $\delta^{13}\text{C}$  of DIC at the chemocline of both past lacustrine and marine environments (van Breugel et al., 2005). In the Kiliran oil shale the  $\delta^{13}\text{C}$  value of isorenieratane (-24‰) is depleted by about 9‰ relative to the average of strongly enriched  $\delta^{13}\text{C}$  values of biomarkers from green sulfur bacteria (about -15‰; calculated from van Breugel et al., 2005). This indicates the presence of DIC depleted in <sup>13</sup>C at the chemocline of the former Kiliran lake. The <sup>13</sup>C-depleted DIC might occur not only at the chemocline, but also in the entire epilimnion zone leading to a general  $\delta^{13}\text{C}$  negative excursion of biomass of algae including *B. braunii*.

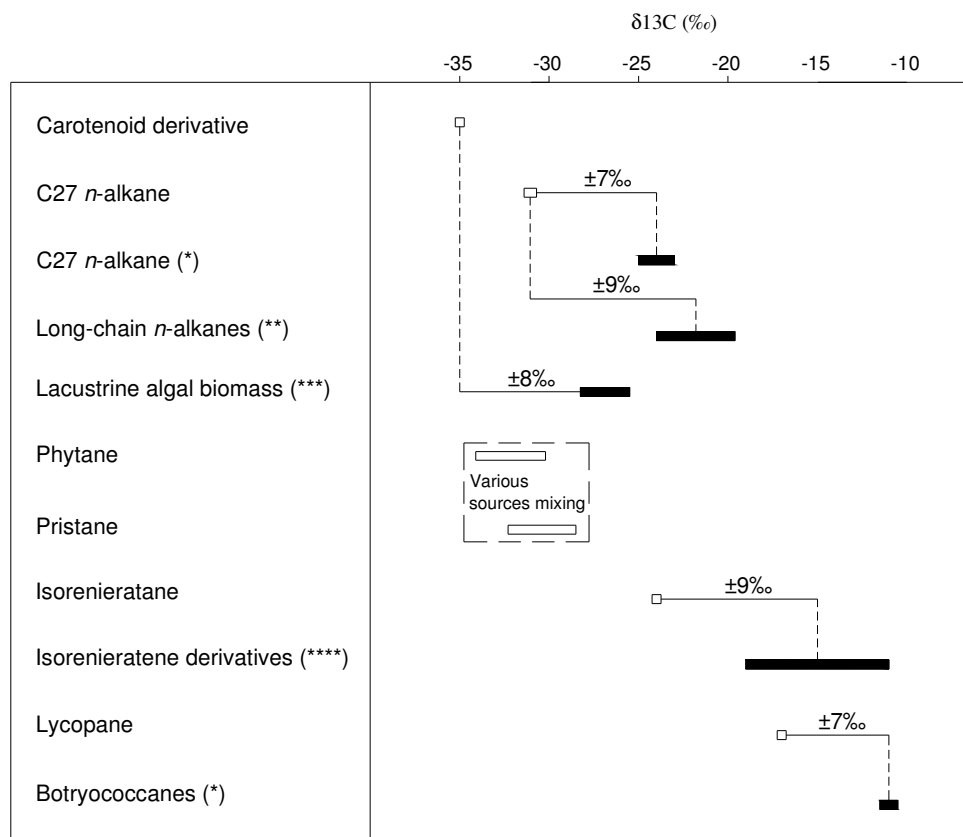


Figure 6. General  $\delta^{13}\text{C}$  depletion of about 7-9‰ in certain biomarkers of Kiliran oil shale (open rectangles) relative to respective common values reported in literatures (filled rectangles), \*: crude oils from Sumatra (Dowling et al., 1995), \*\*: torbanites from different paleogeographical locations (Audino et al., 2001; Grice et al., 2001), \*\*\* Meyers (1997, 2003), \*\*\*\*: isorenieratene derivatives (van Breugel et al., 2005). Pristane and phytane might be derived from mixing various sources having both depleted and enriched  $\delta^{13}\text{C}$ .

The general  $\delta^{13}\text{C}$  negative excursion is also recognized from other algal biomarkers summarized in Figure 4.6. The  $\delta^{13}\text{C}$  value of the carotenoid derivative (compound Cd), likely derived from common algae, is depleted by about 8‰ relative to common lacustrine algal biomass (-26 to -28‰; Meyers, 1997; 2003). The  $\delta^{13}\text{C}$  of the  $\text{C}_{27}$  n-alkane in samples G-74 and G-50 derived mainly from *B. braunii* race A exhibit depleted values of about -31‰. These values are about 7‰ lighter than those reported for  $\text{C}_{27}$  n-alkane in the Balam and Minas crude oils (about -24‰; Dowling et al., 1995). The  $\delta^{13}\text{C}$  values of  $\text{C}_{27}$  n-alkane of the Kiliran oil shale are also depleted by about 9‰ relative to long-chain n-alkanes of *B. braunii* race A-rich torbanites from different paleogeographical locations (-19 to -24‰; Audino et al., 2001; Grice et al., 2001). Although lycopane shows a heavy carbon isotopic composition (-17.2‰), the value is still depleted relative to the botryococcanes observed from the Balam, Duri and Minas crude oils (-10 to -11‰). In the present case, the  $\delta^{13}\text{C}$  values of botryococcanes are compared with the value of lycopane considering several reasons. First, although the lycopane and

botryococcanes have been reported from various sub-basins, they still originate from the same Brown Shale Fm of Central Sumatra Basin. Second, lycopadiene and botryococcones originate likely from the same biosynthetic pathways (Metzger et al., 1991), so that different  $\delta^{13}\text{C}$  values between them due to different isotopic fractionation during biosynthesis is unlikely (Grice et al., 1998a). Although the  $\delta^{13}\text{C}$  value of lycopane is the heaviest among those published in the geological record, it might still be possible that the lycopane could be as enriched as the botryococcanes in  $^{13}\text{C}$  where *B. braunii* race L in the Kiliran lake did not significantly fix  $^{13}\text{C}$ -depleted DIC.

Some of the biomarkers discussed above indicate a concomitant negative  $\delta^{13}\text{C}$  excursion, but the values for  $\text{C}_{27}$  *n*-alkane are quite different (about 14‰) with that of lycopane. The reason for this large difference is probably the presence of additional sources for  $\text{C}_{27}$  *n*-alkane having depleted  $^{13}\text{C}$  (i.e. higher plant and other algae). Additionally, different isotopic fractionation during biosynthesis of lycopane and  $\text{C}_{27}$  *n*-alkane has to be considered.

#### 4.7. Conclusions

Palynological analyses revealed the occurrence of *B. braunii* in varying abundance along the Kiliran oil shale profile. Biomarkers of this organism are recognized by organic geochemical analyses. The  $\text{C}_{27}$  *n*-alkane is known to be a specific biomarker for *B. braunii* race A. This compound is present in high abundance in the saturated hydrocarbon fractions and is by far exceeding the concentrations of other *n*-alkanes. The concentration variation of the  $\text{C}_{27}$  *n*-alkane along the profile is comparable to the abundance of *B. braunii* palynomorph. Carbon isotopic analysis for  $\text{C}_{27}$  *n*-alkane exhibits  $\delta^{13}\text{C}$  values of about -31‰, which are enriched up to 2‰ relative to the other long-chain *n*-alkanes. *B. braunii* race A is therefore suggested to be dominant in the algal population and generate mainly  $\text{C}_{27}$  *n*-alkane.

Lycopane is present in many of the studied oil shale samples but in lower concentrations compared to the  $\text{C}_{27}$  *n*-alkane. The carbon isotope measurement for lycopane exhibited a  $\delta^{13}\text{C}$  value of -17.2‰, which is much heavier than those values determined from other biomarkers. This suggests that this compound originates to *B. braunii* race L. The concentration of lycopane generally develops in opposite with the concentration of the  $\text{C}_{27}$  *n*-alkane. This

suggests that both of the *B. braunii* races generally bloom in alternation, probably due to different specific water chemistry preferences.

Isorenieratane is recognized in all samples and regarded to be derived from brown-pigmented green sulfur bacteria. Carbon isotope measurement for isorenieratane reveals  $\delta^{13}\text{C}$  value -24.0‰. This value is also depleted by about 9‰ relative to common  $\delta^{13}\text{C}$  values for green sulfur bacteria biomarkers. The depletion is attributed to the fixation of  $^{13}\text{C}$ -depleted DIC by the bacteria. The presence of  $^{13}\text{C}$ -depleted DIC is thought to occur not only at the chemocline, but also in the entire epilimnion, since a concomitant  $\delta^{13}\text{C}$  depletion of all biomarkers including those of algal biomass has been observed in the Kiliran oil shale (7-9‰).

## Chapter 5: Paleoecological changes during deposition of the Late Eocene Kiliran oil shale, Central Sumatra Basin, Indonesia

### 5.1. Abstract

Forty two samples from a 102 m long core of the Late Eocene Kiliran oil shale have been investigated to reconstruct paleoecological changes during the deposition. Palynological analysis exhibited the presence of *B. braunii* as the only morphologically preserved autochthonous organisms. Organic geochemical analysis reveals the occurrence of 30-norneohop-13(18)-ene and neohop-13(18)-ene as biomarkers of methanotrophic bacteria ( $\delta^{13}\text{C}$  about -45.2 to 50.2‰) in high amount. These bacteria played an important role in the former Kiliran lake with respect to carbon cycling. The other dominant biomarkers are  $\text{C}_{27}$  *n*-alkane ( $\delta^{13}\text{C}$  about -31‰) derived from *B. braunii* and 4-methylsterane ( $\text{C}_{28}$ - $\text{C}_{30}$ ) and 4-methyldiasterene ( $\text{C}_{28}$ ,  $\text{C}_{30}$ ) homologues ( $\delta^{13}\text{C}$  about -37‰). The latter compounds are hypothesized to originate from freshwater *Dinoflagellates* as organisms frequently reported in Central Sumatra Basin depocenters.

The  $\delta^{13}\text{C}$  values of bulk organic carbon range from -27.0 to -30.5‰. The  $\delta^{13}\text{C}$  variation is interpreted to reflect productivity changes in the lake. Higher values are attributed to higher productivity and vice versa. Calcium (Ca) is the most abundant element in the oil shale and shows variations along the profile, most likely reflecting alkalinity changes of the lake waters. The abundance of *B. braunii* in the organic matter assemblage and the concentration of 4-methylsterane and 4-methyldiasterene homologues in the saturated hydrocarbon fractions develop in opposite along the profile. This suggests that *B. braunii* and *Dinoflagellates* bloomed in alternation during the deposition of the sediment. *B. braunii* preferred less trophic and less alkaline environments, whereas *Dinoflagellates* preferred more trophic and more alkaline environments. Such alternations between both organisms due to water chemistry changes have previously been reported for other Eocene lake environments. Results from the present study support the hypothesis that the 4-methylsterane and 4-methyldiasterene homologues originate from freshwater *Dinoflagellates*.

## 5.2. Introduction

Brown Shale Formation (Fm) has been reported as the most important lacustrine petroleum source rocks in the Central Sumatra Basin (Williams et al., 1985; Wain and Jackson, 1995; Williams and Eubank, 1995). Palynofacies and organic geochemical studies were commonly carried out to characterize the organic matter by the authors. Algal amorphous organic matter is dominant in the Brown Shale Fm. Palynomorphs identified in the source rocks include *B. braunii*, *Pediastrum* and *Dinoflagellates*. They were regarded as the most responsible organisms for petroleum generation in the Central Sumatra Basin.

Although organic matter facies of the Brown Shale Fm have been widely discussed with respect to the three algae as the dominant contributors, bacterial assemblage contributing to the organic matter has been less studied. The Brown Shale Fm was deposited in relatively anoxic environments (e.g. Katz, 1991). In lakes with anoxic bottom water environments, bacteria are present and play important processes including methanogenesis and organic matter degradation with respect to carbon cycling (e.g. Hollander et al., 1993; Hollander and Smith, 2001). On the other hand, the Brown Shale Fm studies mostly dealt only on spot and spatial samples from different sub-basins. Palynofacies and organic geochemical studies based on detailed stratigraphic series of this formation have never been done.

The Kiliran oil shale is equivalent to the Brown Shale Formation (Fm) deposited in Kiliran Sub-basin, southeastern border of the Central Sumatra Basin. In the present study, the organic matter of this oil shale is investigated to reconstruct in detail the trophic level and paleoecological changes in detail during the deposition. Geochemical and palynological analyses are carried out to identify both algae and bacteria contributing to the oil shale.

## 5.3. Geological Setting of the Study Area

The Kiliran Sub-basin location is shown in Figure 5.1a. The enlarged area in Figure 5.1b shows various sub-basins in the arbitrary boundary including the Kiliran Sub-basin. The sub-basins have been referred as part of the Central Sumatra Basin, since they show analogous sediment successions (Wain and Jackson, 1995; Carnel et al., 1998).

### 5.3.1. Central Sumatra Basin

The geological setting and history of the Central Sumatra Basin have been described in detail e.g. by de Coster (1974), Williams et al. (1985) and Doust and Noble (2008). This rift basin is situated in a tectonically active region as a result of the Indian-Australian plate subduction beneath the Eurasian plate during Late Eocene-Oligocene. It consists of many troughs and grabens which show analogous sedimentary successions. Tectonic events, sedimentation rates, isostatic subsidence and eustatic sea level changes have been proposed as controlling factors for Tertiary sedimentation in the basin (de Coster, 1974). The generalized tectonostratigraphy of the Central Sumatra Basin is shown in Figure 5.2a. Brown Shale Fm contains the most important source rocks for the occurrence of oil in the basin. It was deposited in deep and shallow anoxic lacustrine environments during rapid rift development in Late Eocene. Most of the source rocks are mature especially those that occur in the basin center and deep grabens.

### 5.3.2. Geology of the Kiliran Sub-basin

Kiliran Sub-basin has been regarded as a small rift basin formed during Late Eocene (Carnell et al., 1998). The morphology of the sub-basin is uncertain, since it has been integrated into the Barisan compressional belt and is now fragmented and faulted on both flanks. It had also been thought to terminate abruptly against the Pre-Tertiary Timpe lineament (Wain and Jackson, 1995). Further geological mapping and drilling programs carried out by the Indonesian Center for Geological Resources (PSDG) in 2006 revealed the occurrence of thick oil shale sequences in Padanglawas graben (Figure 5.1b) in the southern part of the Timpe fault. It is thought as the extension of Kiliran Sub-basin.

In Figure 5.2b, the general sediment succession in Kiliran Sub-basin based on Carnell et al. (1998) and PSDG (2006) is presented. Pre-graben paleosol most probably corresponds to Lower Red Bed Fm. It is composed of carbonaceous and grey mudstones with locally red and green mottles. Above the paleosol, a coal bed varying from very thin to 17.5 m thickness was deposited in a slowly subsiding reed swamp. A more rapid subsidence rate occurred later by the deposition of algal-rich coal interbeds which pass laterally into freshwater carbonates. A conformably lithofacies change occurred by the deposition of the >90 m thick brown to grey colored shales. Sedimentological appraisal of well exposed shales in the northwestern tip of Kiliran graben suggests a shallow lake setting (10-50 m deep) which exhibit anoxic



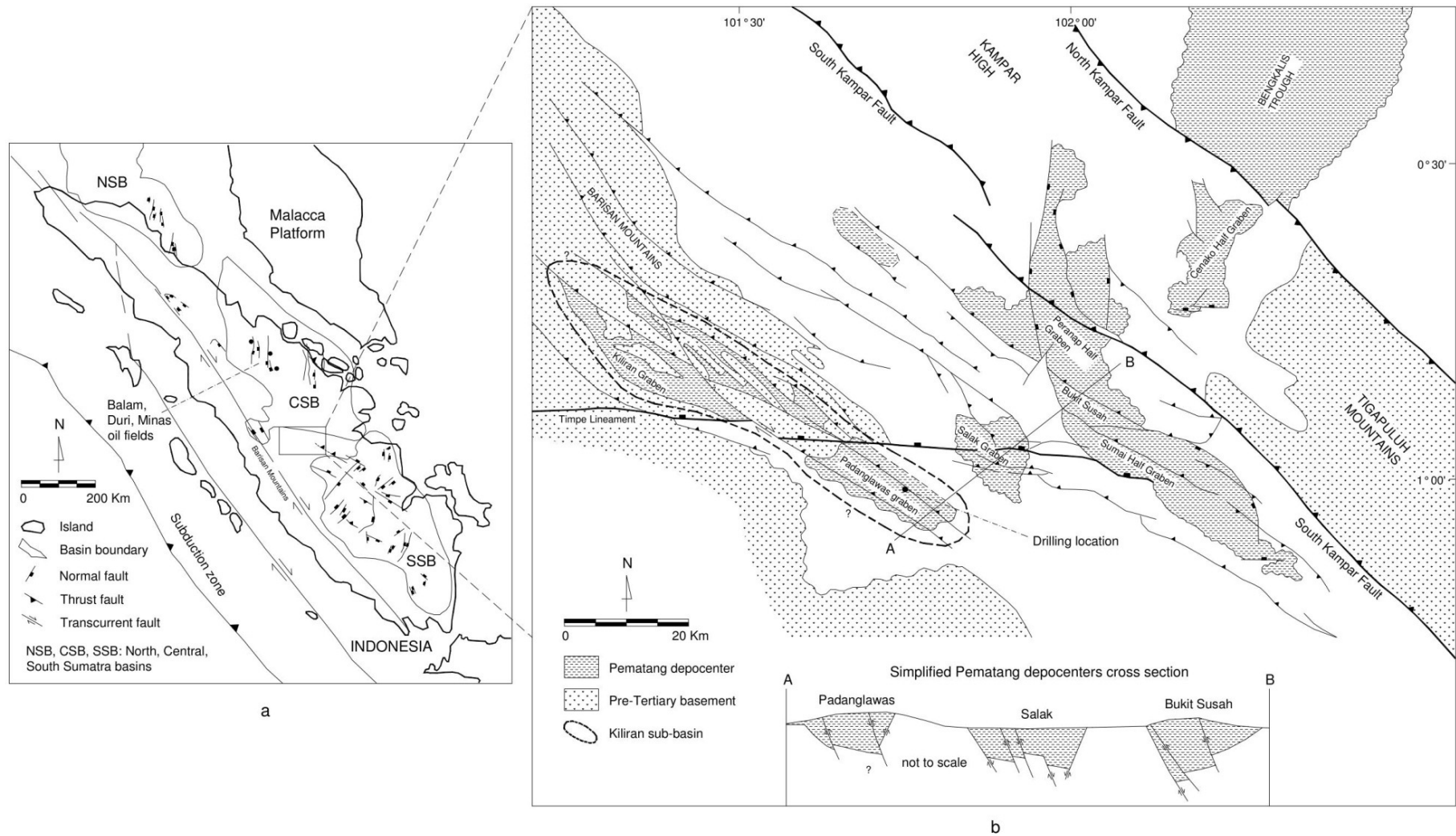


Figure 5.1. Map of Sumatra Basins with main graben structures (modified after Darman and Sidi, 2000) (a). Enlarged map of the arbitrary boundary between Central and South Sumatra Basins containing Pematang depocenters, and the drilling location in Padanglawas graben (modified after Wain and Jackson, 1995 and PSDG, 2006) (b).

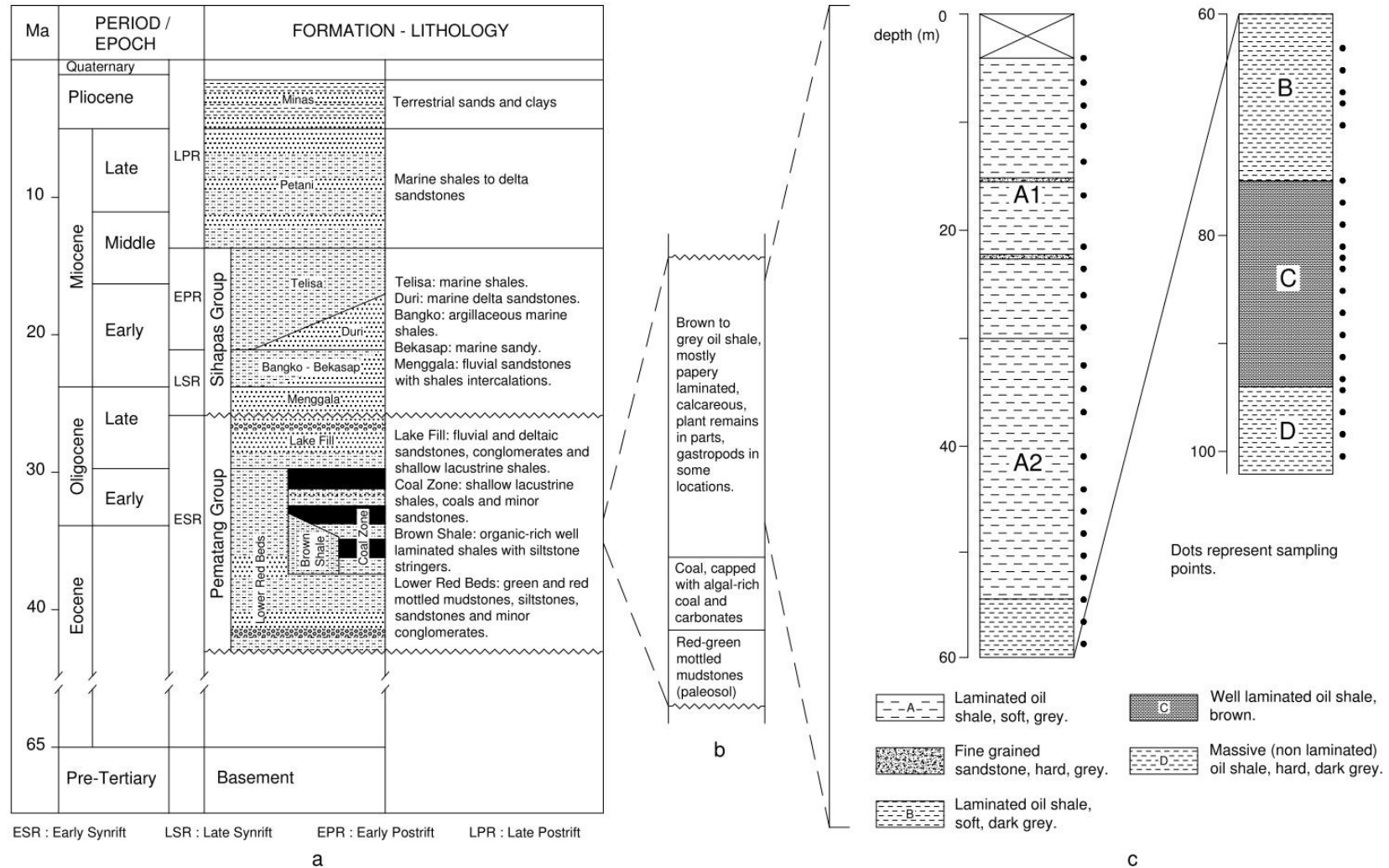


Figure 5.2. Generalized stratigraphic column of Central Sumatra Basin (adopted from Williams et al., 1985 and Doust and Noble, 2008) (a) and Kiliran Sub-basin (modified after Carnell et al., 1998 and PSDG, 2006) (b), and drill core profile of oil shale in Padanglawas graben of Kiliran sub-basin (c).

depositional environments. The presence of abundant gastropods and bioturbation in the uppermost part profile was interpreted to indicate intermittently oxic conditions of sediment deposition (Carnell et al., 1998). There is no exposure which corresponds to the Oligocene Lake Fill Fm and younger lithofacies in this area.

## 5.4. Sample Material and Methods

### 5.4.1. Sample material

Forty two samples were collected from a 102 m long drilling core (representing about 90 m thick oil shales) available in the depository warehouse of PSDG, Bandung, Indonesia. The core was drilled in Padanglawas graben of Kiliran Sub-basin. Gastropods and bioturbation are not observed in the entire oil shale core. Plant remains are occasionally present in minor amount as woody organic detritus and leaves. The sediment profile of the core drilling and the sampling positions in the core are shown in Figure 5.2c. The vertical section consists of fine-grained shales with the following variation of the physical characteristics:

- e. soft, grey and well-laminated shale in the upper part (section A), thin fine sandstone intervals are present in the upper part
- f. soft, dark grey and well-laminated shale (section B)
- g. soft, brown and well-laminated shale (section C)
- h. hard, dark grey and non-laminated shale in the lowermost part (section D).

Section A is further divided into A1 and A2 based on geochemical composition (see below).

### 5.4.2. Elemental analysis

Oil shale rock samples were first crushed, pulverized and sieved to obtain particle size <63 micron. Calcium (Ca) was analyzed by Actlabs, Ancaster, Canada. A 0.25 g sample was totally digested at 260°C employing HF, HClO<sub>4</sub>, HNO<sub>3</sub> and HCl. The sample was then analyzed using a Perkin Elmer ELAN 9000 ICP-MS. Total organic carbon contents (TOC) was analyzed using Euro EA (CAP 20) Elemental Analyzer. For TOC determination, pulverized samples were treated with diluted (10%) hydrochloric acid prior to the analysis to remove carbonates from the sample and then rinsed with distilled water until neutrality. The TOC values were then corrected to the original sample weight due to calcite loss.

For analysis of carbon isotopic composition of bulk organic matter, the carbonate free samples were measured with an IsoPrime<sup>TM</sup> (GV Instruments, UK) continuous-flow isotope ratio mass spectrometer. Isotope ratios are given in  $\delta$ -notation,  $\delta = (R_s/R_{st} - 1) \times 1000$ , with  $R_s$  and  $R_{st}$  as isotope ratios of sample and the standards VPDB. Analytical precision was 0.08‰.

#### 5.4.3. Palynological analysis

Palynological processing was carried out at the Natural History Museum of London, UK. The samples were treated with HCl (37% aq.), and HF (40% aq.) in alternating steps to remove carbonates and silicates, respectively, and, after washing to neutrality, sieved with a 15 micrometer mesh sieve. Organic matter particles were counted at minimum 300 points using a transmitted-light microscope at a 400x magnification. In the present study, only palynomorph of *B. braunii* will be presented to compare with geochemical data.

#### 5.4.4. Biomarker analysis

Twenty five grams of pulverized oil shale sample material (<63 micron) were extracted for 24 hours in a soxhlet extraction apparatus using 200 ml dichloromethane (DCM) as solvent. The extract was then separated into four fractions using column chromatography (1.5 cm diameter) over 14 grams activated silica gel. Sequential elution was performed to obtain fractions of saturated hydrocarbons, aromatic hydrocarbons, ketones/esters and more polar compounds using 40 ml n-hexane, 100 ml of n-hexane/DCM (9/1 v/v), 40 ml DCM and 40 ml methanol, respectively. In the present study, saturated hydrocarbon fraction was analyzed by gas chromatography and mass spectrometry (GC-MS) using a Thermo Scientific Ultra series gas chromatograph coupled to a Thermo Scientific DSQ II mass spectrometer. GC separation of the compounds was achieved using a Thermo Scientific TR-5MS fused silica capillary column (30 m x 0.25 mm ID x 0.25  $\mu$ m film thickness). The oven temperature was programmed from 60 to 320 °C at a rate of 4 °C /min, with a 35 min isothermal period at 320 °C. The samples were injected in the splitless mode with the injector temperature at 280°C. Helium was used as carrier gas. The mass spectrometer was operated in the electron impact mode (EI) at 70 eV ionization energy. Mass spectra were obtained by scanning from 50 to 600 daltons at a cycle time of 1 second. For data processing, the Xcalibur Qual Browser software was used. Per-deuterated tetracosane was used as internal standard for quantification.

#### 5.4.5. Compound-specific isotope analysis

Compound-specific isotope analysis (CSIA) for carbon of the saturated hydrocarbons was carried out in the Stable Isotope Laboratory of the Department of Applied Geosciences and Geophysics at the University of Leoben (Austria). A Thermo Fisher Delta V mass spectrometer connected to a Ultra series gas chromatograph, fitted with a similar column specification to that used in GC-MS analysis, were used for the analysis. The GC oven, injection conditions and carrier gas were also the same as those used in GC-MS analysis. Eluting compounds from the GC were converted to CO<sub>2</sub> in a combustion oven and measured relative to a reference CO<sub>2</sub>. The  $\delta^{13}\text{C}$  values were reported relative to the Pee Dee Belemnite (PDB) standard. An *n*-alkane carbon isotope external standard mixture (*n*-C<sub>15</sub>; *n*-C<sub>20</sub>; *n*-C<sub>25</sub>) was used for the control of the analytical results.

### 5.5. Results

#### 5.5.1. Elemental and palynological data

Concentrations of Ca range from 5.0 to 16.7% (average 9.4%). The Ca concentrations are generally high in sections D and C, moderately high in section B, low in the top of section B and section A2 and subsequently increase in section A1 (Figure 5.3a). Ca in the oil shale represents calcite considering the well correlation between Ca concentrations and loss weights during carbonate removal ( $R^2=0.85$ , not shown). TOC ranges from 1.9 to 12.5% averaging at 5.9% (Figure 5.3b). Upwards increase of TOC is observed in section D and C. Subsequently, the TOC values decrease upwards in section B and A2 and A1.  $\delta^{13}\text{C}$  varies from -27.0 to -30.5‰ with an average value of -28.3‰ (Figure 5.3c).  $\delta^{13}\text{C}$  generally increases upwards in section D and C and slightly decreases in the bottom part of section B. A remarkable decrease of  $\delta^{13}\text{C}$  is observed at the bottom part of section A2. Subsequently the  $\delta^{13}\text{C}$  increases upwards. In order to relate with the  $\delta^{13}\text{C}$  variation and to interpret the paleoecology, the abundances of *B. braunii* palynomorph are shown in Figure 5.3d. They range from 3 to 16% averaging at 8%, generally develop in opposite with the of  $\delta^{13}\text{C}$  values along the profile. The detailed palynological and geochemical data are presented in Appendices 2 and 3, respectively.

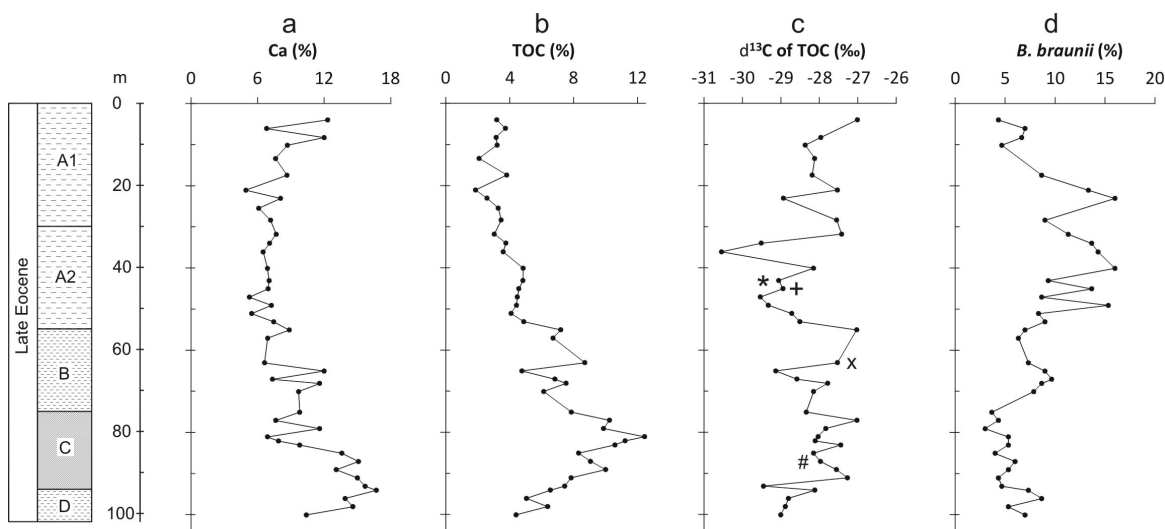


Figure 5.3. Vertical concentration variations of Ca (a), TOC (b),  $\delta^{13}\text{C}$  of TOC (c) and *B. braunii* (d). Signs (c) denote samples: \* (G-30), + (G-32), x (G-50), # (G-74). The detailed palynological and geochemical data are presented in Appendices 2 and 3, respectively.

### 5.5.2. Biomarkers

The total ion chromatogram (TIC) from GC-MS analysis of saturated hydrocarbon fraction (Figure 5.4a) is obtained from the solvent extract of the representative sample G-32. *n*-Alkane peaks are noted with asterisks. The  $\text{C}_{27}$  *n*-alkane is derived from *B. braunii* race A, and will be discussed in detail elsewhere. Pristane (Pr) and phytane (Ph) are dominant in all samples. Mass fragmentograms for  $m/z$  191, 231, 271 of the saturated hydrocarbon fraction are presented in Figure 5.4b,c,d showing hopanes, 4-methylsteranes and 4-methyldiasterenes distributions respectively. Peaks assignment for the biomarkers is listed in Table 5.1. The detailed organic geochemical data are presented in Appendix 4.

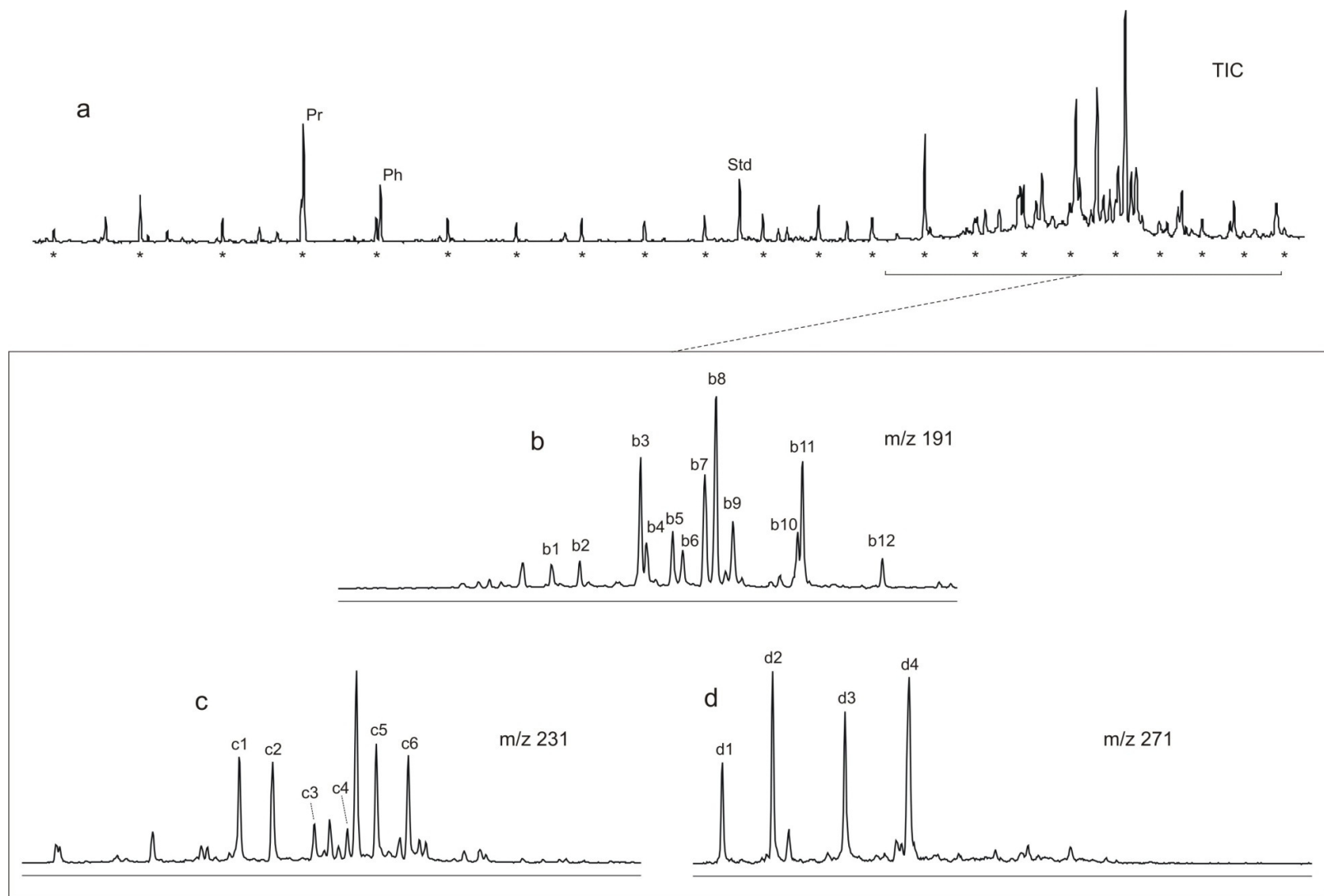


Figure 5.4. Mass chromatogram of saturated hydrocarbon fraction of representative sample (G-32) for total ion (TIC, a),  $m/z$  191 (b), 231 (c) and 271 (d). Asterisks denote peaks of *n*-alkanes. Chemical structures of the compounds are shown in Figure 5.5.

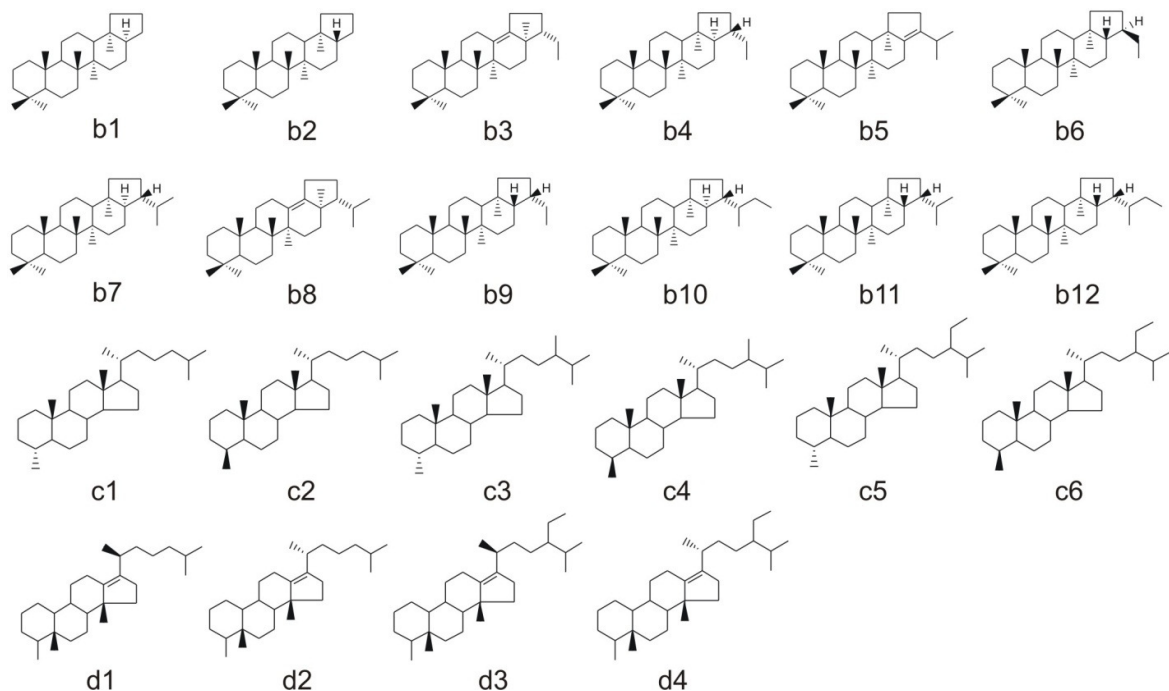


Figure 5.5. Chemical structures of the identified compounds shown in Figure 5.4.

Table 5.1. Peaks assignment of compounds shown in Figure 5.4.

Peak	Compound	Base peak	Mass weight	Reference
Pr	Pristane	57	268	1
Ph	Phytane	57	282	1
Std	Internal standard			
b1	17 $\alpha$ (H)-22,29,30-Trisnorhopane	191	370	2
b2	17 $\beta$ (H)-22,29,30-Trisnorhopane	149	370	2
b3	30-Norneohop-13(18)-ene	191	396	2
b4	17 $\alpha$ (H),21 $\beta$ (H)-30-Norhopane	191	398	2
b5	Hop-17(21)-ene	191	410	2
b6	17 $\beta$ (H),21 $\alpha$ (H)-Normoretane	177	398	2
b7	17 $\alpha$ (H),21 $\beta$ (H)-Hopane	191	412	2
b8	Neohop-13(18)-ene	191	410	2
b9	17 $\beta$ (H),21 $\beta$ (H)-30-Norhopane	177	398	2
b10	22R-17 $\alpha$ (H),21 $\beta$ (H)-Homohopane	191	426	2
b11	17 $\beta$ (H),21 $\beta$ (H)-Hopane	191	412	2
b12	17 $\beta$ (H),21 $\beta$ (H)-Homohopane	205	426	2
c1	4 $\alpha$ -Methylsterane	231	386	3
c2	4 $\beta$ -Methylsterane	231	386	3
c3	4 $\alpha$ -Methyl-24-methylsterane	231	386	3
c4	4 $\beta$ -Methyl-24-methylsterane	231	386	3
c5	4 $\alpha$ -Methyl-24-ethylsterane	231	386	3
c6	4 $\beta$ -Methyl-24-ethylsterane	231	386	3
d1	20R-Methyldiasterene	271	384	4
d2	20S-Methyldiasterene	271	384	4
d3	20R-Methyl-24-ethyldiasterene	271	412	4
d4	20S-Methyl-24-ethyldiasterene	271	412	4

Note: Compound identification is based on mass spectra and/or relative retention time published in the references. 1: Wiley Library (2008), 2: Philp (1985), 3: Wolf et al. (1986b), 4: Püttmann and Goth (1988).



### 5.5.2.1. Hopanoids

Hopanoids in the studied oil shale samples are characterized by the presence of hopenes and a series of hopane homologues ranging from C<sub>27</sub> to C<sub>31</sub> with the absence of bisnorhopanes (C<sub>28</sub>) (Figure 5.4b). Hopenes are present as major compounds. They consist of 30-norneohop-13(18)-ene (compound b3), hop-17(21)-ene (compound b5) and neohop-13(18)-ene (compound b8). Their concentrations range from 25.8-207.2 (average 97.6) µg/g TOC, 13.9-202.5 (average 79.8) µg/g TOC and 14.7-235.6 (average 82.5) µg/g TOC, respectively. These hopenes are in parallel along the profile. The concentration sums of compounds b3 and b8 (neohopenes) along the profile are presented in Figure 5.6a, showing generally two cycles of upwards concentration decreases. One cycle covers sections A and one cycle covers sections B, C and D of the profile. The most abundant compound of hopane homologues is 17 $\alpha$ (H),21 $\beta$ (H)-hopane (compound b7), ranging from 6.0 to 79.2 averaging at 35.4 µg/g TOC (not shown). Most of the hopane homologues develop generally in parallel with the hopenes along the profile. The total concentrations of the hopanoid hydrocarbons are shown in Figure 5.6b, varying from 153.9 to 899.8 averaging at 431.7 µg/g TOC.

### 5.5.2.2. Pristane and phytane

Pristane and phytane are dominant compounds in the oil shale. Pristane concentrations range from 51.4 to 359.0 averaging at 142.6 µg/g TOC (Figure 5.6c). Phytane is less abundant and varies from 34.5 to 173.6 with an average value of 76.2 µg/g TOC (Figure 5.6c). Their concentration variation is largely parallel along the profile and the high concentrations are observed in section B. The pristane/phytane ratio varies from 1.3 to 2.4 with an average value of 1.9 (Figure 5.6d). The pristane/phytane ratio shows two cycles of concentration variation. These cycles develop in opposite to the cyclicity of the neohopenes concentrations. Pristane/phytane ratio increases upwards in sections D-B and again in sections A2 and A1.

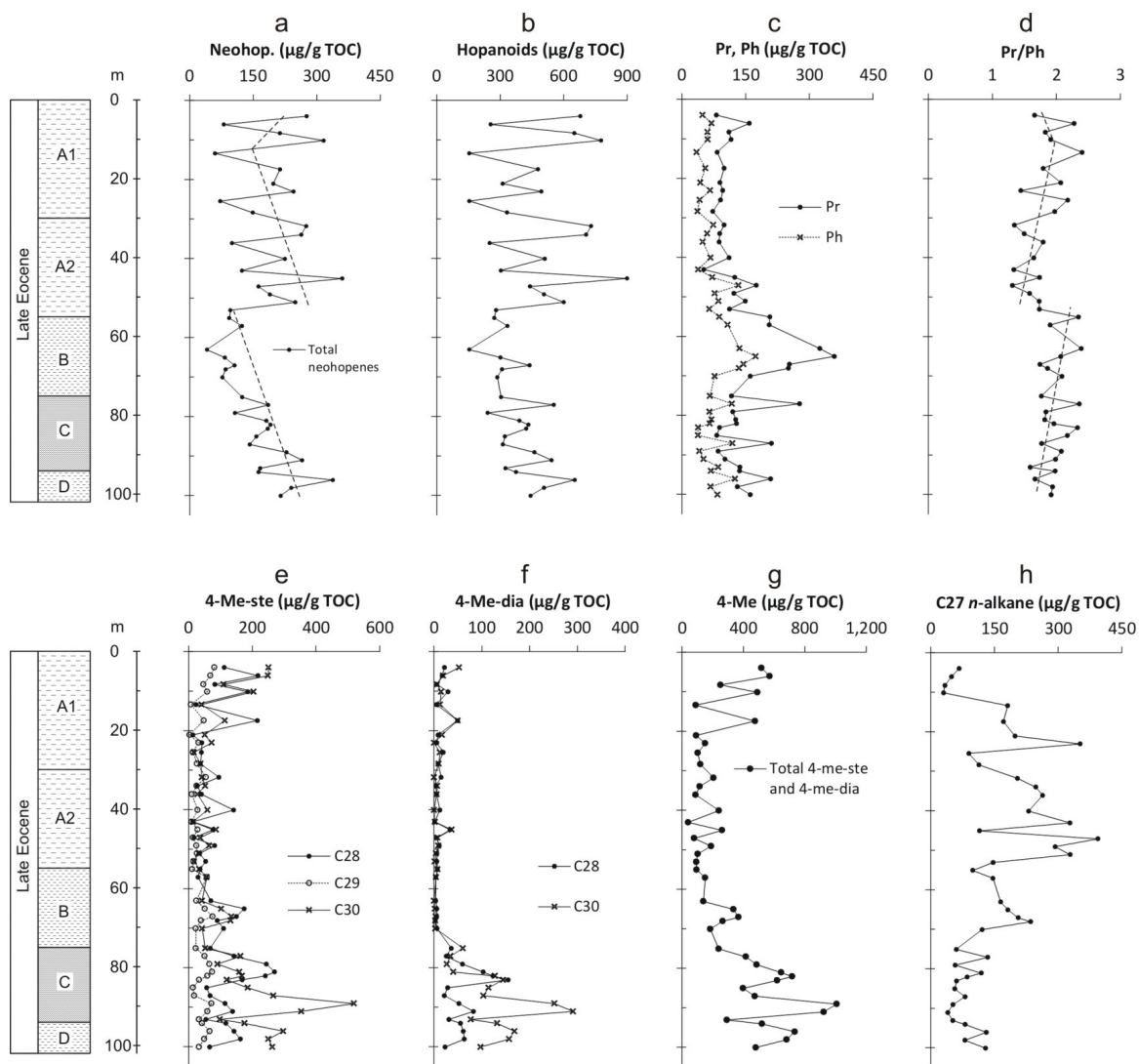


Figure 5.6. Vertical variation of some major biomarkers and parameter in the Kiliran oil shale: total neohopenes (a), total hopanoid hydrocarbons (b), pristane and phytane (c), pristane/phytane (d), C<sub>28</sub>-C<sub>30</sub> 4-methylsteranes (e), C<sub>28</sub> and C<sub>30</sub> 4-methyldiasteranes (f), sum of 4-methylsterane and 4-methyldiasterane homologues (g) and C<sub>27</sub> *n*-alkane (h). The detailed organic geochemical data are presented in Appendix 4.

### 5.5.2.3. Steroids

The 4-methylsteranes comprise C<sub>28</sub>-C<sub>30</sub> homologues, namely 4-methylsteranes, 4-methyl-24-methylsteranes and 4-methyl-24-ethylsteranes (Figure 5.4c). Dinosteranes are not present in the extracts. Each compound is represented by two isomers (4 $\alpha$  and 4 $\beta$ ). The 4-methylsteranes occur in all samples and their concentrations (sum of both isomers of the C<sub>28</sub>, C<sub>29</sub> and C<sub>30</sub> homologues) vary from 13.1 to 269.9 (average 101.4)  $\mu\text{g/g TOC}$ , 3.3-81.2 (average 38.0)  $\mu\text{g/g TOC}$  and 14.2-519.5 (average 125.7)  $\mu\text{g/g TOC}$ , respectively (Figure 5.6e). They show parallel

vertical variations which are generally decreasing upwards in the lower half of the investigated profile (sections B, C and D), low concentrations in the top of section B and section A2 and subsequently increase upwards in section A1. The 4-methyldiasterenes also occur in all samples in lower abundance than the 4-methylsteranes, varying 1.4-155.2 (average 29.2) and 0-291.0 (average 50.4)  $\mu\text{g/g}$  TOC for sum of both isomers of the  $\text{C}_{28}$  and  $\text{C}_{30}$  homologues, respectively (Figure 5.6f). The concentrations develop largely in parallel with the 4-methylsteranes along the profile. Total concentrations of both 4-methylsteranes and 4-methyldiasterenes homologues are 40.3-1,009.2  $\mu\text{g/g}$  TOC with an average value of 344.7  $\mu\text{g/g}$  TOC (Figure 5.6g). These total concentrations generally tend to be low in those parts of the section where abundances of *B. braunii* (Figure 5.3d) and  $\text{C}_{27}$  *n*-alkane (Figure 5.6h) are high.

#### 5.5.2.4. Compound-specific carbon isotopic composition

CSIA measurements are carried out for 4 representative samples (G-30, G-32, G-50 and G-74) and the results are listed in Table 5.2. Carbon isotopic composition of 4-methylsteranes are consistently depleted ( $-36.7 \pm 1\%$ ). The  $\delta^{13}\text{C}$  of neohopenes are extremely depleted, ranging from  $-45.2$  to  $-50.2\%$ . Common  $\delta^{13}\text{C}$  values of pristane and phytane are obtained. Moderate  $\delta^{13}\text{C}$  differences of pristane and phytane are observed ranging from 1.1 to 2.8‰. The  $\delta^{13}\text{C}$  values of  $\text{C}_{27}$  *n*-alkanes are about  $-31\%$ , which are up to 2‰ heavier than those of the other long-chain *n*-alkanes (not shown).

Table 5.2. Carbon isotopic composition of compounds identified from 4 samples of Kiliran oil shale. Sample positions are shown in Figure 5.3c.

Compound	$\delta^{13}\text{C}$ (‰)			
	G-30	G-32	G-50	G-74
4 $\beta$ -Methylsterane		-35.4		
4 $\alpha$ -Methyl-24-ethylsterane			-36.4	-35.9
4 $\beta$ -Methyl-24-ethylsterane		-37.0	-37.2	-38.1
30-Norneohop-13(18)-ene		-50.2	-46.5	-50.4
Neohop-13(18)-ene		-47.6	-49.1	-45.2
Pristane	-32.3	-28.5	-28.6	-29.8
Phytane	-34.1	-31.3	-30.2	-30.9
$\Delta\text{Pr-Ph}$	1.8	2.8	1.6	1.1
$\text{C}_{27}$ <i>n</i> -alkane			-30.7	-31.4

## 5.6. Discussions

### 5.6.1. Hopanoids

Hopanes are widespread in crude oils, source rocks and coals. They originate from diploptene and diplopterol for  $\leq C_{30}$  hopanes and from bacteriohopanetetrol for the extended hopanes ( $> C_{30}$ ). These precursors have been found in almost all hopanoid-producing bacteria (Rohmer, 1987). Additionally, to a lesser extent, hopanoid hydrocarbons were also reported to be present in some ferns (Bottari et al., 1972; Ageta and Arai, 1983). In clay rich environments, diploptene may be rearranged generating neohop-13(18)-ene through hop-17(21)-ene during diagenesis (Ishiwatari et al., 1994a; Farrimond and Telnaes, 1996; and references therein).

Hopanoid hydrocarbons in the Kiliran oil shale account a major constituent of the solvent extracts. Considering the minor amount of higher plants debris (unpublished), the high amounts of hopanoid hydrocarbon are attributed to bacterial origin. The  $\delta^{13}C$  values of neohopenes (compounds d3 and d8) are significantly depleted (-45 to -50‰) suggesting an origin from methanotrophic bacteria. Methanogenesis will produce methane with depleted carbon isotopic composition ranging from -50 to -60‰ (Whiticar, 1999). Fixation of the methane by the methanotrophic bacteria results in a depletion of  $\delta^{13}C$  values of their biomass.

### 5.5.2. Pristane and phytane

Pristane and phytane are ubiquitous in sediments and usually the most dominant compounds among the acyclic isoprenoids. The common origin of them is the phytyl side chain of chlorophyll a in phototrophic organisms and bacteriochlorophyll a and b in purple sulfur bacteria (e.g. Powell and McKirdy, 1973; Peters et al., 2005b). Didyk et al. (1978) proposed that redox conditions control the relative proportion of pristane and phytane preserved during diagenesis. Anoxic conditions lead to the reduction of the phytyl side chain to phytol and then to phytane giving low Pr/Ph ratios. On the other hand, more oxic conditions promote to the oxidation of phytol to pristane resulting high Pr/Ph ratio. The ratio has thus commonly been used to infer redox conditions of depositional environments.

However, pristane and phytane may also originate from archaeobacterial membrane lipids (Chappe et al., 1982; Rowland, 1990). Tocopherols have also been proposed as major

precursors of pristane in sediments and crude oils deposited in environments with high primary production or strongly anoxic conditions (Goossens et al., 1984; Rontani et al., 2010). The compounds are relatively abundant in both higher land plants and aquatic phototrophic organisms (Goossens et al., 1984). Li et al. (1995) proposed that methyltrimethyltridecylchromans (MTTC) could also generate pristane. Considering these additional sources, the use of the Pr/Ph ratio as redox indicator is consequently not always successful and should be applied with care (see e.g. Rontani et al., 2010).

Complexity of the origin of pristane and phytane can be inferred by their  $\delta^{13}\text{C}$  values. A common origin is shown by the  $\delta^{13}\text{C}$  similarity of these isoprenoids, which usually differ by no more than  $\pm 0.3\text{‰}$  (e.g. Li et al., 1995; Peters et al., 2005b). According to Collister (1992), uniform  $\delta^{13}\text{C}$  values may also imply an origin from multiple producers using the same source of dissolved inorganic carbon (DIC). A significant difference of the  $\delta^{13}\text{C}$  value between pristane and phytane by about  $6\text{‰}$  was reported in case of Messel shale indicating distinct multiple sources. The depleted  $\delta^{13}\text{C}$  of phytane was attributed to a significant contribution from lipids of methanotrophic bacteria. The enriched  $\delta^{13}\text{C}$  of pristane was ascribed to origin from lipids of common phototrophic algae (Freeman et al., 1990).

In the Kiliran oil shale the differences of  $\delta^{13}\text{C}$  values between pristane and phytane vary from 1.1 to  $2.8\text{‰}$  (Table 5.2) with  $\delta^{13}\text{C}$  values of pristane being always heavier than those of phytane. This suggests that the compounds were not derived solely from the phytyl side chain of chlorophyll a, but also from other sources. In the present case, therefore, the pristane/phytane ratios are not suggested to infer redox changes in the sediments during deposition of the sediments. Moreover, the high abundance of biomarkers from methanotrophic bacteria (neohopenes) strictly indicate anoxic bottom water during deposition of the entire profile, so that phytol oxidation to pristane during diagenesis resulting in increased pristane/phytane ratios is unlikely. The variation of the pristane/phytane ratios along the profile shows an inverse correlation with the amount of the sum of neohopenes. The generally opposite trends between them may indicate that phytane was contributed significantly from lipids of methanotrophic bacteria.

### 5.6.3. Steroids

The homologues of 4-methylsterane have commonly been considered to originate from 4-methylsterols in living dinoflagellates (e.g. Robinson et al., 1984; Fu Jiamo et al., 1990). They may also be derived from prymnesiophyte microalgae of the genus *Pavlova* (Volkman et al., 1990). A world wide spread macrophyte *Utricularia neglecta* has also been reported as important source for sedimentary 4-methylsterols of lacustrine environments (Klink et al., 1992). Additionally, 4-methylsteranes may also be derived as diagenetic products of methylsteroids through methylation of sterols from primary producers by bacterial activity under anaerobic conditions (Auras and Püttmann, 2004).

Although the biological source of the 4-methylsterane homologues in sediments is ambiguous, their presence in sediments is an important key to indicate their depositional environment (Peters et al., 2005b). For example, the occurrence of 4-methyl-24-ethylsteranes along with dinosteranes (principal and specific biomarkers of *Dinoflagellates*) is usually interpreted as indication for marine *Dinoflagellates* input. On the other hand, 4-methyl-24-ethylsteranes are commonly dominant and often not co-occurring with dinosteranes in lacustrine sediments (Summons et al., 1987; Goodwin et al., 1988; Summons et al., 1992), although some freshwater *Dinoflagellates* are known (e.g. Herrmann, 2010). Fu Jiamo et al. (1990) attributed the occurrence of 4-methylsteranes in Chinese non-marine sediments to an origin from freshwater *Dinoflagellates* although dinosteranes were absent from the sediments. The relative distribution of C<sub>28</sub>, C<sub>29</sub> and C<sub>30</sub> 4-methylsteranes was suggested to be caused by different species and genus composition of *Dinoflagellates* in different environments (Fu Jiamo et al., 1999).

The similar concentration variations between 4-methylsteranes and 4-methyldiasterenes in the oil shale profile indicate the occurrence of both compound series from the same biological sources. Freshwater *Dinoflagellates* as common sources of these compounds could not be observed from palynological study. However, freshwater *Dinoflagellates* were frequently recognized in Brown Shale Fm from different sub-basins of Central Sumatra Basin as reported by Longley et al. (1990) and Wain and Jackson (1995). This leads to hypothesis that the 4-methylsteranes were derived from freshwater *Dinoflagellates*, considering the analogous stratigraphy and geological history of the Central Sumatra Basin depocenters. Further discussion on paleoecological changes supports this hypothesis (see below). An absence of

certain freshwater *Dinoflagellates* cysts from palynological sample must not necessarily mean that there were no *Dinoflagellates* in a lake (see Herrmann, 2010). Unfavourable conditions could lead to their lack cysts preservation.

#### 5.6.4. Carbon isotopic composition in response to eutrophication of lake systems

Variations of the carbon isotopic composition of sedimentary organic matter have often been used to indicate changes of primary productivity in aquatic systems. In eutrophic environments, diverse types of anaerobic activities including respiration and methanogenesis can enhance the production of respired CO<sub>2</sub> and biogenic methane which are significantly depleted in <sup>13</sup>C. Carbon fixation of the <sup>13</sup>C-depleted CO<sub>2</sub> and methane by chemoautotrophs in hypolimnion and methanotrophic bacteria in chemocline, respectively, would deplete the δ<sup>13</sup>C of bacterial biomass (Whiticar et al., 1986; Hollander and Smith, 2001). Water overturn and/or diffusion can provide the <sup>13</sup>C-depleted CO<sub>2</sub> from hypolimnion to epilimnion, resulting in <sup>13</sup>C-depletion in overall DIC reservoir. Photosynthesis utilizing this DIC would also result in δ<sup>13</sup>C depletion of the biomass of phototrophic organisms. The biomass derived from both bacteria and phototrophic organisms can therefore contribute significantly to negative excursions of δ<sup>13</sup>C values of sedimentary organic matter during eutrophication (Küspert, 1982; Hollander and Smith, 2001).

On the other hand, most authors suggested that during periods of high primary productivity, limited availability of DIC can decrease carbon isotopic fractionation during photosynthesis. The progressive increase of productivity would therefore result in a positive excursion of δ<sup>13</sup>C values represented on the sedimentary organic matter (e.g. McKenzie, 1985; Hollander et al., 1993; Hodell and Schelske, 1998).

Hollander and Smith (2001) proposed three models of carbon isotope excursions during consecutive lake-eutrophications. In moderate eutrophication lake, bacterial biomass derived from chemoautotrophs and methanotrophs fixing <sup>13</sup>C-depleted CO<sub>2</sub> and methane, respectively, contribute to δ<sup>13</sup>C negative excursion of sedimentary organic matter. In moderate-severe eutrophication lake, the higher productivity leads to additional sources of <sup>13</sup>C-depleted biomass associated with biogenic methane oxidation. The chemocline moves upwards and the oxidation of biogenic methane will become a primary influence on δ<sup>13</sup>C values of DIC in epilimnion. Biomass of both bacterial and phototrophic organisms therefore contributes to significant δ<sup>13</sup>C

negative excursion of sedimentary organic matter. In severe eutrophication lake, high primary productivity leads to the limitation of DIC availability and thus decreases carbon isotope fractionation. The phototrophic biomass export from epilimnion would also overwhelm the  $^{13}\text{C}$ -depleted bacterial biomass in sediments, which consequently implicates a positive excursion of  $\delta^{13}\text{C}$  values in sedimentary organic matter (see Hollander and Smith, 2001).

#### 5.6.5. Carbon isotopic composition and eutrophication in the Kiliran lake

The aquatic ecosystem corresponding to  $\delta^{13}\text{C}$  excursions of organic matter in the former Kiliran lake is represented in Figure 5.7. Oxidation of biogenic methane is the most important process in the former Kiliran lake, as the concentrations of methanotrophic bacteria biomarkers (neohopenes) are very high, ranging from 40.6 to 360.0  $\mu\text{g/g}$  TOC. According to models proposed by Hollander and Smith (2001), the abundant of methanotrophic bacteria may indicate that high primary productivity condition prevailed in the lake, enhancing the production export to hypolimnion and thus methanogenesis at the bottom water and/or upper sediment. The sources of  $^{13}\text{C}$ -depleted DIC would therefore be both of bacterial respiration during the organic matter decomposition in hypolimnion and oxidation of biogenic methane in chemocline. Seasonal water overturn was responsible to introduce the  $^{13}\text{C}$ -depleted DIC to the epilimnion. Under such circumstances, the phototrophic organisms would fix this DIC leading to the  $\delta^{13}\text{C}$  negative excursion of their biomass. This negative excursion is evidenced by the relative  $\delta^{13}\text{C}$  depletion of algal biomarkers such as 4-methylsteranes (about -37‰) and  $\text{C}_{27}$  *n*-alkane (about -31‰). The first compounds are depleted in  $^{13}\text{C}$  relative to common lacustrine algal biomass (about -27‰; see e.g. Meyers, 1997, 2003). The latter compound is depleted in  $^{13}\text{C}$  relative to those commonly reported to *B. braunii* race A-rich torbanites (-19 to -24‰; Audino et al., 2001; Grice et al., 2001).

The  $\delta^{13}\text{C}$  variation of bulk organic matter along the oil shale profile ranging from -27.0 to -30.5‰ (Figure 5.3c) may generally infer eutrophication history during the oil shale deposition. Increase of trophic level or productivity would lead to higher phototrophic biomass export, overwhelming the bacterial biomass in the sediment. These conditions lead to the enrichment of the oil shale organic matter in  $^{13}\text{C}$ , because phototrophic biomass has higher  $\delta^{13}\text{C}$  values relative to biomass of bacteria dominated by methanotrophic bacteria. Inversely, the decrease of trophic level or productivity would lead to the depletion of the oil shale organic matter in  $^{13}\text{C}$ . The  $\delta^{13}\text{C}$  variation of TOC along the profile can be divided into several steps (Figure



5.3c). In the lower part of the profile (sections D, C) the  $\delta^{13}\text{C}$  of TOC generally tends to increase upwards, indicating increasing productivity of the lake during the deposition. Subsequently, slight decreases of  $\delta^{13}\text{C}$  are observed in section B. A remarkable  $\delta^{13}\text{C}$  decrease is recognized in the bottom part of section A2, suggesting sudden decreases of the lake productivity. Afterwards, during deposition of sections A2 and A1, the lake productivity might increase as indicated by the upwards increase of  $\delta^{13}\text{C}$ .

Although the  $\delta^{13}\text{C}$  values of bulk organic matter show a variation of productivity as discussed above, the  $\delta^{13}\text{C}$  values of individual algal biomarkers (4-methylsteranes) (Table 5.2) from different samples deposited during different trophic levels of the lake do not show such variation. According to the carbon cycling models of lake systems in response to eutrophication Hollander and Smith (2001), it is expected that the  $\delta^{13}\text{C}$  of algal biomarkers would exhibit variation with respect to productivity changes (see above). However, the proposed models considered lake productivities where nutrients availability is not only from recycling but primarily also from external sources in response to cultural eutrophications. In the present study, nutrients from external sources are not important (see discussion in Chapter 2). The availability of both nutrients and recycled DIC in the epilimnion of the former Kiliran lake was dependent on the weaker or absent thermocline (Figure 5.7). Under such circumstances, the significant fractionation of carbon isotopes to more positive values during high productivity due to limited availability of recycled DIC was unlikely. The  $^{13}\text{C}$ -depleted DIC in epilimnion was probably always not limited.

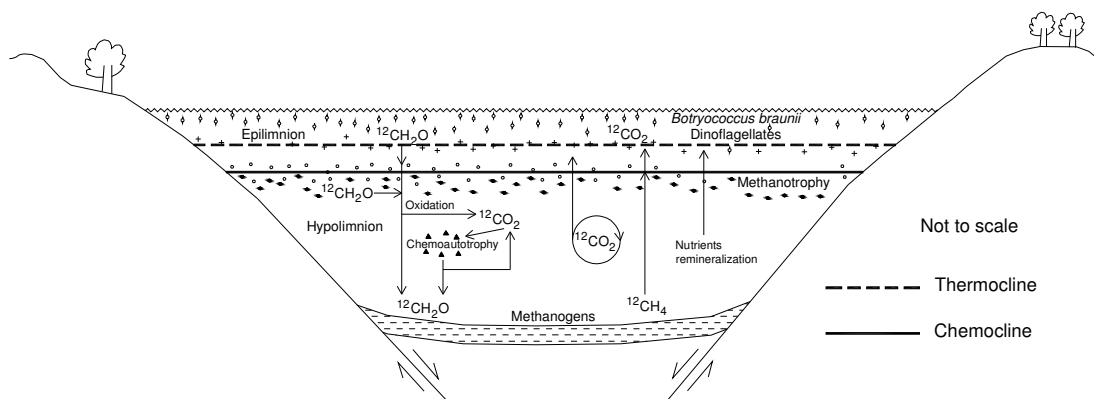


Figure 5.7. Aquatic ecosystem of the former Kiliran lake with respect to carbon and nutrients cycling. Carbon cycling leads to  $\delta^{13}\text{C}$  negative excursions of biomass of phototrophic organisms. The carbon cycling scheme is adopted from Hollander and Smith (2001). The availability of both  $^{13}\text{C}$ -depleted DIC and nutrients in epilimnion was dependent on the lake stratification.

#### 5.6.6. Paleoeological changes

Lenz et al. (2007) reported the occurrence of freshwater *Dinoflagellates* and *B. braunii* in Middle Eocene Messel lake oil shale. They concluded that both of organisms occurred in close alternation during holomictic phase of Messel lake. They were mutually exclusive during meromictic phase of Messel lake, *Dinoflagellates* tend to be dominant where *B. braunii* disappears and vice versa. This antagonistic relation has been regarded to changes in the chemistry of water body. Further, Herrmann (2010) reported also the competition of both organisms in Oligocene Enspel lake where *Dinoflagellates* were dominant in more alkaline and higher trophic level environments, and *B. braunii* was dominant in more acidic and lower trophic level environments.

In the studied oil shale, Ca concentrations probably reflect the alkalinity of water body during the deposition. Ca (Figure 5.3a) tends to be high where 4-methylsteranes are abundant in the profile, implying that the organisms deriving these compounds favoured more alkaline environments. On the other hand, *B. braunii* tend to be more abundant where Ca and 4-methylsteranes are lower in concentration. Additionally, *B. braunii* develops in opposite with  $\delta^{13}\text{C}$  of TOC, indicating that this organism favoured less trophic conditions. This is consistent with the well known of *B. braunii* blooming in environments which relatively less trophic by other authors (e.g. Tyson, 1995; Smittenberg et al., 2005). The general alternation of *B. braunii* abundances and 4-methylsteranes along the oil shale profile was likely induced by environmental changes which are comparable with those reported by Herrmann (2010) in Enspel lake. This may support the hypothesis that the 4-methylsteranes were derived from freshwater *Dinoflagellates*.

### 5.7. Conclusions

Palynological and organic geochemical data revealed the occurrence of both bacterial and algal organic matter in the Kiliran oil shale. Hopanoid hydrocarbons are among the dominating compounds in the saturated hydrocarbon fractions. 30-Norneohop-13(18)-ene and neohop-13(18)-ene are the most abundant hopanoid compounds. These hopenes are attributed to originate from methanotrophic bacteria due to their strongly depleted  $\delta^{13}\text{C}$  values (-45.2 to -50.2‰). The methanotrophic bacteria were responsible for methane oxidation in the

chemocline of the former Kiliran lake, resulting in the generation of  $^{13}\text{C}$ -depleted DIC. This led to the  $\delta^{13}\text{C}$  depletion of phototrophic organisms fixing the  $^{13}\text{C}$ -depleted DIC through photosynthesis.

The  $\delta^{13}\text{C}$  variation of bulk organic matter along the profile may reflect the lake productivity changes during deposition of the sediment. The lower productivity in the middle part of the profile (section A2) promoted lower phototrophic biomass export to the sediment. These conditions lead to the depletion of the organic matter in  $^{13}\text{C}$ , because phototrophic biomass has higher  $\delta^{13}\text{C}$  relative to biomass of organisms such as methanogenic and methanotrophic bacteria. Inversely, the increase of the trophic level or productivity in the bottom and top part of the profile led to the enrichment of the oil shale organic matter in  $^{13}\text{C}$ .

*B. braunii* tends to be more abundant during lower lake productivity and relatively less alkaline (more acidic) waters. 4-Methylsterane and 4-methyldiasterene homologues generally develop in opposite with *B. braunii* along the profile. Their biological sources likely preferred a higher trophic level and alkaline waters. These compounds are hypothesized to originate from freshwater *Dinoflagellates*, considering the alternation between these organisms and *B. braunii* with respect to changes in water chemistry.

## Chapter 6: Summary

Various geochemical and palynological methods were applied to investigate 42 samples of the Late Eocene Brown Shale Fm of the Kiliran Sub-basin of the Central Sumatra Basin. Investigations were carried out to interpret the evolution of the former Kiliran lake, as well as paleoecological and paleoenvironmental changes during deposition of the oil shale section. Particular biomarkers were used to unravel the specific biological source material of the sedimentary organic matter. Corresponding to the general aims of this study, the results are summarized as follows.

### 6.1. Paleoenvironmental changes and evolution of the former Kiliran lake

Development of lakes is controlled by two major controls: tectonic subsidence and climate (see discussions in Carrol and Bohacs, 1999; Bohacs et al., 2000). Tectonic subsidence is responsible to create accommodation space, in which the autochthonous and terrigenous materials will be deposited. Climate governs the supply of water and terrigenous material into lakes. Interaction between both tectonic subsidence and climate variation characterize the water level fluctuation and thus the composition of sediments including organic matter.

In order to reconstruct the depositional history of the Kiliran oil shale, palynological and geochemical analyses were carried out (Chapter 2). Although palynological data revealed the occurrence of amorphous organic matter (AOM) in high amount (76-96%), the structured organic matter provided excellent indication of compositional changes along the studied oil shale profile (see Chapter 2). *B. braunii* is the only autochthonous organism that could be recognized by transmitted light microscopy. Pollen and fungal remains were considered as terrigenous organic palynomorphs recognized in the samples. Geochemical analyses were performed for both inorganic and organic parameters. The element Al was used as proxy for terrigenous matter, whereas TOC, S, U and Mo are proxies indicating increasing incorporation of autochthonous matter into sediments. Salinity variation of bottom water during the oil shale deposition was inferred from the inverse variation of TOC/S values. The Zr/Rb ratio was considered as grain size indicator. Both elements are of terrigenous origin, where Zr and Rb

are generally associated with coarse and fine fractions of fine-grained sediments, respectively. Carbon isotopic composition of organic matter ( $\delta^{13}\text{C}$ ) was also determined to interpret the productivity changes during the Kiliran lake development.

Sudden decreases of the (Zr/Rb) ratio observed along the oil shale profile indicate rapid changes to finer grain size, suggesting rapid deepening events during lake development. Subsidence was responsible to enlarge the extent of the water column, so that bottom water anoxia could develop resulting in better organic matter preservation. Relatively higher rates of subsidence than sediment and water supply rates will promote higher autochthonous input to the sediment. This is particularly shown in the lower part of the oil shale profile where autochthonous proxies are generally higher than terrigenous proxies.

Climatic control was interpreted to be the cause for paleoenvironmental changes, especially salinity and productivity. Climatic changes could be recognized from the abundance of fungal remains, which are generally higher in the middle part of the profile indicating relatively warmer climate. Warmer climate would lead to higher rates of sediment and water supply which is confirmed by the higher terrigenous input recognized in the middle part of the profile. TOC/S ratios indicate salinity changes which are also depending on the climatic changes. The ratios show slightly higher values in the middle part of the profile, indicating lower water salinity. Productivity changes could also closely be linked to climatic changes. Warmer climate promoted the establishment of a thermocline, inhibiting the supply of recycled nutrients from hypolimnion to epilimnion and thus less productivity (see Chapter 2). The presence of a thermocline will result in a shoaling of chemocline when the climate becomes warmer. This is confirmed by the increasing abundances of isorenieratane, a specific biomarker for green sulfur bacteria dwelling at photic zone euxinia, in the middle part of the profile (Chapter 3).

## **6.2. Paleoecological changes**

Water chemistry differs from lake to lake, and also varies with respect to timeline during development of lakes. Chemistry of lake waters can be ascribed to e.g. concentrations of oxygen, nutrients and specific elements such as calcium determining water alkalinity. The water chemistry determines the productivity of respective organisms dwelling in lakes. The

reconstruction of paleoenvironments with respect to water chemistry and ecology has previously been carried out (see e.g. Smittenberg et al., 2004, 2005; Herrmann, 2010).

For reconstruction of paleoecology, geochemical and palynological data were used. Productivity was inferred from the carbon isotopic composition of bulk organic matter ( $\delta^{13}\text{C}$ ). Calcium abundances were regarded as alkalinity proxy of water during deposition of the oil shale. Palynological data revealed the occurrence of *B. braunii* in the former Kiliran lake. Although this alga is the only organism recognized in palynological analysis, its occurrence and abundance is an excellent indicator for both changes in the paleoenvironment and paleoecology. To assist the palynological data, organic geochemical analyses were performed to unravel the occurrence of further organisms by their biomarkers.

Abundances of isorenieratane and aryl isoprenoids were used to infer the extent and dynamics of photic zone euxinia. As discussed in Chapter 3, the chemocline was shoaling, mostly due to the presence of thermocline preventing water column mixing in epilimnion during deposition of the middle part of the oil shale profile. This resulted in an increasing extent of photic zone euxinia and thus the increasing abundance of green sulfur bacteria in the water column.

Corresponding to nutrient concentrations and alkalinity, *B. braunii* is an alga favoring less trophic (less nutrients) and less alkaline (less Ca) environments (Herrmann, 2010). In the middle part of oil shale profile, *B. braunii* is generally more abundant (Chapter 5). This is consistent with the generally less trophic environment indicated by the relatively more depleted  $\delta^{13}\text{C}$ . In this part, the lower supply of nutrients from hypolimnion favoured the growth of *B. braunii*, since other faster growing algae suffered from the low availability of nutrients. Warmer climate during deposition of this middle part of the oil shale profile would also lead the water supply increase to the lake, promoting relatively less alkaline or more acidic environments and thus supporting *B. braunii* population to develop.

Organic geochemical data were also used to unravel the major organism contributing to the lower and upper parts of the oil shale profile where *B. braunii* algae are less abundant. Homologues of 4-methylsterane ( $\text{C}_{28}$ - $\text{C}_{30}$ ) and 4-methyldiasterene ( $\text{C}_{28}$ ,  $\text{C}_{30}$ ) are the major identified biomarkers. These compounds have commonly been attributed to *Dinoflagellates*. In the study, the 4-methylsterane and 4-methyldiasterene homologues were hypothesized to originate from freshwater *Dinoflagellates*. Beside these algae have commonly been reported in

Brown Shale Fm, the ecological preferences are consistent for their development. In the lower and upper parts of the oil shale profile, relatively more alkaline (higher Ca) and more trophic environments were present (see Chapter 5). Herrmann (2010) reported alternation or antagonistic developments between *B. braunii* and *Dinoflagellates* with respect to trophic level and alkalinity changes, which are likely the case also in the present study assuming that the 4-methylsteranes homologues in the Kiliran oil shale are originating from *Dinoflagellates*.

### 6.3. Significance of particular biomarkers

In the present study, the organic geochemical composition of the sediment extracts was investigated with respect to both, molecular composition and carbon isotopic composition of individual compounds. The organic geochemical composition of the extracts is strongly dependent on the biological sources in the water column contributing to organic-rich sediments, as well as microbial processes in the sediments (e.g. Peters et al., 2005). Analyses of biomarkers and their carbon isotopic composition are helpful in the absence of the ability to visually identify morphologically preserved organisms by microscopical methods. Results from organic geochemical investigations with respect to particular biomarkers are discussed in Chapters 4 and 5.

Hopanoid hydrocarbons are among the dominant constituents of the soluble organic matter indicating a significant contribution of bacterial biomass. The strongly depleted carbon isotopic compositions measured for these compounds (about -50‰) suggest the occurrence of methanotrophic bacteria in significant amounts. The presence of abundant methanotrophic bacteria-derived compounds (neohopenes) strongly indicates the presence of anoxic environments during the deposition of the entire oil shale profile (Chapter 5). Additionally, the occurrence of isorenieratane and its derivatives argues for euxinic depositional environments (Chapter 3). Pristane and phytane are abundant. Based on the comparable vertical variation along the profile between pristane/phytane ratio and biomarkers of methanotrophic bacteria, the isoprenoids especially phytane is interpreted to originate mainly from these bacteria (Chapter 5).

*n*-Alkanes are further major constituents of sediment extracts. The C<sub>27</sub> *n*-alkane is the dominating *n*-alkane in all analyzed samples of the oil shale. Its vertical concentration

variation along the profile is in parallel with that of *B. braunii* abundances observed from palynological analysis. This suggests that the compound might originate mainly from *B. braunii* race A. The relatively heavy  $^{13}\text{C}$  values of this compound (about  $-31\text{‰}$ ) in relation to the adjacent long-chain *n*-alkanes (about  $-33\text{‰}$ ) confirm its origin from *B. braunii* race A. Lycopane was detected in many samples and shows strongly enriched  $\delta^{13}\text{C}$  values ( $-17.2\text{‰}$ ). This value suggests the presence of *B. braunii* race L as the origin of lycopane. Along the profile, concentration variations of both,  $\text{C}_{27}$  *n*-alkane and lycopane develop largely in opposite. This may indicate that both of the *B. braunii* races grew in alternation in the Kiliran lake, probably due to specific water chemistry changes (Chapter 4).

One important paleoenvironmental process occurring in the aquatic system of the Kiliran lake was carbon cycling (Chapter 5). Evidence for the presence of major carbon cycling in the lake system is the concomitant depletion of particular biomarkers in  $^{13}\text{C}$ . Isorenieratane has  $\delta^{13}\text{C}$  value of  $-24\text{‰}$ , which is about  $9\text{‰}$  more depleted than common values for  $\delta^{13}\text{C}$  of green sulfur bacteria biomarkers ( $\sim -15\text{‰}$ ). Other biomarkers such as the 4-methylsterane homologues, other carotenoid derivative,  $\text{C}_{27}$  *n*-alkane and lycopane are interpreted to be also depleted in  $^{13}\text{C}$  with comparable shifts ( $-7$  to  $-9\text{‰}$ ) relatively to the expected values (see discussion in Chapter 4). This concomitant depletion is related to bacterial activity in the Kiliran lake responsible for the carbon recycling in the anoxic hypolimnion. Water overturn was also ascribed to be the important factor for the availability of the recycled carbon to epilimnion.



## Chapter 7: Suggestion for further studies

### 7.1. Carbonate as possible indicator for paleoenvironment

Carbonate is the most dominant component in the Kiliran oil shale. Ca is assumed to represent  $\text{CaCO}_3$  considering the strong correlation between Ca concentrations and loss weights during carbonate removal ( $R^2=0.85$ ). This element constitutes the oil shale from 5.0 to 16.7% (average 9.4%) of total weight.

Müller et al. (1972) classified the occurrence of carbonate assemblages from differing lake environments into: (a) calcite and/or high-Mg calcite; (b) high-Mg calcite with aragonite, dolomite, huntite and magnesite; and (c) aragonite. The lakes showing assemblages a and c contain only primary carbonates, whereas those showing assemblage b contains diagenetic minerals in addition. The occurrence of primary carbonates was associated into three main processes: (a) loss or extraction of  $\text{CO}_2$ ; (b) evaporation concentration; and (c) mixing of different water bodies. The first and second processes commonly occur in humid and dry climates, respectively. Additionally, carbonates precipitated by evaporation concentration are characterized by very high of Mg/Ca ratio (Müller et al., 1972).

Although carbonates commonly occur in lakes in different mode of formation, their chemical characteristics have often been used to reconstruct of paleoenvironments during sediments deposition. High primary productivity would deplete the carbon isotopic compositions of not only organic matter but also precipitated carbonate (e.g. Hollander et al., 1993; Hollander and Smith, 2001). On the other hand, the precipitation of carbonate in lakes has often also been related to the induction of specific picoplankton (e.g. Hodell et al., 1998).

In the Kiliran lake, although the abundance variation of Ca may indicate relative alkalinity of water, the occurrence of carbonate in the lake is still poorly understood. The relatively much lower of Mg to Ca ( $\text{Mg}/\text{Ca} < 0.1$ ) might give a clue for non-evaporative precipitation, but other aspects relating to the detailed carbonate mode of formation and respective paleoenvironment need to be further investigated. Some methods involving visual analysis (thin section

petrography or scanning electron microscope) and carbon isotope measurement for carbonate can be applied.

## 7.2. Artificial maturation study

Beneficiation of oil shales involves heating process to extract the shale oil. The Kiliran oil shale is immature with vitrinite reflectance about  $0.25\pm 0.3$  (PSDG, 2006). Retorting in laboratory scale has been applied for oil shales from Indonesia, but such study dealt only on oil yield as a simple parameter for oil shale prospecting. Rock-Eval analysis has also been performed, but the thermal data were not supported by other geochemical data.

In natural process, organic matter would undergo physicochemical changes against heating during diagenesis, catagenesis and metagenesis. During diagenesis, the main process is elimination of heteroatomic bonds and functional groups. The next organic matter evolution is elimination of hydrocarbon chains and cycles during catagenesis. Crude oils and then gas are successively formed during this stage. After that, metagenesis rearranges aromatic sheets to form larger clusters. At this stage, only dry gas is generated (Tissot and Welte, 1984).

Studies concerning on the evolution of organic matter during artificial maturation have been widely undertaken (e.g. Peters et al., 1981; Huang, 1996; Han et al., 2001). The studies principally adopt the processes occurring in the nature, simulating thermal, pressure and time as the key factors. Closed-system pyrolysis is commonly used to perform the artificial maturation.

From the present study, distinct changes of paleoecology as well as organic matter composition constituting to the oil shale are apparent. *B. braunii* has been well known to contain very high of hydrocarbon and thus potential for oil yield. It is interesting to carry a study concerning the effects of artificial maturation on the hydrocarbon characteristics and oil generation potency of the oil shale showing differing compositional of *B. braunii*. In such study, the fate of each biomarker during maturation can be well understood. Closed-system pyrolysis and then biomarker analysis can be taken to follow such study.

## References

- Ageta, H. and Arai, Y. (1983) Fern constituents: pentacyclic triterpenoids isolated from *Polypodium niponicum* and *P. formosanum*. *Phytochemistry* 22, 1801-1808.
- Aichner, B., Herzsuh, U. and Wilkes, H. (2010) Influence of aquatic macrophytes on the stable carbon isotopic signatures of sedimentary organic matter in lakes on the Tibetan Plateau. *Organic Geochemistry* 41, 706-718.
- Aizenshtat, Z. (1973) Perylene and its geochemical significance. *Geochimica et Cosmochimica Acta* 37, 559-567.
- Allgaier, M. and Grossart, H.P. (2006) Diversity and seasonal dynamics of actinobacteria populations in four lakes in Northeastern Germany. *Applied and Environmental Microbiology* 72, 3489-3497.
- Amijaya, H., Schwarzbauer, J. and Littke, R. (2006) Organic geochemistry of the Lower Suban coal seam, South Sumatra Basin, Indonesia: Palaeoecological and thermal metamorphism implications. *Organic Geochemistry* 37, 261-279.
- Anggayana, K. (1996) Mikroskopische und organisch-geochemische Untersuchungen an Kohlen aus Indonesien, ein Beitrag zur Genese und Fazies verschiedener Kohlenbecken. Dissertation, RWTH Aachen, Germany, pp. 224.
- Audino, M., Grice, K., Alexander, R., Boreham, C.J. and Kagi, R.I. (2001) Unusual distribution of monomethylalkanes in *Botryococcus braunii*-rich samples: origin and significance. *Geochimica et Cosmochimica Acta* 65, 1995-2006.
- Auras, S. and Püttmann, W. (2004) Zusammensetzung und Herkunft der 4-Methylsterioide im Messeler Ölschiefer. *Courier Forschungsinstitut Senckenberg* 252, 139-149.
- Batten, D.J. (1983) Identification of amorphous sedimentary organic matter by transmitted light microscopy. In: *Petroleum Geochemistry and Exploration of Europe* (J. Brooks, ed), Geological Society Special Publications 12, 275-287.
- Berner, R.A. (1984) Sedimentary pyrite formation: An update. *Geochimica et Cosmochimica Acta* 48, 605-615.
- Berner, R.A. and Raiswell, R. (1984) C/S method for distinguishing freshwater from marine sedimentary rocks. *Geology* 12, 365-368.

- Bohacs, K.M., Carroll, K.M., Neal, J.E. and Mankiewicz, P.J. (2000) Lake-basin type, source potential, and hydrocarbon character: an integrated sequence-stratigraphic-geochemical framework. *AAPG Studies in Geology* 46, 3-34.
- Boreham, C.J., Summons, R.E., Roksandic, Z., Dowling, L.M. and Hutton, A.C. (1994) Chemical, molecular and isotopic differentiation of organic facies in the Tertiary lacustrine Duaringa oil shale deposit, Queensland, Australia. *Organic Geochemistry* 21, 685-712.
- Bottari, F., Marsili, A., Morelli, I. and Pacchiani, M. (1972) Aliphatic and triterpenoid hydrocarbons from ferns. *Phytochemistry* 11, 2519-2523.
- BP (2010) BP Statistical Review of World Energy June 2010, <http://bp.com/statisticalreview/>.
- Brassell, S.C. (1990) Biomarkers in recent and ancient sediments: The importance of the diagenetic continuum. In: *Organic Matter: Productivity, Accumulation, and Preservation in Recent and Ancient Sediments* (J.K. Whelan and J.W. Farrington, eds), Hunt Symposium Volume, Columbia Univ. Press.
- Bredholt, H., Fjærvik, E., Johnsen, G. and Zotchev, S.B. (2008) Actinomycetes from sediments in the Trondheim Fjord, Norway: Diversity and biological activity. *Marine Drugs* 6, 12-24.
- Brendow, K. (2003) Global oil shale issues and perspectives. *Oil Shale* 20, 81-92.
- Brocks, J.J., Love, G.D., Summons, R.E., Knoll, A.H., Logan, G.A. and Bowden, S.A. (2005) Biomarker evidence for green and purple sulfur bacteria in a stratified Palaeoproterozoic sea. *Nature* 437, 866-870.
- Burnham, A.K. and McConaghy, J.R. (2006) Comparison of the acceptability of various oil shale processes. 26<sup>th</sup> Oil Shale Symposium December 11, 2006, Golden-Colorado, pp. 17.
- Carnell, A., Butterworth, P., Hamid, B., Livsey, A., Barton, J. and Bates, C. (1998) The Brown Shale of Central Sumatra: a detailed geological appraisal of a shallow lacustrine source rock. *Proceedings Indonesian Petroleum Association 26th Annual Convention May 1998, Jakarta*, pp. 51-69.
- Carroll, A.R. and Bohacs, K.M. (1999) Stratigraphic classification of ancient lakes: Balancing tectonic and climatic controls. *Geology* 27, 99-102.
- Chappe, B., Albrecht, P. and Michaelis, W. (1982) Polar lipids of archaebacteria in sediments and petroleum. *Science* 217, 65-66.
- Chikaraishi, Y. and Naraoka, H. (2003) Compound-specific  $\delta D$ - $\delta^{13}C$  analyses of *n*-alkanes extracted from terrestrial and aquatic plants. *Phytochemistry* 63, 361-371.

- Chikaraishi, Y. and Naraoka, H. (2007)  $\delta^{13}\text{C}$  and  $\delta\text{D}$  relationships among three *n*-alkyl compound classes (*n*-alkanoic acid, *n*-alkane and *n*-alkanol) of terrestrial higher plants. *Organic Geochemistry* 38, 198-215.
- Cole, J.M. and Crittenden, S. (1997) Early Tertiary basin formation and the development of Lacustrine and quasi-lacustrine/marine source rocks on the Sunda Shelf of SE Asia. In: *Petroleum Geology of Southeast Asia* (A.J. Fraser, S.J. Matthews and R.W. Murphy, eds), Geological Society Special Publications 126, 147-183.
- Collister, J.M. (1992) An Isotopic Biogeochemical Study of the Green River Oil Shale (Piceance Creek Basin, Colorado). PhD Thesis, Indiana University, USA, pp. 192.
- Collister, J.W., Rieley, G., Stern, B., Eglinton, G. and Fry, B. (1994) Compound-specific  $\delta^{13}\text{C}$  analyses of leaf lipids from plants with differing carbon dioxide metabolisms. *Organic Geochemistry* 21, 619-627.
- Cook, A.C. and Sherwood, N.R. (1991) Classification of oil shales, coals and other organic-rich rocks. *Organic Geochemistry* 17, 211-222.
- Cranwell, P.A., Eglinton, G. and Robinson, N. (1987) Lipids of aquatic organisms as potential contributors to lacustrine sediments – II. *Organic Geochemistry* 11, 513-527.
- Darman, H. and Sidi, F.H. (2000) *An Outline of The Geology of Indonesia*. Indonesian Association of Geologists, Jakarta, pp. 254.
- de Coster, G.L. (1974) The geology of Central and South Sumatra Basins. *Proceedings Indonesian Petroleum Association 3rd Annual Convention June 1974, Jakarta*, pp. 77-110.
- Dehmer, J. (1988) Petrographische und organisch-geochemische Untersuchungen an rezenten Torfen und tertiären Braunkohlen-Ein Beitrag zur Fazies und Genese gebänderter Braunkohlen. PhD Thesis, RWTH Aachen, Germany, pp. 340.
- Didyk, B.M., Simoneit, B.R.T., Brassell, S.C. and Eglinton, G. (1978) Organic geochemical indicators of palaeoenvironmental conditions of sedimentation. *Nature* 272, 216-222.
- DJMIGAS (2010) *Energy Development in Indonesia: Opportunities and Challenge*. Presentation of Direktorat Jenderal Minyak dan Gas Bumi (DJMIGAS), Indonesian Ministry of Energy and Mineral Resources in Rotes Rathaus, Berlin, October 13, 2010.
- Doust, H. and Noble, R.A. (2008) Petroleum systems of Indonesia. *Marine and Petroleum Geology* 25, 103-129.
- Dowling, L.M., Boreham, C.J., Hope, J.M., Murray, A.P. and Summons, R.E. (1995) Carbon isotopic composition of hydrocarbons in ocean-transported bitumens from the coastline of Australia. *Organic Geochemistry* 23, 729-737.

- Dyni, J.R. (2006) Geology and resources of some world oil-shale deposits: U.S. Geological Survey Scientific Investigations Report 2005-5294, pp. 42.
- Dypvik, H. and Harris, N. B. (2001) Geochemical facies analysis of fine-grained siliciclastics using Th/U, Zr/Rb and (Zr+Rb)/Sr ratios. *Chemical Geology* 181, 131-146.
- Eglinton G. and Hamilton R.J. (1967) Leaf epicuticular waxes. *Science* 156, 1322-1335.
- EIA (2010) U.S. Energy Information Administration, Independent Statistic and Analysis, <http://www.eia.doe.gov/>.
- Elsik, W.C. (1996) Fungi. In: *Palynology: Principles and Applications Vol. 1* (J. Jansonius and D.C. McGregor, eds), American Association of Stratigraphic Palynologists Foundation, Publishers Press, Utah, pp. 293-305.
- Eusterhues, K., Heinrichs, H. and Schneider, J. (2005) Geochemical response on redox fluctuations in Holocene lake sediments, Lake Steisslingen, Southern Germany. *Chemical Geology* 222, 1-22.
- Farrimond, P. and Telnaes, N. (1996) Three series of rearranged hopanes in Toarcian sediments (northern Italy). *Organic Geochemistry* 25, 165-177.
- Ficken, K.J., Li, B., Swain, D.L. and Eglinton, G. (2000) An *n*-alkane proxy for the sedimentary input of submerged/floating freshwater aquatic macrophytes. *Organic Geochemistry* 31, 745-749.
- Freeman, K.H., Hayes, J.M., Trendel, J.M. and Albrecht, P. (1990) Evidence from carbon isotope measurements for diverse origins of sedimentary hydrocarbons. *Nature* 343, 254-256.
- Fu Jiamo., Sheng Guoying, Xu Jiayou, Eglinton G., Gowar A.P., Jia Rongfen, Fan Shanfa and Peng Pingan (1990) Application of biological markers in the assessment of paleoenvironments of Chinese non-marine sediments. *Organic Geochemistry* 16, 769-779.
- Gelpi, E., Schneider, H., Mann, J. and Oró, J. (1970) Hydrocarbons of geochemical significance in microscopic algae. *Phytochemistry* 9, 603-612.
- Geopetro Library (2003) *Geo- & Petrochemicals and Biomarkers*, 2nd Edition. Wiley-VCH Verlag GmbH & Co. KGaA, Weinheim.
- Gocht, T., Barth, J.A.C., Epp, M., Jochmann, M., Blessing, M., Schmidt, T.C. and Grathwohl, P. (2007) Indications for pedogenic formation of perylene in a terrestrial soil profile: Depth distribution and first results from stable carbon isotope ratios. *Applied Geochemistry* 22, 2652-2663.

- Goldman, C.R. (1988) Primary productivity, nutrients, and transparency during the early onset of eutrophication in ultra-oligotrophic Lake Tahoe, California-Nevada. *Limnol. Oceanogr.* 33, 1321-1333.
- Goodfellow, M. and Williams, S.T. (1983) Ecology of Actinomycetes. *Annual Reviews of Microbiology* 37, 189-216.
- Goodwin N.S., Mann A.L. and Patience R.L. (1988) Structure and significance of C30 4-methylsteranes in lacustrine shales and oils. *Organic Geochemistry* 12, 495-506.
- Goossens, H., de Leeuw, J.W., Schenck, P.A. and Brassell, S.C. (1984) Tocopherols as likely precursors of pristane in ancient sediments and crude oils. *Nature* 312, 440-442.
- Grice, K., Audino, M., Boreham, C.J., Alexander, R. and Kagi, R.I. (2001) Distributions and stable carbon isotopic compositions of biomarkers in torbanites from different palaeogeographical locations. *Organic Geochemistry* 32, 1195-1210.
- Grice, K., Cao, C., Love, G.D., Böttcher, M.E., Twitchett, R.J., Grosjean, E., Summons, R. E., Turgeon, S.C., Dunning, W. and Jin, Y. (2005) Photic zone euxinia during the Permian-Triassic superanoxic event. *Science* 307, 706-709.
- Grice, K., Lu, H., Atahan, P., Asif, M., Hallmann, C., Greenwood, P., Maslen, E., Tulipani, S., Williford, K. and Dodson, J. (2009) New insights into the origin of perylene in geological samples. *Geochimica et Cosmochimica Acta* 73, 6531-6543.
- Grice, K., Schaeffer, P., Schwark, L. and Maxwell, J.R. (1996) Molecular indicators of palaeoenvironmental conditions in an immature Permian shale (Kupferschiefer, Lower Rhine Basin, north-west Germany) from free and S-bound lipids. *Organic Geochemistry* 25, 131-147.
- Grice, K., Schouten, S., Nissenbaum, A., Charrach, J. and Sinninghe-Damsté, J.S. (1998a) A remarkable paradox: Sulfurised freshwater algal (*Botryococcus braunii*) lipids in an ancient hypersaline euxinic ecosystem. *Organic Geochemistry* 28, 195-216.
- Grice, K., Schouten, S., Peters, K.E. and Sinninghe Damsté, J.S. (1998b) Molecular isotopic characterization of hydrocarbon biomarkers in Palaeocene-Eocene evaporitic, lacustrine source rocks from the Jiangnan Basin, China. *Organic Geochemistry* 29, 1745-1764.
- Hartgers, W.A., Schouten, S., Lopez, J.F., Sinninghe-Damsté, J.S. and Grimalt, J.O. (2000) <sup>13</sup>C-contents of sedimentary bacterial lipids in a shallow sulfidic monomictic lake (Lake Cisó, Spain). *Organic Geochemistry* 31, 777-786.
- Hartgers, W.A., Sinninghe Damsté, J.S., Requejo, A.G., Allan, J., Hayes, J.M., Ling, Y., Xie, T., Primack, J. and de Leeuw, J.W. (1994) A molecular and carbon isotopic study

- towards the origin and diagenetic fate of diaromatic carotenoids. *Organic Geochemistry* 22, 703-725.
- Hayes, J.M., Freeman, K.H., Popp, B.N. and Hoham, C.H. (1990) Compound-specific isotopic analyses: A novel tool for reconstruction of ancient biogeochemical processes. *Organic Geochemistry* 16, 1115-1128.
- Herrmann, M. (2010) Palaeoecological reconstruction of the late Oligocene Maar Lake of Enspel, Germany using lacustrine organic walled algae. *Palaeodiversity and Palaeoenvironments* 20, 29-37.
- Hodell, D.A. and Schelske, C.L. (1998) Production, sedimentation, and isotopic composition of organic matter in Lake Ontario. *Limnology and Oceanography* 43, 200-214.
- Hollander, D., McKenzie, J., Hsu, K. and Huc, A. (1993) Application of an eutrophic lake model to the origin of ancient organic-carbon-rich sediments. *Global Biogeochemical Cycles* 7, 157-179.
- Hollander, D.J. and Smith, M.A. (2001) Microbially mediated carbon cycling as a control on the  $\delta^{13}\text{C}$  of sedimentary carbon in eutrophic Lake Mendota (USA): new models for interpreting isotopic excursions in the sedimentary record. *Geochimica et Cosmochimica Acta* 65, 4321-4337.
- Huang, W.Y. and Meinschein, W.G. (1979) Sterols as ecological indicators. *Geochimica et Cosmochimica Acta* 43, 739-745.
- Huang, X., Xie, S., Zhang, C.L., Jiao, D., Huang, J., Yu, J., Jin, F. and Gu, Y. (2008) Distribution of aliphatic des-A-triterpenoids in the Dajiuhu peat deposit, southern China. *Organic Geochemistry* 39, 1765-1771.
- Huang, Y., Street-Perrott, F.A., Perrott, R.A., Metzger, P. and Eglinton, G. (1999) Glacial-interglacial environmental changes inferred from molecular and compound-specific  $\delta^{13}\text{C}$  analyses of sediments from Sacred Lake, Mt. Kenya. *Geochimica et Cosmochimica Acta* 63, 1383-1404.
- Hutton, A.C. (1987) Petrographic classification of oil shales. *International Journal of Coal Geology* 8, 203-231.
- Ishiwatari, R., Hirakawa, Y., Uzaki, M., Yamada, K. and Yada, T. (1994a) Organic geochemistry of the Japan Sea sediments—1: Bulk organic matter and hydrocarbon analyses of core KH-79-3, C-3 from the Oki Ridge for paleoenvironment assessments. *Journal of Oceanography* 50, 179-195.
- Ishiwatari, R., Uzaki, M. and Yamada, K. (1994b) Carbon isotope composition of individual *n*-alkanes in recent sediments. *Organic Geochemistry* 21, 801-808.



- Jiang, C., Alexander, R., Kagi, R.I. and Murray, A.P. (2000) Origin of perylene in ancient sediments and its geological significance. *Organic Geochemistry* 31, 1545-1559.
- Kalgutkar, R.M. (1997) Fossil fungi from the lower Tertiary Iceberg Bay Formation, Eukeka Sound Group, Axel Heiberg Island, Northwest Territories, Canada. *Review of Palaeobotany and Palynology* 97, 197-226.
- Kar, R., Mandaokar, B.D. and Kar, R.K. (2010) Fungal taxa from the Miocene sediments of Mizoram, northeast India. *Review of Palaeobotany and Palynology* 158, 240-249.
- Katz, B.J. (1991) Controls on lacustrine source rock development: a model for Indonesia. *Proceedings Indonesian Petroleum Association 20th Annual Convention October 1991, Jakarta*, pp. 587-619.
- Katz, B.J. (2001) Lacustrine basin hydrocarbon exploration - current thoughts. *Journal of Paleolimnology* 26, 161-179.
- Killops, S.D. (1991) Novel aromatic hydrocarbons of probable bacterial origin in a Jurassic lacustrine sequence. *Organic Geochemistry* 17, 25-36.
- Klink, G., Dreier, F., Buchs, A. and Gülaçar, F.O. (1992) A new source for 4-methyl sterols in freshwater sediments: *Utricularia neglecta* L. (Lentibulariaceae). *Organic Geochemistry* 18, 757-763.
- Komárek, J. and Marvan, P. (1992) Morphological differences in natural populations of the genus *Botryococcus* (*Chlorophyceae*). *Archiv für Protistenkunde* 141, 65-100.
- Koopmans, M.P., Köster, J., van Kaam-Peters, H.M.E., Kenig, F., Schouten, S., Hartgers, W.A., de Leeuw, J.W. and Sinninghe Damsté, J.S. (1996a) Diagenetic and catagenetic products of isorenieratene: Molecular indicators for photic zone anoxicity. *Geochimica et Cosmochimica Acta* 60, 4467-4496.
- Koopmans, M.P., Schouten, S., Kohlen, M.E.L. and Sinninghe Damsté, J.S. (1996b) Restricted utility of aryl isoprenoids as indicators for photic zone anoxicity. *Geochimica et Cosmochimica Acta* 60, 4873-4876.
- Krügel, H., Krubasik, P., Weber, K., Saluz, H.P. and Sandmann, G. (1999) Functional analysis of genes from *Streptomyces griseus* involved in the synthesis of isorenieratene, a carotenoid with aromatic end groups, revealed a novel type of carotenoid desaturase. *Biochimica et Biophysica Acta* 1439, 57-64.
- Kuhn, T.K., Krull, E.S., Bowater, A., Grice, K. and Gleixner, G. (2010) The occurrence of short chain *n*-alkanes with an even over odd predominance in higher plants and soils. *Organic Geochemistry* 41, 88-95.

- Kumar, P. (1990) Fungal remains from the Miocene Quilon Beds of Kerala State, South India. *Review of Palaeobotany and Palynology* 62, 13-28.
- Küspert, W. (1982) Environmental changes during oil shale deposition as deduced from stable isotope ratios. In: *Cyclic and Event Stratification* (G. Einsele and A. Seilacher, eds.), Springer, Heidelberg, pp. 482–501.
- Lenz, O.K., Wilde, V., Riegel, W. and Heinrichs, T. (2007) Distribution and paleoecologic significance of the freshwater dinoflagellates cyst *Messeledonium thielepfeifferae* Gen. et sp. nov from the Middle Eocene of lake Messel, Germany. *Palynology* 31, 119-134.
- Lewis, W.M. (1987) Tropical limnology. *Annual Reviews Ecology Systematics* 18, 159-184.
- Li, M., Larter, S.R., Taylor, P., Jones, D.M., Bowler, B. and Bjoroy, M. (1995) Biomarkers or not biomarkers? A new hypothesis for the origin of pristane involving derivation from methyltrimethyltridecylchromans (MTTCs) formed during diagenesis from chlorophyll and alkylphenols. *Organic Geochemistry* 23, 159-167.
- Liaaen-Jensen, S., Renstrøm, B., Ramdahl, T., Hallenstvet, M. and Bergquist, P. (1982) Carotenoids of marine sponges. *Biochemical Systematics and Ecology* 10, 167-174.
- Lichtfouse, É., Derenne, S., Mariotti, A. and Largeau, C. (1994) Possible algal origin of long chain odd *n*-alkanes in immature sediments as revealed by distributions and carbon isotope ratios. *Organic Geochemistry* 22, 1023-1027.
- Longley, I.M., Barraclough, R., Bridden, M.A. and Brown, S. (1990) Pematang lacustrine petroleum source rocks from the Malacca Strait PSC, Central Sumatra, Indonesia. *Proceedings Indonesian Petroleum Association 19th Annual Convention October 1990, Jakarta*, pp. 279-297.
- Maresca, J.A., Romberger, S.P. and Bryant, D.A. (2008) Isorenieratene biosynthesis in green sulfur bacteria requires the cooperative actions of two carotenoid cyclases. *Journal of Bacteriology* 190, 6384-6391.
- McKenzie, J.A. (1985) Carbon isotopes and productivity in the lacustrine and marine environment. In: *Chemical Processes in Lakes* (W. Stumm, ed), Wiley, pp. 99-118.
- McManus, J., Berelson, W.M., Severmann, S., Poulson, R.L., Hammond, D.E., Klinkhammer, G.P. and Holm, C. (2006) Molybdenum and uranium geochemistry in continental margin sediments: Paleoproxy potential. *Geochimica et Cosmochimica Acta* 70, 4643-4662.
- Menzel, D., Hopmans, E.C., van Bergen, P.F., de Leeuw, J.W. and Sinninghe-Damsté, J.S. (2002) Development of photic zone euxinia in the eastern Mediterranean Basin during deposition of Pliocene sapropels. *Marine Geology* 189, 215-226.

- Metzger, P. and Casadevall, E. (1987) Lycopadiene, a tetraterpenoid hydrocarbon from new strains of the green alga *Botryococcus braunii*. *Tetrahedron Letters* 28, 3931-3934.
- Metzger, P. and Largeau, C. (2005) *Botryococcus braunii*: a rich source for hydrocarbons and related ether lipids. *Applied Microbiology and Biotechnology* 66, 486-496.
- Metzger, P., Berkaloff, C., Casadevall, E. and Coute, A. (1985b) Alkadiene- and botryococcene-producing races of wild strains of *Botryococcus braunii*. *Phytochemistry* 24, 2305-2312.
- Metzger, P., Casadevall, E. and Coute, A. (1988) Botryococcene distribution in strains of the green alga *Botryococcus braunii*. *Phytochemistry* 27, 1383-1388.
- Metzger, P., Casadevall, E., Pouet, M.J. and Pouet, Y. (1985a) Structures of some botryococcenes: branched hydrocarbons from the b-race of the green alga *Botryococcus braunii*. *Phytochemistry* 24, 2995-3002.
- Metzger, P., Largeau, C. and Casadevall, E. (1991) Lipids and macromolecular lipids of the hydrocarbon-rich microalga *Botryococcus braunii*. Chemical structure and biosynthesis. Geochemical and biotechnological importance. In: *Progress in the Chemistry of Organic Natural Products* (W. Herz et al., eds), Springer Verlag, Berlin, pp. 1-70.
- Metzger, P., Pouet, Y. and Summons, R. (1997) Chemotaxonomic evidence for the similarity between *Botryococcus braunii* L race and *Botryococcus neglectus*. *Phytochemistry* 44, 1071-1075.
- Metzger, P., Villarreal-Rosales, E., Casadevall, E. and Coute, A. (1989) Hydrocarbons, aldehydes and triacylglycerols in some strains of the a-race of the green alga *Botryococcus braunii*. *Phytochemistry* 28, 2349-2353.
- Meyers, P.A. (1997) Organic geochemical proxies of paleoceanographic, paleolimnologic, and paleoclimatic processes. *Organic Geochemistry* 27, 213-250.
- Meyers, P.A. (2003) Applications of organic geochemistry to paleolimnological reconstructions: a summary of examples from the Laurentian Great Lakes. *Organic Geochemistry* 34, 261-289.
- Meyers, P.A. and Ishiwatari, R. (1993) Lacustrine organic geochemistry – an overview of indicators of organic matter sources and diagenesis in lake sediments. *Organic Geochemistry* 20, 867-900.
- Moldowan, J.M. and Seifert, W.K. (1980) First discovery of botryococcane in petroleum. *Journal of the Chemical Society, Chemical Communications* 1980, 912-914.

- Moldowan, J.M., Seifert, W.K. and Gallegos, E.J. (1985) Relationship between petroleum composition and depositional environment of petroleum source rocks. *AAPG Bulletin* 69, 1255-1268.
- Murray, A.P., Summons, R.E., Boreham, C.J. and Dowling, L.M. (1994) Biomarker and *n*-alkane isotope profiles for Tertiary oils: relationship to source rock depositional setting. *Organic Geochemistry* 22, 521-542.
- Nytoft, H.P., Bojesen-Koefoed, J.A., Christiansen, F.G. and Fowler, M.G. (2002) Oleanane or lupane? Reappraisal of the presence of oleanane in Cretaceous-Tertiary oils and sediments. *Organic Geochemistry* 33, 1225-1240.
- O'Reilly, C.M., Alin, S.R., Plisnier, P.D., Cohen, A.S. and McKee, B.A. (2003) Climate change decreases aquatic ecosystem productivity of Lake Tanganyika, Africa. *Nature* 424, 766-768.
- Pedentchouk, N., Freeman, K. H., Harris, N. B., Clifford, D. J. and Grice, K. (2004) Sources of alkylbenzenes in Lower Cretaceous lacustrine source rocks, West African rift basins. *Organic Geochemistry* 35, 33-45.
- Peters, K.E., Walters, C.C. and Moldowan, J.M. (2005a) *The Biomarker Guide Vol. 1: Biomarkers and Isotopes in the Environment and Human History*, 2nd Edition. Cambridge University Press, New York, pp. 471.
- Peters, K.E., Walters, C.C. and Moldowan, J.M. (2005b) *The Biomarker Guide Vol. 2: Biomarkers and Isotopes in Petroleum Exploration and Earth History*, 2nd Edition. Cambridge University Press, New York, pp. 475-1155.
- Petrominer (2010) *Petrominer Monthly Magazine XXXVI(1)*, January 15, 2010.
- Philp, R. P. (1985) *Fossil fuel biomarker: Applications and spectra*. Elsevier, Amsterdam, pp. 294.
- Powell, T.G. and McKirdy, D.M. (1973) Relationship between ratio of pristane to phytane, crude oil composition and geological environment in Australia. *Nature Physical Science* 243, 37-39.
- PSDG (2006) *Laporan Inventarisasi Kegiatan Pengeboran Bitumen Padat di Daerah Padanglawas, Kabupaten Dharmasraya, Sumatera Barat*. Pusat Sumber Daya Geologi, Bandung, pp. 112. (in Bahasa Indonesia).
- Püttmann W. and Goth K. (1988) Analysis of hydrocarbon in algal-rich Messel Shale samples. *Courier Forschungsinstitut Senckenberg* 107, 105-117.
- PWC (2010) *Oil and Gas in Indonesia, Investment and Taxation Guide*. PricewaterhouseCoopers Indonesia.

- Radke, M., Welte, D.H. and Willsch, H. (1986) Maturity parameters based on aromatic hydrocarbons: Influence of the organic matter type. *Organic Geochemistry* 10, 51-63.
- Ramírez, J.J. and Corbacho, M. (2005) Population dynamics of *Botryococcus braunii* Kützing 1849 in a shallow tropical eutrophic lake. *Algological Studies* 115, 129-143.
- Requejo, A. G., Allan, J., Creaney, S., Gray, N. R. and Cole, K. S. (1992) Aryl isoprenoids and diaromatic carotenoids in Paleozoic source rocks and oils from the Western Canada and Williston Basins. *Organic Geochemistry* 19, 245-264.
- Robinson, N., Eglinton, G., Brassell, S.C. and Cranwell, P.A. (1984) Dinoflagellate origin for sedimentary 4 $\alpha$ -methylsteroids and 5 $\alpha$ (H)-stanols. *Nature* 308, 439-442.
- Rohling, E.J., Hopmans, E.C. and Sinninghe-Damsté, J.S. (2006) Water column dynamics during the last interglacial anoxic event in the Mediterranean (sapropel S5). *Paleoceanography* 21, PA2018, doi:10.1029/2005PA001237.
- Rohmer, M. (1987) The hopanoids, prokaryotic triterpenoids and sterols surrogates. In: *Surface Structures of Microorganisms and Their Interactions with the Mammalian Host* (E. Schriener et al., eds), VCH Publishing, Weinlein, Germany, pp. 227-242.
- Rontani, J.F., Nassiry, M., Michotey, V., Guasco, S. and Bonin, P. (2010) Formation of pristane from  $\alpha$ -tocopherol under simulated anoxic sedimentary conditions: A combination of biotic and abiotic degradative processes. *Geochimica et Cosmochimica Acta* 74, 252-263.
- Rowland, S.J. (1990) Production of acyclic isoprenoid hydrocarbons by laboratory maturation of methanogenic bacteria. *Organic Geochemistry* 15, 9-16.
- Schaeffer, P., Adam, P., Wehrung, P. and Albrecht, P. (1997) Novel aromatic carotenoid derivatives from sulfur photosynthetic bacteria in sediments. *Tetrahedron Letters* 38, 8413-8416.
- Schmidt, K. (1978) Biosynthesis of carotenoids. In: *Photosynthetic Bacteria* (R.K. Clayton and W.R. Sistrom, eds), Plenum Press, New York, pp. 729-730.
- Schouten, S., Hartgers, W.A., Lòpez, J.F., Grimalt, J.O. and Sinninghe-Damsté, J.S. (2001) A molecular isotopic study of <sup>13</sup>C-enriched organic matter in evaporitic deposits: recognition of CO<sub>2</sub>-limited ecosystems. *Organic Geochemistry* 32, 277-286.
- Seip, K.L. (1994) Phosphorus and nitrogen limitation of algal biomass across trophic gradients. *Aquatic Science* 56, 16-28.
- Senousy, H.H., Beakes, G.W. and Hack, E. (2004) Phylogenetic placement of *Botryococcus braunii* (*Trebouxiophyceae*) and *Botryococcus sudeticus* isolate utex 2629 (*Chlorophyceae*). *Journal of Phycology* 40, 412-423.

- Silliman, J.E., Meyers, P.A., Ostrom, P.H., Ostrom, N.E. and Eadie, B.J. (2000) Insights into the origin of perylene from isotopic analyses of sediments from Saanich Inlet, British Columbia. *Organic Geochemistry* 31, 1133-1142.
- Sinninghe Damsté, J.S., Frewin, N.L., Kenig, F. and de Leeuw J.W. (1995) Molecular indicators for palaeoenvironmental change in a Messinian evaporitic sequence (Vena del Gesso, Italy). I: Variations in extractable organic matter of ten cyclically deposited marl beds. *Organic Geochemistry* 23, 471-483.
- Sinninghe Damsté, J.S., Schouten, S. and van Duin A.C.T. (2001) Isorenieratene derivatives in sediments: Possible controls on their distribution. *Geochimica et Cosmochimica Acta* 65, 1557-1571.
- Sinninghe-Damsté, J.S., Kuypers, M.M.M., Schouten, S., Schulte, S. and Rullkötter, J. (2003) The lycopane/C<sub>31</sub> *n*-alkane ratio as a proxy to assess palaeoacidity during sediment deposition. *Earth and Planetary Science Letters* 209, 215-226.
- Sinninghe-Damsté, J.S., Rijpstra, W.I.C. and Reichert, G. (2002) The influence of oxic degradation on the sedimentary biomarker record II. Evidence from Arabian Sea sediments. *Geochimica et Cosmochimica Acta* 66, 2737-2754.
- Sladen, C. (1997) Exploring the lake basins of East and Southeast Asia. In: *Petroleum Geology of Southeast Asia* (A.J. Fraser, S.J. Matthews and R.W. Murphy, eds) Geological Society Special Publications 126, 49-76.
- Smittenberg, R.H., Baas, M., Schouten, S. and Sinninghe-Damsté, J.S. (2005) The demise of the alga *Botryococcus braunii* from a Norwegian fjord was due to early eutrophication. *The Holocene* 15, 133-140.
- Smittenberg, R.H., Pancost, R.D., Hopmans, E.C., Paetzel, M. and Sinninghe Damsté, J.S. (2004) A 400-year record of environmental change in an euxinic fjord as revealed by the sedimentary biomarker record. *Palaeogeography, Palaeoclimatology, Palaeoecology* 202, 331-351.
- Sosrowidjojo, I.B., Alexander, R., Kagi, R.I. (1994) The biomarker composition of some crude oils from Sumatra. *Organic Geochemistry* 21, 303-312.
- Staplin, F.L., Fournier, G.R., Leblanc, A.E. (1976) Tertiary biostatigraphy, Mackenzie Delta region, Canada. *Bulletin of Canadian Petroleum Geology* 24, 117-136.
- Stout, S. A. (1992) Aliphatic and aromatic triterpenoid hydrocarbons in a Tertiary angiospermous lignite. *Organic Geochemistry* 18, 51-66.
- Stout, S.A. (1992) Aliphatic and aromatic triterpenoid hydrocarbons in a Tertiary angiospermous lignite. *Organic Geochemistry* 18, 51-66.

- Summons R.E., Thomas J., Maxwell J.R. and Boreham C.J. (1992) Secular and environmental constraints on the occurrence of dinosteranes in sediments. *Geochimica et Cosmochimica Acta* 56, 2437-2444.
- Summons, R.E., Metzger, P., Largeau, C., Murray, A.P. and Hope, J.M. (2002) Polymethylsqualanes from *Botryococcus braunii* in lacustrine sediments and crude oils. *Organic Geochemistry* 33, 99-109.
- Summons, R.E., Volkman, J.K. and Boreham, C.J. (1987) Dinosterane and other steroidal hydrocarbons of dinoflagellate origin in sediments and petroleum. *Geochimica et Cosmochimica Acta* 51, 3075-3082.
- Suwarna, N., Heryanto, R., Hermanto, B., Sundari, D. and Panggabean, H. (2001) Kajian Oil Shale di Cekungan Ombilin dan Sub-cekungan Kiliranjao, Sumatera Barat. Geological Research and Development Center (GRDC) Internal Report, Bandung, pp. 53.
- Tissot B.P. and Welte D.H. (1984) *Petroleum Formation and Occurrence*. Springer-Verlag, New York.
- Tobing, S.M. (2005) Prospek bitumen padat Pulau Buton, Propinsi Sulawesi Tenggara. Kolokium Hasil Lapangan – DIM 2005 (in Bahasa Indonesia).
- Trendel, J.M., Lohmann, F., Kintzinger, J.P., Albrecht, P., Chiarone, A., Riche, C., Cesario, M., Guilhem, J. and Pascard, C. (1989) Identification of des-A-triterpenoid hydrocarbons occurring in surface sediments. *Tetrahedron* 45, 4457-4470.
- Tribovillard, N., Algeo, T., Lyons, T.W. and Riboulleau, A. (2006) Trace metals as paleoredox and paleoproductivity proxies: an update. *Chemical Geology* 232, 12-32.
- Tu, T.T.N., Derenne, S., Largeau, C., Mariotti, A., Bocherens, H. and Pons, D. (2000) Effects of fungal infection on lipid extract composition of higher plant remains: comparison of shoots of a Cenomanian conifer, uninfected and infected by extinct fungi. *Organic Geochemistry* 31, 1743-1754.
- Tyson, R.V. (1995) *Sedimentary Organic Matter, Organic Facies and Palynofacies*. Chapman & Hall, London, pp. 615.
- van Breugel, Y., Schouten, S., Paetzel, M., Ossebaar, J. and Sinninghe Damsté, J.S. (2005) Reconstruction of  $\delta^{13}\text{C}$  of chemocline  $\text{CO}_2$  (aq) in past oceans and lakes using the  $\delta^{13}\text{C}$  of fossil isorenieratene. *Earth and Planetary Science Letters* 235, 421-434.
- Volkman J.K., Kearney, P. and Jeffrey S.W. (1990) A new source of 4-methyl and 5 $\alpha$ (H)-stanols in sediments: prymnesiophyte microalgae of the genus *Pavlova*. *Organic Geochemistry* 15, 489-497.

- Wain, A.S. and Jackson, B.A. (1995) New Pematang Depocentres on the Kampar Uplift, Central Sumatra. Proceedings Indonesian Petroleum Association 24th Annual Convention October 1995, Jakarta, pp. 215-233.
- Wakeham, S.G., Freeman, K.H., Pease, T.K. and Hayes, J.M. (1993) A photoautotrophic source for lycopane in marine water columns. *Geochimica et Cosmochimica Acta* 57, 159-165.
- Wakeham, S.G., Schaffner, C., Giger, W., Boon, J.J. and de Leeuw, J.W. (1979) Perylene in sediments from the Namibian Shelf. *Geochimica et Cosmochimica Acta* 43, 1141-1144.
- Ward, A.C. and Bora, N. (2006) Diversity and biogeography of marine actinobacteria. *Current Opinion in Microbiology* 9, 279-286.
- Webster, N.S., Wilson, K.J., Blackall, L.L. and Hill, R.T. (2001) Phylogenetic diversity of bacteria associated with the marine sponge *Rhopaloeides odorabile*. *Applied and Environmental Microbiology* 67, 434-444.
- WEC (2010) 2010 Survey of Energy Resources. World Energy Council, <http://www.worldenergy.org/>.
- Whiticar, M.J. (1999) Carbon and hydrogen isotope systematics of bacterial formation and oxidation of methane. *Chemical Geology* 161, 291-314.
- Whiticar, M.J., Faber, E. and Schoell, M. (1986) Biogenic methane formation in marine and freshwater environments: CO<sub>2</sub> reduction vs. acetate fermentation – Isotope evidence. *Geochimica et Cosmochimica Acta* 50, 693-709.
- Widodo, S. (2008) Organic petrology and geochemistry of Miocene coals from Kutai Basin, Mahakam Delta, East Kalimantan, Indonesia: Genesis of coal and depositional environment. PhD Thesis, Goethe-Universität, Germany, pp. 173.
- Widodo, S., Bechtel, A., Anggayana, K. and Püttmann, W. (2009) Reconstruction of floral changes during deposition of the Miocene Embalut coal from Kutai Basin, Mahakam Delta, East Kalimantan, Indonesia by use of aromatic hydrocarbon composition and stable carbon isotope ratios of organic matter. *Organic Geochemistry* 40, 206-218.
- Wiley Library (2008) Wiley Registry, 8th Edition/NIST. SIS Inc., Ringoes-New Jersey.
- Wilkinson, H.P. (2003) Fossil actinomycete filaments and fungal hyphae in dicotyledonous wood from the Eocene London Clay, Isle-of-Sheppey, Kent, England. *Botanical Journal of the Linnean Society* 142, 383-394.
- Williams, H.H. and Eubank, R.T. (1995) Hydrocarbon habitat in the rift graben of the Central Sumatra Basin, Indonesia. In: *Hydrocarbon Habitat in Rift Basins* (J.J. Lambiase, ed), Geological Society Special Publications 80, 331-371.



- Williams, H.H., Fowler, M. and Eubank, R.T. (1995) Characteristics of selected Palaeogene and Cretaceous lacustrine source basins of Southeast Asia. In: Hydrocarbon Habitat in Rift Basins (J.J. Lambiase, ed), Geological Society Special Publications 80, 241-282.
- Williams, H.H., Kelley, P.A., Janks, J.S. and Christensen, R.M. (1985) The Paleogene rift basin source rocks of Central Sumatra. Proceedings Indonesian Petroleum Association 14th Annual Convention October 1985, Jakarta, pp. 57-90.
- Wolff G.A., Lamb N.A. and Maxwell J.R. (1986) The origin and fate of 4-methyl steroids – II. Dehydration of stanols and occurrence of C30 4-methyl steranes. *Organic Geochemistry* 10, 965-974.
- Xu, Y. and Jaffé, R. (2009) Geochemical record of anthropogenic impacts on Lake Valencia, Venezuela. *Applied Geochemistry* 24, 411-418.
- Zhang, Z., Metzger, P. and Sachs, J.P. (2007) Biomarker evidence for the co-occurrence of three races (A, B and L) of *Botryococcus braunii* in El Junco Lake, Galápagos. *Organic Geochemistry* 38, 1459-1478.

**Appendix 1: Sample list**

Table A1.1. List of samples and profile-depths

Samples	Profile depth (m)	Samples	Profile depth (m)
G-01	4.0	G-44	57.1
G-03	6.1	G-50	63.1
G-05	8.3	G-52	65.1
G-06	10.2	G-54	67.1
G-08	13.4	G-55	68.1
G-11	17.4	G-57	70.1
G-14	21.1	G-62	75.1
G-16	23.1	G-64	77.1
G-18	25.5	G-66	79.1
G-20	28.4	G-68	81.1
G-22	31.8	G-69	82.1
G-24	34.0	G-70	83.1
G-26	36.1	G-72	85.1
G-28	40.1	G-74	87.1
G-30	43.1	G-76	89.1
G-32	45.1	G-78	91.1
G-34	47.1	G-80	93.1
G-36	49.1	G-81	94.1
G-38	51.1	G-83	96.1
G-40	53.1	G-85	98.1
G-42	55.1	G-87	100.1

**Appendix 2: Palynological Data**

Table A2.1. Organic matter composition of the studied Kiliran oil shale (%).

Samples	B. b.	Po.	Fu.	Sp.	Ph.	AOM
G-01	4.33	5.00	-	0.67	0.67	89.33
G-03	7.00	3.00	-	0.67	0.33	89.00
G-05	6.67	4.33	-	0.33	0.33	88.34
G-06	4.75	3.00	-	0.50	0.25	91.50
G-08						
G-11	8.67	5.33	-	0.67	0.67	84.66
G-14	13.33	6.00	-	0.67	1.00	79.00
G-16	16.00	5.00	0.33	0.67	2.00	76.00
G-18						
G-20	9.00	4.67	0.67	1.00	1.00	83.66
G-22	11.33	3.67	1.33	0.67	0.33	82.67
G-24	13.67	3.67	1.67	-	0.67	80.32
G-26	14.33	5.00	1.00	-	0.67	79.00
G-28	16.00	3.00	2.67	1.00	0.67	76.66
G-30	9.33	3.33	1.33	0.67	1.00	84.34
G-32	13.67	3.67	2.33	-	1.33	79.00
G-34	8.67	1.67	2.00	-	1.00	86.66
G-36	15.33	2.33	1.67	1.00	0.33	79.34
G-38	8.36	3.33	3.00	0.33	1.67	83.31
G-40	9.00	2.00	0.67	0.33	0.67	87.33
G-42	7.00	1.75	-	0.25	0.50	90.50
G-44	6.50	1.00	0.75	-	0.25	91.50
G-50	7.50	1.25	-	0.25	-	91.00
G-52	9.00	1.67	1.00	0.33	0.33	87.67
G-54	9.67	0.67	1.00	-	0.33	88.33
G-55	8.67	0.67	1.33	-	1.33	88.00
G-57	7.87	1.67	0.67	0.33	0.33	89.13
G-62	3.75	1.00	0.75	-	0.25	94.25
G-64	4.25	0.75	0.50	-	0.25	94.25
G-66	3.00	0.25	0.50	-	0.25	96.00
G-68	5.25	1.25	0.50	0.50	-	92.50
G-69						
G-70	5.25	0.75	-	0.50	-	93.50
G-72	4.00	1.00	-	-	-	95.00
G-74	6.00	0.75	-	-	-	93.25
G-76	5.25	0.75	-	-	-	94.00
G-78	4.25	0.75	-	-	1.00	94.00
G-80	4.75	1.00	-	-	1.00	93.25
G-81	7.25	1.25	-	-	0.25	91.25
G-83	8.67	2.00	-	-	1.67	87.66
G-85	5.33	0.33	0.33	-	3.33	90.68
G-87	7.00	2.00	0.33	0.67	1.33	88.67

B. b.: *Botryococcus braunii*; Po.: pollen; Fu.: fungal remains including hyphae, spores and fruiting bodies; Sp.: spores; Ph.: phytoclasts including cuticles and wood debris; AOM: amorphous organic matter.

A.2.2. Photomicrographs

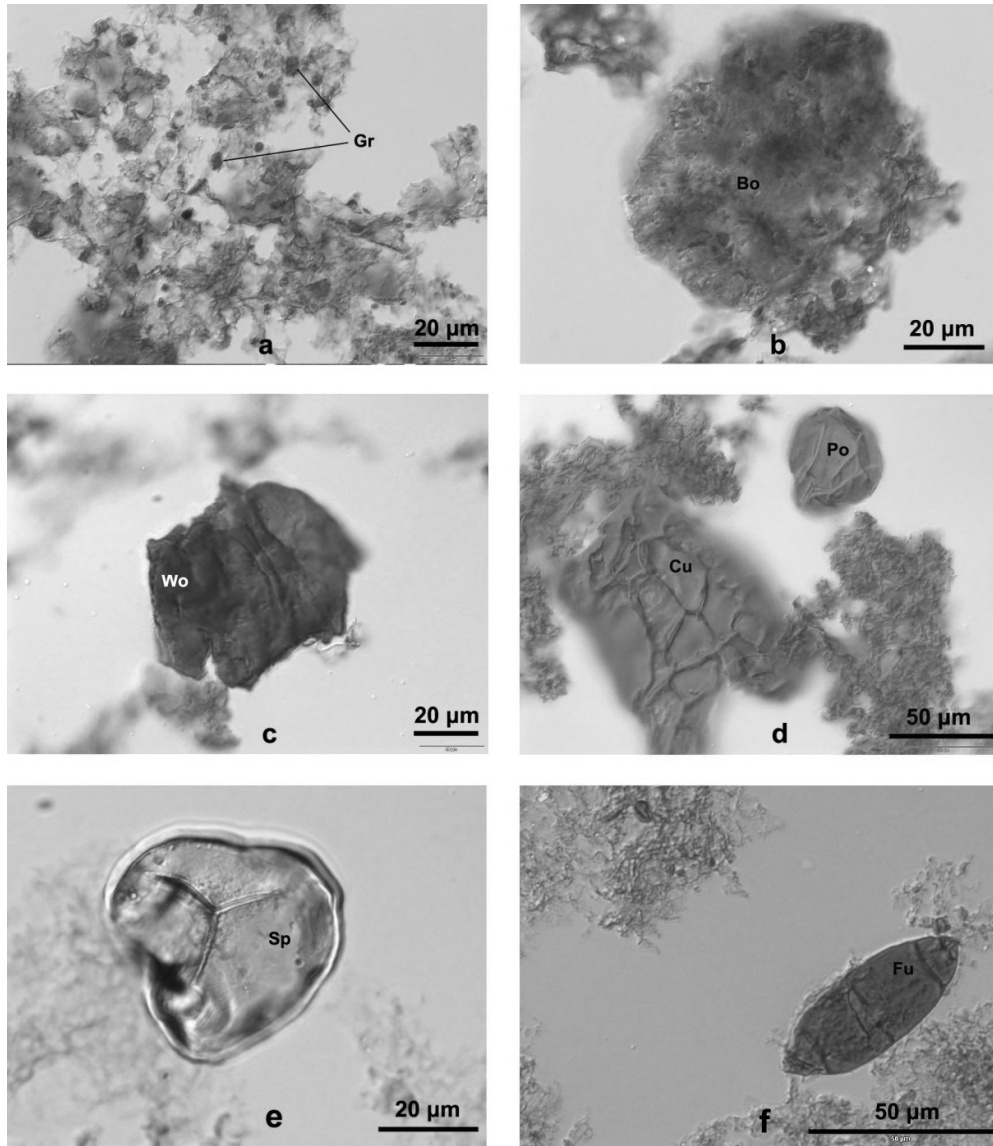


Figure A1.1. Photomicrographs of the Kiliran oil shale organic matter showing amorphous organic matter (AOM) dominated by fibrous and membraneous debris with granular features (Gr) (a), *B. braunii* palynomorph (Bo) (b), wood debris (Wo) (c), cuticles (Cu) and pollen (Po) (d), trilete spore (Sp) (e) and fungal remains (Fu) (f).

**Appendix 3: Elemental data**

Table A3.1. Geochemical composition of the Kiliran oil shale including the carbon isotopic composition of organic carbon.

Samples	TOC (%)	$\delta^{13}\text{C}$ (‰)	S (%)	Al (%)	Ca (%)	U (ppm)	Mo (ppm)	Zr (ppm)	Rb (ppm)	TOC/S	Zr/Rb
G-01	3.2	-27.0	0.7	5.3	12.3	4.3	1.3	73	98.8	4.6	0.7
G-03	3.7		0.5	6.1	6.8	4.0	1.5	88	105.0	7.1	0.8
G-05	3.2	-28.0	0.4	4.1	12.0	3.2	1.8	94	99.8	8.2	0.9
G-06	3.2	-28.4	1.1	6.5	8.7	4.5	1.8	87	107.0	2.9	0.8
G-08	2.1	-28.1	0.2	6.3	7.6	3.7	0.2	107	92.4	12.2	1.2
G-11	3.8	-28.2	0.6	6.3	8.7	3.8	1.2	89	91.2	6.9	1.0
G-14	1.9	-27.5	0.1	6.1	5.0	3.8	0.2	103	81.0	15.8	1.3
G-16	2.6	-28.9	0.4	7.6	8.1	4.0	0.7	108	101.4	7.4	1.1
G-18	3.3		0.2	6.0	6.1	3.7	0.7	110	107.0	13.6	1.0
G-20	3.5	-27.5	0.4	6.1	7.2	3.8	1.3	127	115.0	9.0	1.1
G-22	3.0	-27.4	1.0	5.3	7.7	4.0	1.9	85	97.6	3.2	0.9
G-24	3.8	-29.5	1.1	7.3	7.1	4.8	1.8	117	120.0	3.5	1.0
G-26	3.6	-30.5	0.7	6.5	6.5	3.6	1.7	74	112.0	5.2	0.7
G-28	4.8	-28.1	0.9	5.5	6.9	3.9	2.1	78	92.5	5.1	0.8
G-30	4.8	-29.1	0.6	6.0	7.0	3.8	1.8	66	104.0	8.0	0.6
G-32	4.6	-28.9	0.8	6.0	7.0	4.1	2.1	109	93.2	5.5	1.2
G-34	4.5	-29.5	0.6	8.1	5.3	4.4	1.9	140	131.0	7.0	1.1
G-36	4.4	-29.3	1.1	6.3	7.3	3.7	1.6	110	107.0	4.0	1.0
G-38	4.1	-28.7	0.6	6.2	5.5	4.1	1.8	123	112.0	7.3	1.1
G-40	4.9	-28.5	0.8	5.6	7.5	3.5	1.5	92	92.3	6.0	1.0
G-42	7.2	-27.0	0.8	4.1	8.9	3.8	2.2	94	106.0	9.6	0.9
G-44	6.7		0.6	5.4	6.9	4.5	2.0	86	109.0	10.4	0.8
G-50	8.7	-27.5	1.3	3.7	6.6	4.0	4.6	76	60.5	6.8	1.3
G-52	4.8	-29.1	0.7	4.1	12.0	4.1	3.0	46	69.1	7.2	0.7
G-54	6.8	-28.6	1.0	5.6	7.4	4.8	3.8	63	92.3	6.7	0.7
G-55	7.5	-27.8	1.1	4.1	11.6	5.5	3.6	46	67.0	7.0	0.7
G-57	6.1	-28.1	1.4	5.6	9.7	5.0	3.7	53	93.6	4.5	0.6
G-62	7.9	-28.3	1.4	4.3	9.8	6.4	4.7	45	72.0	5.7	0.6
G-64	10.3	-27.0	1.3	5.0	7.6	6.6	6.8	54	88.5	7.6	0.6
G-66	9.9	-27.8	1.8	4.0	11.6	5.7	5.9	37	66.4	5.4	0.6
G-68	12.4	-28.0	1.5	4.6	6.9	7.5	6.3	35	86.5	8.3	0.4
G-69	11.2	-28.1	1.8	4.1	7.9	6.7	5.8	34	75.4	6.2	0.5
G-70	10.6	-27.4	1.8	3.9	9.8	6.0	5.6	36	71.4	6.0	0.5
G-72	8.3	-28.1	1.7	3.8	13.6	5.4	3.5	30	59.3	5.0	0.5
G-74	9.1	-28.0	1.5	3.7	15.1	4.0	2.8	26	56.5	6.2	0.5
G-76	10.0	-27.6	1.6	3.9	13.1	5.8	4.0	28	61.7	6.1	0.5
G-78	7.8	-27.3	1.8	3.8	15.0	4.9	3.4	28	63.2	4.4	0.4
G-80	7.4	-29.5	1.7	3.6	15.7	4.2	5.0	26	59.0	4.3	0.4
G-81	6.5	-28.1	1.4	3.7	16.7	4.1	2.8	30	61.5	4.6	0.5
G-83	5.1	-28.8	2.0	4.6	13.9	3.4	2.1	46	75.4	2.5	0.6
G-85	6.4	-28.9	1.2	4.6	14.6	3.8	2.1	45	74.3	5.2	0.6
G-87	4.4	-29.0	0.9	6.5	10.4	3.7	1.7	69	112.0	4.9	0.6

TOC: total organic carbon;  $\delta^{13}\text{C}$ : carbon isotopic composition of TOC; S: sulfur; Al: aluminum, Ca: calcium; U: uranium; Mo: molybdenum; Zr: zirconium; Rb: rubidium.

**Appendix 4: Organic geochemical data**

Table A4.1. Concentrations of isoprenoids and *n*-alkanes (µg/g TOC).

Samples	Pr	Ph	Ly	nC14	nC15	nC16	nC17	nC18	nC19	nC20
G-01	80.9	48.7	-	4.3	5.8	2.6	7.8	5.4	4.2	3.6
G-03	158.6	69.6	-	39.2	135.9	58.0	27.7	19.0	8.5	6.9
G-05	110.5	60.4	-	0.9	1.9	6.0	4.7	8.2	4.2	4.1
G-06	116.0	60.6	-	3.1	6.8	6.1	9.9	6.9	4.8	5.3
G-08	83.0	34.5	3.2	1.6	6.2	13.8	12.8	22.8	8.9	11.2
G-11	99.5	55.4	-	6.8	12.4	9.1	19.8	11.6	11.0	8.4
G-14	89.4	43.2	4.9	5.0	9.9	7.9	16.7	11.7	10.8	8.8
G-16	96.1	66.5	9.6	6.3	16.4	11.4	22.1	15.6	15.5	12.6
G-18	91.0	41.8	-	99.7	325.6	113.6	35.9	28.5	10.4	13.6
G-20	72.6	36.7	-	34.5	79.2	31.0	17.4	11.6	7.0	5.0
G-22	99.4	73.8	4.0	3.2	8.4	8.4	22.6	18.0	16.2	9.8
G-24	88.9	59.3	2.3	3.1	28.6	9.4	15.8	13.8	12.3	11.9
G-26	87.5	48.8	6.1	4.1	12.1	11.6	17.3	20.5	12.9	18.8
G-28	110.9	67.3	8.2	2.7	7.6	9.9	12.3	10.3	9.3	9.5
G-30	51.4	38.4	3.1	1.5	5.6	7.8	10.3	17.5	9.0	13.1
G-32	124.5	71.6	54.7	25.7	44.2	25.0	39.5	18.0	17.9	11.4
G-34	175.2	133.4	8.1	6.2	18.0	18.6	26.4	20.5	23.3	19.0
G-36	122.4	77.4	3.1	5.2	15.4	14.1	22.9	14.3	16.4	13.3
G-38	149.2	86.2	3.9	4.9	12.1	12.6	20.5	23.7	15.2	18.7
G-40	112.1	64.6	4.5	3.8	10.9	9.3	15.8	9.4	10.7	8.1
G-42	207.1	88.2	3.4	6.7	13.7	13.7	17.0	20.7	12.9	16.2
G-44	205.7	108.0	11.4	4.1	7.6	7.6	11.4	11.2	15.3	11.4
G-50	324.6	135.7	-	22.1	46.4	33.7	40.9	32.9	22.8	22.2
G-52	359.0	173.6	11.9	23.0	44.8	28.4	31.8	22.2	19.7	17.9
G-54	253.0	145.0	27.2	10.4	20.4	20.0	25.2	20.1	19.2	17.8
G-55	250.5	134.4	23.2	24.7	40.5	30.0	34.8	24.1	23.2	19.8
G-57	161.0	77.1	14.1	35.4	46.4	24.0	18.6	12.0	11.8	11.4
G-62	116.8	66.1	-	19.2	23.6	13.9	10.3	10.8	6.9	8.0
G-64	277.0	117.4	-	19.1	24.3	20.2	23.3	14.7	12.8	8.9
G-66	119.4	64.9	-	2.0	3.8	4.6	5.0	5.2	4.2	3.2
G-68	126.7	69.6	-	8.4	16.8	10.2	12.2	11.3	8.2	7.9
G-69	128.5	65.5	-	4.9	13.0	13.7	11.3	14.0	8.2	8.7
G-70	88.7	38.1	-	7.5	11.2	7.5	8.7	5.7	5.2	4.9
G-72	81.9	37.7	22.5	3.1	5.7	5.3	6.1	5.8	5.4	5.0
G-74	210.6	118.9	16.1	5.8	13.5	10.1	12.5	10.8	6.9	8.5
G-76	85.5	41.1	29.5	4.0	8.3	6.0	6.1	3.9	4.0	2.9
G-78	101.4	51.0	21.1	5.5	11.1	8.1	10.2	5.0	4.5	3.5
G-80	136.4	85.7	6.6	2.9	5.1	5.3	9.3	5.6	7.6	7.1
G-81	135.3	68.2	22.3	2.5	5.9	7.5	8.6	12.1	8.1	7.4
G-83	209.0	125.4	35.2	12.0	28.6	20.2	27.3	18.5	18.4	17.0
G-85	130.5	67.2	17.1	7.3	18.3	12.9	17.3	10.9	10.3	8.4
G-87	161.0	83.9	7.6	15.9	28.8	25.8	30.2	30.6	17.1	16.9

Pr: pristane; Ph: phytane; Ly: lycopane; nC14: C<sub>14</sub> *n*-alkane.

Table A4.1. (continued)

Samples	nC21	nC22	nC23	nC24	nC25	nC26	nC27	nC28	nC29	nC30
G-01	4.2	4.4	5.1	4.5	13.8	7.5	66.7	8.5	17.9	7.8
G-03	8.4	7.2	9.0	9.1	12.9	5.7	49.2	6.8	14.6	5.2
G-05	7.3	5.1	6.9	5.1	11.0	7.6	33.3	9.7	16.1	6.4
G-06	8.3	4.2	10.2	3.2	6.9	4.5	30.1	4.7	11.3	6.6
G-08	9.0	9.0	15.8	8.9	26.6	16.5	181.3	15.3	46.1	10.3
G-11	15.3	11.5	17.2	11.5	38.2	16.6	171.2	14.2	32.8	9.7
G-14	12.4	9.3	15.8	9.6	34.7	19.2	198.5	16.9	47.7	10.7
G-16	20.2	15.0	20.9	18.2	52.0	33.6	351.9	27.5	77.6	17.8
G-18	13.6	11.1	15.2	5.9	12.3	5.2	89.8	3.8	7.5	2.2
G-20	7.7	4.6	5.8	5.0	11.0	7.5	113.5	8.7	18.4	5.3
G-22	15.8	11.0	12.6	11.7	22.3	16.2	204.3	13.5	38.6	11.3
G-24	20.2	15.4	22.6	16.5	42.6	26.0	247.2	17.3	41.8	19.0
G-26	19.4	14.5	19.1	14.7	35.0	31.8	263.6	21.7	51.4	11.6
G-28	16.0	12.6	21.7	13.1	35.0	22.7	230.5	19.4	46.3	14.5
G-30	12.5	11.1	16.3	10.9	42.0	27.0	328.0	23.5	58.2	14.8
G-32	24.3	15.8	23.3	16.9	28.4	21.7	114.9	17.1	34.5	13.3
G-34	33.4	28.5	39.2	28.2	66.5	53.3	393.7	37.5	20.2	19.5
G-36	23.9	16.4	24.1	18.6	42.6	31.9	292.9	24.4	62.4	18.4
G-38	20.8	14.5	21.1	14.8	36.4	30.4	328.3	19.6	49.2	11.0
G-40	14.4	10.0	12.9	10.4	27.8	21.8	146.9	15.6	35.1	8.8
G-42	14.8	9.0	11.1	6.3	13.7	10.3	98.9	7.3	13.5	5.0
G-44	18.2	14.3	18.1	13.4	26.9	21.0	146.6	16.7	34.4	10.0
G-50	30.2	20.5	31.9	13.0	24.0	17.6	164.5	9.7	24.7	7.1
G-52	31.8	24.3	35.9	18.0	31.5	21.5	181.7	16.0	44.1	12.3
G-54	33.8	27.0	40.9	23.9	43.3	31.4	205.9	22.9	62.7	16.4
G-55	33.1	27.9	45.6	25.0	49.0	34.4	235.3	27.0	64.0	18.0
G-57	17.6	13.4	20.7	10.4	20.1	15.1	121.1	11.7	29.7	9.5
G-62	9.1	6.1	9.2	5.7	12.2	6.9	60.2	8.8	12.8	4.6
G-64	17.0	11.0	17.2	11.5	24.0	17.4	134.2	13.1	25.6	9.0
G-66	7.5	4.4	6.6	3.9	10.9	27.0	57.7	4.8	10.3	4.0
G-68	10.8	8.9	10.4	8.0	24.0	15.2	119.0	23.1	22.2	9.9
G-69	10.9	7.7	8.7	6.7	17.8	12.2	85.6	11.0	14.6	8.0
G-70	7.9	4.9	7.8	4.2	13.0	8.3	60.9	11.0	10.3	6.0
G-72	7.8	6.1	9.4	5.4	13.7	10.0	56.5	10.9	14.5	6.2
G-74	9.5	8.9	9.3	6.6	20.1	14.6	80.8	14.4	19.0	7.8
G-76	5.1	3.5	4.7	3.4	11.8	6.1	52.5	12.3	12.1	4.4
G-78	7.5	5.9	8.5	5.3	12.4	6.9	40.0	14.6	9.9	5.8
G-80	11.2	8.9	12.8	7.3	18.5	10.1	51.7	8.6	12.4	5.4
G-81	11.7	10.9	12.2	7.4	23.0	12.7	80.9	12.6	16.8	4.2
G-83	32.2	28.4	25.3	21.5	35.5	24.5	130.9	21.3	29.7	13.1
G-85	13.9	9.8	13.2	8.6	22.5	3.2	80.4	12.5	18.0	6.1
G-87	21.6	17.8	20.3	12.1	28.6	16.6	128.9	5.5	30.1	10.7

nC21: C<sub>21</sub> n-alkane

Table A4.1. (continued)

Samples	nC31	nC32	nC33	nC34
G-01	14.7	4.2	11.7	2.3
G-03	13.4	7.6	10.4	1.7
G-05	9.2	3.9	6.7	1.0
G-06	14.3	3.3	10.4	-
G-08	38.7	9.4	27.5	3.1
G-11	22.0	5.1	12.2	1.8
G-14	47.7	11.6	32.1	3.2
G-16	39.0	11.6	20.3	3.4
G-18	6.1	2.3	4.4	-
G-20	23.0	6.2	19.0	2.4
G-22	28.4	7.9	17.1	3.4
G-24	20.3	2.2	9.0	-
G-26	23.1	7.1	13.1	2.7
G-28	20.8	11.7	11.3	2.4
G-30	24.0	8.6	11.2	2.3
G-32	25.4	8.3	13.4	3.4
G-34	9.1	14.3	15.9	-
G-36	27.4	12.5	4.1	3.6
G-38	17.2	5.6	8.4	1.6
G-40	15.2	6.9	7.8	2.4
G-42	6.8	3.3	4.0	-
G-44	14.7	3.9	5.7	1.3
G-50	7.7	5.3	2.1	1.0
G-52	19.4	11.4	7.7	3.2
G-54	22.5	10.5	6.1	2.1
G-55	22.8	9.5	7.3	3.1
G-57	10.2	6.3	3.5	1.4
G-62	5.3	1.3	2.7	-
G-64	10.0	1.6	4.4	-
G-66	4.4	0.8	2.1	-
G-68	12.1	3.1	6.3	0.7
G-69	8.2	1.4	3.4	0.4
G-70	7.1	0.7	2.9	-
G-72	8.8	2.5	3.2	0.5
G-74	8.0	4.0	4.5	0.8
G-76	8.2	-	-	-
G-78	8.2	-	3.3	4.6
G-80	6.1	-	2.0	-
G-81	8.6	-	3.8	-
G-83	16.4	3.5	6.0	-
G-85	13.4	1.2	5.3	-
G-87	21.5	4.0	9.3	-

nC31: C<sub>31</sub> *n*-alkane



Table A4.2. Concentrations of steroidal hydrocarbons ( $\mu\text{g/g}$  TOC).

Samples	C27b	C27a	C28b	C28a	C29b	C29a	c1	c2	c3	c4
G-01	3.9	16.8	-	3.9	1.5	7.3	37.8	74.0	41.5	39.7
G-03	2.7	11.2	-	2.4	1.1	4.4	83.3	134.4	37.5	31.3
G-05	3.7	14.7	-	2.9	-	8.2	34.1	48.1	24.1	22.6
G-06	2.5	11.2	-	2.3	-	8.3	87.0	98.5	32.2	26.5
G-08	-	2.6	-	0.8	-	3.5	6.9	16.8	4.2	3.8
G-11	1.6	7.1	-	3.7	2.4	6.4	77.6	138.4	25.5	22.1
G-14	0.4	2.9	-	-	-	3.6	5.0	8.1	1.6	1.6
G-16	2.0	9.0	-	4.5	3.8	12.2	17.0	24.7	16.5	14.8
G-18	-	3.6	-	-	-	-	15.0	25.5	7.8	6.0
G-20	2.0	9.4	-	2.4	0.7	1.8	13.2	23.3	14.5	12.2
G-22	18.3	30.9	-	19.8	4.5	16.2	37.2	57.8	35.0	19.6
G-24	3.4	13.3	-	3.8	2.4	8.0	8.9	18.3	10.6	15.0
G-26	1.4	6.2	-	12.9	1.5	4.0	17.0	23.2	5.4	5.1
G-28	1.4	6.2	0.9	2.5	1.9	4.3	55.7	85.8	16.3	12.2
G-30	0.7	3.0	1.0	1.9	0.8	3.1	5.6	7.9	6.4	3.0
G-32	5.5	26.5	1.7	7.6	5.5	17.7	27.4	49.2	22.4	6.1
G-34	2.5	9.7	1.6	6.1	1.5	3.3	7.5	9.4	8.4	5.3
G-36	1.9	8.2	2.3	9.2	4.2	9.8	32.4	49.5	19.3	5.4
G-38	3.1	13.2	-	2.3	-	3.5	11.3	23.3	15.2	11.1
G-40	1.7	7.0	-	5.1	1.5	6.2	21.1	32.5	9.1	6.7
G-42	0.8	1.9	-	-	-	-	13.7	22.3	6.5	5.0
G-44	3.7	14.3	1.2	4.7	1.2	4.5	13.2	16.5	31.3	25.8
G-50	1.7	6.8	-	2.6	0.5	1.6	28.9	40.8	13.4	11.4
G-52	1.5	7.5	1.2	7.7	1.6	5.3	71.2	103.6	30.2	20.7
G-54	2.3	12.2	1.0	5.0	3.0	10.2	63.1	86.9	42.9	32.7
G-55	2.4	10.3	-	3.4	4.2	10.6	37.5	52.1	20.9	18.4
G-57	1.6	5.5	-	2.2	1.5	3.5	41.2	68.9	12.0	11.0
G-62	0.5	3.4	5.4	3.4	-	-	30.9	36.7	12.4	10.4
G-64	1.2	5.9	-	7.3	-	4.3	56.3	86.4	26.9	23.5
G-66	-	2.5	-	-	-	0.6	104.4	139.8	33.6	31.7
G-68	0.4	1.9	-	-	-	1.5	131.3	138.6	38.5	35.4
G-69	-	1.5	-	-	-	-	115.2	125.5	29.4	29.4
G-70	-	1.5	-	-	-	-	59.8	108.2	16.6	16.6
G-72	-	0.9	-	-	-	-	28.2	28.1	6.9	7.0
G-74	-	1.7	-	-	-	-	32.4	34.5	8.6	8.8
G-76	0.8	2.4	-	-	-	-	55.5	58.6	36.6	35.0
G-78	-	1.9	-	-	-	-	66.2	71.6	30.4	28.4
G-80	-	1.3	-	-	-	-	22.2	31.6	18.7	14.1
G-81	-	1.1	-	-	-	-	54.8	62.2	22.1	20.1
G-83	2.3	7.5	-	1.7	-	1.9	62.7	79.7	39.0	27.1
G-85	0.5	2.4	-	0.8	-	1.3	73.6	88.6	25.6	23.6
G-87	0.7	2.0	-	0.9	-	2.0	27.4	38.6	16.8	15.8

C27b: 5 $\beta$ -Sterane; C27a: 5 $\alpha$ -Sterane; C28b: 24-Methyl-5 $\beta$ -sterane; C28a: 24-Methyl-5 $\alpha$ -sterane; C29b: 24-Ethyl-5 $\beta$ -sterane; C29a: 24-Ethyl-5 $\alpha$ -sterane; c1: 4 $\alpha$ -Methylsterane; c2: 4 $\beta$ -Methylsterane; c3: 4 $\alpha$ -Methyl-24-methylsterane; c4: 4 $\beta$ -Methyl-24-methylsterane.

Table A4.2. (continued)

Samples	c5	c6	d1	d2	d3	d4
G-01	95.1	155.9	7.6	14.2	18.1	34.3
G-03	103.2	145.9	6.5	10.7	5.6	13.3
G-05	47.7	61.9	1.8	4.3	-	6.5
G-06	97.3	106.3	7.3	22.0	-	14.7
G-08	16.4	24.3	2.3	2.5	5.4	7.3
G-11	46.3	67.5	19.4	29.8	18.1	31.3
G-14	20.1	30.8	3.6	4.7	7.0	9.8
G-16	32.7	39.8	2.4	3.3	-	-
G-18	7.0	9.8	8.6	10.9	3.4	8.9
G-20	17.2	20.7	3.5	5.2	4.3	5.6
G-22	18.4	23.1	5.1	9.6	-	-
G-24	23.8	28.4	1.4	2.4	2.5	4.4
G-26	12.4	15.5	2.3	3.1	2.5	3.0
G-28	23.6	35.8	4.7	7.5	-	-
G-30	6.4	7.8	0.6	0.8	0.5	1.2
G-32	38.8	47.4	11.5	22.1	12.6	24.5
G-34	17.5	19.0	2.5	2.8	3.6	3.8
G-36	31.4	32.6	4.8	6.2	3.7	5.1
G-38	14.7	16.9	2.2	3.8	-	4.4
G-40	6.8	10.3	2.5	3.5	-	1.4
G-42	16.2	17.3	2.7	4.5	2.0	5.4
G-44	25.4	31.2	1.4	2.3	-	4.4
G-50	19.1	22.9	1.5	2.1	-	-
G-52	47.4	54.8	2.2	3.7	-	2.0
G-54	58.1	76.1	2.1	3.4	-	3.5
G-55	56.7	75.2	1.0	1.8	-	2.6
G-57	17.7	24.6	1.9	4.4	1.1	1.7
G-62	18.2	34.0	14.7	21.5	24.6	35.8
G-64	72.2	91.1	8.1	17.5	13.7	20.6
G-66	37.0	53.8	22.0	37.6	15.7	11.2
G-68	65.1	94.6	42.3	60.7	-	40.3
G-69	61.0	106.7	49.3	74.2	54.5	73.0
G-70	45.1	74.6	59.2	96.0	57.8	87.0
G-72	71.8	113.8	11.2	17.3	42.3	71.9
G-74	106.0	159.8	7.8	13.6	43.4	59.8
G-76	205.4	314.1	22.4	29.6	117.1	185.0
G-78	144.8	208.8	35.6	47.0	135.4	206.6
G-80	38.6	59.2	11.6	19.5	34.1	42.9
G-81	70.7	104.9	21.9	33.4	49.0	83.1
G-83	131.0	166.3	21.1	40.0	68.2	100.4
G-85	94.3	156.2	25.9	37.4	57.6	99.5
G-87	105.9	156.8	8.7	14.6	46.4	51.1

c5: 4 $\alpha$ -Methyl-24-ethylsterane; c6: 4 $\beta$ -Methyl-24-ethylsterane; d1: 20R-Methyldiasterene; d2: 20S-Methyldiasterene; d3: 20R-Methyl-24-ethyldiasterene; d4: 20S-Methyl-24-ethyldiasterene.

Table A4.3. Concentrations of hopanoid hydrocarbons ( $\mu\text{g/g}$  TOC).

Samples	b1	b2	b3	b4	b5	b6	b7	b8	b9	b10
G-01	7.3	18.1	138.3	23.0	132.8	19.5	61.3	137.7	46.5	12.8
G-03	4.5	10.7	40.1	8.8	14.7	13.5	42.3	40.0	30.8	11.8
G-05	8.8	17.7	112.5	39.0	141.4	24.4	79.2	100.3	41.8	22.6
G-06	4.5	20.5	122.8	21.2	181.8	16.8	31.8	193.4	56.4	9.5
G-08	1.7	5.2	25.8	6.1	13.9	-	23.6	33.9	16.6	2.1
G-11	6.3	14.2	112.6	11.2	81.2	10.2	33.6	100.6	35.9	9.5
G-14	6.5	9.7	100.3	2.2	41.0	-	6.0	96.8	20.3	1.5
G-16	6.0	16.7	143.6	13.7	51.3	16.4	35.3	101.3	43.2	8.0
G-18	3.3	6.3	37.0	5.6	23.1	-	12.4	34.7	11.2	4.3
G-20	5.3	13.3	68.7	9.1	43.2	6.3	21.3	79.8	24.1	7.6
G-22	9.9	19.0	154.1	38.1	173.7	22.4	73.6	120.8	44.2	14.0
G-24	6.2	17.5	115.9	23.6	186.6	15.2	47.2	147.3	44.1	13.2
G-26	3.8	6.9	57.7	12.8	35.4	7.9	26.2	41.9	20.5	7.9
G-28	6.5	14.6	117.2	21.3	67.6	15.1	51.4	107.4	33.2	16.7
G-30	4.4	9.5	72.2	11.1	56.5	8.5	22.3	51.0	23.3	7.0
G-32	10.7	25.7	124.4	30.1	202.5	20.6	58.2	235.6	41.5	16.0
G-34	7.9	15.4	100.0	21.3	68.7	15.0	45.4	62.4	35.5	14.5
G-36	7.1	15.6	118.4	22.4	103.8	16.2	38.4	70.9	37.4	14.4
G-38	6.3	16.5	82.3	16.4	153.0	8.4	32.7	167.1	32.8	11.2
G-40	4.1	9.1	61.0	16.1	50.1	10.7	28.7	35.0	21.8	11.2
G-42	2.6	5.8	54.5	14.8	68.3	5.7	21.1	38.6	20.0	9.7
G-44	6.3	11.2	81.8	17.7	64.6	9.4	26.6	41.4	26.6	11.2
G-50	2.4	4.6	25.9	9.3	38.1	7.7	17.1	14.7	12.0	4.0
G-52	6.0	8.0	56.7	18.5	66.5	19.5	33.0	25.9	20.8	7.6
G-54	8.9	12.1	72.8	33.7	87.6	22.2	70.8	33.1	35.6	15.7
G-55	5.4	9.8	61.7	26.0	54.6	18.3	47.3	22.7	17.4	11.9
G-57	4.2	7.0	56.4	24.1	62.5	13.5	33.4	20.6	25.0	9.5
G-62	5.1	7.3	58.4	14.2	62.5	8.8	17.1	65.1	20.1	8.5
G-64	6.3	10.5	108.8	35.4	157.6	13.4	44.2	76.4	30.8	18.1
G-66	3.3	5.8	66.0	6.2	54.1	6.8	6.9	40.7	20.2	3.1
G-68	4.6	7.9	96.0	12.9	69.6	6.3	18.6	84.9	33.6	7.7
G-69	4.9	8.8	104.9	26.0	67.2	12.4	33.9	86.0	25.3	12.0
G-70	3.0	6.1	97.1	39.6	75.3	9.1	43.5	87.0	19.7	13.7
G-72	4.1	9.5	95.2	20.4	33.2	8.0	22.2	62.1	23.2	10.1
G-74	2.6	6.3	80.0	18.6	52.4	7.8	31.0	61.9	13.7	15.2
G-76	4.3	9.4	128.5	26.5	57.5	12.6	40.3	100.1	16.1	24.2
G-78	5.0	9.6	137.9	30.0	94.2	15.4	44.0	127.4	23.6	15.9
G-80	4.1	5.4	108.2	18.8	41.3	6.6	23.2	58.1	20.0	9.8
G-81	6.3	10.7	107.5	28.5	47.3	10.3	38.9	55.1	22.2	13.2
G-83	7.6	16.7	207.2	20.6	111.9	14.9	32.4	130.8	38.0	12.6
G-85	3.9	13.0	133.3	22.0	74.5	10.3	35.2	106.5	30.3	18.8
G-87	6.0	11.6	136.0	17.5	58.4	10.6	32.6	78.7	36.5	10.6

b1: 17 $\alpha$  (H)-22,29,30-Trisnorhopane; b2: 17 $\beta$ (H)-22,29,30-Trisnorhopane; b3: 30-Norneohop-13(18)-ene; b4: 17 $\alpha$ (H),21 $\beta$ (H)-30-Norhopane; b5: Hop-17(21)-ene; b6: 17 $\beta$ (H),21 $\alpha$ (H)-Normoretane; b7: 17 $\alpha$ (H),21 $\beta$ (H)-Hopane; b8: Neohop-13(18)-ene; b9: 17 $\beta$ (H),21 $\beta$ (H)-30-Norhopane; b10: 22R-17 $\alpha$ (H),21 $\beta$ (H)-Homohopane.

Table A4.3. (continued)

Samples	b11	b12
G-01	44.7	36.3
G-03	13.8	23.5
G-05	32.0	30.3
G-06	68.6	49.2
G-08	17.3	8.1
G-11	37.3	25.5
G-14	12.9	14.3
G-16	36.9	22.3
G-18	7.3	9.1
G-20	34.8	19.3
G-22	34.1	26.0
G-24	60.4	28.8
G-26	14.8	13.9
G-28	33.8	25.9
G-30	22.7	14.3
G-32	72.7	61.9
G-34	29.0	26.0
G-36	32.3	30.0
G-38	48.7	25.2
G-40	15.1	17.6
G-42	14.2	17.0
G-44	16.4	20.6
G-50	9.2	8.7
G-52	17.7	20.8
G-54	18.9	27.2
G-55	13.6	19.8
G-57	11.8	18.3
G-62	13.8	22.9
G-64	21.9	29.8
G-66	14.8	13.0
G-68	27.1	22.1
G-69	38.6	13.1
G-70	11.3	17.5
G-72	17.2	16.5
G-74	8.1	15.3
G-76	14.0	27.5
G-78	10.7	29.4
G-80	13.8	15.2
G-81	16.2	18.6
G-83	22.1	36.9
G-85	26.5	32.3
G-87	19.4	25.9

b11: 17 $\beta$ (H),21 $\beta$ (H)-Hopane; b12: 17 $\beta$ (H),21 $\beta$ (H)-Homohopane.

Table A4.4. Concentrations of des-A-triterpenoids ( $\mu\text{g/g}$  TOC).

Samples	Ole	Lup	Urs
G-01	3.6	17.8	6.8
G-03	1.9	13.8	4.3
G-05	2.5	13.0	3.5
G-06	5.3	10.0	4.1
G-08	4.8	14.9	10.0
G-11	3.4	11.5	5.3
G-14	6.3	23.3	14.6
G-16	2.9	13.2	6.8
G-18	2.2	8.7	4.5
G-20	2.4	9.4	5.6
G-22	3.0	14.9	4.3
G-24	3.5	9.9	4.0
G-26	2.1	7.6	3.0
G-28	1.9	8.8	3.2
G-30	1.5	6.9	2.8
G-32	3.0	12.3	5.3
G-34	2.4	10.6	4.6
G-36	2.0	10.4	3.2
G-38	3.0	10.5	4.3
G-40	2.2	7.4	3.2
G-42	1.7	5.9	1.7
G-44	1.5	5.9	1.5
G-50	1.3	3.7	0.9
G-52	1.5	5.3	1.0
G-54	2.0	6.7	1.5
G-55	1.6	5.2	0.9
G-57	1.7	4.9	1.3
G-62	1.3	5.0	0.6
G-64	1.5	5.8	0.9
G-66	1.2	4.2	1.1
G-68	1.3	4.7	0.9
G-69	1.3	5.1	0.8
G-70	1.0	3.7	1.1
G-72	0.6	3.3	0.5
G-74	1.0	4.3	0.8
G-76	2.0	4.0	1.1
G-78	1.4	5.1	1.3
G-80	1.2	5.6	-
G-81	1.2	5.5	0.5
G-83	3.4	8.2	2.0
G-85	1.3	7.8	1.9
G-87	2.1	6.8	2.0

Ole: des-A-olean-13(18)-ene; Lup: des-A-lupane, Urs: des-A-ursane.

Table A4.5. Concentrations of aromatic hydrocarbons ( $\mu\text{g/g}$  TOC).

Samples	C13-Aryl	C14-Aryl	C15-Aryl	Cad	TMTHN	Per	MECPC	Cd1	Cd2	Isore
G-01	2.8	6.0	2.0	3.7	2.4	2.8	8.2	-	-	10.0
G-03	2.7	5.4	2.2	6.4	2.5	0.7	-	-	-	7.6
G-05	2.0	5.6	2.6	1.2	1.5	1.0	7.7	-	3.5	5.8
G-06	2.4	7.3	3.9	2.9	2.5	3.8	-	4.6	-	3.7
G-08	-	0.7	1.0	1.9	0.6	4.2	5.4	-	-	3.9
G-11	3.1	2.7	4.0	12.8	8.3	9.4	14.9	-	4.2	7.4
G-14	1.8	2.9	3.9	13.3	11.2	16.8	-	-	-	4.9
G-16	2.1	3.8	4.5	10.1	6.4	8.2	7.0	-	3.0	5.9
G-18	9.1	8.4	9.0	12.8	15.1	0.7	-	-	-	0.6
G-20	8.3	7.2	6.4	7.3	12.2	5.6	-	-	3.3	6.9
G-22	3.5	9.0	5.1	9.7	9.4	19.2	17.1	-	-	18.1
G-24	3.1	6.8	8.9	7.7	5.5	5.9	5.7	-	-	14.4
G-26	1.8	3.8	2.9	6.6	5.2	4.0	-	-	-	9.7
G-28	1.6	4.1	5.2	6.0	5.3	2.1	-	-	3.7	10.0
G-30	1.1	2.2	2.7	3.3	2.4	1.9	4.9	-	-	3.7
G-32	5.8	10.5	11.3	14.6	14.5	15.3	20.1	11.9	12.2	13.9
G-34	3.1	5.9	6.3	11.9	8.1	4.8	6.3	-	-	10.4
G-36	2.5	5.5	4.6	9.4	7.3	3.8	14.4	-	-	9.7
G-38	2.7	5.4	8.0	10.2	8.2	3.5	-	-	4.8	5.7
G-40	1.9	3.8	6.6	5.3	4.9	2.5	6.1	-	-	4.0
G-42	2.9	5.1	7.7	6.3	6.8	1.0	-	-	-	2.6
G-44	3.2	6.5	8.2	5.3	5.3	2.0	-	-	-	7.7
G-50	3.2	6.7	5.4	4.3	4.8	0.6	-	-	-	1.0
G-52	1.8	4.3	4.5	2.3	3.5	1.4	-	-	0.4	8.9
G-54	2.7	6.2	8.6	3.8	4.8	1.8	-	-	-	8.1
G-55	2.8	5.8	8.8	3.3	4.3	1.8	-	-	-	7.2
G-57	2.5	5.2	5.4	2.5	2.9	0.9	-	-	-	3.6
G-62	1.6	2.9	5.9	2.3	1.9	0.8	-	-	-	1.3
G-64	0.4	1.5	1.9	5.3	6.7	3.7	-	-	-	5.0
G-66	0.8	2.8	3.3	2.1	2.4	2.1	11.4	-	-	1.4
G-68	2.2	4.8	2.4	2.7	7.9	3.8	-	-	1.3	3.6
G-69	1.1	3.2	2.1	3.4	7.1	2.9	6.0	-	0.9	2.3
G-70	1.9	4.2	1.5	3.7	8.0	2.9	8.0	-	-	1.4
G-72	-	0.5	1.7	0.6	1.4	3.4	6.6	-	1.2	2.2
G-74	1.0	2.9	1.1	2.8	4.0	3.5	-	-	-	1.2
G-76	0.6	1.7	0.9	1.3	2.3	5.3	-	-	-	1.5
G-78	1.5	3.3	2.0	3.9	7.5	7.1	13.6	-	-	2.2
G-80	-	0.7	2.3	-	-	1.1	28.8	-	-	0.8
G-81	-	0.8	1.7	-	-	1.9	-	-	-	1.1
G-83	2.8	5.7	2.3	9.6	13.8	10.0	7.4	-	-	4.0
G-85	0.6	2.9	1.0	2.1	3.4	2.6	13.8	-	3.5	0.4
G-87	1.4	3.7	2.5	3.7	8.9	3.9	6.6	-	-	4.1

C13-Aryl: C13 aryl isoprenoid; Cad: cadalene, TMTHN: 1,1,5,6-Tetramethyl-1,2,3,4-tetrahydronaphthalene; Per: perylene; MECPC: 7-Methyl-1'-ethyl-1,2-cyclopentenochrysen; Cd1: carotenoid derivative 1; Isore: isorenieratane.

Table A4.6. Compound specific carbon isotopic composition of some biomarkers in the Kiliran oil shale.

Compound		$\delta^{13}\text{C}$ (‰, PDB)			
		B3-30	B3-32	B3-50	B3-74
n-Alkanes	C15		-30.2		
	C16		-29.0		
	C17	-32.3	-29.5	-32.4	-31.4
	C18	-30.4	-29.0	-30.9	-30.1
	C19	-33.0	-30.5	-33.7	-32.9
	C20	-29.3	-29.9	-31.2	-31.3
	C21	-34.2	-33.5	-34.4	-34.0
	C22	-33.0	-30.4	-33.1	-33.3
	C23	-34.7	-33.9	-34.9	-34.0
	C24	-32.3	-30.5	-33.5	-32.3
	C25	-34.8	-32.2	-33.8	-34.5
	C26	-34.2	-31.3	-32.9	-33.4
	C27	-33.5	-31.0	-30.7	-31.4
C28	-35.2	-29.7	-32.6	-33.9	
C29	-33.5	-30.8	-32.9	-33.6	
Pristane		-32.3	-28.5	-28.6	-29.8
Phytane		-34.1	-31.3	-30.2	-30.9
4 $\beta$ -Methylsterane			-35.4		
30-Norneohop-13(18)-ene			-50.2	-46.5	-50.4
Neohop-13(18)-ene			-47.6	-49.1	-45.2
4 $\alpha$ -Methyl-24-ethylsterane				-36.4	-35.9
4 $\beta$ -Methyl-24-ethylsterane			-37.0	-37.2	-38.1
Lycopane			-17.2		
Cadalene			-30.5		
Des-A-arbora-5,7,9-triene			-33.1		
Perylene			-29.7		
Methylethylcyclopenteno-chrysene			-30.3		
Carotenoid derivatives			-34.9		
Carotenoid derivatives			-35.1		
Isorenieratene			-24.0		

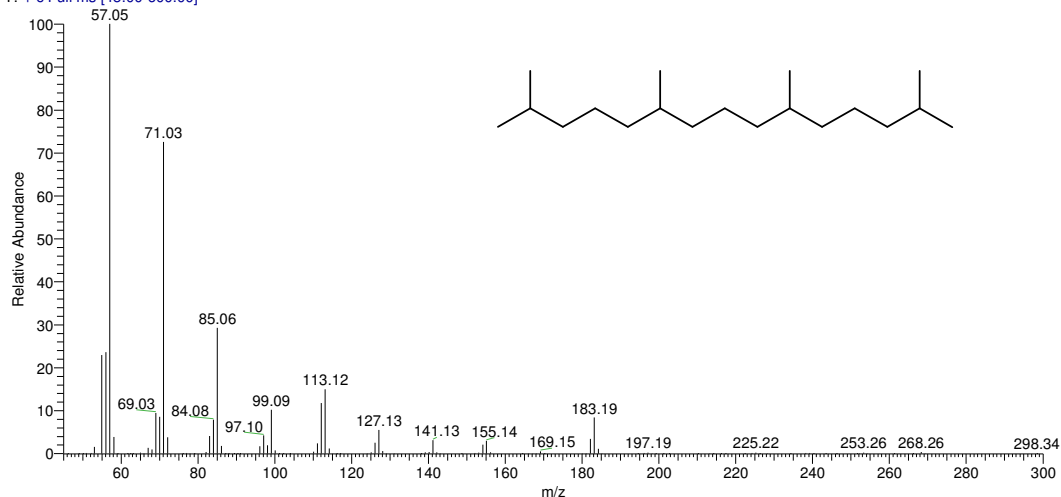
## Appendix 5: Mass spectra of identified biomarkers in the Kiliran oil shale

Compound identification is based on mass spectra and/or retention time published in the references written in the brackets.

### A5.1. Biomarkers in saturated hydrocarbon fraction

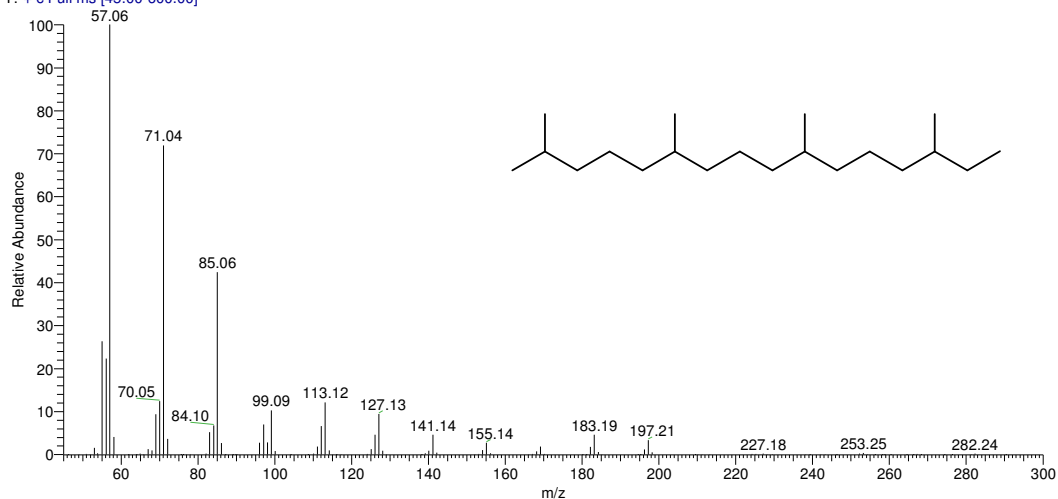
#### Pristane (Wiley Library)

gumai\_B3-32-alkane #1271 RT: 28.97 AV: 1 SB: 2 63.90 , 64.23 NL: 5.43E7  
T: + c Full ms [45.00-600.00]



#### Phytane (Wiley Library)

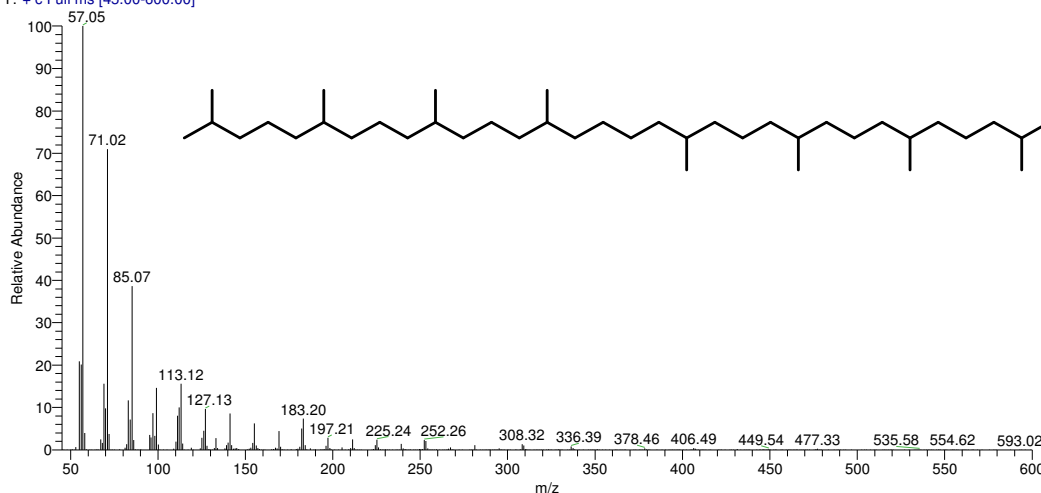
gumai\_B3-32-alkane #1418 RT: 31.74 AV: 1 SB: 2 63.90 , 64.23 NL: 2.38E7  
T: + c Full ms [45.00-600.00]





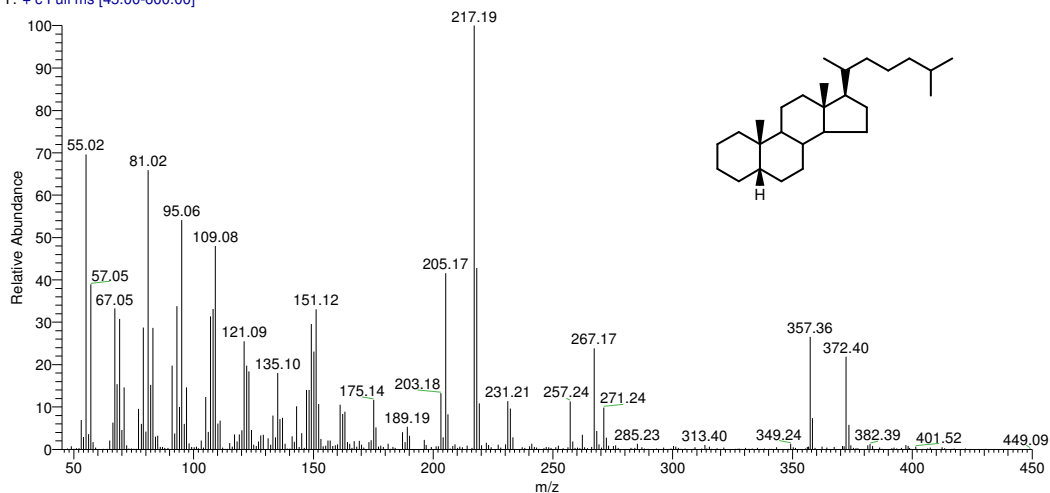
Lycopane (Sinninghe-Damsté et al., 2003)

gumai\_B3-32-alkane #3042 RT: 64.06 AV: 1 SB: 2 63.90, 64.23 NL: 1.19E7  
T: + c Full ms [45.00-600.00]



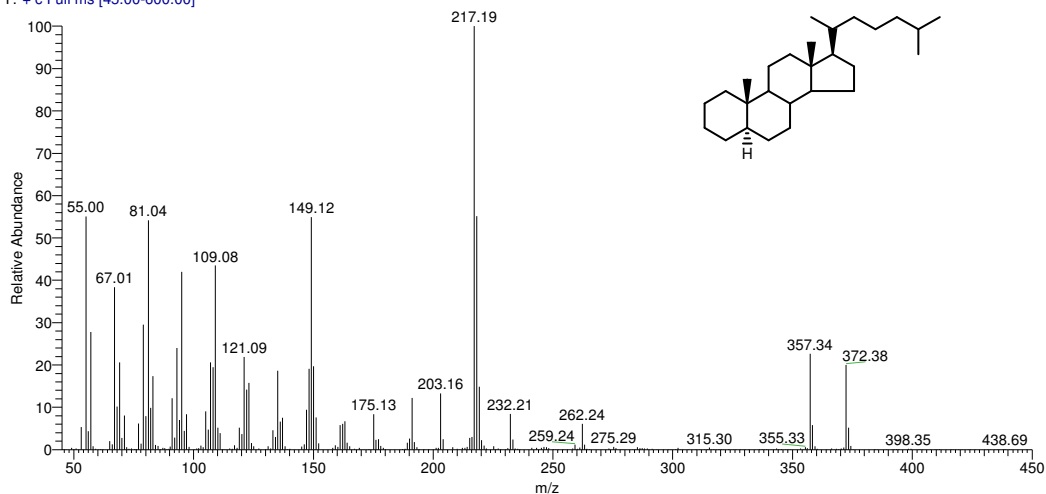
5 $\beta$ -Sterane (Philp, 1985)

gumai\_B3-32-alkane #2503 RT: 52.88 AV: 1 SB: 7 52.42-52.53, 53.05 NL: 9.42E5  
T: + c Full ms [45.00-600.00]



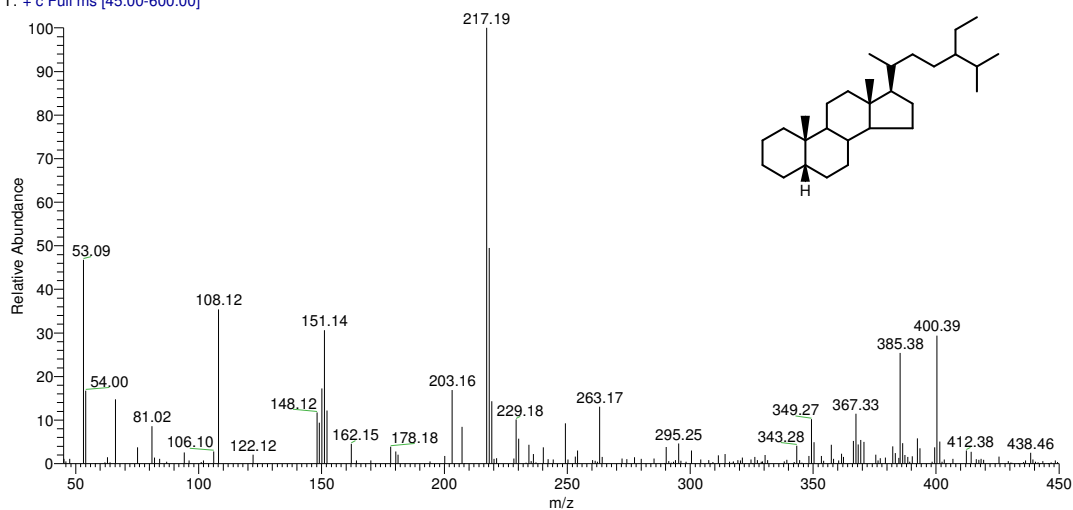
5 $\alpha$ -Sterane (Philp, 1985)

gumai\_B3-32-alkane #2535 RT: 53.55 AV: 1 SB: 2 53.37, 53.80 NL: 3.94E6  
T: + c Full ms [45.00-600.00]



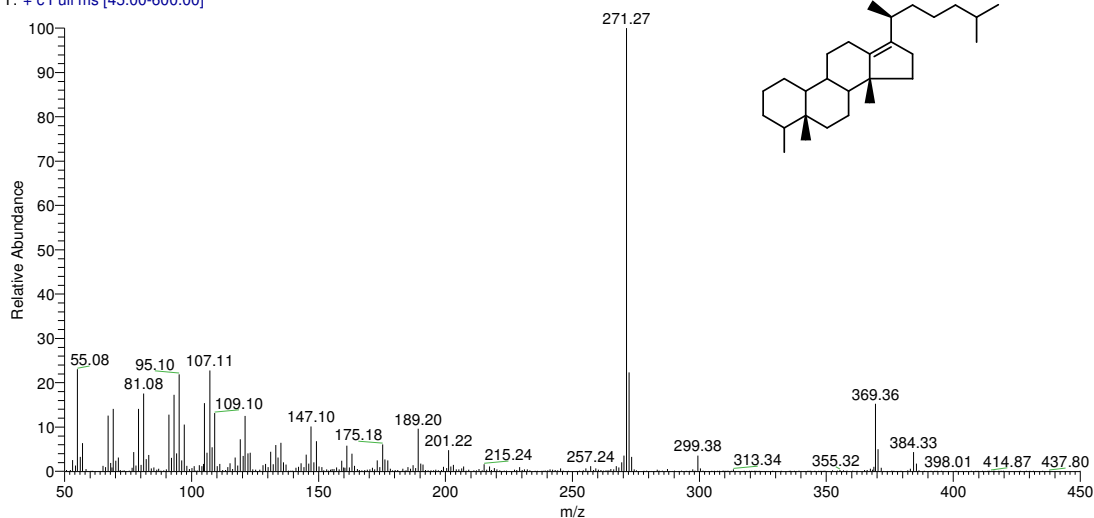
24-Ethyl-5 $\beta$ -sterane (Philp, 1985)

gumai B3-32-alkane #2659 RT: 56.17 AV: 1 SB: 2 56.06, 56.32 NL: 2.55E5  
T: + c Full ms [45.00-600.00]



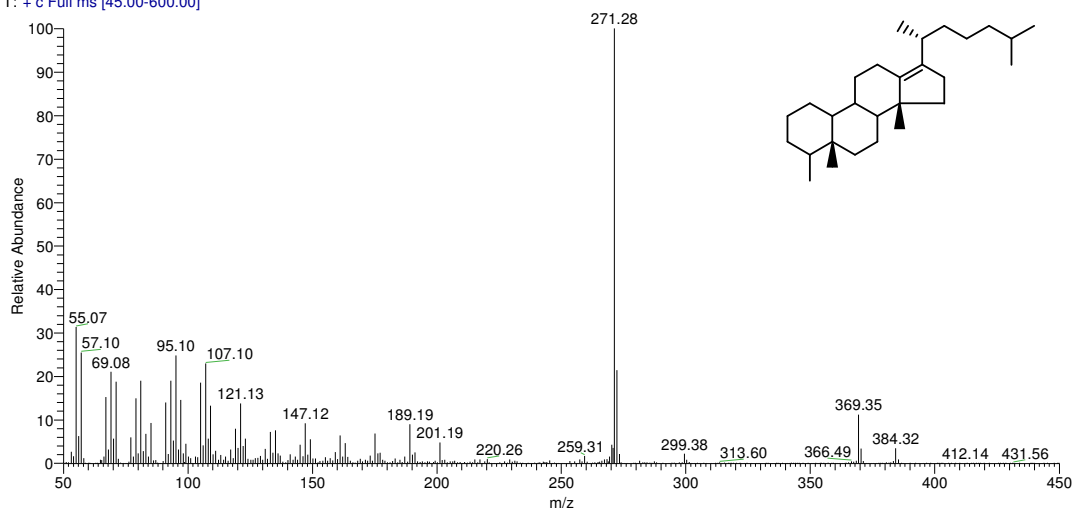
20R-Methyldiasterene (Püttmann and Goth, 1986)

haris051008\_03 #1996 RT: 42.65 AV: 1 NL: 1.74E6  
T: + c Full ms [45.00-600.00]



20S-Methyldiasterene (Püttmann and Goth, 1986)

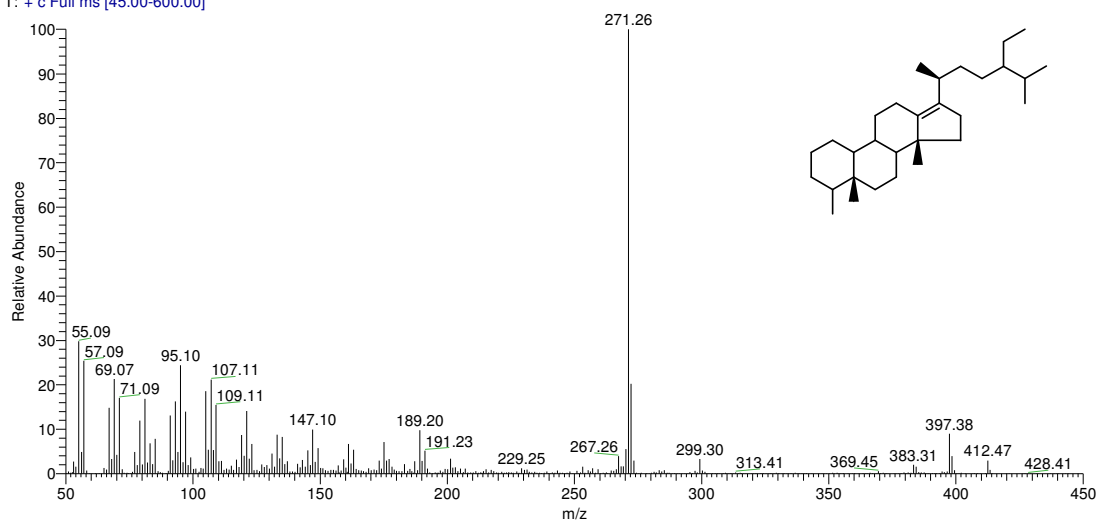
haris051008\_03 #2064 RT: 43.94 AV: 1 NL: 2.33E6  
T: + c Full ms [45.00-600.00]



**20R-Methyl-24-ethyldiasterene (Püttmann and Goth, 1986)**

haris051008\_03 #2150 RT: 45.56 AV: 1 NL: 1.54E6

T: + c Full ms [45.00-600.00]

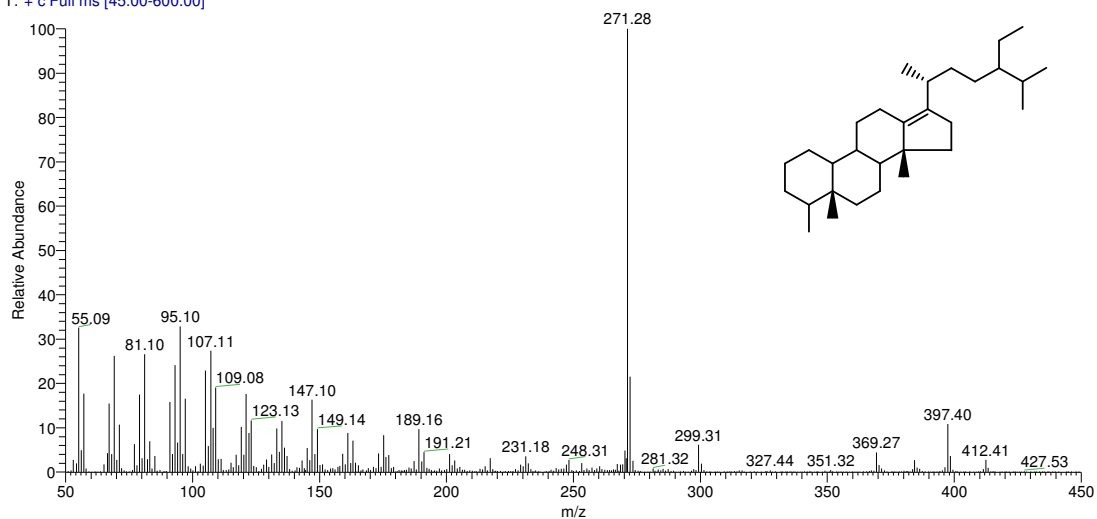


2

**0S-Methyl-24-ethyldiasterene (Püttmann and Goth, 1986)**

haris051008\_03 #2232 RT: 47.11 AV: 1 NL: 2.31E6

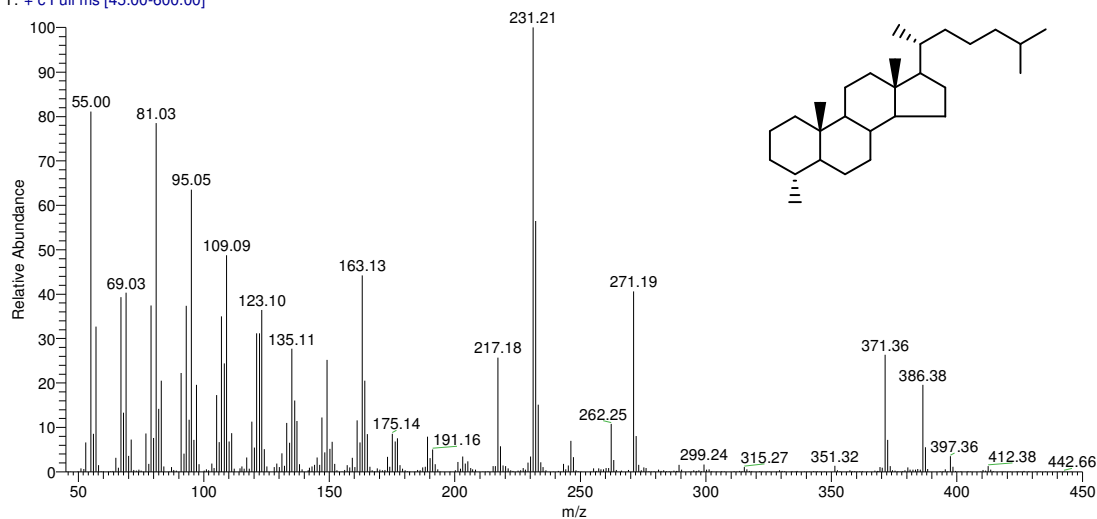
T: + c Full ms [45.00-600.00]



**4 $\alpha$ -Methylsterane**

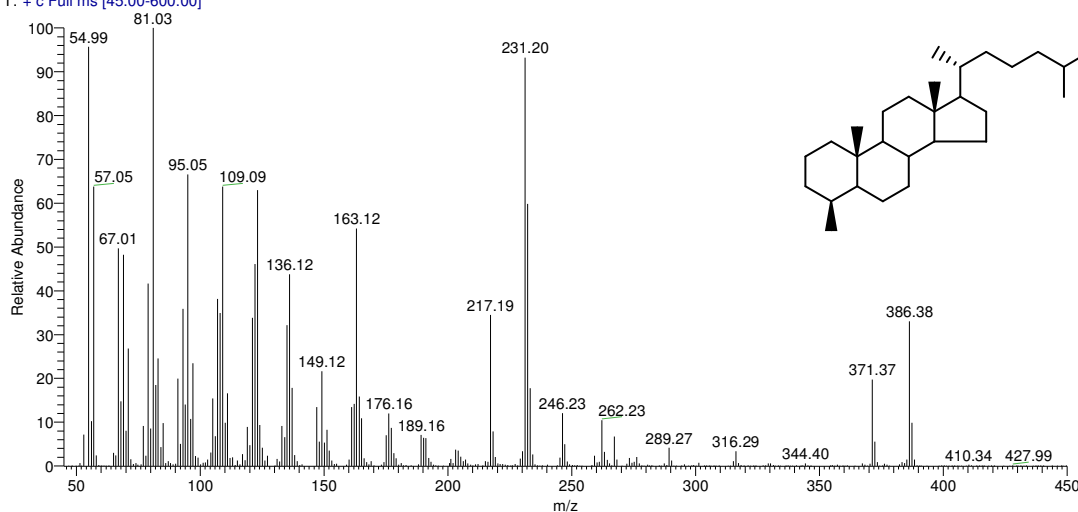
gumai\_B3-32-alkane #2595 RT: 54.81 AV: 1 SB: 2 54.66, 55.08 NL: 4.77E6

T: + c Full ms [45.00-600.00]



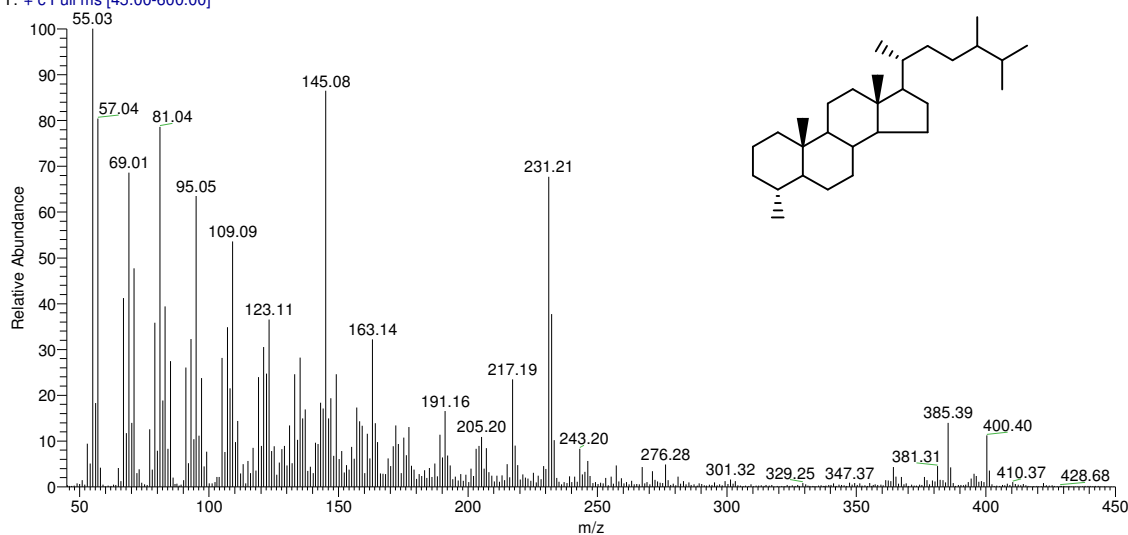
### 4 $\beta$ -Methylsterane

gumai\_B3-32-alkane #2633 RT: 55.60 AV: 1 SB: 2 55.45 , 55.82 NL: 4.97E6  
T: + c Full ms [45.00-600.00]



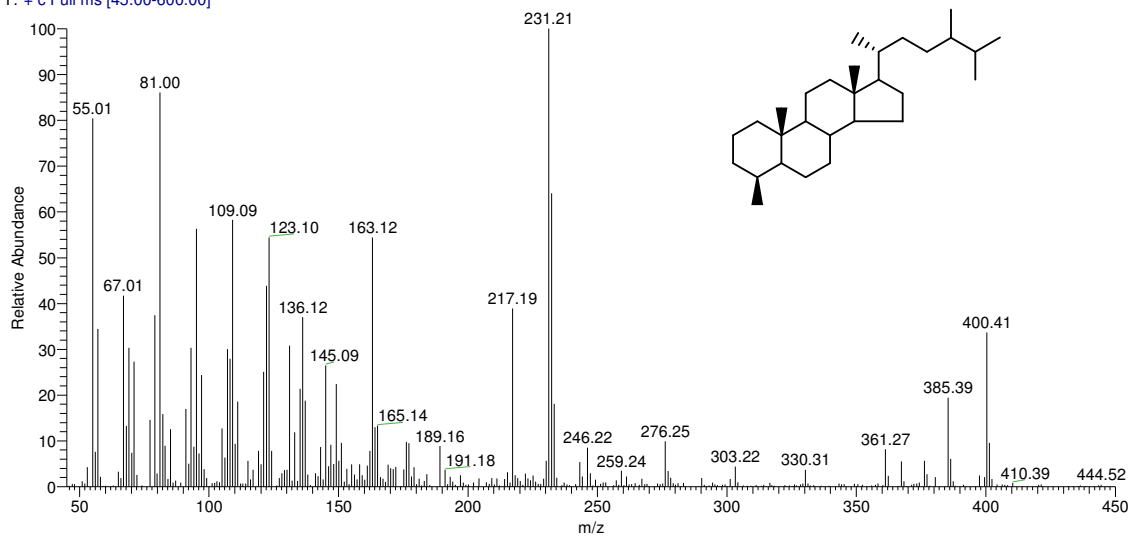
### 4 $\alpha$ -Dimethylsterane mixed with another compound

gumai\_B3-32-alkane #2678 RT: 56.58 AV: 1 NL: 2.64E6  
T: + c Full ms [45.00-600.00]



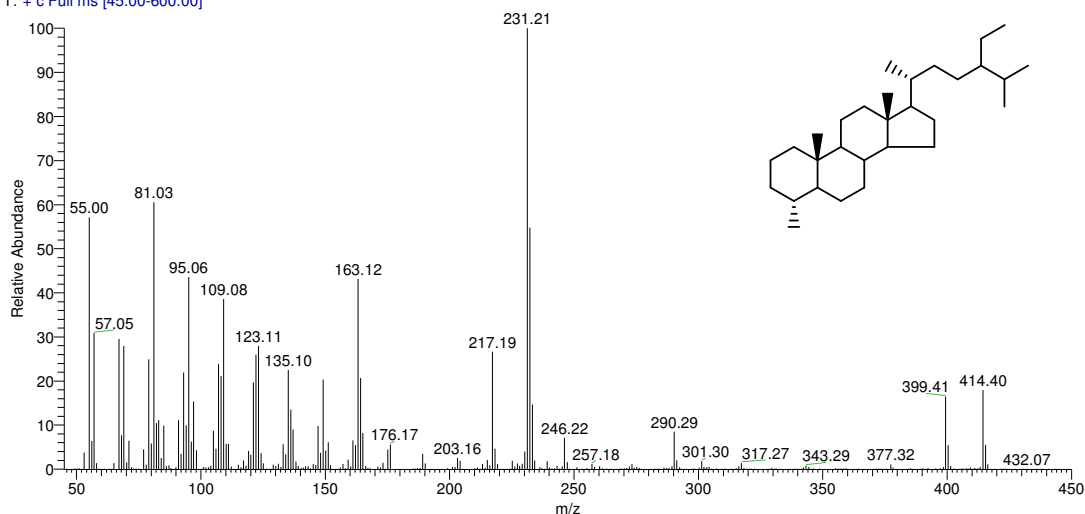
### 4 $\beta$ -Dimethylsterane

gumai\_B3-32-alkane #2715 RT: 57.36 AV: 1 SB: 2 57.27 , 57.46 NL: 1.14E6  
T: + c Full ms [45.00-600.00]



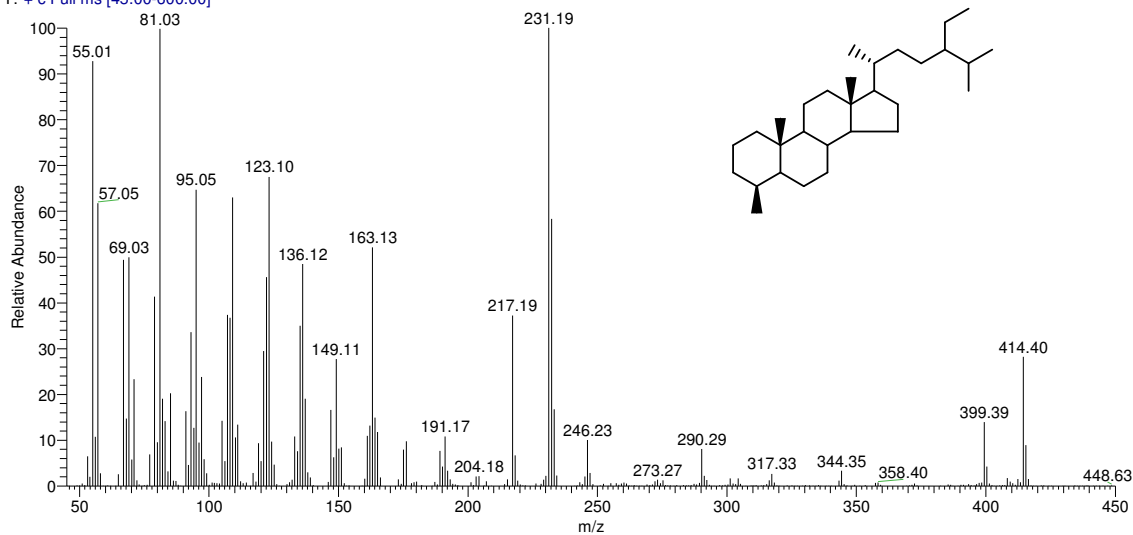
**4 $\alpha$ -Methyl-24-ethylsterane (Wolff et al., 1986)**

gumai B3-32-alkane #2749 RT: 58.06 AV: 1 SB: 2 57.89, 58.18 NL: 5.18E6  
T: + c Full ms [45.00-600.00]



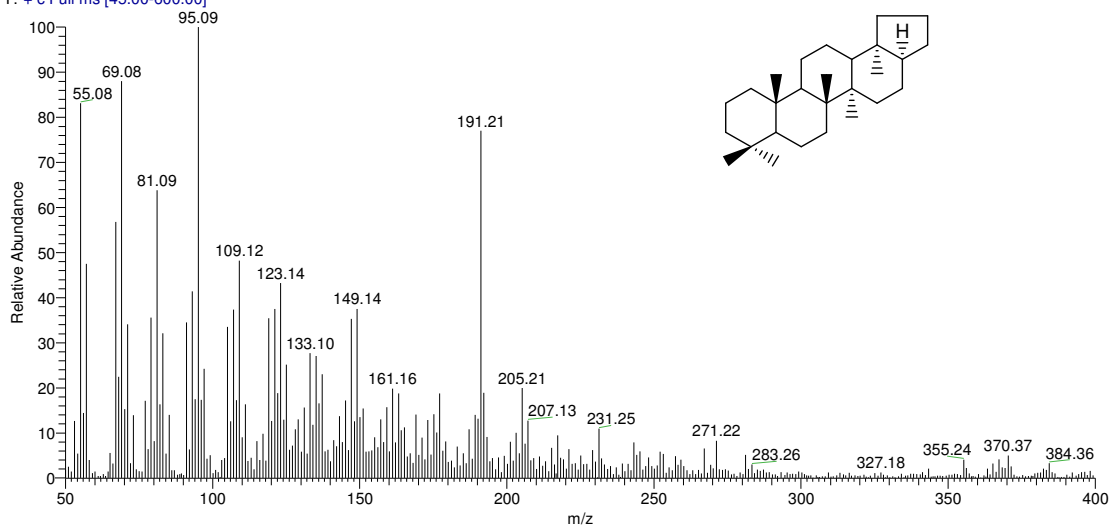
**4 $\beta$ -Methyl-24-ethylsterane (Wolff et al., 1986)**

gumai B3-32-alkane #2786 RT: 58.82 AV: 1 SB: 2 58.70, 58.94 NL: 4.72E6  
T: + c Full ms [45.00-600.00]



**17 $\alpha$ (H)-22,29,30-Trisnorhopane (Philp, 1985)**

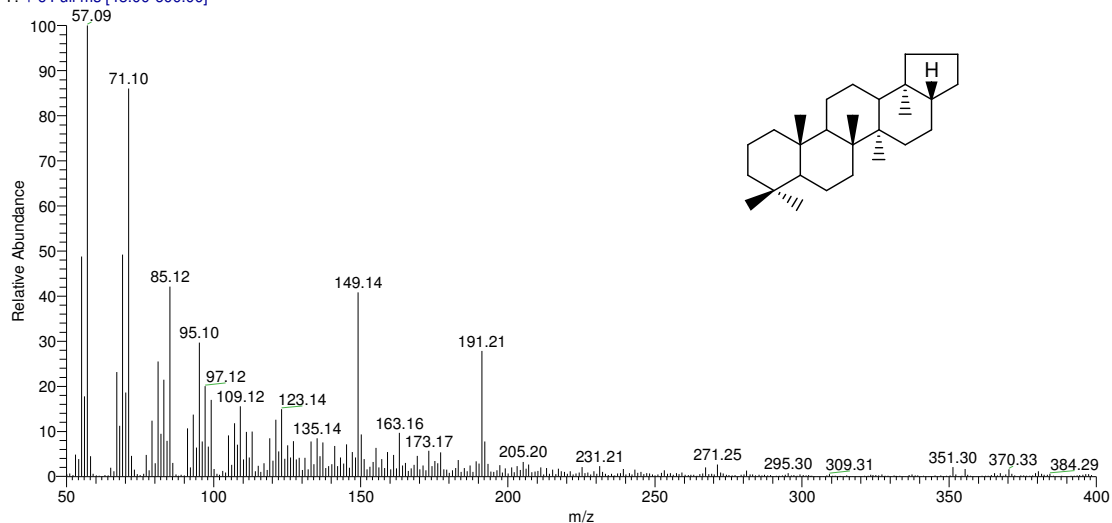
B3-32\_haris090908\_03 #2218 RT: 46.93 AV: 1 NL: 8.98E5  
T: + c Full ms [45.00-600.00]



17 $\beta$ (H)-22,29,30-Trisnorhopane (Philp, 1985) mixed with C<sub>29</sub> *n*-alkane

B3-32\_haris090908\_03 #2248 RT: 47.53 AV: 1 NL: 4.20E6

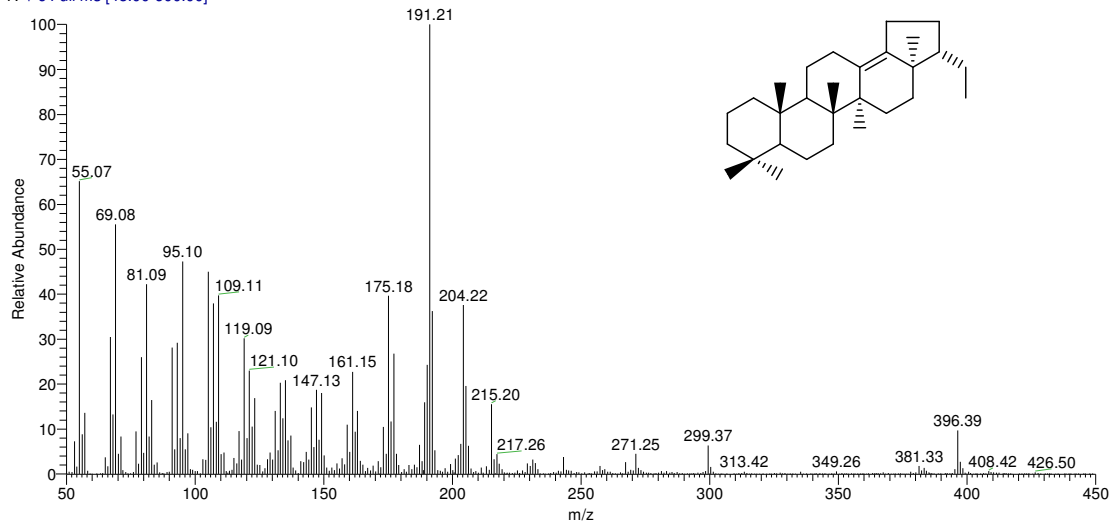
T: + c Full ms [45.00-600.00]



30-Norneohop-13(18)-ene (Philp, 1985)

haris051008\_03 #2323 RT: 48.83 AV: 1 NL: 2.66E6

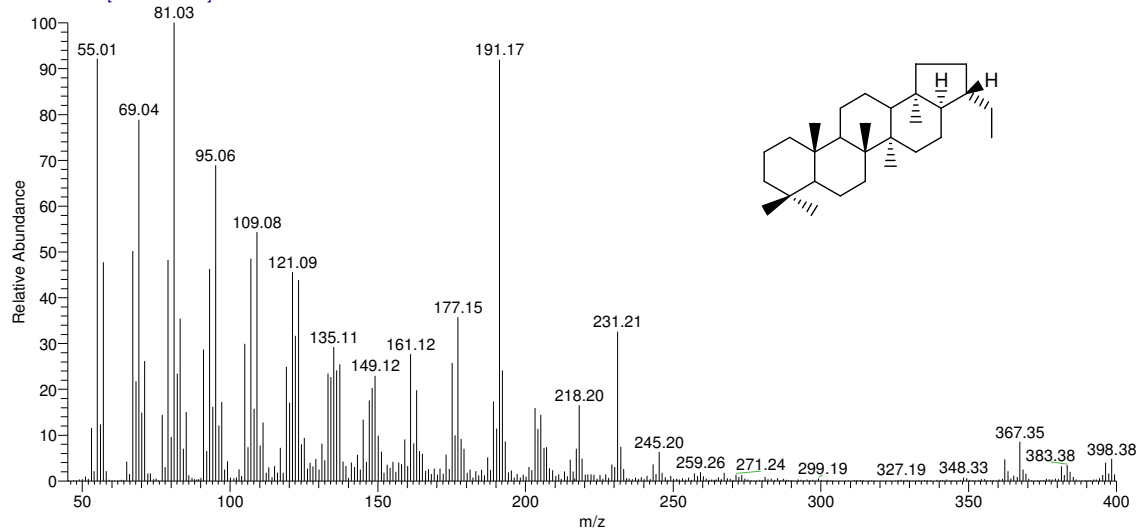
T: + c Full ms [45.00-600.00]



17 $\alpha$ (H),21 $\beta$ (H)-30-Norhopane (Philp, 1985) mixed with other compounds

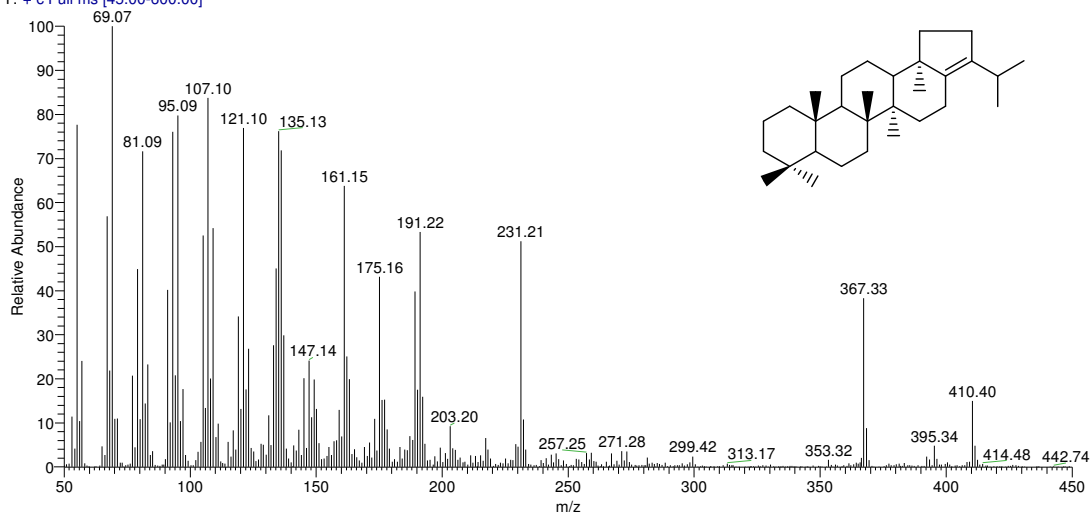
gumai\_B3-32-alkane #2697 RT: 56.98 AV: 1 NL: 5.55E6

T: + c Full ms [45.00-600.00]



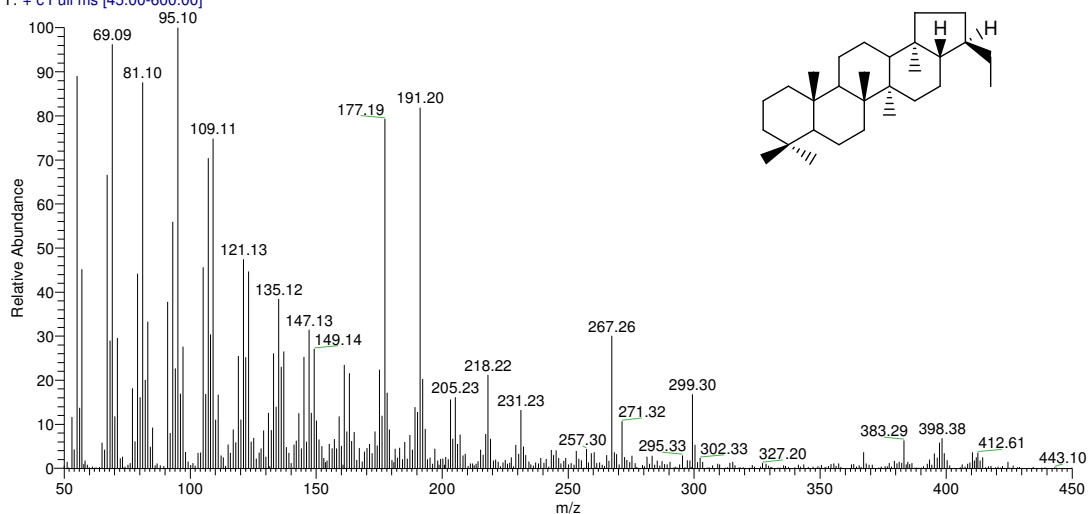
**Hop-17(21)-ene (Philp, 1985)**

haris051008\_03 #2361 RT: 49.54 AV: 1 NL: 9.99E5  
T: + c Full ms [45.00-600.00]



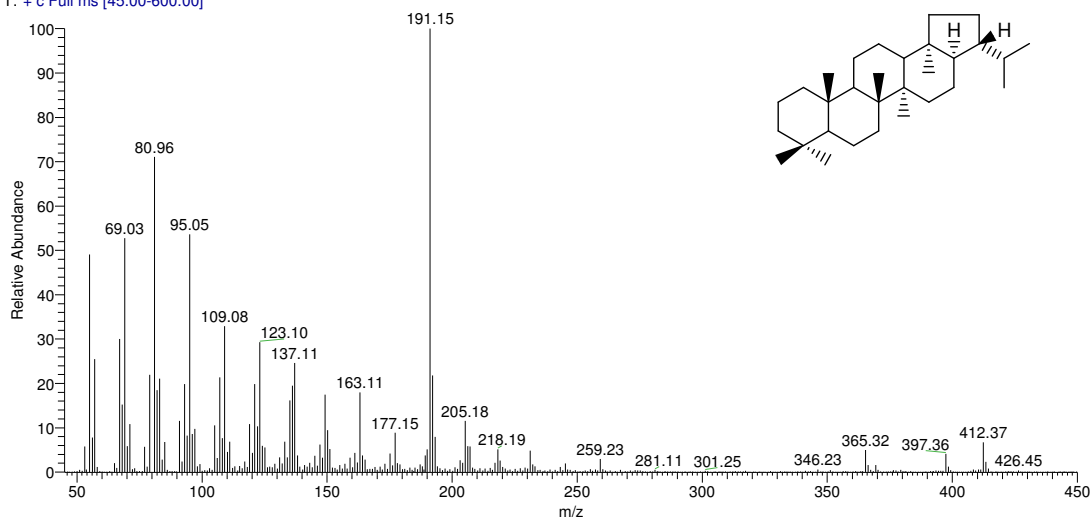
**17 $\beta$ (H),21 $\alpha$ (H)-30-Normoretane (Philp, 1985)**

haris051008\_03 #2369 RT: 49.69 AV: 1 NL: 3.86E5  
T: + c Full ms [45.00-600.00]



**17 $\alpha$ (H),21 $\beta$ (H)-Hopane (Philp, 1985)**

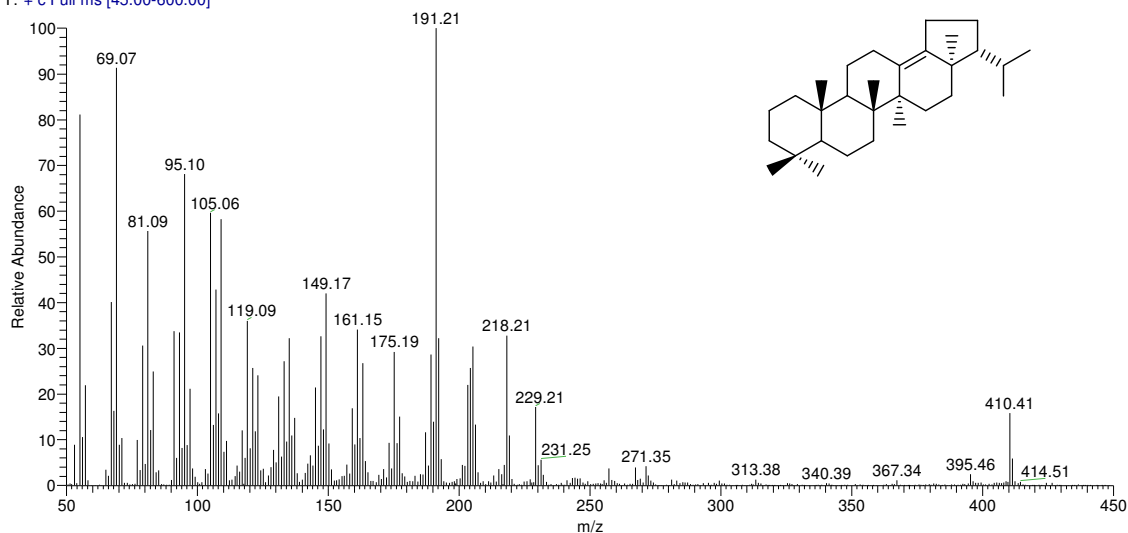
qumai B3-32-alkane #2762 RT: 58.33 AV: 1 NL: 1.11E7  
T: + c Full ms [45.00-600.00]



**Neohop-13(18)-ene (Philp, 1985)**

haris051008\_03 #2414 RT: 50.55 AV: 1 NL: 1.58E6

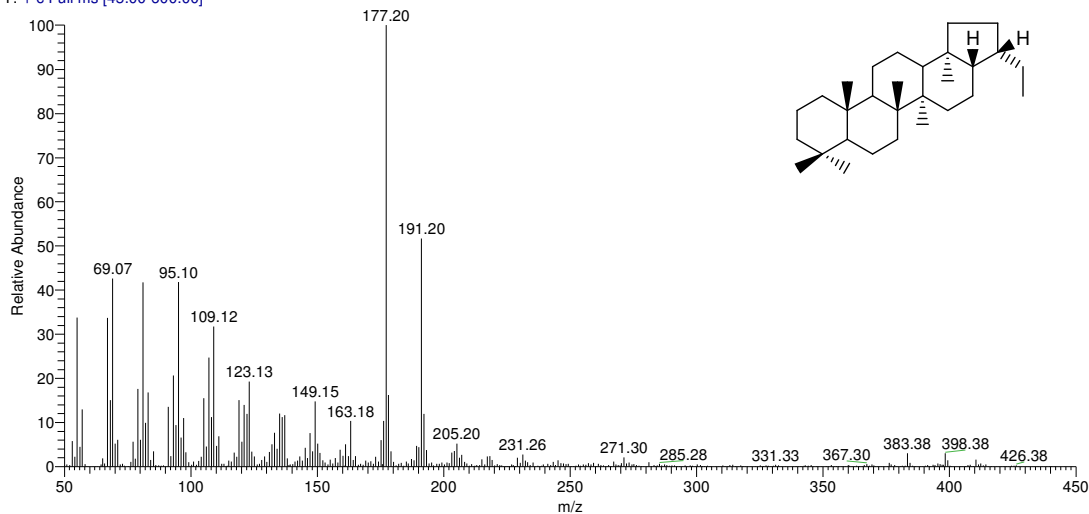
T: + c Full ms [45.00-600.00]



**17 $\beta$ (H),21 $\beta$ (H)-30-Norhopane (Philp, 1985)**

haris051008\_03 #2425 RT: 50.75 AV: 1 NL: 1.62E6

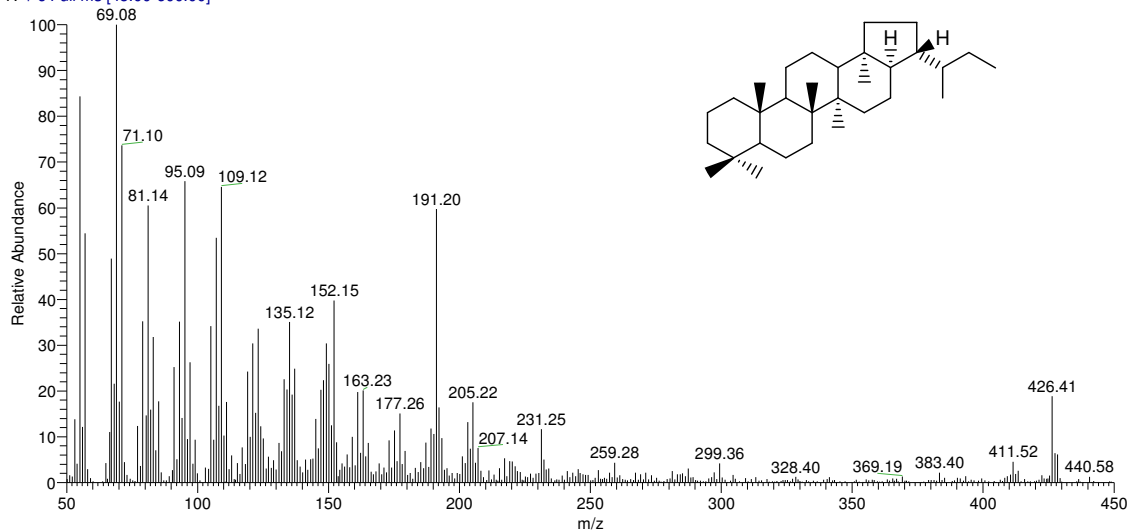
T: + c Full ms [45.00-600.00]



**22R-17 $\alpha$ (H),21 $\beta$ (H)-Homohopane (Philp, 1985)**

haris051008\_03 #2489 RT: 51.96 AV: 1 NL: 4.76E5

T: + c Full ms [45.00-600.00]

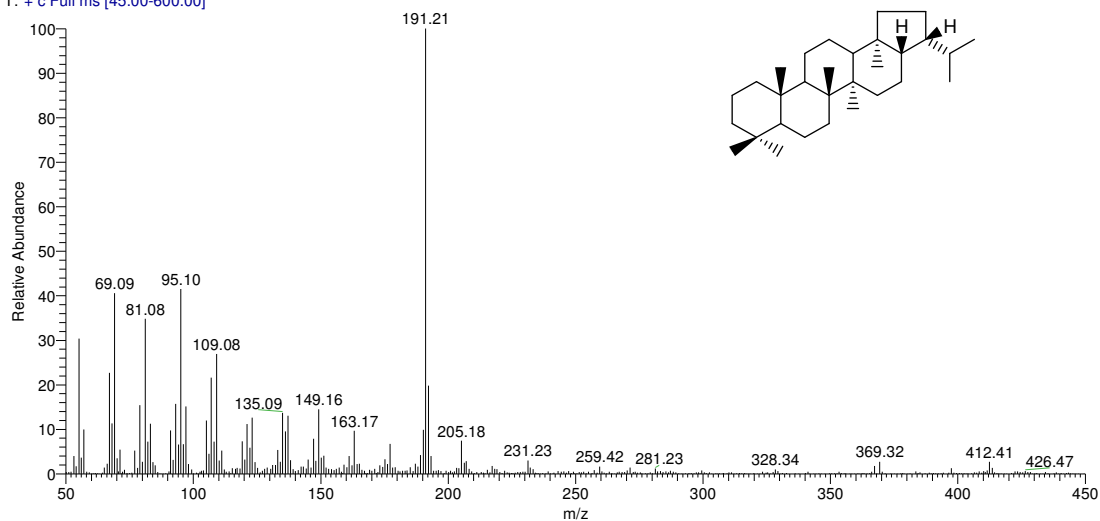




17 $\beta$ (H),21 $\beta$ (H)-Hopane (Philp, 1985)

haris051008\_03 #2512 RT: 52.40 AV: 1 NL: 1.06E6

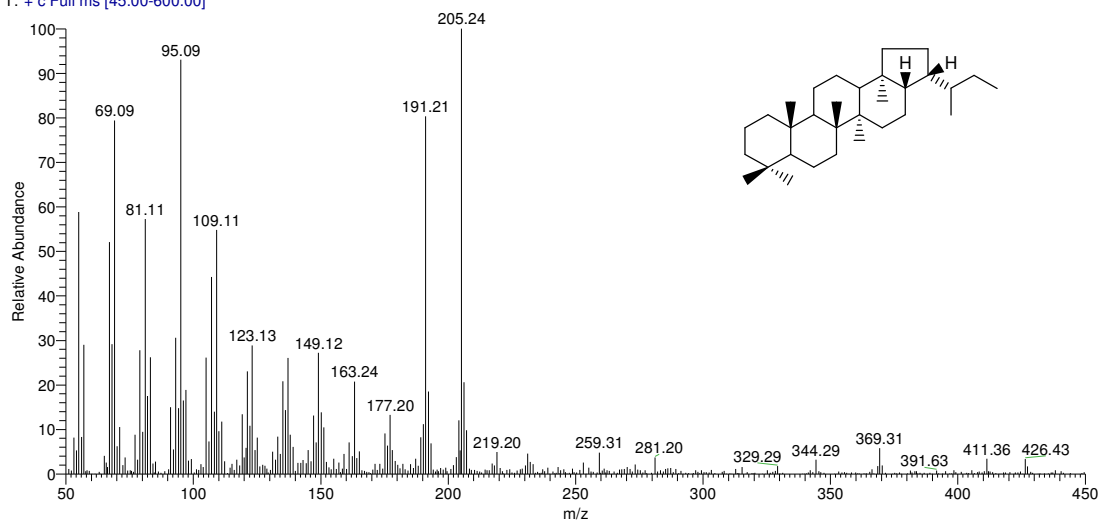
T: + c Full ms [45.00-600.00]



17 $\beta$ (H),21 $\beta$ (H)-Homohopane (Philp, 1985)

haris051008\_03 #2611 RT: 54.27 AV: 1 NL: 4.04E5

T: + c Full ms [45.00-600.00]

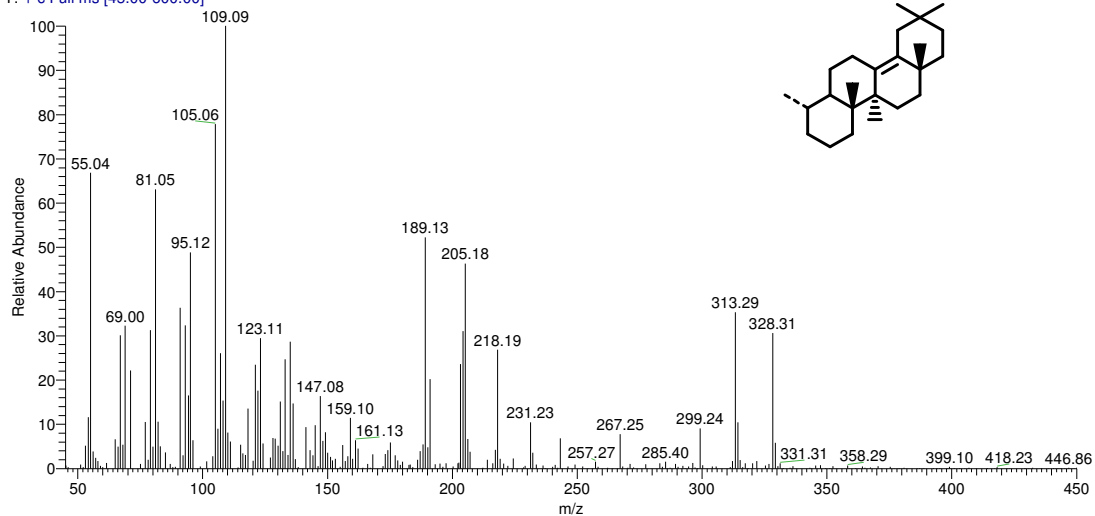


d

es-A-olean-13(18)-ene (Widodo, 2008)

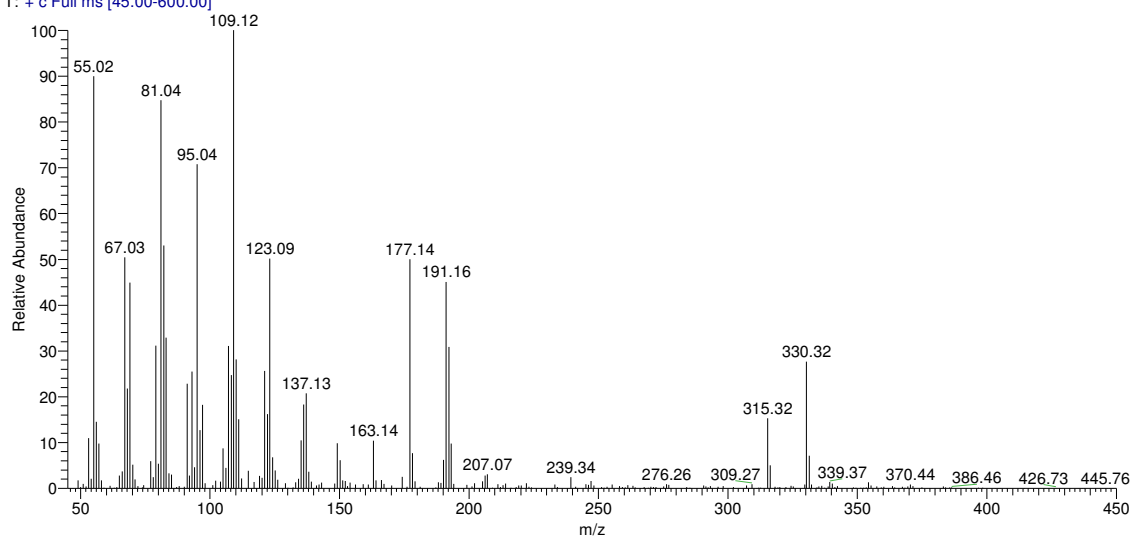
gumai\_B3-32-alkane #2068 RT: 44.05 AV: 1 SB: 2 43.95, 44.13 NL: 2.84E5

T: + c Full ms [45.00-600.00]



des-A-ursane (Widodo, 2008)

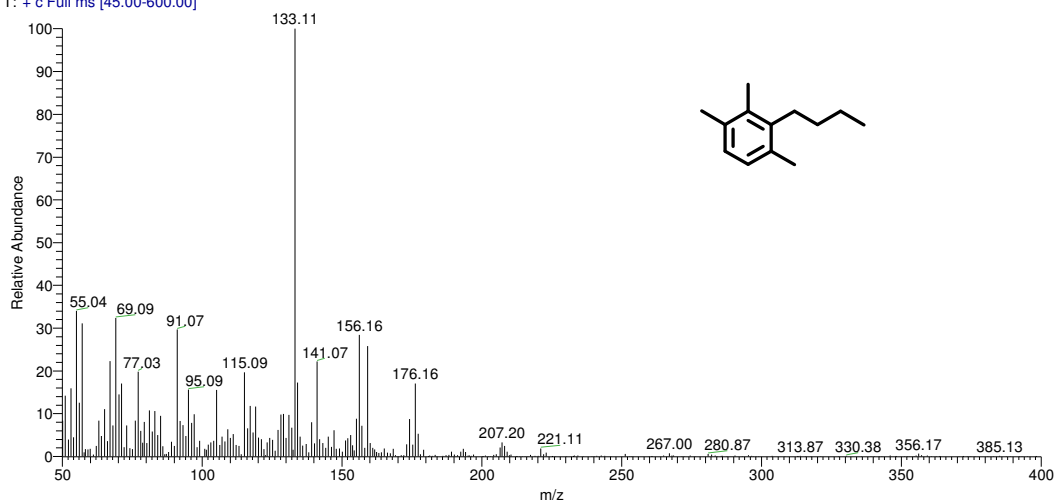
gumai\_B3-32-alkane #2235 RT: 47.27 AV: 1 SB: 2 47.17, 47.35 NL: 5.37E5  
T: + c Full ms [45.00-600.00]



A5.2. Biomarkers in aromatic hydrocarbon fraction

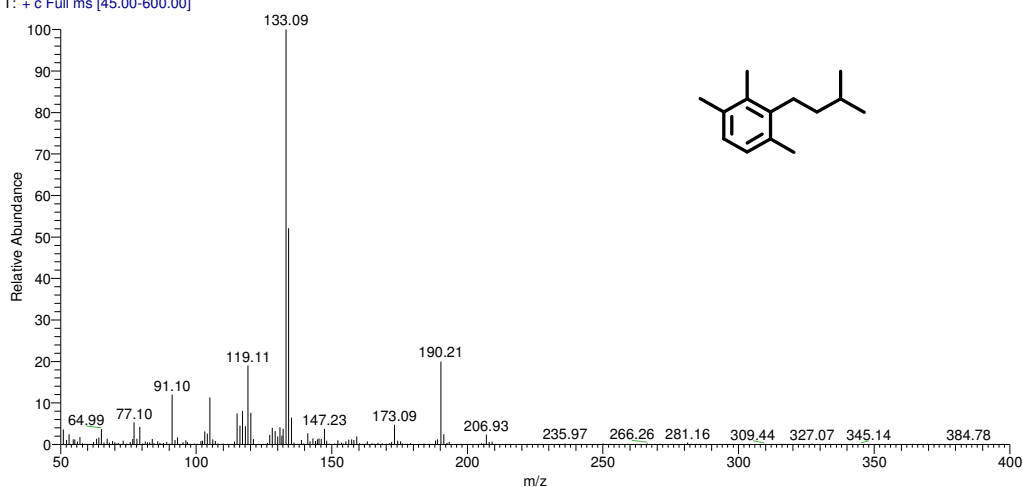
C<sub>13</sub> Aryl isoprenoids (mixed with dimethylnaphthalene)

B3-28C\_haris120908\_15 #475 RT: 13.95 AV: 1 NL: 2.20E5  
T: + c Full ms [45.00-600.00]



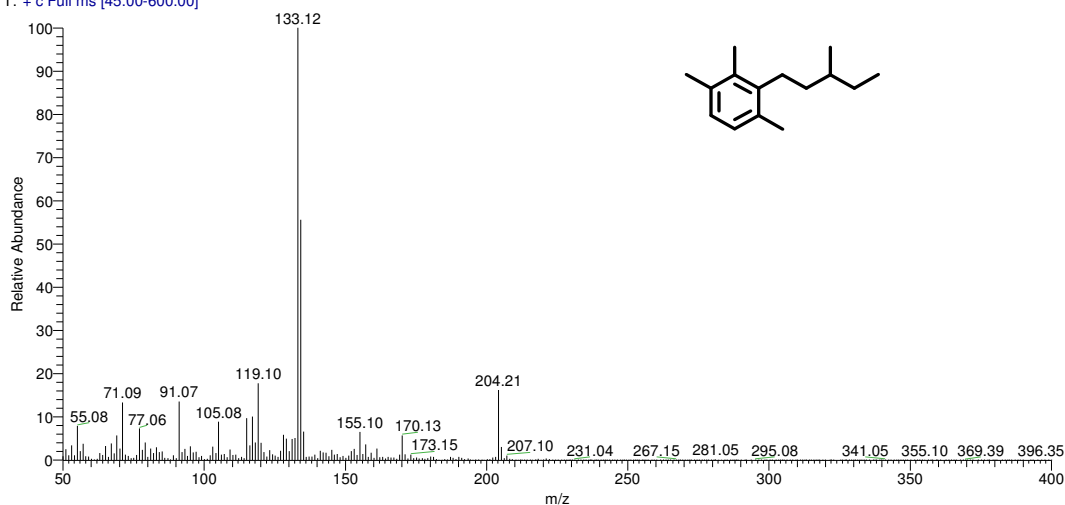
C<sub>14</sub> Aryl isoprenoids (Requejo et al, 1992)

haris051008\_04 #557 RT: 15.49 AV: 1 NL: 6.36E5  
T: + c Full ms [45.00-600.00]



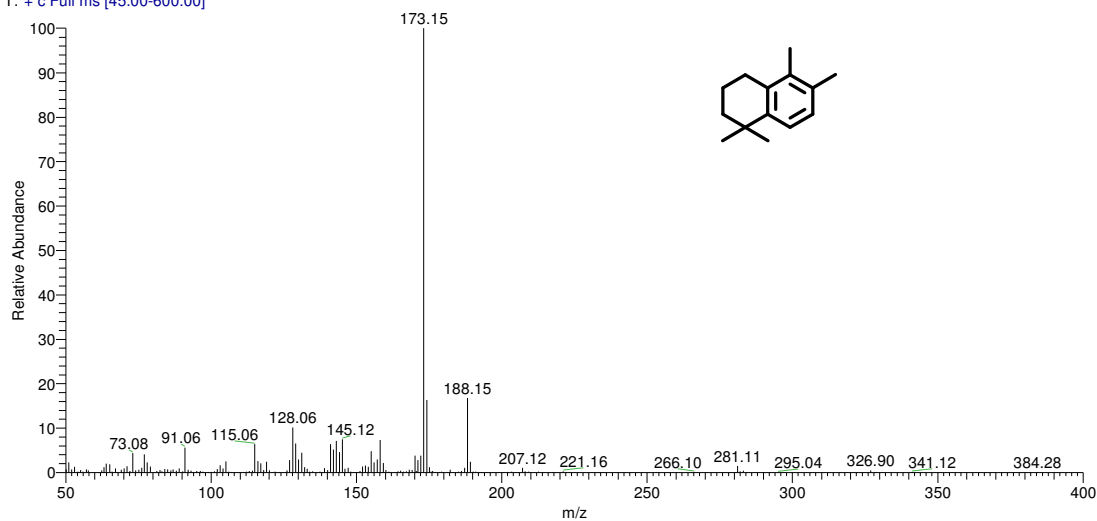
C<sub>15</sub> Aryl isoprenoids

B3-32\_haris090908\_03 #694-696 RT: 18.08-18.12 AV: 3 NL: 4.11E6  
T: + c Full ms [45.00-600.00]



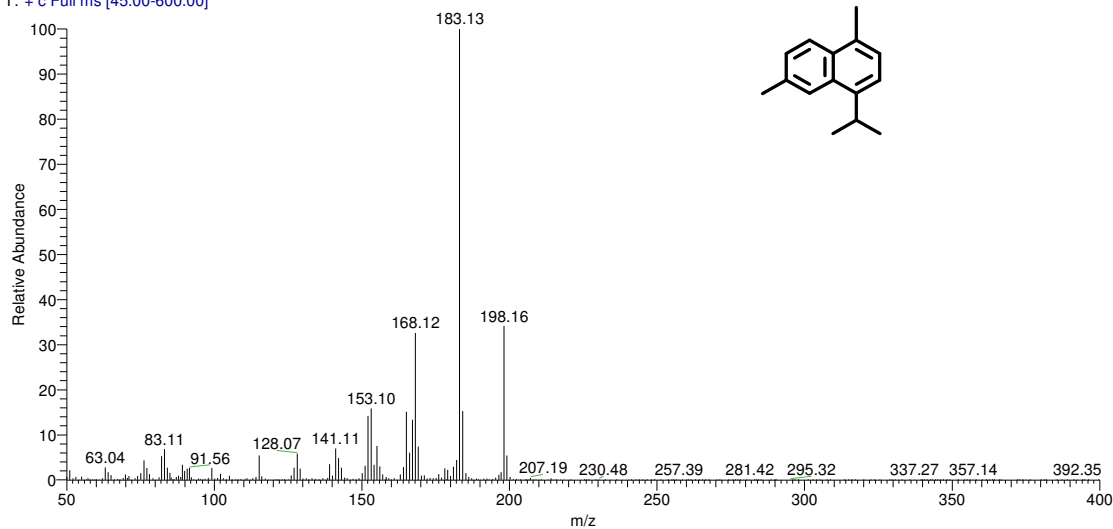
1,1,5,6-Tetramethyl-1,2,3,4-tetrahydronaphthalene (Killops, 1991)

haris051008\_04 #639 RT: 17.04 AV: 1 NL: 1.61E6  
T: + c Full ms [45.00-600.00]



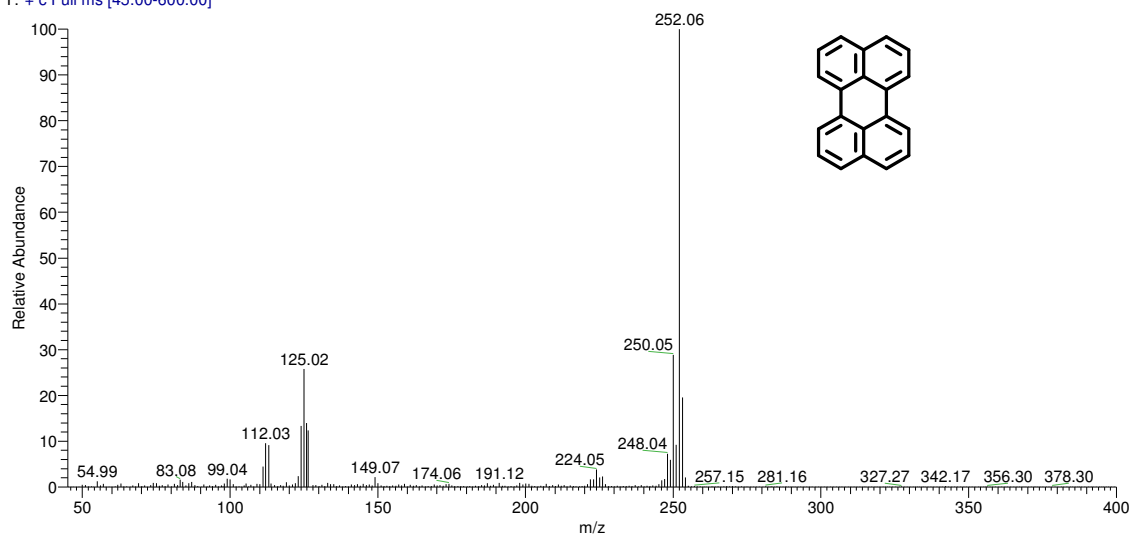
Cadalene (Geopetro and Wiley Libraries)

haris051008\_04 #870 RT: 21.40 AV: 1 NL: 2.16E6  
T: + c Full ms [45.00-600.00]



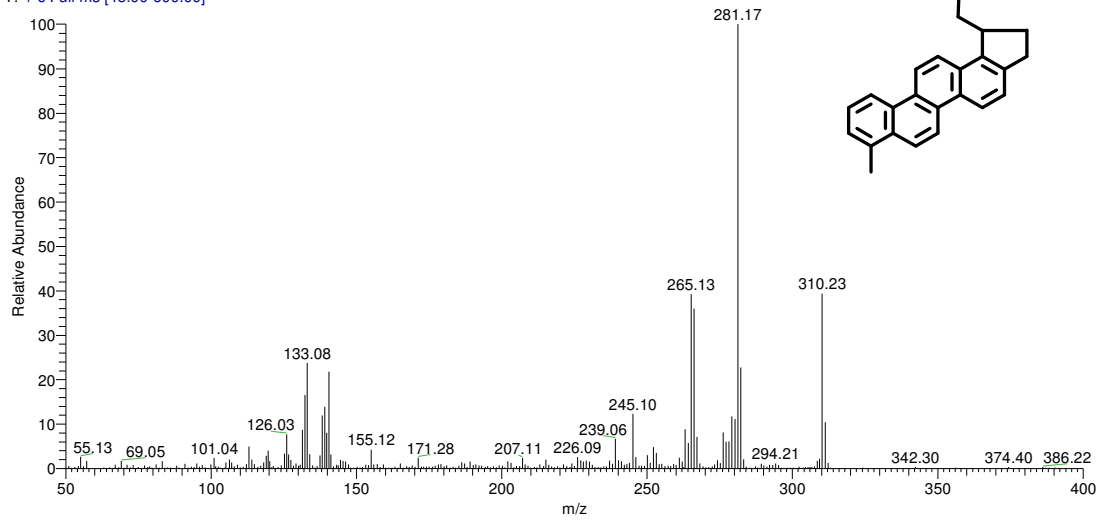
Perylene (Geopetro and Wiley Libraries)

gumai B3-32-aromatic #2558 RT: 54.07 AV: 1 NL: 3.07E7  
T: + c Full ms [45.00-600.00]



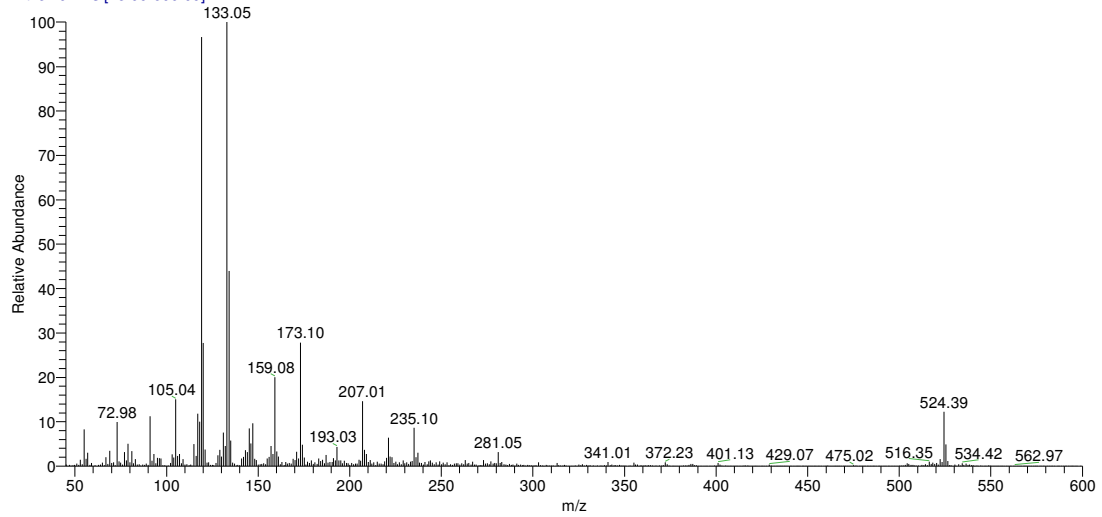
Methylethylcyclopentenochrysene (Dehmer, 1988; Wiley Library)

haris051008\_04 #2547 RT: 53.05 AV: 1 NL: 1.97E6  
 T: + c Full ms [45.00-600.00]



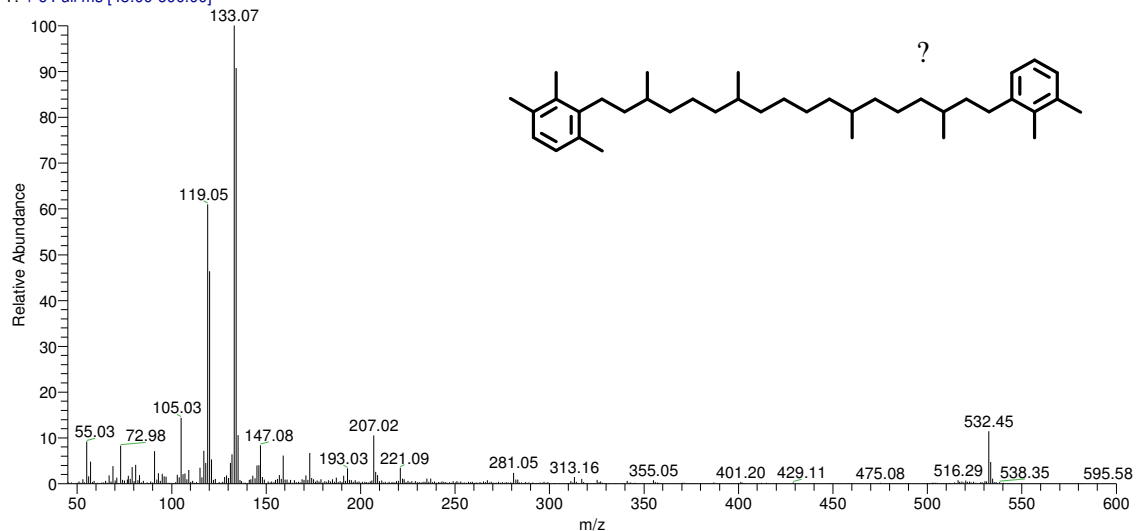
Carotenoid derivative 1

gumai\_B3-32-aromatic #3369 RT: 71.14 AV: 1 NL: 9.21E6  
 T: + c Full ms [45.00-600.00]



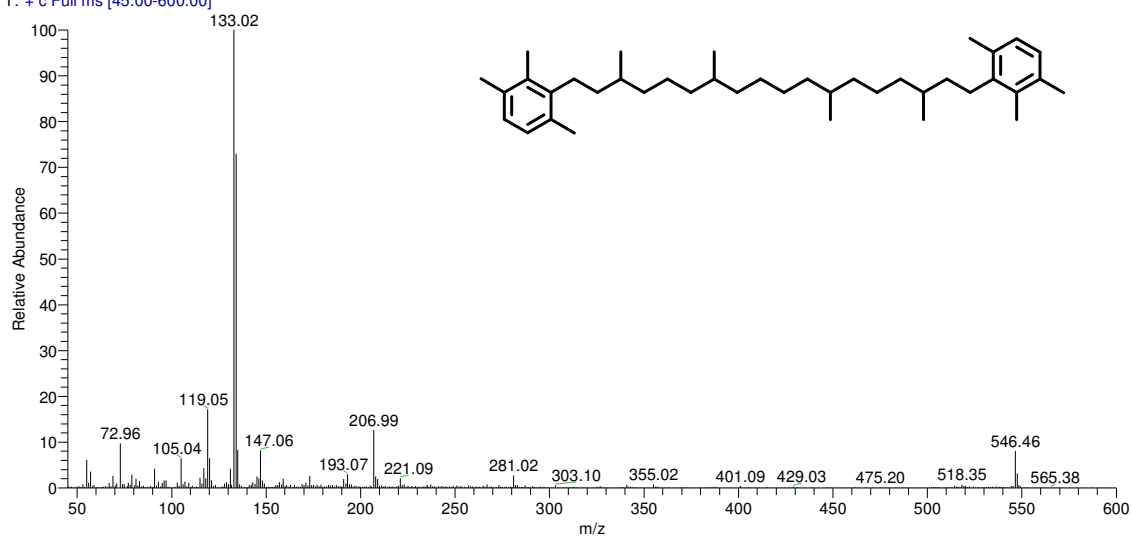
Carotenoid derivative 2

gumai\_B3-32-aromatic #3443 RT: 72.68 AV: 1 NL: 1.20E7  
 T: + c Full ms [45.00-600.00]



Isorenieratane (Hartgers et al., 1994)

gumai\_B3-32-aromatic #3549 RT: 74.91 AV: 1 NL: 1.04E7  
T: + c Full ms [45.00-600.00]



## Curriculum Vitae

### Personal Detail

Name : Agus Haris Widayat  
Date of birth : 12 May 1978  
Place of birth : Kulonprogo (Indonesia)  
Nationality : Indonesian



### Education

2007-2011 : PhD study at the Department of Environmental Analytical Chemistry, Institute of Atmospheric and Environmental Sciences, Johann Wolfgang Goethe University, Frankfurt am Main, Germany  
2003-2005 : Master study at the Department of Mining Engineering, Institut Teknologi Bandung, Indonesia  
Subject of interest: Organic petrology  
1997-2001 : Bachelor study at the Department of Mining Engineering, Institut Teknologi Bandung, Indonesia  
Major study: Earth resources exploration and evaluation  
1994-1997 : Senior High School at SMAN 1 Yogyakarta, Indonesia  
1991-1994 : Junior High School at SMPN 1 Brosot, Kulonprogo, Indonesia  
1985-1991 : Elementary School at SDN Bunder II, Kulonprogo, Indonesia

### Work Experience

2011-present : Academic staff at the Faculty of Mining and Petroleum Engineering Institut Teknologi Bandung, Indonesia  
2005-2007 : Academic assistant at the Faculty of Earth Science and Mineral Technology, Institut Teknologi Bandung, Indonesia  
2002-2003 : Engineer on coal reserves evaluation at Banpuindo Inc., South Kalimantan, Indonesia

### Scholarship

2007-2011 : German Academic Exchange Service (DAAD) for PhD study at the Department of Environmental Analytical Chemistry, Institute of Atmospheric and Environmental Sciences, Johann Wolfgang Goethe University, Frankfurt am Main, Germany  
2003-2005 : Graduate Scholarship Program (BPPS) of Indonesian Education Ministry for master study at the Department of Mining Engineering, Institut Teknologi Bandung, Indonesia

### Professional Membership

2009-present : American Association of Petroleum Geologists (AAPG)  
2010-present : The Geological Society of London (GSL)